Preliminary Design of Four Aircraft to Service the California Corridor in the Year 2010

The California Condor
California Sky-Hopper
High Capacity Short Range Transport
Tilt Rotor Aircraft Needed to Simlify Intercity Transportation

Presented to

Dr. Doral R. Sandlin

by
The Senior Design Class
Aeronautical Engineering Department
California Polytechnic State University
San Luis Obispo

22 May 1989

THE CALIFORNIA CONDOR

BUSINESS TRANSPORT
FOR THE CALIFORNIA CORRIDOR

FLIGHT VEHICLE DESIGN
AERO 445
SPRING 1989

Candace Chan
Michael Salazar
Mark Sousa
Mark Spence
Celso Velarde Jr.

AERONAUTICAL ENGINEERING DEPARTMENT
CALIFORNIA POLYTECHNIC STATE UNIVERSITY
SAN LUIS OBISPO, CALIFORNIA


3B
CC-3B

Abstract

The major objective of this project was to design an aircraft for use in the California Corridor in the year 2010. The design process, completed by students in a senior design class at California Polytechnic State University, San Luis Obispo, used a Class I airplane design analysis from Jan Roskam's Airplane Design. The California Condor (CC-38), a 38 passenger, 400 mph aircraft, was designed to meet the needs of tomorrow's passengers while conforming to the California Corridor's restrictons. Assumptions were made using today's technology with forecasts into 21st Century technology. Doubling today's commuter aircraft passenger capacity, travelling at Mach .57 with improved cruise efficiencies of over 10%, with the ability to land within field lengths of 4000 feet, are the CC- 38's strongest points. The California Condor has a very promising future in helping to relieve the air traffic and airport congestion in the 21st Century.

TABLE OF CONTENTS

LIST OF TABLES

LIST OF FIGURES

LIST OF SYMBOLS

a	Lift curve slope	1/degree
AR	Aspect Ratio	
A.C.	Aerodynamic Center	
b	Wing Span	ft
c	Wing chord	ft
C	Fuel fraction parameter	
cf	Equivalent Skin friction coefficient	
c.g.	Center of Gravity	in.,ft.
cj	Specific fuel consumption	lbs/lbs/hr
cp	Specific fuel consumption	lbs/hp/hr
cr	Root chord	ft
ct	Tip chord	ft
Cd	Drag coefficient	
Cd_0	Zero lift drag coefficient	
CGR	Climb Gradient	rad
CGRP	Climb Gradient parameter	rad
C_L	Total Lift Coefficient	
Ce	Engine Cost	dollars
Cfca	Material ($/cycle)	$/cycle
Cfce	Material ($/cycle)	$/cycle
Cfha	Material ($/FH)	$/FH
Cfhc	Material ($/FH)	$/FH
Cft	Cost of fuel	dollars
Cl	Section lift coefficient	
Cm	Pitching moment coefficient	
Cot	Cost of oil for turbin	dollars
Ct	Cost of total airplane	dollars
Ctm	Cost of material	dollars
D	Drag	lbs
D	Trip Distance	statute miles
Di	Induced Drag	lbs
Do	Parasite Drag	lbs
Df	Diameter of fuselage	ft
Dp	Propeller Diameter	ft
e	Oswald's Efficiency factor	
ehp	Equivalent horsepower	hp
E	Endurance	hours
f	Equivalent parasite area	ft^2
F	Weight sensitivity parameter	lbs
Fam	Fuel air maneuver	lbs
Fb	Block Fuel	lbs
Fcl	Fuel to climb	lbs
Fcr	Fuel to cruise	lbs
Fgm	Fuel ground maneuver	lbs
FH	Flight Hours	hours
FRES	Fuel Reserve	lbs
FAR	Federal Aviation Regulation	
g	acceleration of gravity	ft/sec^2

h	altitude	ft
Ip	Power Index	$(hp/ft^2)^{.33}$
i_w	wing incidence angle	degree
Kfca	Direct Labor (MH/cycle)	hours
Kfha	Direct Labor (MH/FH)	
Kfhc	Direct Labor (MH/Fh)	
Kfhe	Direct Labor (MH/cycle)	hours
lf	length of fuselage	ft
lm	Dist. cg to main gear	ft
ln	Dist. cg to nose gear	ft
L	Lift	lbs
L/D	Lift to drag ratio	
mph	Miles per hour	mph
mi	mile	mi
M	Mach number	
Mff	Mission Fuel Fraction	
MH	Man Hours	hours
n	Load factor	
nm	Nautical mile (6076ft)	nm
N	Number of engines	
P	Power, Horse-power	hp
P	Payload	tons
Pbl	Blade power loading	hp/ft^2
Ps	Specific excess power	ft/sec
q	Dynamic pressure	psf
R	Range	nm or mi.
Rn	Reynold's number	
RC	Rate of climb	fpm or fps
RCP	Rate of climb parameter	hp/lbs
RL	Labor Rate	dollars/hour
s	Distance in takeoff and landing	ft
S	Wing surface area	ft^2
sm	Statute mile	sm
SHP	Shaft horspower	hp
Swet	Wetted Area	ft^2
t	time	sec,min,hr
tb	time block	hours
t/c	thickness ratio	
Tam	Time air maneuver	hours
Tcl	Time to climb	hours
Tcr	Time at cruise altitude	hours
Tgm	Time ground maneuver	hours
TOGW	Takeoff Gross Weight	lbs
TOP_{25}	FAR 25 takeoff parameter	lbs/ft^2
Vbar	Volume coefficient	
V	Velocitymph,fps,kts	
Vb	Velocity block	mph,fps,kts
Vf	Velocity Final	mph,fps,kts
Vo	Velocity Initial	mph,fps,kts
VA	Velocity Approach	mph,fps,kts
Vs	Velocity Stall	mph,fps,kts
W	Weight	lbs
W/P	Power Loading	lbs/hp

W/S	Wing Loading	lbs/ft^2
Xac	Distance from l.e. to a.c.	ft
Xv,Xh,Xc	Distance from c.g. to a.c. of surface	ft

Greek Symbols

α	Angle of attack	degrees
β	Sideslip angle	degrees
η	Efficiency of prop	
K_λ	Taper ratio correction factor	
λ	Taper ratio	
Λ	Wing sweep	
ρ	Density	$slugs/ft^3$
σ	Density ratio	

Introduction

California is currently one of the fastest growing states in the United States and its population trends are expected to continue. The major metropolitan areas within the state are already saturated causing many other developing areas to take the inflow of people and industry. It is foreseen that there will be necessary changes in transportation due to the increased population and dispersion of business throughout the state. The California Corridor, ranging from the San Diego area to the Sacramento Valley, (see Figure 1), is the focus of this design project. By the year 2010, it is foreseen that there will be a need for necessary changes in air transportation within the California Corridor. Cities such as Bakersfield, Fresno, Ventura, Santa Barbara, San Luis Obispo, Salinas, Stockton, and Tracy have high growth potentials. These cities often have airports much smaller than those of San Francisco and Los Angeles. With smaller airports come smaller runways, some less than 5000 feet. The CC-38 was designed so that airports such as these can be accessed.

It is expected that by the year 2010, air transportation in California will be utilized more extensively due to increases in automobile traffic. Recently there have been problems in the airline industry with air traffic and airport congestion. If something is not done to relieve these problems soon, California could become a huge gridlock, both on the ground and in the air. In the next century it will be necessary to keep ground and air traffic to a minimum.

The California Condor (CC-38), a medium speed, medium range, 38 passenger aircraft may be a partial answer to these problems. One way to reduce ground and air congestion is to decrease the number of aircraft using the airport facilities. The current commuter regional turboprop aircraft can accomodate up to 19 passengers due to Federal Aviation Regulations. Aircraft with 19 passengers or less are not required to have flight attendents on board, thus cutting the airline's expenses. However, these 19 passenger aircraft are posing increased ground and air traffic at major airports. With a 38 passenger aircraft, fewer commuter flights will be needed thus cutting congestion into and out of the major California airports. At the same time, a cruise velocity of 348 knots can cut the transit time of todays commuter aircraft significantly. Along with its high cruise speed, and 38 passenger capacity, the CC-38 has been designed to land at field lengths of 4000 feet. Many cities, like those mentioned above, can accomodate the CC-38 because of its ability to land in less than 4000 feet. The use of counter-rotating propellers can greatly impove the cruise efficiency of the aircraft, and at the same time allow the CC-38 to cruise to velocities of Mach .57 at altitude.

Meeting the demands of the 21st Century, the CC-38 will provide highly efficient air transportation servicing the diverse needs of tomorrow's passenger.

Mission Specifications

Keeping the needs of the California Corridor in mind, the mission specifications for the California Condor (CC-38) were established. Table I shows the list of mission specifications for the CC-38.

TABLE I MISSION SPECIFICATIONS

Range	600 nm (plus 100 nm loiter)
Cruise speed	348 knots (M=0.57 AT 20,000 ft)
Altitude	20,000 ft
Take-off distance	4,000 ft @ 5,000 ft elevation
Landing distance	4,000 ft @ 5,000 ft elevation
Payload	38 passengers (7790 lbs)
Crew	1 pilot (205 lbs)
	2 attendants (410 lbs)

The range of 600 nautical miles with a 100 nautical mile loiter was chosen by looking at the distances from one major airport to another in California. (see Figure 1) For example, the 600 nautical miles will span from San Diego to San Francisco as well as from Los Angeles to Sacramento. The 100 nautical mile loiter was decided upon to accomodate for traffic congestion and the changing weather experienced on the California coastline.

The payload is 38 passengers, catering to mostly business class people who commute between major metropolitan areas. The 38 passenger capacity was based on growth trends forecasted in Aviation Forecasts (Reference 7). As can be seen from Figures 2a and 2b below, the trends look to favor the 20-40 passenger sizes by the year 2000. Figure 3 shows that the number of 40 passenger aircraft is increasing, and is expected to keep increasing into the 21st century. The 38 passenger capacity doubles that of the current commuter turboprop aircraft, which means fewer flights into airports, less air traffic, and less ground congestion. With the population increasing, the need for larger commuter aircraft will definitely help the air traffic problems that the nation faces already.

FIGURE 1 THE CALIFORNIA CORRIDOR

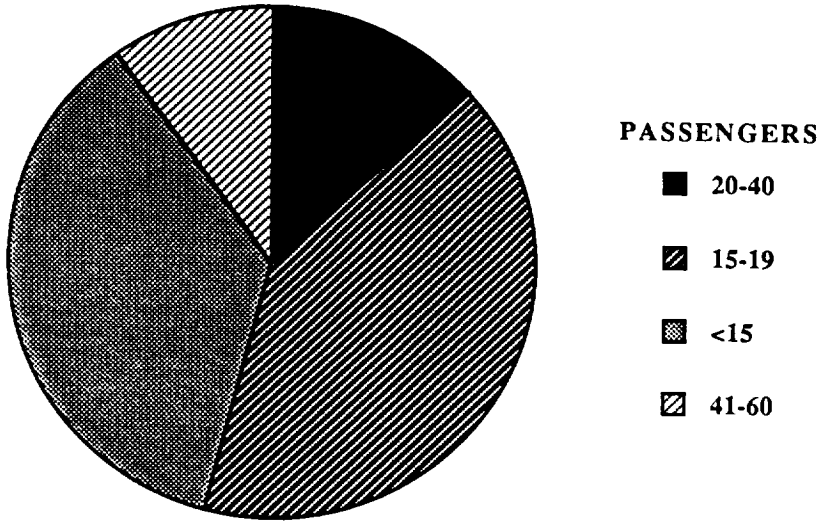

FIGURE 2a PERCENT BY SEAT SIZE 1987

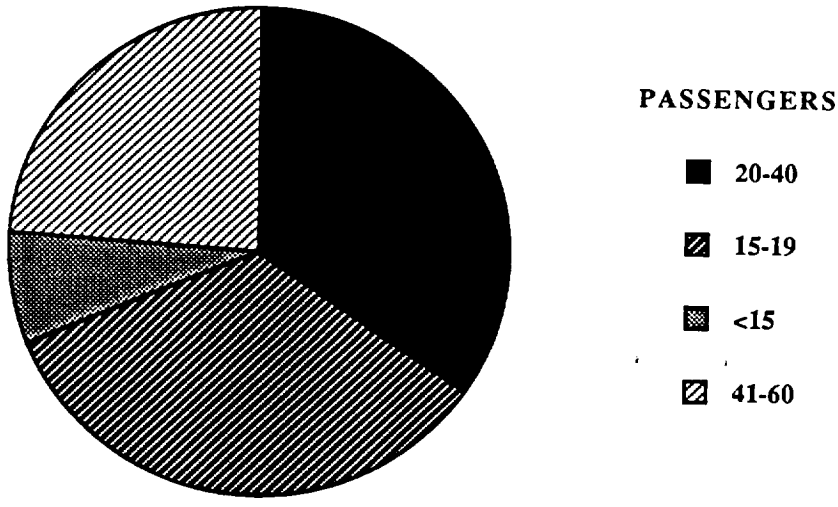

FIGURE 2b PERCENT BY SEAT SIZE 1999

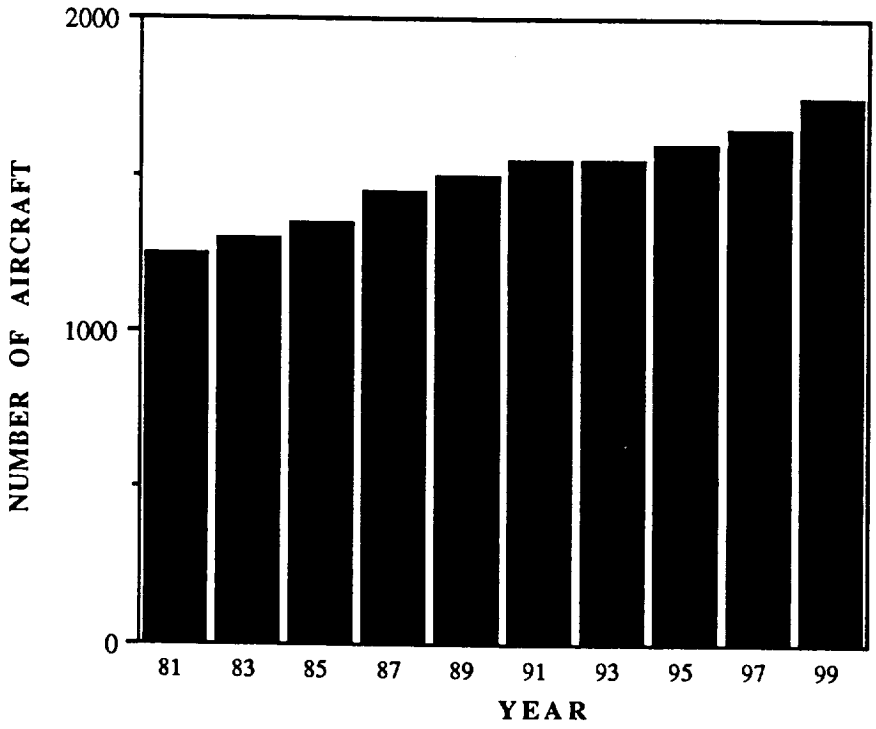

FIGURE 3 40 PASSENGER AIRCRAFT (REFERENCE 7)

A cruise speed of 348 knots (400 mph) corresponding to Mach .57 at 20,000ft was chosen so that a minimum amount of time is spent in transit between the airports. At Mach .57, with the airfoils chosen, no compressibility effects such as wave drag are present. Aircraft with speeds above Mach .75 can experience wave drag which would increase the total power required to fly. Flight speeds above Mach 1 in the California Corridor were not considered due to the sonic booms that would be generated and the short distances being travelled.

An altitude of 20,000 feet provided excellent cruise conditions for the CC-38. The counter-rotating propellers were tested a higher altitude and efficiencies of about 86% were found. Pressurization at this altitude would also be required providing more comfort to passengers.

Takeoff and landing distances of 4000 feet at an altitude of 5000 feet, allow the CC-38 to land and takeoff at most metropolitan airports. By looking at cities in California that have populations of over 30,000 people and at already existing runways, a 4000 foot field length was chosen. Constructing a new airport is very time consuming and expensive, therefore it was assumed that already existing airports would be used. By sizing at 5000 feet, it insured that sea level requirements were met. Figure 4 shows the complete mission profile for the CC-38.

The crew of the CC-38 consists of 1 pilot and 2 flight attendants. The 1 pilot has the sole resposibility of monitoring the on-board Flight Management Computer System (FMCS) and the Digital Air Data Computer (DADC). These two systems are currently installed in the Boeing 757's and 767's.

With these on-board computers and with ground systems capable of controlling them, a fully automated flight is very realistic in the future. These components, with the electronic technologies to come, should be light enough and inexpensive enough to install on-board most aircraft. A full set of controls will be provided for the pilot in case of a malfunction. The pilot is also there for passenger security, as most people will be hesitant to fly without one aboard. The two flight attendants should provide enough service for the 38 passengers aboard.

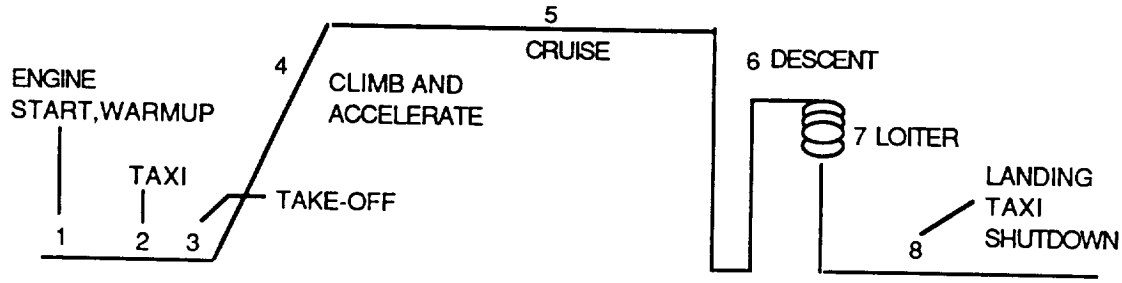

FIGURE 4 MISSION PROFILE FOR THE CC-38

RESULTS

Performance

Weights

Upon completing the preliminary sizing of the CC-38, the weights were calculated. These weights and the calculations are included in Table II and Appendix B, respectively. Composites were assumed to comprise 6% of the wing weight, empennage weight, and fuselage weight. This reduction in weight was taken into account throughout the analysis. A sensitivity analysis was also conducted and used in the weight analysis. The results are included in Table A1.

TABLE II WEIGHTS

Wto	=	31,741.8 lbs.
We	=	18,818.8 lbs.
Wf	=	4,518.0 lbs.
Wp	=	7,790.0 lbs.
Wc	=	615.0 lbs.

Lift and Drag

High lift coefficients for the aircraft were chosen so that the CC-38 could land within a field length of 4000 feet. Table III shows the lift coefficients of the aircraft with the corresponding drag coefficients for the take-off, landing, and cruise configurations. The lift coefficients of 2.5 for take-off and 3.0 for landing were accomplished by using two single slotted Fowler flaps. The inboard flap will be blown by the propeller slipstream and the engine's exhaust. Figure 5 shows drag as a function of velocity at a cruise altitude of 20,000 feet.

TABLE III LIFT COEFFICIENTS

$C_{LMAX\ CLEAN}$	=1.7		
$C_{LCRUISE}$	=0.224	C_D	=0.029
$C_{LMAX\ TO}$	=2.5	C_D	=0.333
$C_{LMAX\ LAND}$	=3.0	C_D	=0.528
$DC_{LMAX\ TO}$	=0.535		
$DC_{LMAX\ LAND}$	=1.07		

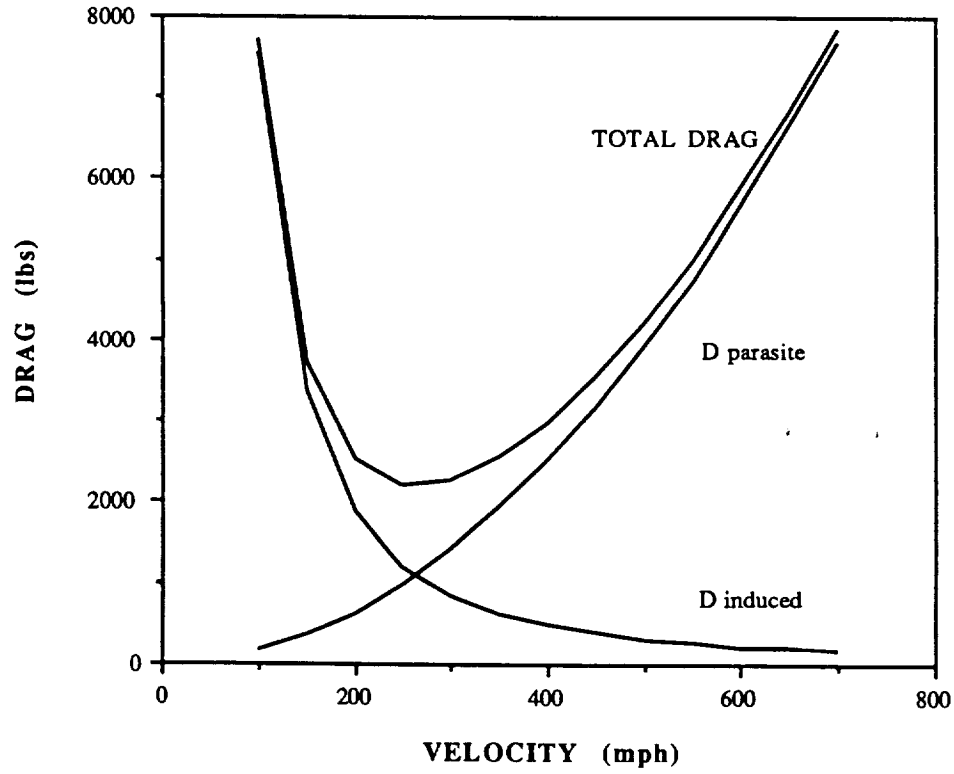

FIGURE 5 DRAG CURVES

Propulsion

The driving factor in the performance of the CC-38 was the cruise velocity of 348 knots (Mach=0.57 at an altitude of 20,000 feet). The cruise speed was found to be the limiting factor in the sizing analysis. A power loading of 6.275 lb/HP was determined from the sizing diagram. The engines were selected to meet this power loading. A propeller diameter of 9.2 feet was calculated using the optimum disk loading given in a Hamilton Standard report. Table IV gives the engine performance parameters and propeller dimensions.

Power required curves at sea level and at an altitude of 20,000 feet are shown in Figures 6a and 6b. The power available from the chosen engines is included in the figures to show the excess power available at a velocity of 400 miles per hour. The cruise flight analysis used 75% of the total available power.

TABLE IV ENGINE AND PROPELLER SPECIFICATIONS

ENGINE

Allison 501-M78 Axial Flow Turboprop

Max Continuos Power:	Takeoff	4910 ehp (4591shp)
Normal		4365 ehp (4061 shp)
Cruise Power (75% at altitude)		2592 shp

SPECIFIC FUEL CONSUMPTION

Max Rating	.501 lbs/hr/hp
Normal Rating	.517 lbs/hr/hp
75% Power	.520 lbs/hr/hp (compared to 501-M62)

PROPELLER

Hamilton Standard	CR-1 (Counter-rotating)
Diameter	9.2ft
Efficiency	.86 (assumed)
Number of blades	12/engine (6/shaft)

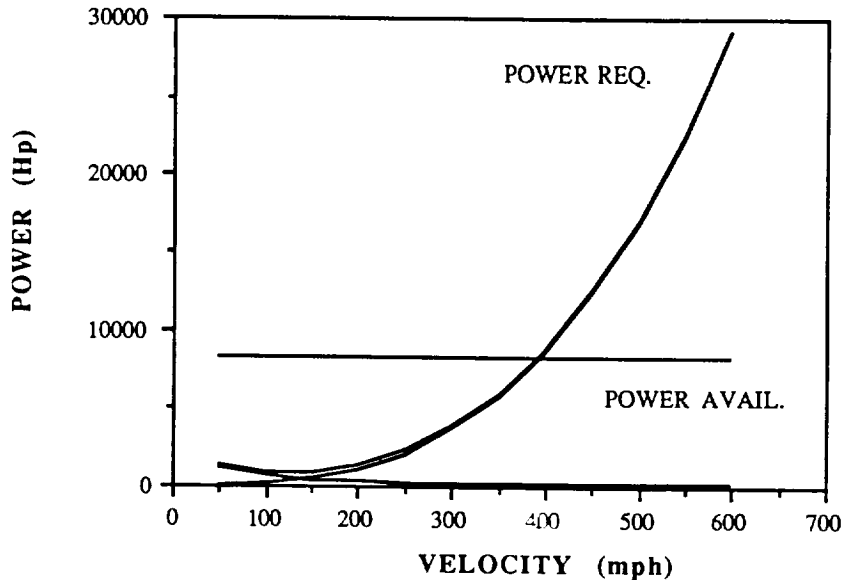

FIGURE 6a POWER REQUIRED AT SEA LEVEL

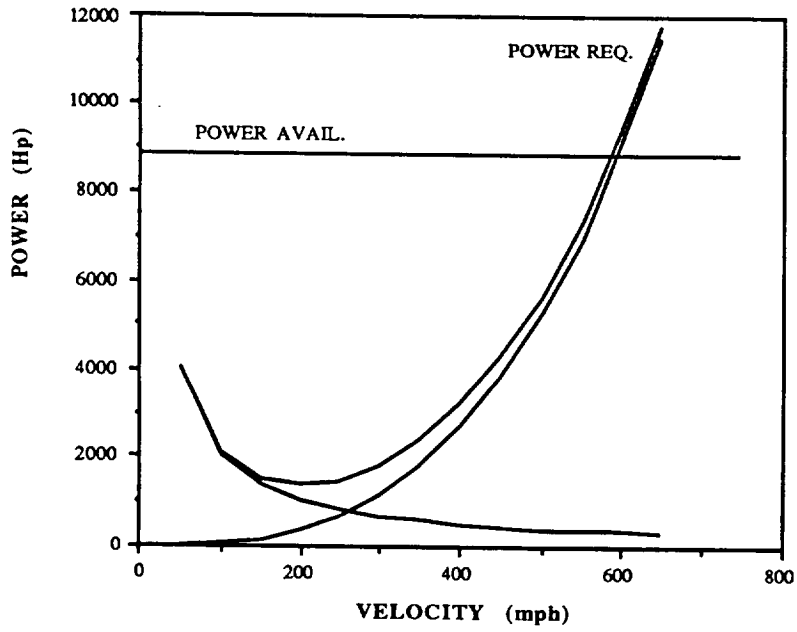

FIGURE 6b POWER REQUIRED AT 20,000 FEET

Velocities

The stall velocities and the approach velocities for the CC-38 were calculated with the designed lift coefficients of Table 3. Table 5 shows the take-off, approach and landing stall velocities as well as the cruise velocity at altitude. The 5,000 foot altitude in Table V was chosen to allow aircraft to operating out of elevated airports. These velocities were found to be comparable to conventional turboprop stalling velocities.

TABLE V VELOCITIES

ALTITUDE = 5000 FT, WITH CORRECT FLAP SETTING

CONDITION	SPEED(KNOTS)	SPEED(MPH)
TAKE-OFF V_{STALL}	79.4	91.4
APPROACH VELOCITY	93.3	107.3
LANDING V_{STALL}	71.8	82.6

ALTITUDE =SEA LEVEL, WITH CORRECT FLAP SETTING

CONDITION	SPEED(KNOTS)	SPEED(MPH)
TAKE-OFF V_{STALL}	73.8	84.8
APPROACH VELOCITY	86.6	99.6
LANDING V_{STALL}	66.6	76.6
CLIMB VELOCITY	260.9	300.0
RATE OF CLIMB	2000 ft/min	

The main parameter in the design of the CC-38 was the landing field length of 4,000 feet. Approximately one-half of this distance is used for take-off and landing ground roll. Ground roll distances are shown in Table VI. These distances were based on passenger comfort during acceleration and deceleration. The take-off acceleration was chosen at 0.25 g's and the landing deceleration was chosen at 0.2 g's. These values are comparable with other commuter aircraft.

TABLE VI TAKEOFF AND LANDING DISTANCE GROUNDROLL

		DISTANCE (FT)	EXCESS (FT)
5000 FT ALTITUDE TAKE-OFF ACCELERATION (TO 1.3 V_{STALL})	FLAPS SET 25° 0.25 G'S	1887.2	2112.8
LANDING DECCELERATION (TO STOP)	FLAPS SET 50° 0.20 G'S	1926.5	2073.5
SEA LEVEL TAKE-OFF ACCELERATION (TO 1.3 V_{STALL})	FLAPS SET 25° 0.25 G'S	1626.1	2373.9
LANDING DECCELERATION (TO STOP)	FLAPS SET 50° 0.20 G'S	1659.8	2340.2

Configuration

The CC-38 is a conventionally configured aircraft. Figure 7 shows the standard tail aft, low wing configuration. This configuration was selected for several reasons. Among these are ease of certification, ease of manufacture, consumer acceptability, and access to ground support services.

Main Wing

A swept and tapered wing is used to maximize aerodynamic efficiency at high speeds. Elliptical winglets were incorporated to reduce the induced drag. The wing has an incidence angle of -2° to accommodate the GA(W)-1 airfoil's zero-lift angle of attack. This supercritical airfoil provided the lift coefficients needed to meet the CC-38's take-off and landing requirements. Table VII shows the wing's planform parameters, while Figure 8 shows the wing's dimensions. The wing also has a 1° dihedral angle for stability augmentation; this angle is illustrated in Figure 9.

ORIGINAL PAGE IS
OF POOR QUALITY

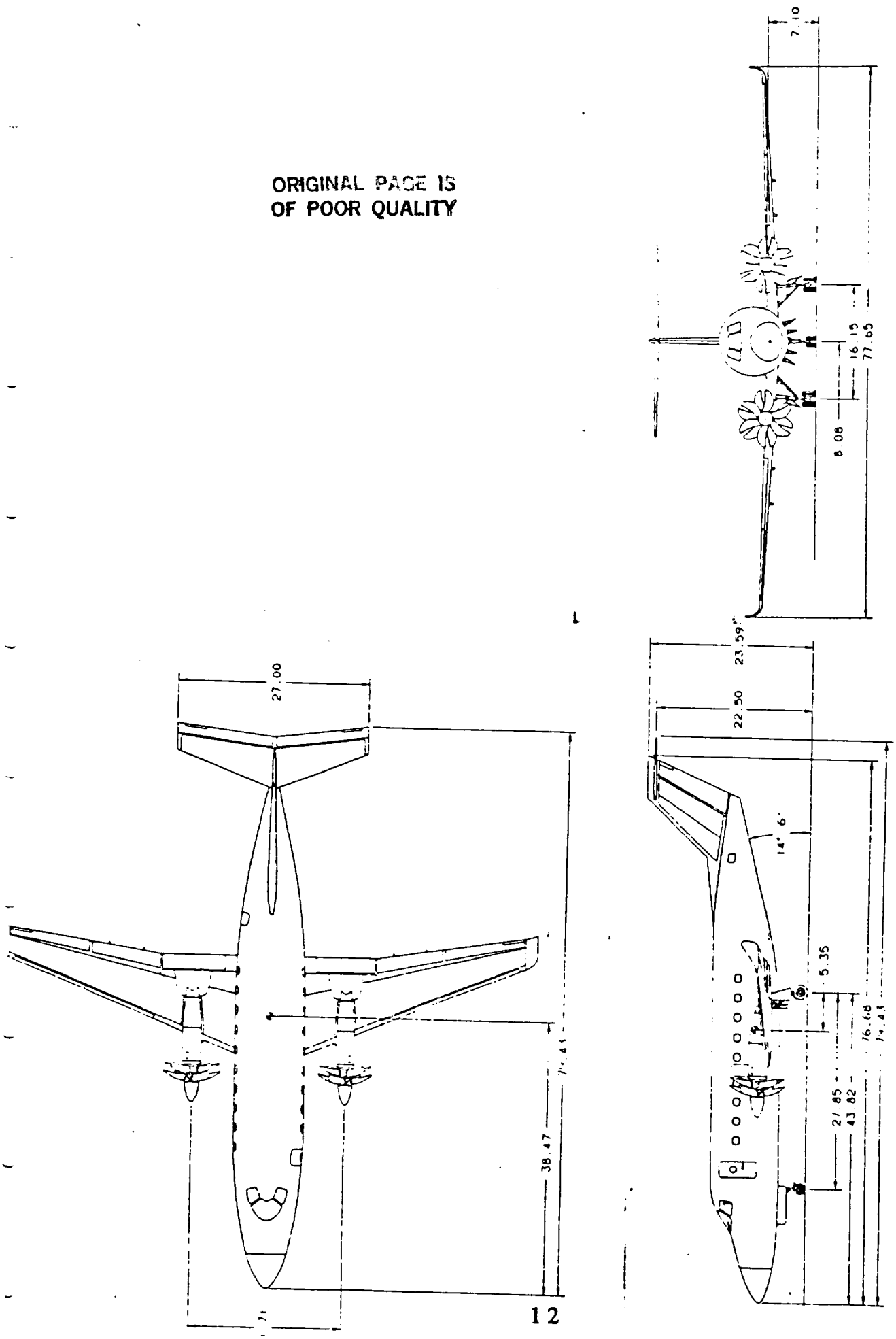

FIGURE 7 THREE VIEW OF THE CC-38

TABLE VII WING PLANFORM PARAMETERS

AREA	=	634.8 ft^2
AR	=	8.89
b	=	77.65 ft
c_{root}	=	13.57 ft
c_{tip}	=	3.97 ft
c_{out}	=	9.516 ft
sweep	=	25 degrees @ 1/4 chord
taper	=	0.333

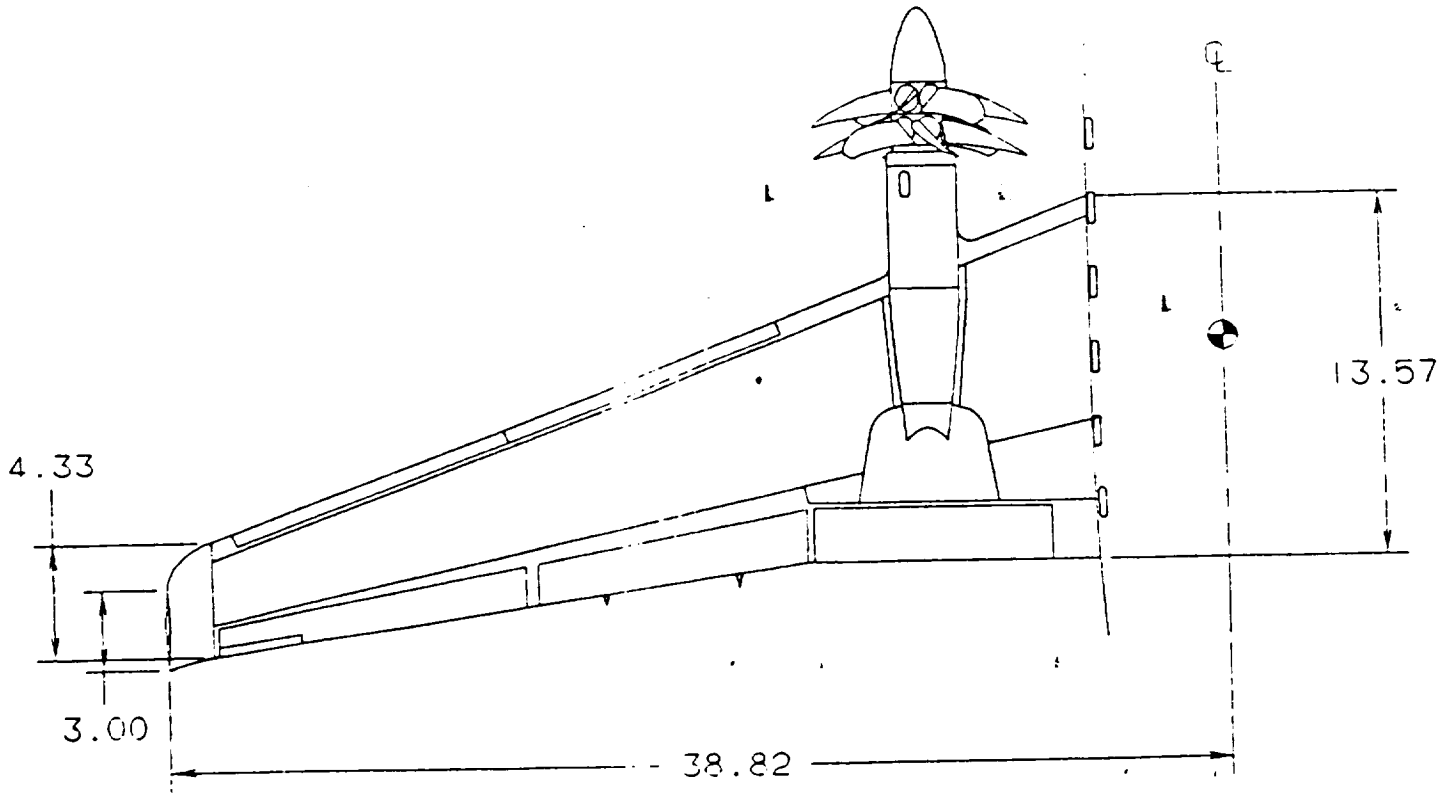

FIGURE 8 WING DIMENSIONS

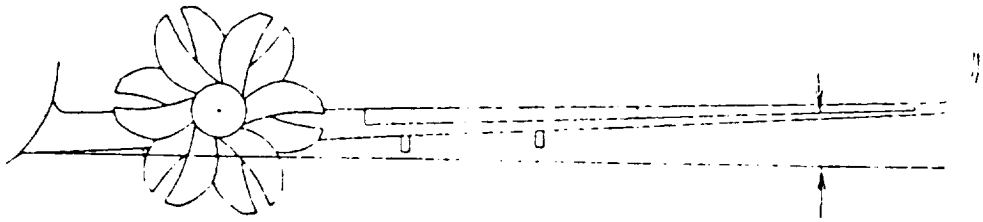

FIGURE 9 WING DIHEDRAL

Horizontal Tail

A NACA 0009 symmetric airfoil was used on the horizontal tail. Initial sizing of this tail was done by comparison to similar aircraft and then adjusted for stability considerations. Table VIII shows the horizontal tail planform parameters and Figure 10 shows the horizontal tail dimensions. The aircraft used for the comparison and their data are included in Table A10.

TABLE VIII HORIZONTAL TAIL PLANFORM

AREA	=	151.47 ft^2
AR	=	5.61
b	=	27.0 ft
c_{root}	=	7.36 ft
c_{tip}	=	3.86 ft
taper	=	0.52

Vertical Tail

The vertical tail size was also based on similar aircraft. The NACA 0009 airfoil was again used. Table IX shows the vertical tail planform parameters and figure 11 shows the vertical tail dimensions.

TABLE IX VERTICAL STABILIZER PLANFORM

AREA	=	93.15 ft^2
c_{root}	=	18.74 ft
c_{tip}	=	6.0 ft
height=		10.77 ft
taper	=	0.33

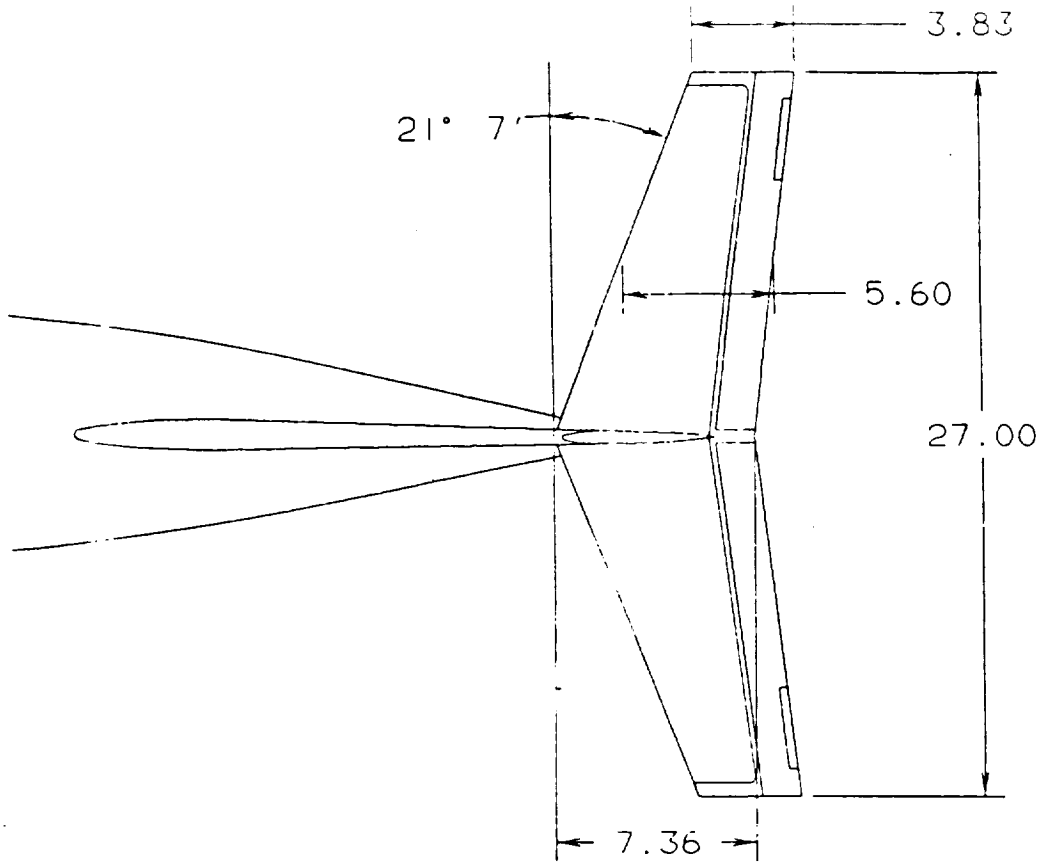

FIGURE 10 HORIZONTAL TAIL DIMENSIONS

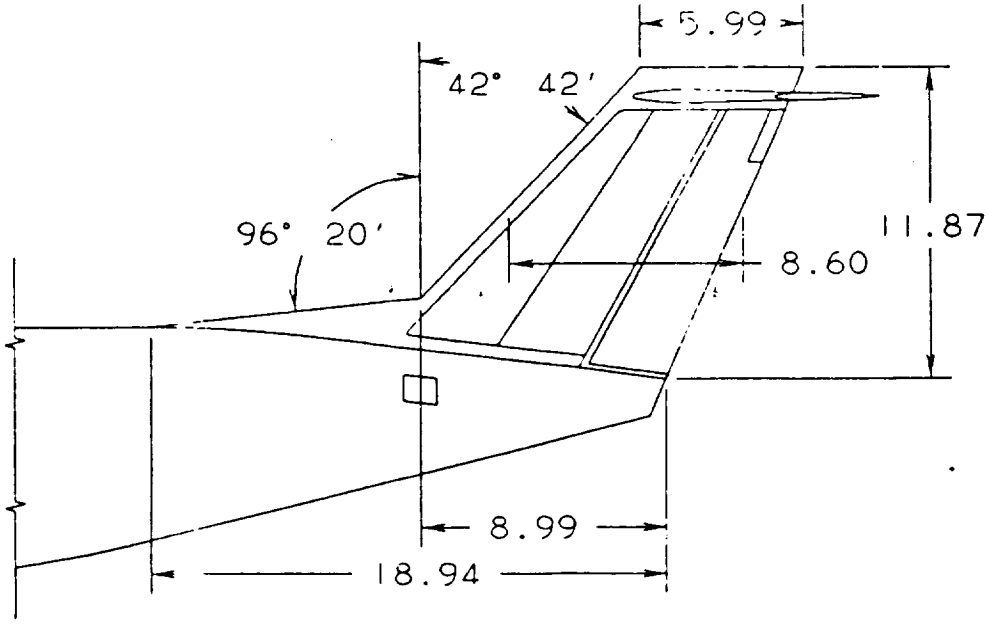

FIGURE 11 VERTICAL TAIL DIMENSIONS

High Lift and Control

The maximum lift coefficients will be achieved using two single slotted Fowler flaps. The flaps are illustrated in Figure 12. The inboard flap is blown with the engine exhaust and the propeller slipstream. The outboard flap is used as a conventional flap. The analysis used in this design did not take the increase in lift coefficient due to blowing into account. Figure 12 also shows the placement of the flaps and the aileron. Flap settings for landing and take-off are 50° and 25°, respectively. Figure 17 shows the wing mounted engine with the counter-rotating propfans. Also present is the extended Fowler flap that will be blown.

Fuselage

The fuselage parameters are listed in Table X. The fuselage dimensions are shown on Figure 13. The placement of the tricycle landing gear can also be seen in this figure.

TABLE X FUSELAGE PARAMETERS

LENGTH	71.59 ft
DIAMETER	9.71 ft
TAIL CONE ANGLE	14° 6"
INTERIOR HEIGHT	6.14 ft

The seats are arranged four abreast with an aisle down the middle. The inboard profile and the seating arrangement are shown in Figure 14. The seats are designed larger than conventional aircraft seats for added passenger comfort. The seat dimensions are shown in Figures 15a and 15b. Overhead storage compartments are provided and baggage compartments are located in the tail cone and the airplane's belly. A galley, restroom, air to air and air to ground telephone, and color FAX system are also included for passenger convenience.

Flight Deck

The CC-38's cockpit incorporates modern technologies which contribute to reducing the pilot's workload. These technologies include a fully automated flight management system. The pilot is provided with a fully operational set of controls for emergency use. Figure 16 shows the cockpit and flight deck arrangement.

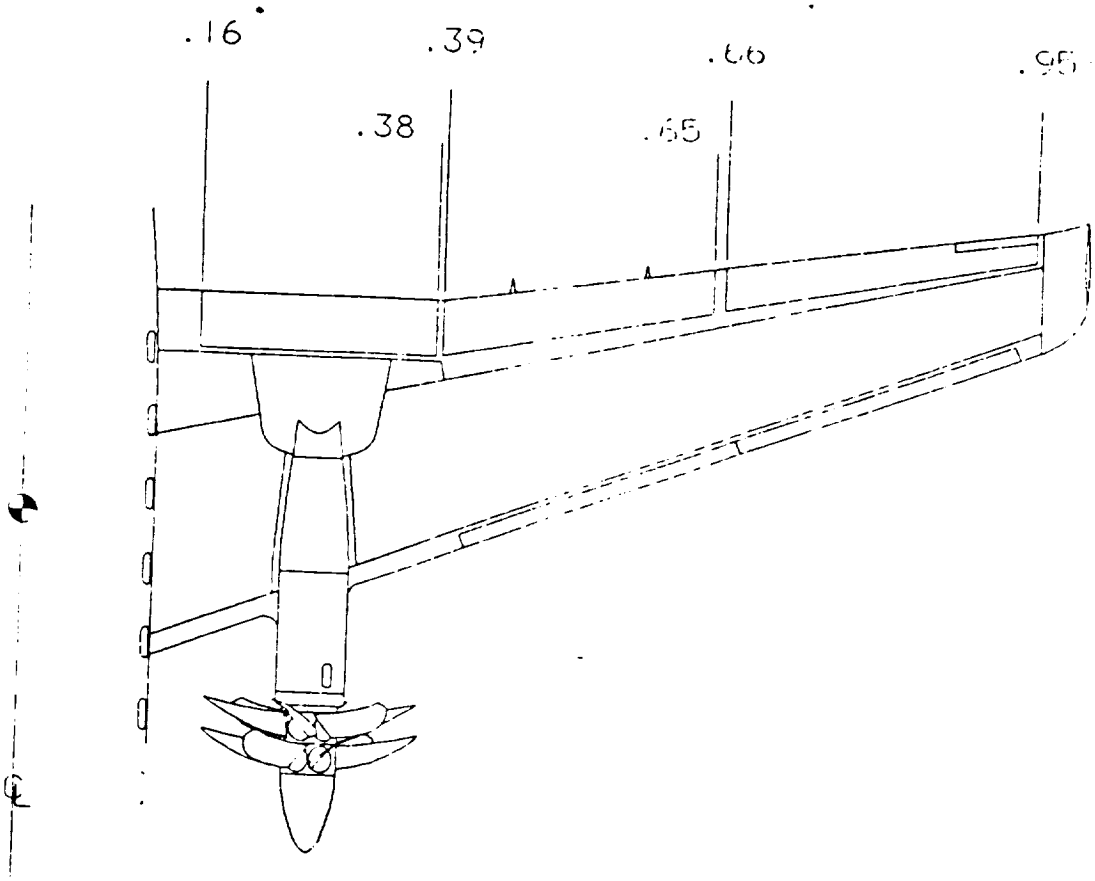

FIGURE 12 FLAP AND AILERON LOCATIONS

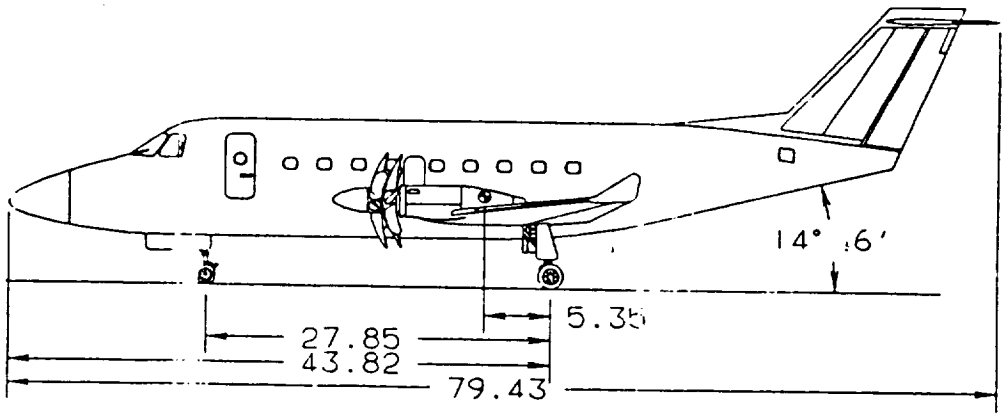

FIGURE 13 FUSELAGE DIMENSIONS

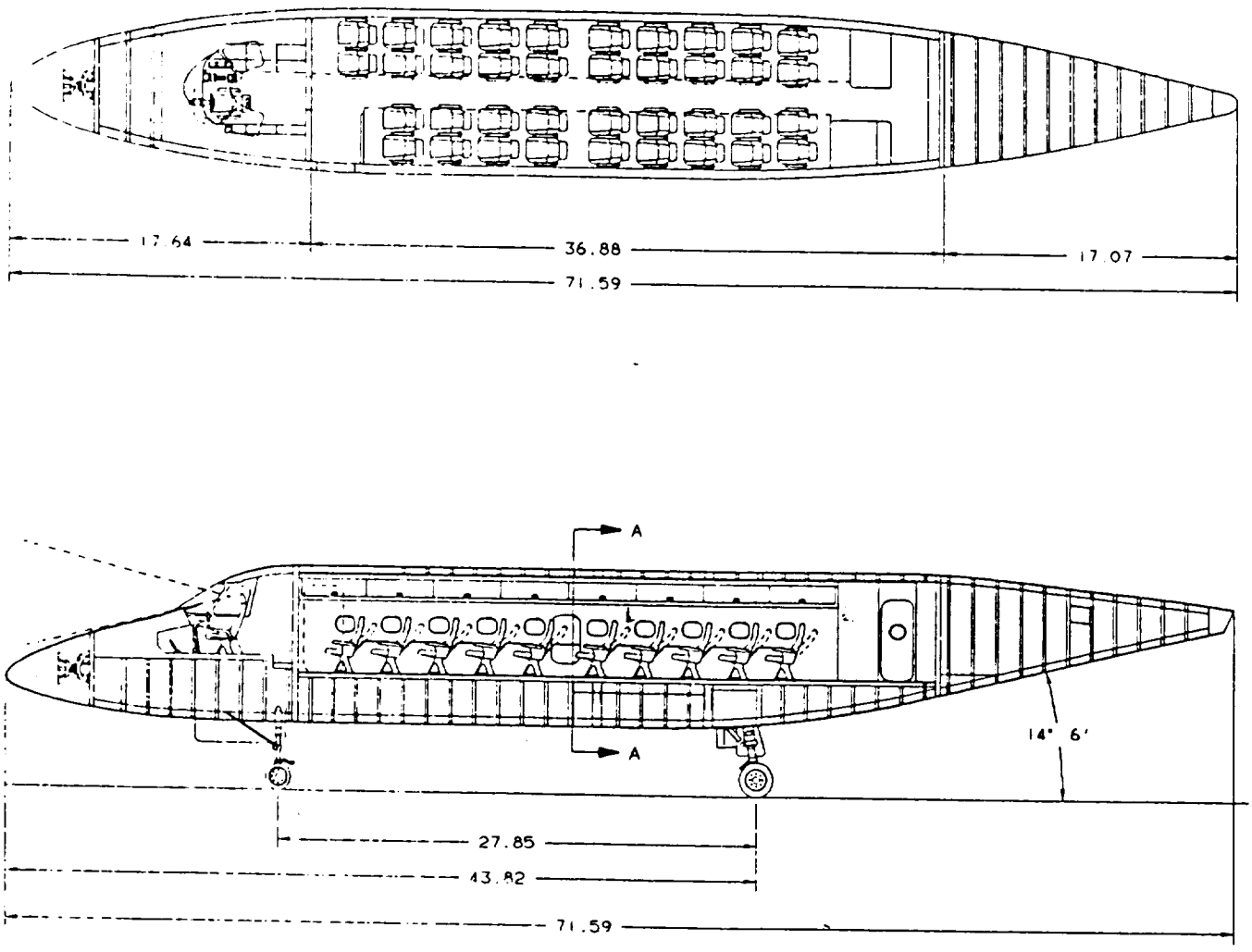

FIGURE 14 INBOARD PROFILES

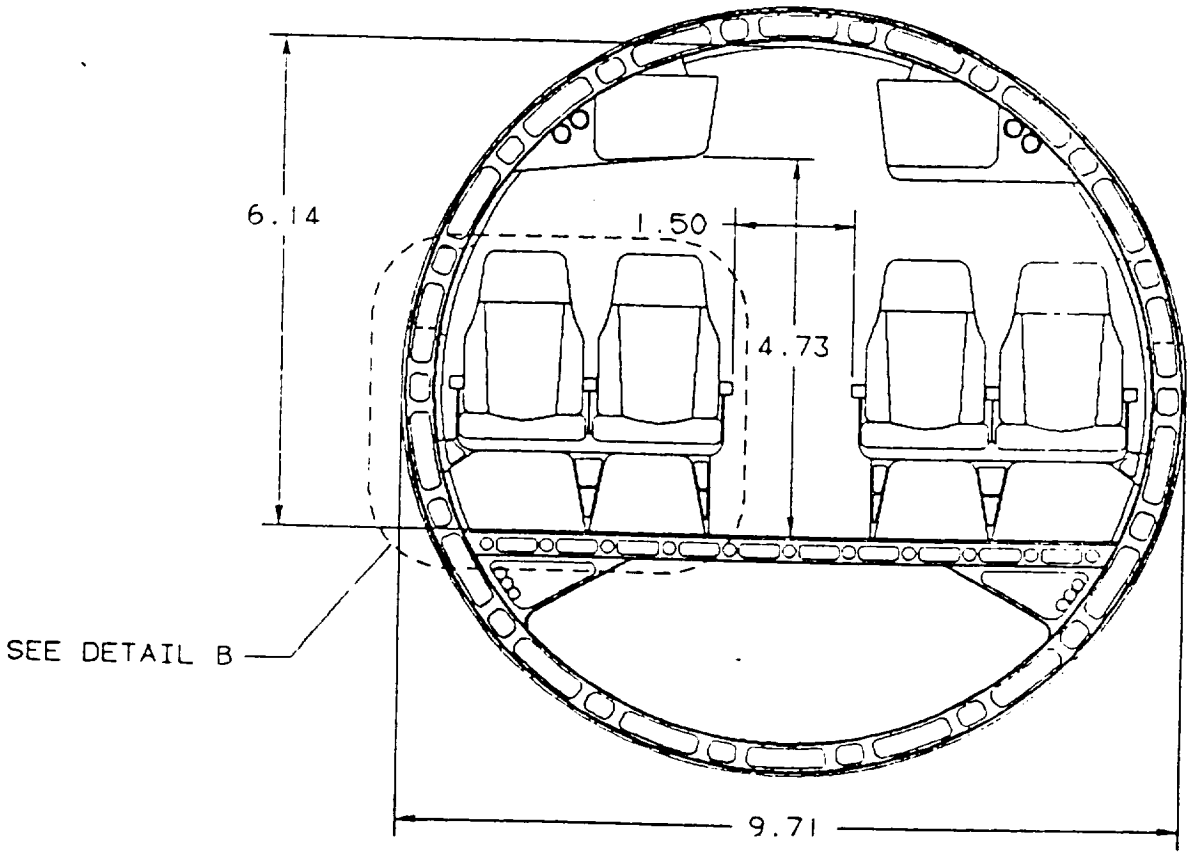

SECTION A-A

FIGURE 15a FUSELAGE CROSS SECTION

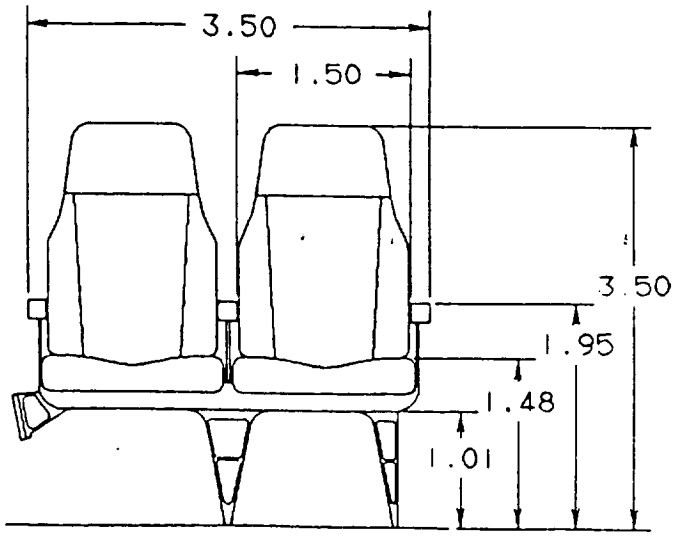

DETAIL B
SEAT ASSEMBLY

FIGURE 15b SEAT DIMENSIONS

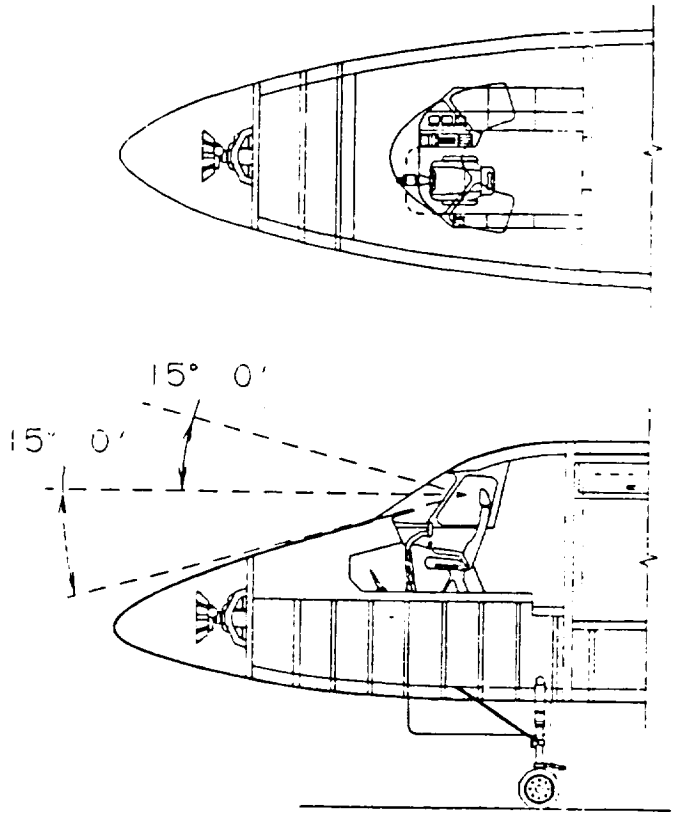

FIGURE 16 FLIGHT DECK ARRANGEMENT

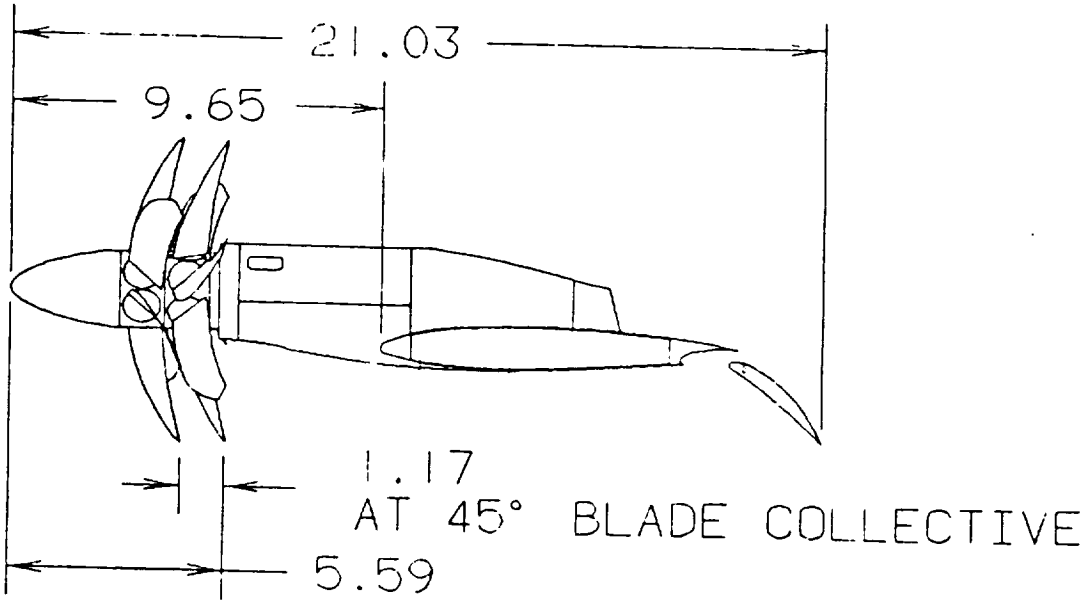

FIGURE 17 WING MOUNTED ENGINE

Structures

A preliminary structural analysis was performed on the wing. Velocity versus load diagrams for sea level and 20,000 feet were constructed. (see Figures 18a, 18b, 19a, 19b) Both maneuver and gust diagrams were constructed so that maximum loads could be obtained for the wing. Table XI shows the values obtained from the above figures.

After these maximum loads were obtained from the V-n diagrams, the total bending moment of the wing was calculated, assuming an elliptical lift distribution.

A structural layout of the wing is seen in Figure 20. This layout shows how the landing gear will retract into the fuselage. Fuel will be stored in the wings in between the main and rear spars. The structural layout was modeled by comparing other aircraft wing layouts.

The fuselage structural layout, seen in Figure 21, was also modeled after similar aircraft. The fuselage was selected to be circular for two reasons. First, the circular cross-section reduces the stress concentration when pressurizing the cabin. Secondly, a circular cross-section is easily manufactured.

TABLE XI STRUCTURAL ANALYSIS OF WING

MAXIMUM MANEUVERING LOAD FACTOR	+2.67
MAXIMUM MANEUVERING LOAD FACTOR	-1.00
FOR SEA LEVEL AND 20,000 FEET	
MAXIMUM GUST LOAD FACTOR	+3.42
MAXIMUM GUST LOAD FACTOR	-1.42
FOR SEA LEVEL	
MAXIMUM GUST LOAD FACTOR	+4.80
MAXIMUM GUST LOAD FACTOR	-2.80
FOR 20,000 FEET	

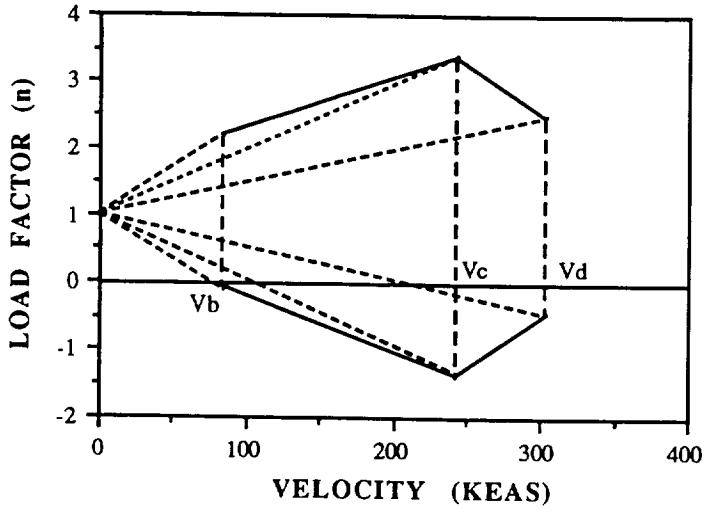

FIGURE 18a V-n GUST DIAGRAM AT SEA LEVEL

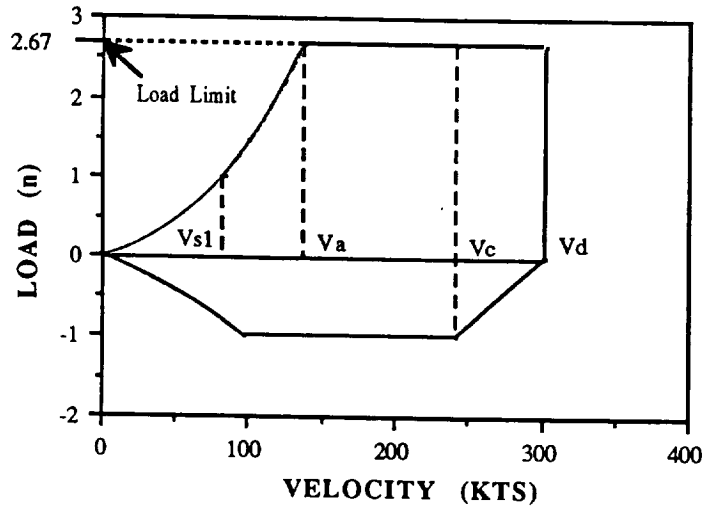

FIGURE 18b V-n MANEUVER DIAGRAM AT SEA LEVEL

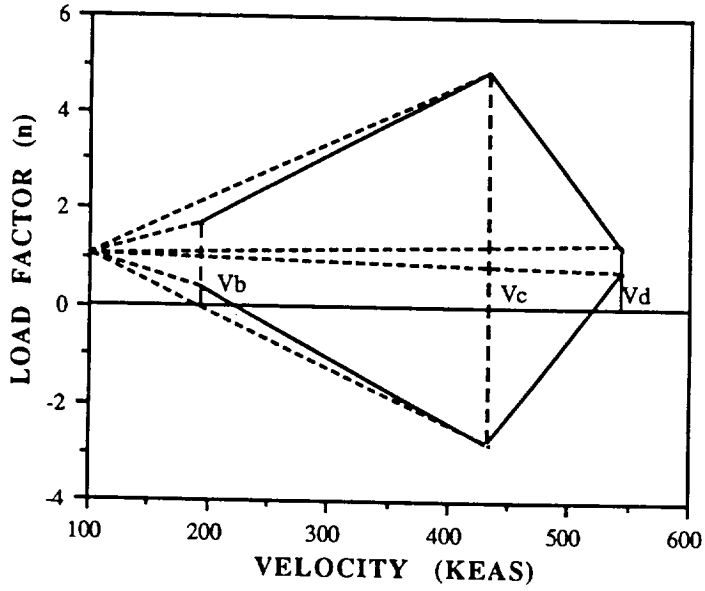

FIGURE 19a V-n GUST DIAGRAM AT 20,000 FEET

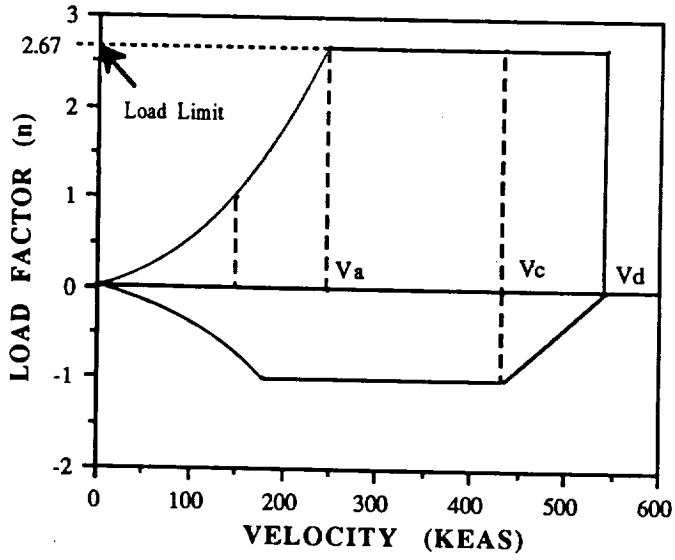

FIGURE 19b V-n MANUEVER DIAGRAM AT 20,000 FEET

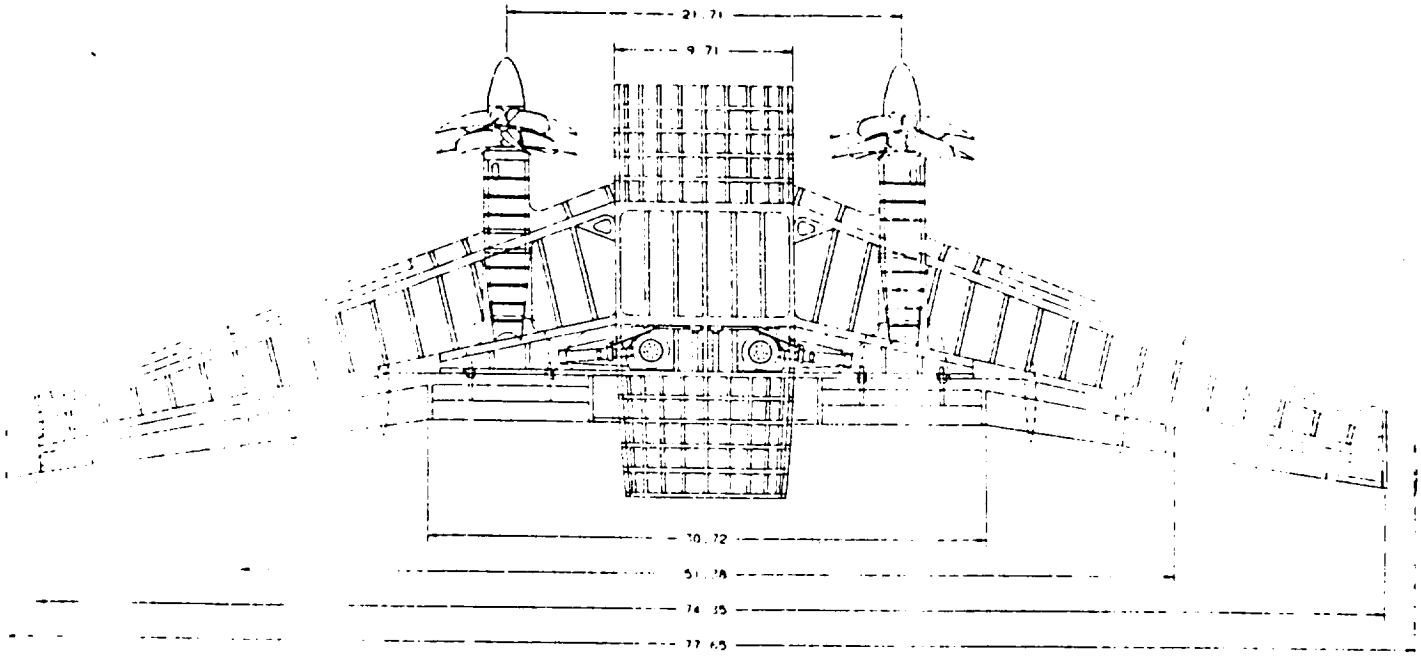

FIGURE 20 WING STRUCTURAL LAYOUT

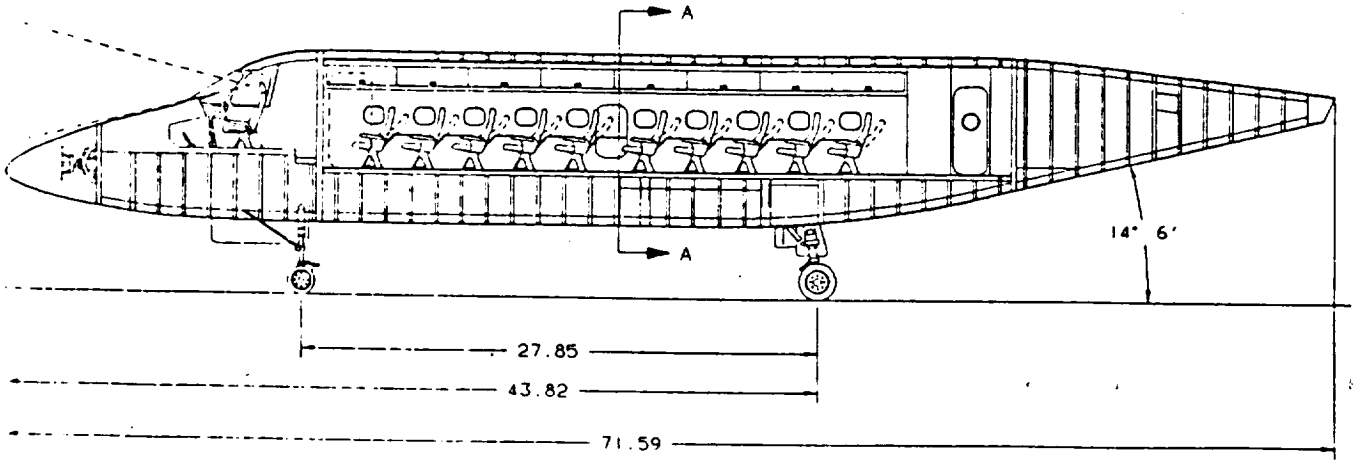

FIGURE 21 FUSELAGE STRUCTURAL LAYOUT

DESIGN METHODOLOGY

Sizing

Roskam's Airplane Design (Reference 1) was used throughout the sizing process. The fuel fraction method was used and a fuel weight was calculated. Then, weights were estimated for the payload and the crew. From this information, the empty weight and the take-off weight were calculated.

Next, Roskam's methods were employed in determining the wing loading and power loading requirements of the various mission components. The sizing calculations were performed for take-off, landing, climb, and cruise. The data revealed that cruise would be the deciding factor and so a power loading and wing loading were chosen to meet this requirement. This data was also used to determine the lift coefficients for the various mission components. A complete listing of the data is included in Tables A4, A5, A8, A9 and the matching of all the sizing requirements are shown below in Figure 22.

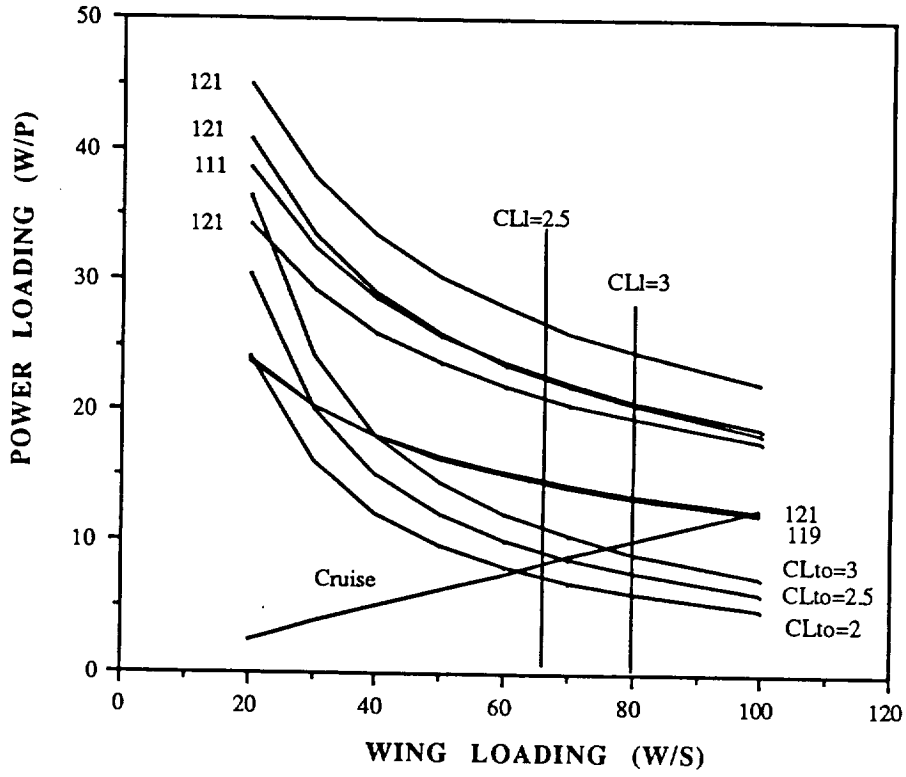

FIGURE 22 SIZING CURVES

Sensitivity

Immediately after completing the preliminary sizing, a sensitivity analysis was conducted in order to investigate possible modifications to the original mission requirements. The methods for determining these sensitivities were taken from Roskam's Airplane Design (Reference 1).

These studies revealed that a substantial savings in weight could be achieved by reducing the aircraft's range. The original range was cut almost in half to the current 600 nautical miles. These studies also revealed the importance of maintaining a high propeller efficiency. The results of these studies are included in Table XII.

TABLE XII SENSITIVITY RESULTS

Assumptions	
c_P=	0.52
n_P=	0.86
L/D=	13.0
R=	690 nm
dW_{TO}/dW_{PL}=	4.115
dW_{TO}/dR=	16.80
dW_{TO}/dc_P=	26014.8
dW_{TO}/dn_P=	-15729.0
$dW_{TO}/d(L/D)$=	-1040.6

Planform

The CC-38 planform, sized using Reference 2, was initially configured like similar regional turboprops. The wings were swept back 25 degrees at the quarter chord to increase the critical mach number. A taper ratio of .333 along with elliptical winglets was incorporated in the design to maximize Oswald's efficiency factor. The elliptical wing tip configuration is currently under extensive study at California Polytechnic State University, San Luis Obispo. The planform also consists of two sets of Fowler flaps. The inboard set, located aft of the propulsion system, is blown. A thin titanium sheet separates the hot engine exhaust from the composite wing sheeting. The second set of flaps are located outboard of the first directly beyond the Yehudi. (see Figure 8)

Airfoil and High Lift Sizing

The airfoil selected for the CC-38 was the supercritical GA(W)-1 (see Figure 23). Cruising at such a high speed while using a conventional airfoil of the same thickness, would produce wave drag due to compressibility effects. This airfoil also has high lift coefficients so that the high lift devices being used can be reduced in size. The thickness of this airfoil is approximately 17%, a little thick for the CC-38 , but the only information found on supercritical airfoils was for this airfoil. A thinner airfoil, approximately 13% thickness, would have been a better choice. The zero lift point on the GA(W)-1's lift curve slope is at -4.0 degrees. In cruise the CC-38 has a lift coefficient of approximately .224 which corresponds to an angle of attack of -2.5 degrees for the GA(W)-1. The wing is at a -2.0 degree incidence to counteract this zero lift coefficient condition. The penalty, however, is higher trim drag. A thinner airfoil would have been used, had the information been obtained in time for this analysis. If this airfoil had been used, the maximum lift coefficients would be less but the high lift devices and the blowing would have made up the difference in lift coefficients.

The wing has zero washout due to the lift curve slope. This does not seem to pose a problem as the elliptical winglets should reduce the stalling tendency of the wingtips.

Table 3, shows the maximum lift coefficients that the aircraft was sized to. These lift coefficients were obtained using the GA(W)-1 supercritical airfoil along with two single slotted Fowler Flaps(see Figure 8). The reason for two flaps is due to one flap will be blown by the propfan slipstream and jet exhaust and the other is simply by the freestream air. Together, these flaps were sized for the aircraft to meet the maximum lift coefficients. Although the inboard flap is being blown, the analysis did not take into account the change in maximum lifts coefficients due to the blowing. Because of this, the size of the flaps should be decreased due to this extra coefficient of lift. Figure 23, shows the change in the maximum lift coefficient for a fully blown flap, but this doesn't apply to the CC-38 which only uses approximately 15% of its thrust and the propeller's slipstream to blow the flaps. See appendix B for flap sizing analysis.

Empennage

The NACA 0009 airfoil was used on the empennage. This was chosen because of its low drag and thin shape. The GA(W)-1's stalling angle of attack is approximately 17 degrees, compared to 15 degrees for the NACA 0009. In aircraft like the CC-38, it was assumed that maneuvers exceeding any angle of attack greater than ten degrees can cause passenger discomfort, therefore the 2 degree difference in stalling angle of attack should not affect the aircraft's stalling tendency.

The empennage was sized and positioned according to Jan Roskam's Airplane Design (Reference 2). The first step was to decide the best configuration for the CC-38. It was decided that a T-tail configuration would be used. The main reason for choosing this tail configuration was to avoid tail buffeting which causes structural fatigue and cabin noise. Another major consideration was the decrease in downwash on the tail due to the T-tail being out of the wing's trailing vortices.

The distances from the center of gravity of the plane to the aerodynamic center of the horizontal and vertical tails were found by comparing these value on other aircraft. Extensive comparisons with the DeHavilland DHC-8 and DHC-7-102 were used since their size and mission specifications were most comparable to the CC-38. Similarly, horizontal and vertical tail volumes were also found through comparisons with the above aircraft. This lead directly to the calculation of the tail surface areas.

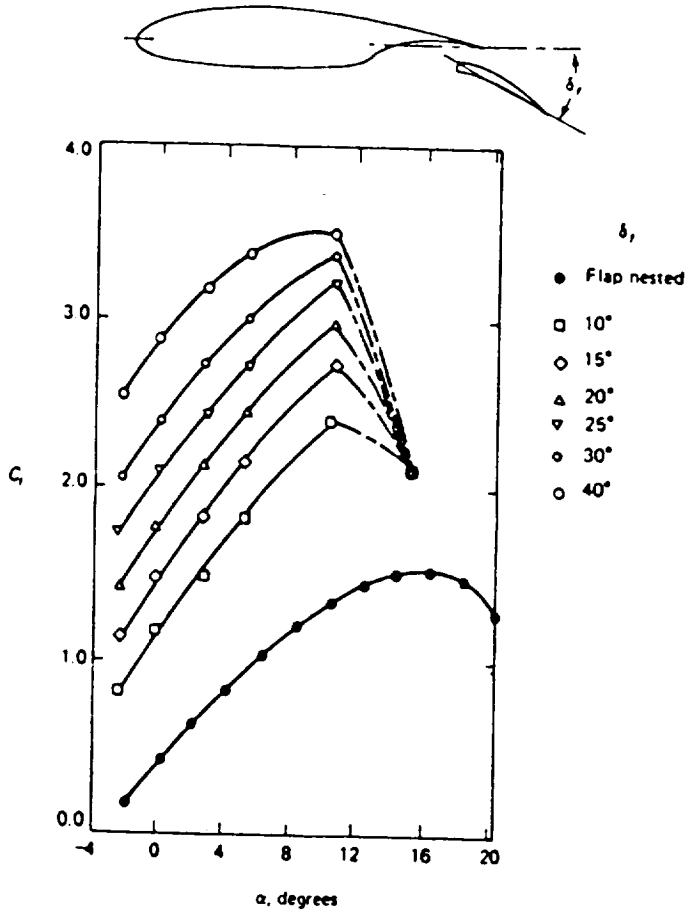

FIGURE 23 GA(W)-1 LIFT CURVE SLOPES (Reference11)

Drag Polar Estimation and Comparison

Initial drag polar estimation was conducted using Reference 1. See Appendix B for the sample calculations and the assumptions used. These values were very rough, and the CC-38 was compared to other regional turbopropeller aircraft in the analysis. The initial drag polars are shown in Table A6.

The parasite and induced drags were plotted against velocity at an altitude of 20,000 feet(Figure 5). The airplane has been designed to be as clean as possible so as to reduce any unnecessary parasite drag, but the CC-38 pays the penalty of a high parasite drag while cruising at 348 knots.

After estimating the drag polars by using comparable aircraft, a further investigation was made to calculate the parasite drag due to the actual dimensions of the CC-38. See Appendix B. The values of the parasite drag only varied by .96%, thus showing that our initial drag polars were very realistic. No further studies of the drag were needed.

Structural Analysis

The first step in the structural analysis was to construct the velocity versus load diagrams from Roskam's Airplane Design (Reference 2). Using FAR 25 parameters, specific load limits were found for stall speed, cruise speed, diving speed, maneuver speed, and design speed for maximum gust intensity. The Ourania, a jet transport used in Roskam's analysis, was compared and analyzed as an aid to attaining accurate load diagrams. Two types of diagrams were found.

First, the maneuver diagram was constructed. However, in order to complete this, the speed for maximum gust intensity was found using the gust line calculation. From there, the dive velocity was found. The curved part of the V-n diagram corresponding to the lower velocities was found using the definition of load factor n=L/W. A maximum normal force coefficient was found using an approximation of 1.1 $C_{L_{max}}$. This was used in the equation just mentioned. Second, the gust load factor diagram was constructed by using the gust line equations in Reference 4. The graphs were also adjusted for the cruise altitude of 20,000 ft.(See Figures 18a,b and 19a,b). Table 12 summarizes the maximum maneuver and gust load factors. This was done by using the density at that altitude and the corresponding gust velocities.

Finally, the total bending moment of the wing was found by applying the maximum load factor limit. Using the equation of an ellipse , an elliptical lift distribution was assumed for the wing. Integrating this and multiplying it by its incremental moment arm, the total bending moment about the center of the wing was found. This calculation was checked by a rough approximation of the lift acting at the midspan of the wing and was found to be of the same relative magnitude. See Figure 20 for the structural layout of the wing.

Fuselage Design

The cabin was primarily designed to meet the needs of the business executive. Its comfortable layout and extensive features are attractive to all business men and women alike. The CC-38, with its full size business class seating, is equipped with a color FAX machine, an automated teller machine, a complete stock updating system, and other helpful business aids.

The fuselage, seen in Figures 13 -15, was sized to accomodate the passengers comfort and needs. It was sized by locating four business class seats abreast with an 18 inch aisle along the center of the fuselage. Leg and head room calculations were then incorporated into the layout. The fuselage length was also driven by passenger comfort along with aerodynamics. The passenger cabin is 8.7 feet wide and 30 feet long.

Weight and Balance

It was necessary to do a preliminary determination of the center of gravity location to ensure that it was adequate for different loading scenarios. Roskam's Class I component weight estimation method was used (Reference 5) This method assumes that within aircraft categories, there are trends in component to takeoff weight fractions.

To determine what these fractions were, a comparison of similar aircraft and their weight fractions was made and the data correlated(Table A11). Average values were used for most fractions, but where specifics were known, actual fractions were calculated and the others adjusted. See Table XIII for the fractions used.

TABLE XIII COMPONENT WEIGHT ESTIMATION

	%GW	COMPONENT WEIGHT ALUM	COMP(6%)
WING	0.106	3,415.53	3,210.60
EMPENAGE	0.03	966.66	908.66
FUESELAGE	0.114	3,673.31	3,452.91
NACELLE	0.032	1,031.10	1,031.10
LANDING GEAR	0.034	1,095.55	1,095.55
POWER PLANT	0.120	3,866.64	3,866.64
FIXED EQUIPMENT	0.1579	5,087.85	5,087.85
EMPTY WEIGHT		19,136.64	18,653.31

The initial weight estimates used aluminum as the primary structure but it was assumed that by the 21st Century, the use of composites in commuter aircraft would be common. In a study done by

Boeing Aircraft (Reference 13), it was predicted that by the mid 1990's, the cost to produce a graphite-epoxy wing structure would be less than that of an aluminum wing. For the CC-38, a 6% weight reduction in the wing, empennage, and fuselage was assumed giving a 483.33 lb decrease in total weight and a final gross takeoff weight of 31,741.8 lbs.

With the weight of the different components having been calculated, a C.G. Excursion diagram was made. The nose was chosen as the datum, and the distances seen on Figure 24 are those distances as measured from the nose of the aircraft.

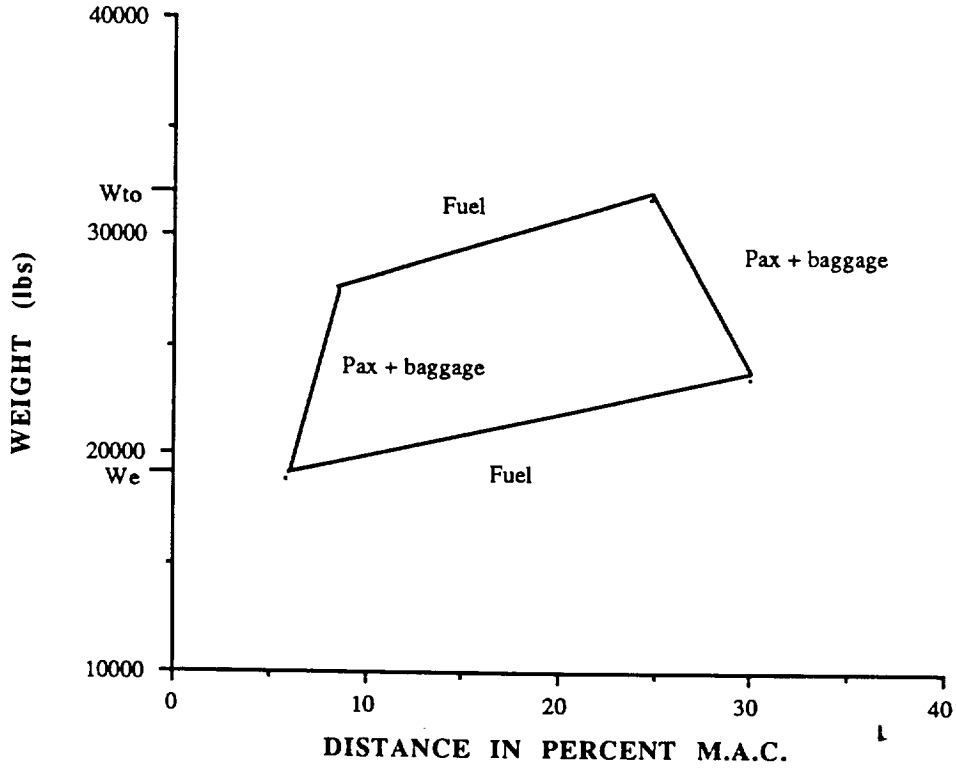

FIGURE 24 C.G. EXCURSION DIAGRAM

Stability

A static stability analysis was conducted on the CC-38's final configuration. This analysis included a horizontal tail longitudinal analysis, a vertical tail side force analysis, and a rudder deflection analysis for the one engine out condition. The results of this stability analysis are shown in Figures 25 and 26.

Appropriate adjustments were made to the horizontal and vertical stabilizer sizes using the results of this analysis. The CC-38's conventional configuration posed no serious stability problems. All initial sizes were determined from a comparison with similar aircraft. These sizes provided very favorable results and no major modifications were necessary.

Propulsion

Upon sizing the aircraft to the FAR 25 requirements, the power for the aircraft was determined to depend on the cruise velocity. Having chosen a wing loading of 50 lb/ft^2 by comparison with other aircraft, the power required in cruise was determined to be 4489.4 Hp. Therefore at 75% power, the engine would need to produce at least 4489.4 Hp. The engine chosen was the Allison Model 501-M78 Axial flow turboprop engine. At an altitude of 20,000 feet the 501-M78 produces 5184.4 Hp at 75% of its maximum continuous power. See Table 4 for the engine's performance. It was decided that two engines would be used for safety in case one engine failed. The engine's performance and weight can be expected to improve with technology. For this analysis it was assumed that the specific fuel consumption rates would remain the same, however these can also be expected to improve in the future.

It was decided that the engines would be placed on the wing (see Figure 17). Wing mounted engines have the advantages of decreasing the wing's bending moments in flight, reducing the vibrations as compared to a fuselage mounted engine, and facilitating maintenance. With these wing mounted engines, the flaps directly behind them could be blown, thus increasing the lift coefficients.

After reviewing the counter-rotating propfan's efficiencies, it was decided that a tractor configuration would be best. This has been studied by Hamilton Standard. A counter-rotating gear box is needed with this engine, and one has been built. The size of this gear box is expected to be a little larger than that found on the 501-M78. With technology, it was assumed that this gear box would be the same size and weight in the future as the one currently used on the 501-M78.

Counter-Rotating Propfans

The CC-38 uses couter-rotating propfans as part of its propulsive system. The high power requirements made it necessary to optimize the efficiency of the propellers. The efficiencies are much

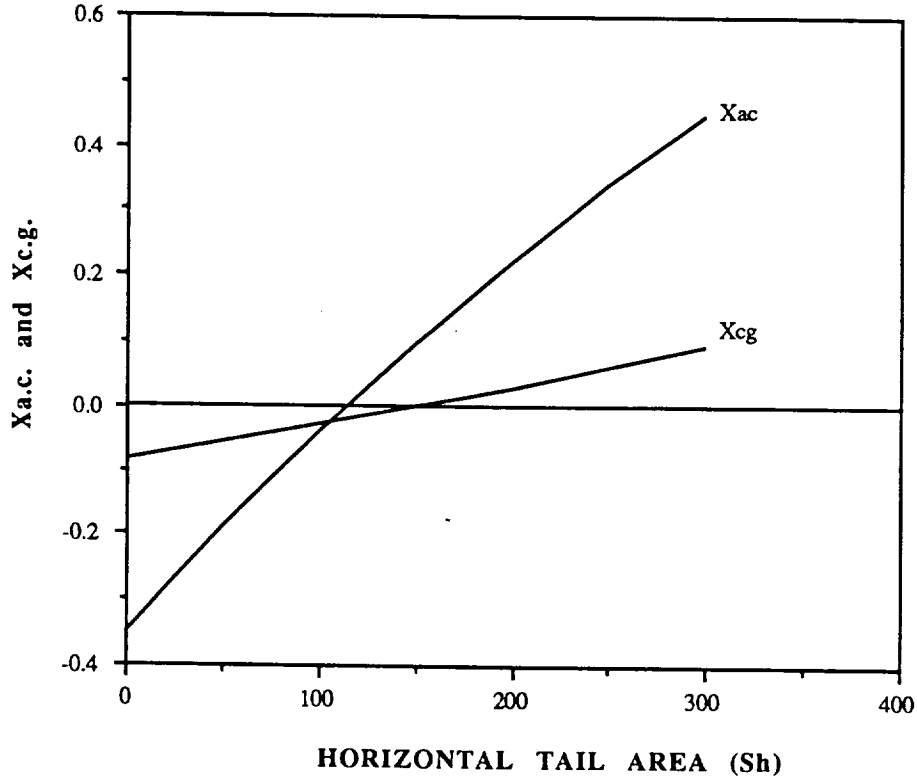

FIGURE 25 LONGITUDINAL X-PLOT

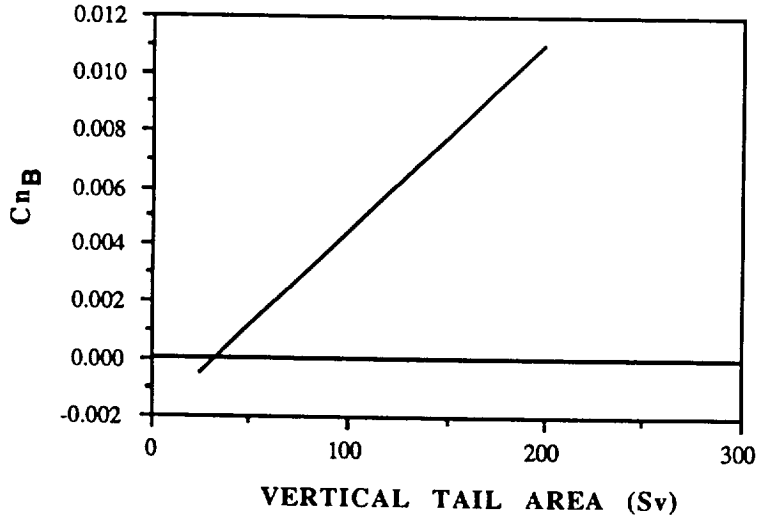

FIGURE 26 DIRECTIONAL X-PLOT

greater for counter-rotating propfans than for single rotation propfans or turbofans (see Figures 27 - 29). The blades were chosen in accordance with a report by Hamilton Standard(Reference 10). The report outlined a comparison of several blades with different taper ratios, twists and sweeps. The CR-1 propeller blade was chosen(Figure 30). These blades have been tested up to Mach .8 and up to 35,000 feet. With these propellers able to operate at such high speeds with almost 90% efficiency makes them the best choice for the CC-38.

The propeller diameter was calculated to be 9.2 feet due to the disk loading that would produce the best efficiency. With the shaft-horsepower known from the engines chosen above and the optimum disk loading of approximately 50 HP/ D^2 from Figure 29, the propeller diameter was calculated. It was dicided that a total of 12 blades would be used per engine(6 blades rotating one way and 6 in the opposite direction). Hamilton Standard has done testing with this many blades and has encountered no problems.

One question that arose is the noise problem with these counter-rotating propfans. As can be seen in Figure 32, these propfans meet the current FAR noise requirements. Even with the lowering of these FAR requirements, the propfans behave much like that of conventional propellers as far as noise is considered. The noise in the cabin will be cut down with insulation. Further noise study tests are being conducted to determine how loud these propfans actually are in the cabin. This is not expected to be a problem.

The flow behind these counter-rotating propfans will be more uniform than the flow behind a single rotation propeller, due to the second propfan rotating in the opposite direction. With this more uniform flow, it is expected that the blowing of the flaps will produce higher lift coefficients than that with single rotation. With the engines mentioned above, it is expected that at least 85% of the total thrust will be produced by the propfans, leaving 15% of the thrust and the propfan's slipstream to blow the flaps.

Landing Gear

The CC-38 is equipped with retractable tricycle landing gear. The nose gear is supported from the forward fuselage bulkhead while the main gear is attached to the aft spar of the wing torque box and the landing gear support beam. The gear was sized using Reference 2. Each of the two main gear struts ride on two Goodyear 26 x 6.6 tires while the nose gear struts rest on two Goodyear 14.5 x 5.5 tires.

Avionics

The on-board avionics to be incorporated in the CC-38 are currently in production and use. The pilot's main role in the airplane is to monitor the instruments and the computer. A full set of

instruments and controls will be available to the pilot in case the computer has a malfunction. Backup systems will also be incorporated into the system. The flight instruments for the pilot will be digital with as few displays as needed. The workload for the pilot, in case of a malfunction, must be minimal since only one person is in the cockpit.

The principle operators of the aircraft will be the Flight Management Computer System (FCMS), and the Digital Air Data Computer (DADC). An Inertial Reference System (IRS) will provide position, velocity, and attitude information to the flight deck displays, FCMS, and DADC. From the IRS the FMCS can provide automatic en-route and terminal navigation and also compute and command both lateral and vertical flight profiles for optimum fuel efficiency maximized by electronic linkage of the FMCS with the automatic flight contol and thrust management systems (Reference 8). Fully automated flights using the above equipment, and the ground support avionics, have been conducted and are currently installed onboard Boeing's 757 and 767 aircraft. With this type of system aboard, and a system on the ground to handle it, the workload of the pilot and of the air traffic controllers should be greatly relieved.

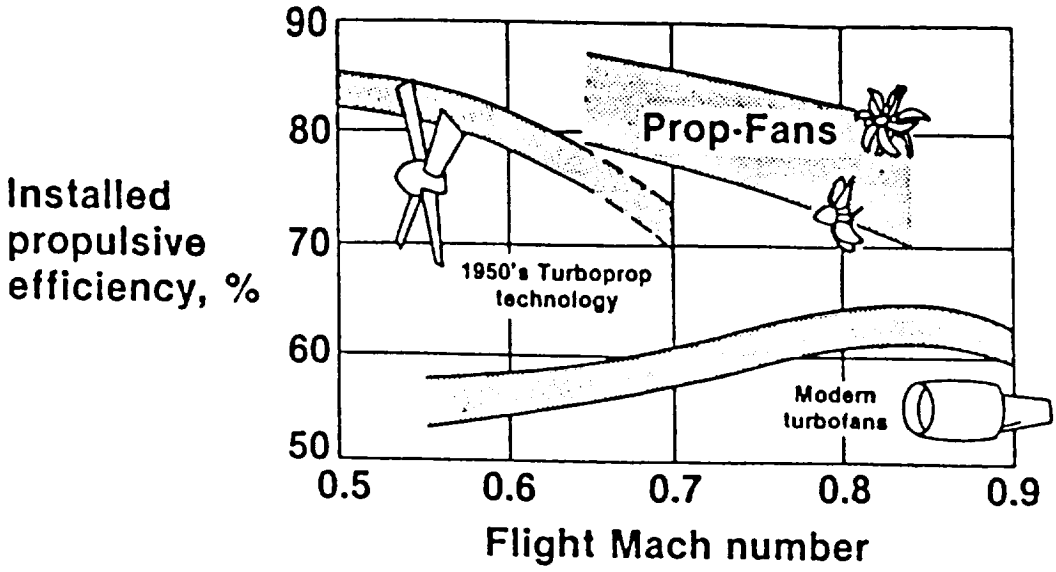

FIGURE 27 INSTALLED EFFICIENCY(Reference 10)

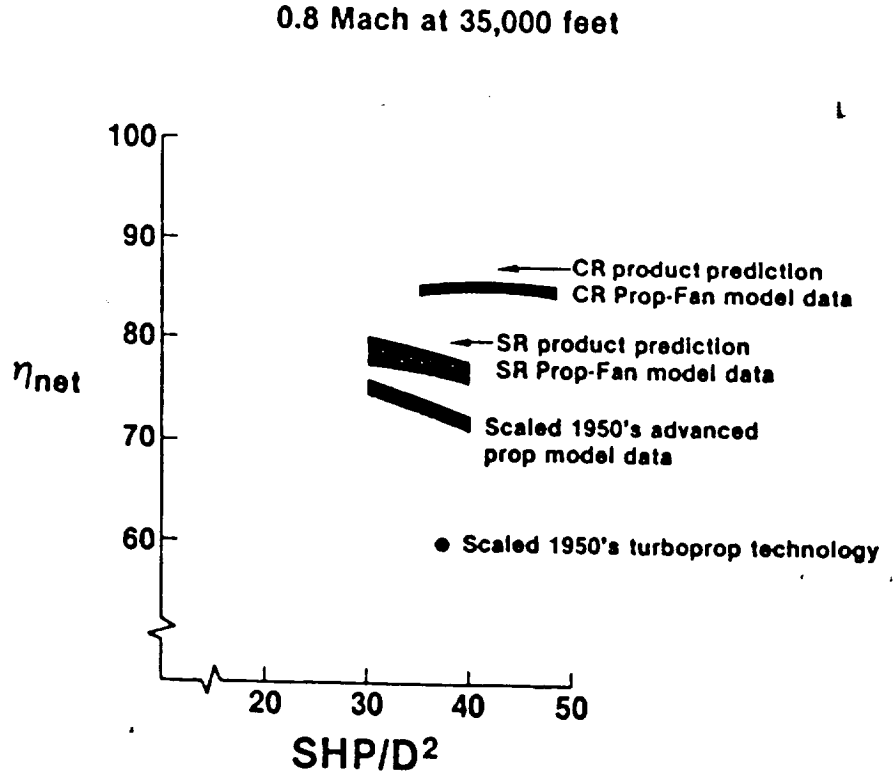

FIGURE 28 PROP-FAN CRUISE EFFICIENCIES(Reference 10)

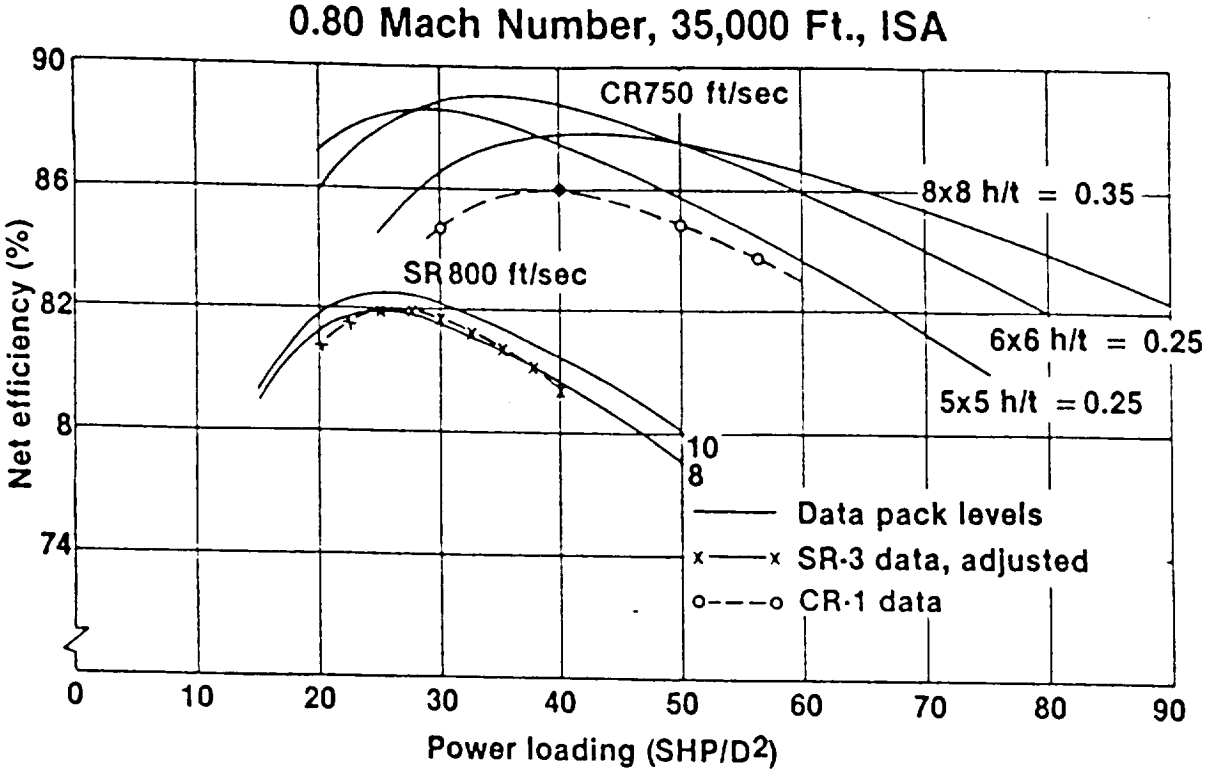

FIGURE 29 EFFICIENCY VS. POWER LOADING(Reference 10)

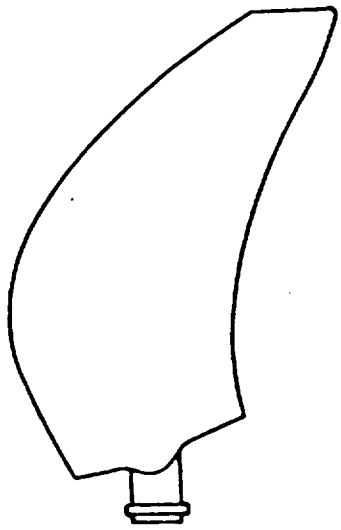

CR-1

FIGURE 30 BLADE SHAPE (Reference 10)

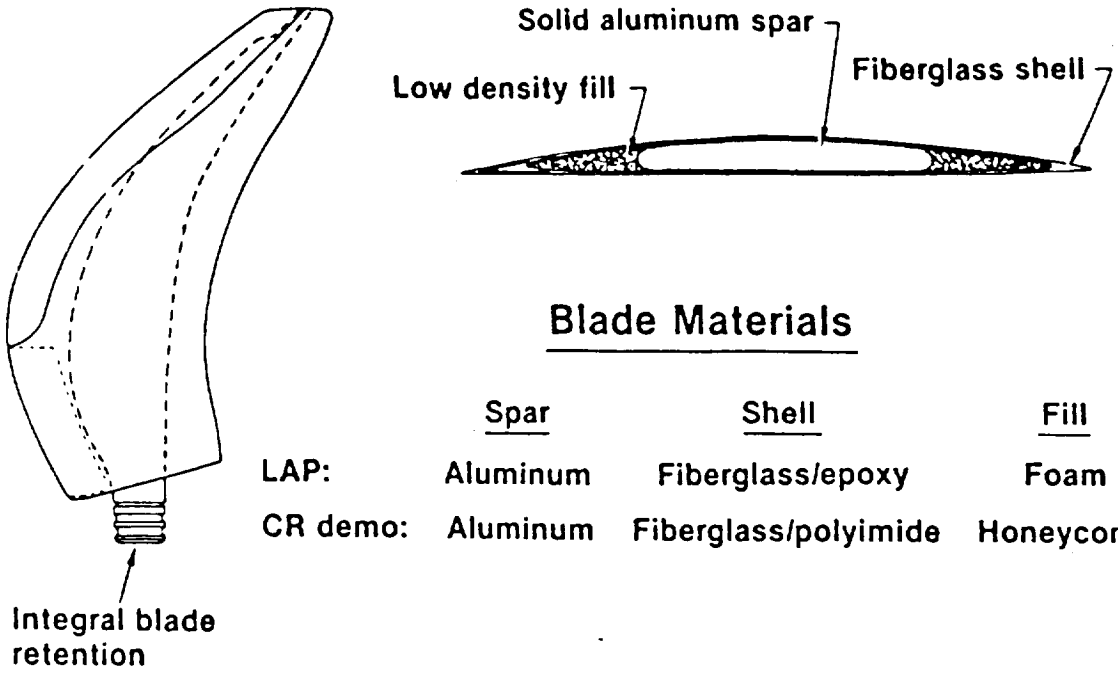

FIGURE 31 BLADE CONSTRUCTION (Reference 10)

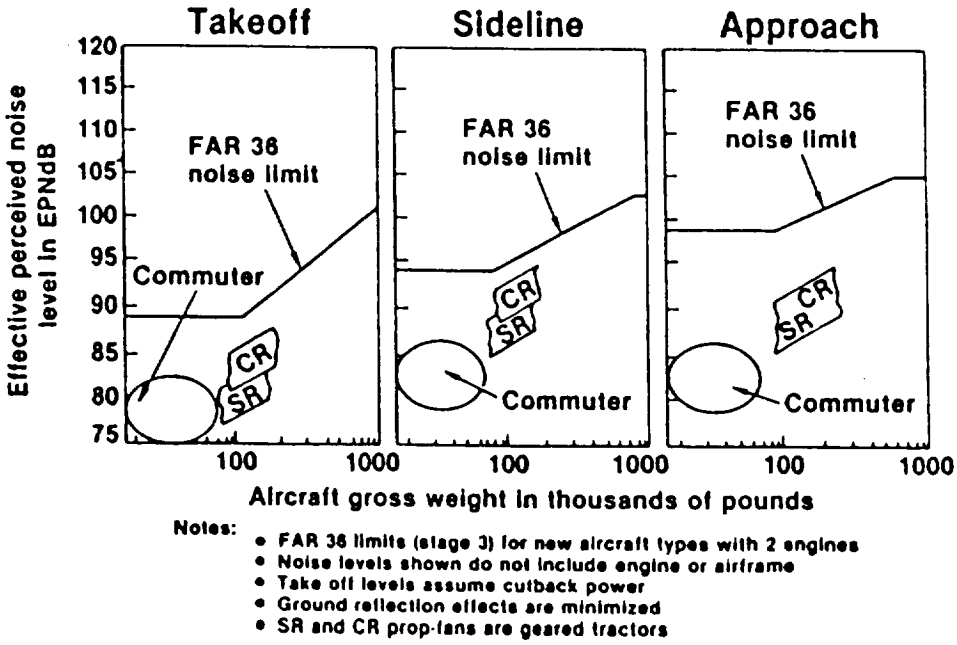

FIGURE 32 NOISE LEVELS (Reference 10)

By the year 2010, the cost and size of this equipment should decrease so that a system like this is feasible to install in commuter aircraft as well as in the larger passenger transports.

Direct Operating Cost

The direct operating cost (DOC) of the CC-38 was conducted using Corning's method(Reference 9). The analysis used by Corning is that for 1975 dollars (Reference 9). With this in mind, the direct operating cost was computed using today's current costs for fuel, maintenance, and crew. See Appendix B for the sample calculations.

Table XIV, below, shows the breakdown of the parts to the final DOC.

TABLE XIV DIRECT OPERATING COST

COMPONENT	COST	
FLYING OPERATING COST	0.2915	$/mile*ton
DIRECT MAINTENANCE	0.0422	$/mile*ton
DEPRECIATION	0.0917	$/mile*ton
TOTAL	0.4254	$/mile*ton

The total DOC for the CC-38 was .4254 $/Mile*Ton relating to a .1025 $/Passenger Mile. Assuming that since 1975 that the prices of airfares have quadrupled, the price for a passenger to fly on the CC-38 from San Diego to Sacramento would be approximately $120.23 in 1989 dollars. It has been estimated that the price of a new CC-38 would be approximately 15-20 million dollars.

CONCLUSIONS

The California Condor, designed to operate within the California Corridor in the year 2010, has tremendous advantages using today's and tomorrow's technologies.

The counter-rotating propfans, with their CR-1 blades, significantly increase efficiency in all phases of flight. At the same time, these propfans are capable of cruising at flight velocities not attainable with conventional propellers. 21st Century technology should provide lighter engines, that can produce higher horsepowers to run these propfans up near Mach .8.

The use of composites in the CC-38 have helped to reduce the weight, increase the performance and therefore conserve fuel. With the extensive use of composites in the aircraft industry, the cost of incorporating composites into aircraft designs should decrease in years to come.

Passenger conveniences, such as larger, more comfortable seats, air to air and air to ground communication, color FAX machines, and an Automated Teller Machine, will give tomorrow's passengers riding on the CC-38 an office in the sky.

The CC-38, with its improved efficiencies, higher speeds, and passenger conveniences, is sure to help alleviate some of the problems arising in the California Corridor in the year 2010.

Recommendations for further study

The California Condor should be given a more extensive analysis in the following areas:

1. Dynamic Stability and Control
2. Structural Design and Configuration
3. Composite Implementation
4. Flight Contol System (Fully Automated)
5. Propfan Noise Limitations and Commercial Usage
6. High Lift Devices with Blowing
7. Elliptical Winglet Configuration
8. Fuels
9. Human Factors

REFERENCES

1. Roskam, J., Airplane Design: Part I. Preliminary Sizing of Airplanes. Roskam Aviation and Engineering Corporation, 1985.

2. Roskam, J., Airplane Design: Part II.Preliminary Configuration Design and Integration of the propulsive system., Roskam Aviation and Engineering Corporation , 1985.

3. Roskam, J., Airplane Design: Part III. Layout. Design of the Cockpit. Fuselage. Wing and Empennage: Cutaways and Inboard Profiles. Roskam Aviation and Engineering Corporation,1985.

4. Roskam,J. , Airplane Design: Part IV. Layout Design for Landing Gear and Systems Roskam Aviation and Engineering Corporation, 1985.

5. Roskam, J., Airplane Design: Part V. preliminary Calculation of Aerodynamic. Thrust.and Power Characteristics, Roskam Aviation and Engineering Corporation, 1985.

6. Roskam,J., Airplane Design: Part VI. Determination of Stability. Control. and Performance Characteristics: FAR and Military Requirements, Roskam Aviation and Engineering Corporation, 1985.

7. U.S. Department of Transportation, Federal Aviation Administration, FAA Aviation Forecasts Fiscal Years 1988-1999, FAA-APO 88-1, February 1988.

8. Taylor, J.W., Jane's All the World's Aircraft '86-'87, Janes Publishing Company, 1986-1987.

9. Corning, G., Supersonic and Subsonic. CTOL and VTOL Airplane Design, 4th Edition, 1986.

10. Gatzen, B.S., Propfan Potential and Technology Readiness, Hamilton Standard Report, 1988.

11. Bertin and Smith, Aerodynamics for Engineers, Prentice-Hall Inc., 1989.

12. Anderson, John D. Jr., Introduction to Flight, McGraw Hill Book Company, 1985.

13. Clay, C.W., Technology for the 1990 Airliner, Boeing Commercial Airplane Company, 12-86.

$CASH$

California Sky-Hopper

STOL Transport For 2010

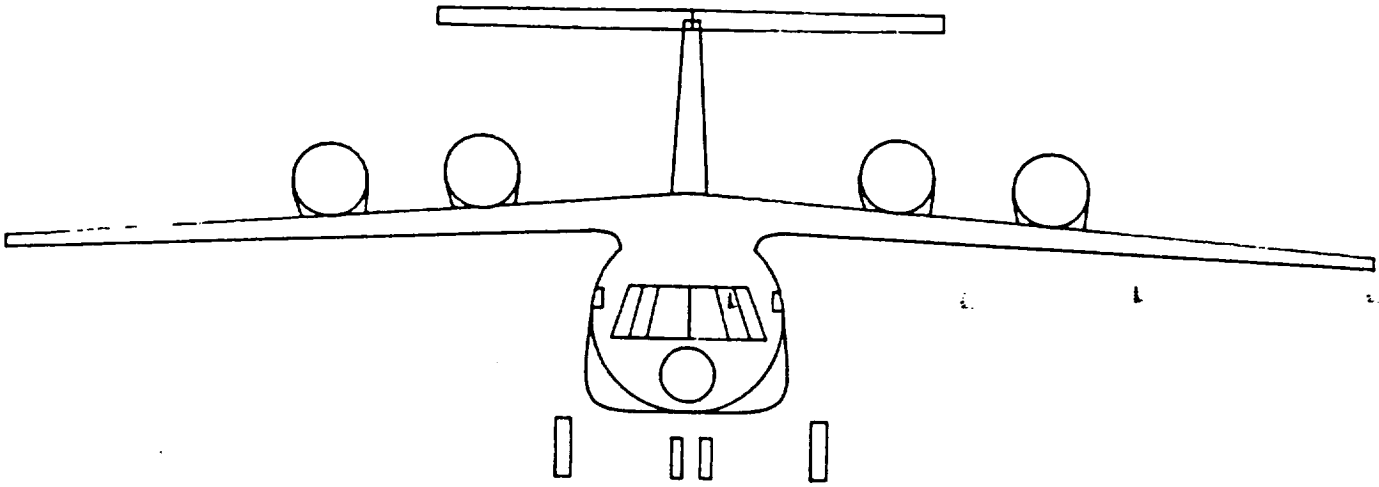

Designed By:

Michael Gorman

Dokyum Kim

Stephen Chiu

Chi Hieu Cao Tran

California Polytechnic State University
Aeronautical Engineering Department
Aero. Design Class 1989

Abstract

This report suggests a partial solution for the air transportation in the California Corridor by the year 2010. After reviewing corridor studies, the **California Sky-Hopper** (CASH) has been designed for short haul regional flights. The CASH is designed to operate on STOL ports at the existing international airports. CASH has a conventional two surface configuration that uses upper surface blown(USB) powered lift technology. The USB technology allows CASH to operate out of fields as short as 2,500 ft. CASH carries 40 passengers and luggage, for the range of 500 nm or two 250 nm hops without refueling.

Table of Contents

List of Tables

List of Figures

List of Symbols

AEO	All Engines Operative
C_d	Drag Coefficient
C_{di}	Induced Drag Coefficient
C_{do}	Parasite Drag Coefficient
C_f	Skin Friction Coefficient
C_j	Specific Fuel Consumption
C_l	Lift Coefficient
C_{lac}	Variation of Lift Coefficient at Canard
C_{lah}	Variation of Lift Coefficient at Horizontal Tail
C_{lav}	Variation of Lift Coefficient of Vertical Tail
C_{lawb}	Variation of Lift Coefficient of Wing and Body
$C_{n\beta}$	Variation of Yawing Moment Coefficient with Sideslip angle
$C_{n\beta b}$	Variation of Yawing Moment Coefficient with Sideslip angle by Body
$C_{n\beta w}$	Variation of Yawing Moment Coefficient with Sideslip angle by wing
$C_{n\beta wb}$	Variation of Yawing Moment Coefficient with Sideslip angle by Wing and Body
C_r	Root Chord
C_t	Tip Chord
C_{lcr}	Cruise Lift Coefficient

CGR	Climb Gradient
c	Mean Aerodynamic Chord
D_p	Parasite Drag Parameter
D_i	Induced Drag Parameter
dC_m / dC_l	Static Margin
dw / dx	Downwash Gradient
E	Endurance
e	Wing Efficiency Factor
F.S.	Front spar
f	Equivalent Parasite Drag
H	Altitude
H_{abs}	Absolute Ceiling
H_{cr}	Cruise Altitude
$H_{service}$	Service Ceiling
L/D	Lift-to-Drag Ration
M	Bending Moment (ft-lb)
M_{ff}	Mission Fuel Fraction
M_{tfo}	Trapped Fuel Fraction
ΔM	Moment increment (ft-lb)
OEI	One Engine Inoperative
QSRA	Quiet Short Haul Research Aircraft
R	Range

R.S.	Rear Spar
Rho_{ser}	Density at Service Ceiling
RC_o	Rate of Climb at Sea Level
S	Wing Area
STOL	Short Takeoff And Landing
S_c	Area of Canard
S_e	Elevator Area
S_H	Horizontal Tail Area
S_R	Rudder Area
S_V	Vertical Tail Area
S_{wet}	Wetted Area
T/W	Thrust-to-Weight Ratio
TOFL	Takeoff Field Length
t/c	Thickness Ratio
V	True Airspeed
V_a	Approach Speed
V_H	Horizontal Tail Volume Coefficient
V_{sl}	Stall Speed
V_v	Vertical Tail Volume Coefficient
v	Shear (lb)
Δv	Shear increment (lb)
W_e	Empty Weight

W_{pl}	Payload Weight
W_{to}	Takeoff Weight
W/S	Wing Loading
$(W/S)_l$	Wing Loading at Landing
$(W/S)_{to}$	Wing Loading at Takeoff
w	Load Intensity (lb/ft)
$X_{a.c.}$	Location of Aerodynamic Center
X_{ach}	Location of Aerodynamic Center of Horizontal Tail
X_{acwh}	Location of Aerodynamic Center with Wing and Body
$X_{c.g.}$	Location of Center of Gravity
X_v	Distance between Aft C.G. and Aerodynamic Center of Vertical Tail
y	Distance From Center Line of Wing (ft)
Δy	Distance Between Wing Station (ft)
Λ	Sweep Angle
Λ_H	Horizontal Tail Sweep Angle
Λ_V	Vertical Tail Sweep Angle
λ	Taper Ratio

Aircraft Mission

The California Corridor is defined as the air traffic between San Diego and San Francisco. This traffic is expected to increase significantly by the year 2010 such that our current transportation system will be insufficient to handle the increased traffic volume.

Our aircraft mission concentrates on providing flights from rural areas or small cities to the two international airports, Los Angeles and San Francisco. **Fig. 1** shows two possible mission profiles. The top profile has a two legged hop. This schedule allows a small regional airline to fly into Los Angeles or San Francisco without refueling. And it also permits fast turn around times and minimizes operational costs. The bottom profile shows a one legged hop. For longer ranged flights, this schedule adds flexibility in selling CASH.

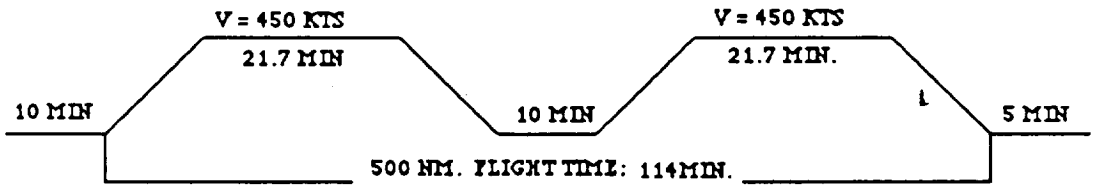

PROFILE A

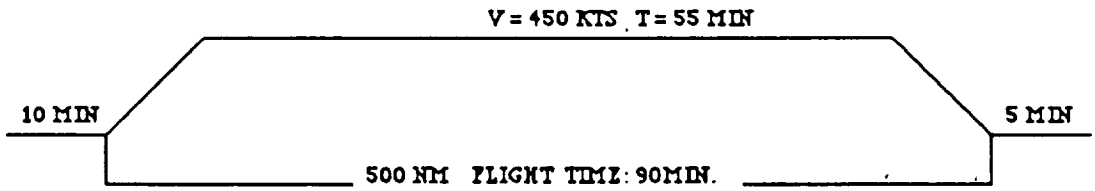

PROFILE B

Figure 1 Mission Profile

The primary purpose of our aircraft mission is to fly short range connecting and commuting flights into the two major airports without adding congestion to the already overcrowded airspace. This can be achieved by installing small short takeoff and landing runways (STOL ports) at the existing

international airports. Fig. 2 is a conceptual Drawing of such a port. A STOL port will have a much smaller traffic pattern, which will not interfere with the larger transports. A microwave landing system, currently being developed, will allow for short non-straight-in approach paths during poor weather. An aircraft that operates at much slower speeds than conventional aircraft would be able to accommodate this tight pattern. Since the speeds are slower, aircraft separation can be lowered without compromising safety.

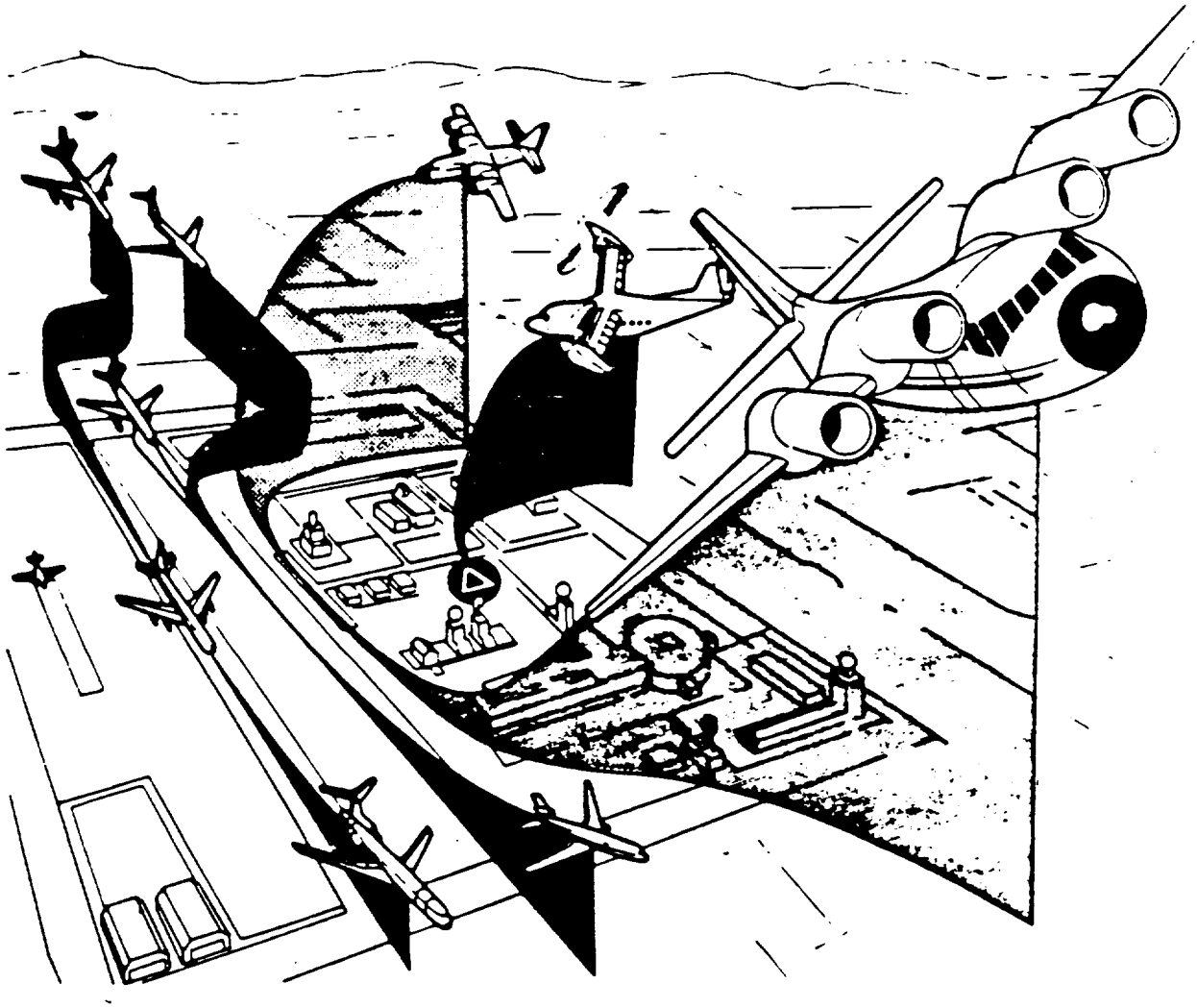

Figure 2 Expanded Airport Operations

Mission Specifications

Table I provides the specifications required to satisfy the needs for flight into STOL ports.

Table I Mission Specifications

Passenger:	40
Crew:	2
Range:	500 NM.
Speed:	450 Knots
Altitude:	25,000 ft.
Field Length:	2,500 ft.

In selecting the number of passengers, two factors were considered. The first factor deals with the shift in regional and commuter air travel. Each year more people chose flying over other methods of transportation for short trip lengths. Based on FAA forecasts from **Ref. 1**, demand for higher capacity short range regionals is steadily increasing. **Fig. 3** demonstrates this in bar graph form. In 1987, the 15 to 19 passenger aircraft was the most demanded aircraft. By the year 2010, this demand is expected to shift to the 20 to 60 passenger range.

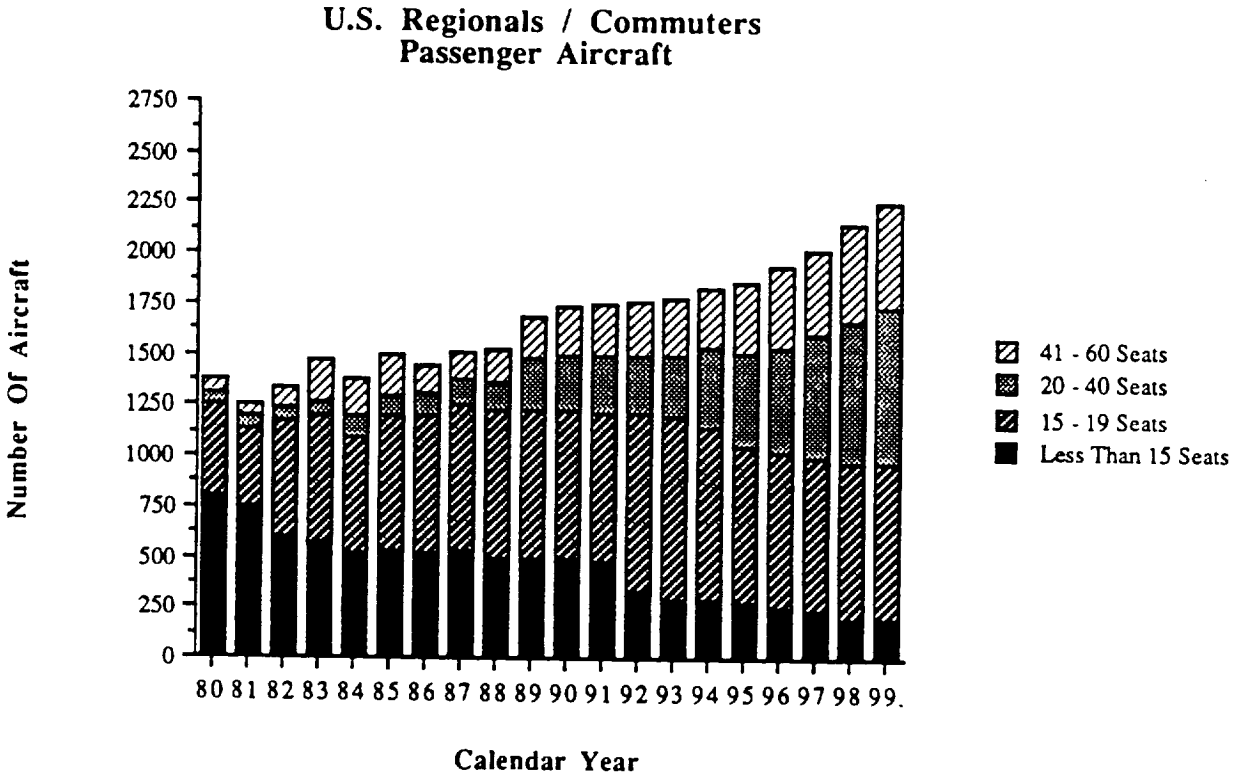

Figure 3 Aircraft Seat Size Demand

The second factor deals with flight frequency. In order to prevent long lay-overs at the international airports, a small regional airline will have to provide more than one flight per day. It is necessary to have a smaller passenger aircraft in order to maintain a full load. In viewing both factors, 40 passengers were selected as a reasonable size for CASH.

The **California Sky-hopper** will have an advanced computer controlled flight system. This system will only require one pilot to monitor flight progress. In order to assure safety, a copilot is required. The copilot will have two tasks. The first is to monitor systems during critical flight conditions (landing and takeoff). His/hers second task is to serve passengers during cruise.

Based on the size of California and the distance between Los Angeles and San Francisco a total range of 500 nm was selected . **Fig. 4** demonstrates that if 250 nm radius circles are plotted about Los Angeles and San Francisco International airports respectively, all of the major areas of California are covered. This range map shows that any regional airline within these limits can provide round trip flights to the international airports without refueling.

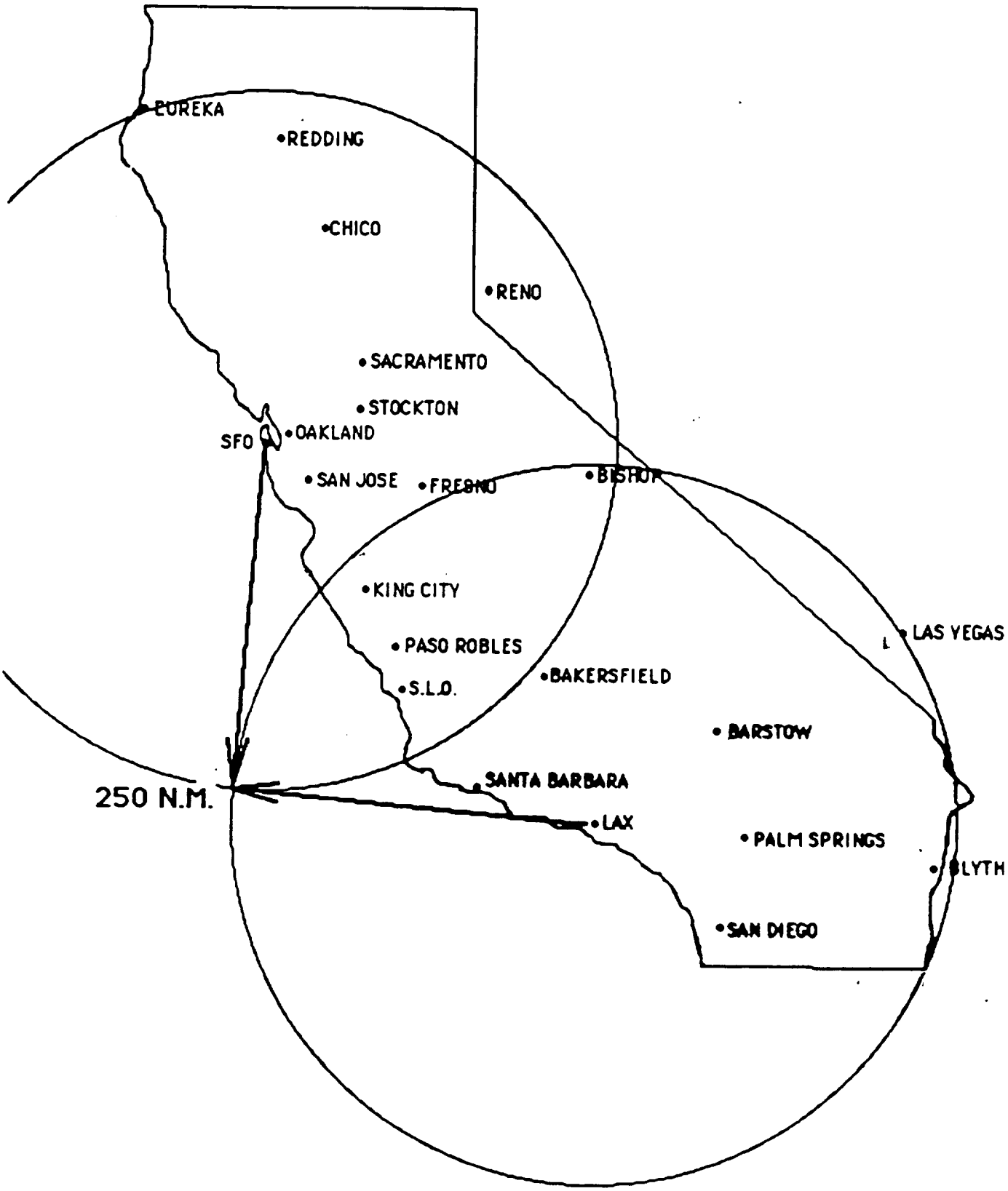

Figure 4 California Sky-hopper Map

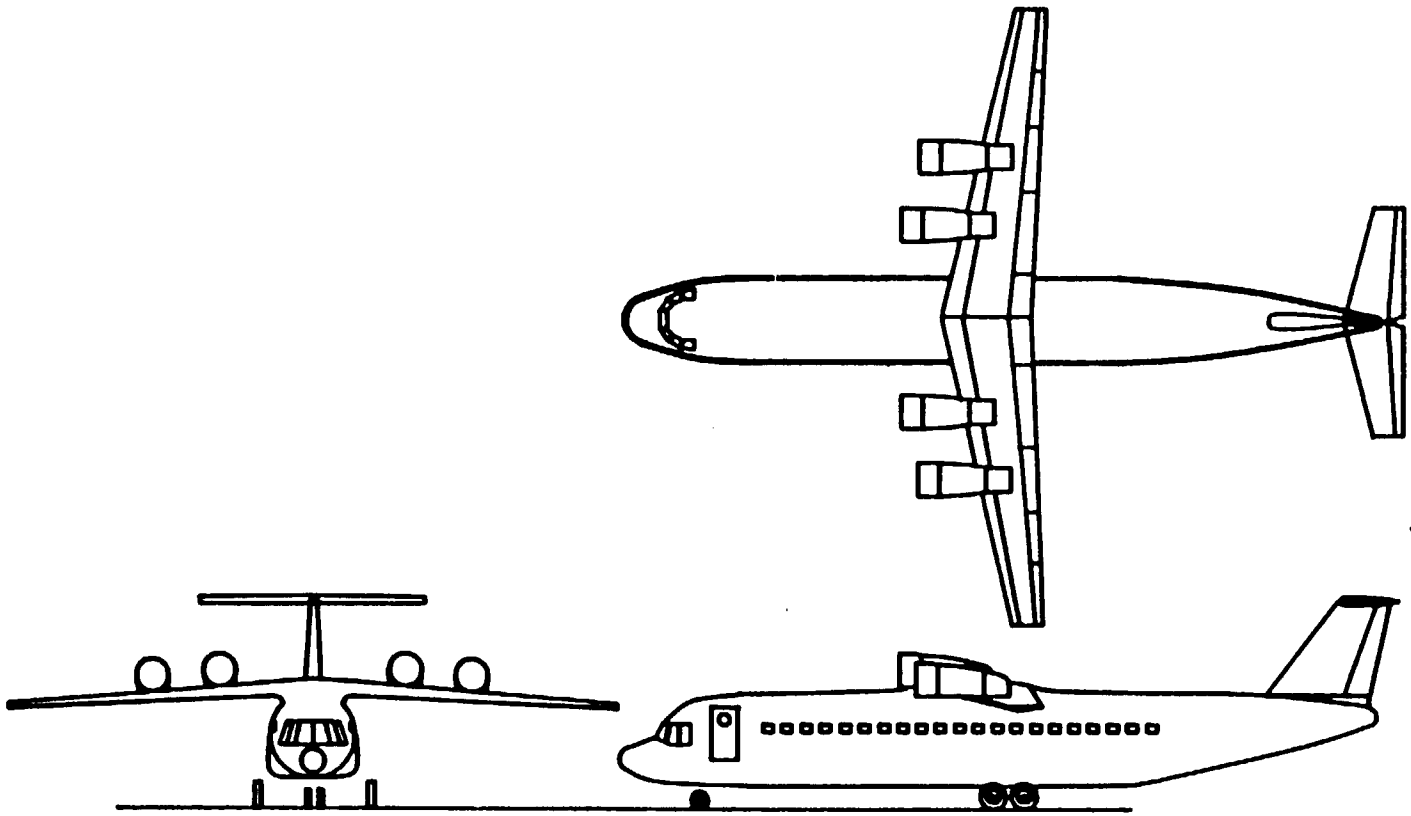

Figure 5 California Sky-hopper Class I Threeview

The cruise speed of 450 knots was selected as a compromise between cost of high speed and passenger convenience. Current regional aircraft fly at approximately 250 knots. The following tabulation compares CASH with two popular competitors. (Table II)

Table II Comparative Aircraft

Airplane Type	W_{pl} (lbs)	W_{to} (lbs)	V_{crmax} (kts)	Range (nm)
BAE 146-100	19,500	84,000	383	935
DASH 7-100	11,310	44,000	227	690
CASH	8,200	36,475	450	500

*Data base on JANE's World of Aircraft

Engine performance and aerodynamics will continue to improve such that it will be economically feasible to cruise at higher speeds. It was also speculated that high speed trains will be developed. **Ref. 2** and 3 indicates that heavily used routes, such as Las Vegas to Los Angeles, may see trains as an alternative to flying. These trains can reach speeds up to 250 mph. In order to compete in this market, CASH must provide service at higher speed and reasonable cost.

In order to reach a cruise speed of 450 kts without introducing wave drag, a cruising altitude of 25,000 ft is necessary. This also allows flight over low level turbulence from weather systems.

A required runway length of 2500 ft is sufficient enough for safe CASH operations. Since this is such a short length, an under used taxi way can easily be converted to provide for STOL ports.(**Fig. 2**)

Performance Summary

Preliminary calculations show a required installed thrust of 2,800 lbs. The closest available engine provides 3,500 lbs. Due to the additional thrust, CASH performs above what is required in cruise conditions. **Figure 6** shows the excess power of the CASH. The top speed is over 500 kts. With the given engine selection, CASH should be able to fly at the design cruise speed. **Figure 7(a)** indicates the various power requirements during the approach, landing and takeoff phases of flight. During the landing phase, drag increases due to the USB flap and gear extension requires more power. However, approach speed of 90 kts is possible. **Figure 7(b)** shows the different lift to drag ratio at various configurations. For low altitude climbout, it can be seen that the best climb speed is 210 kts. **Figure 7(c)** clearly shows that the excess power provides excellent climb performance during takeoff and landing phases of flight. The selected power configuration provides enough power for safe flight while CASH is in the USB configuration.

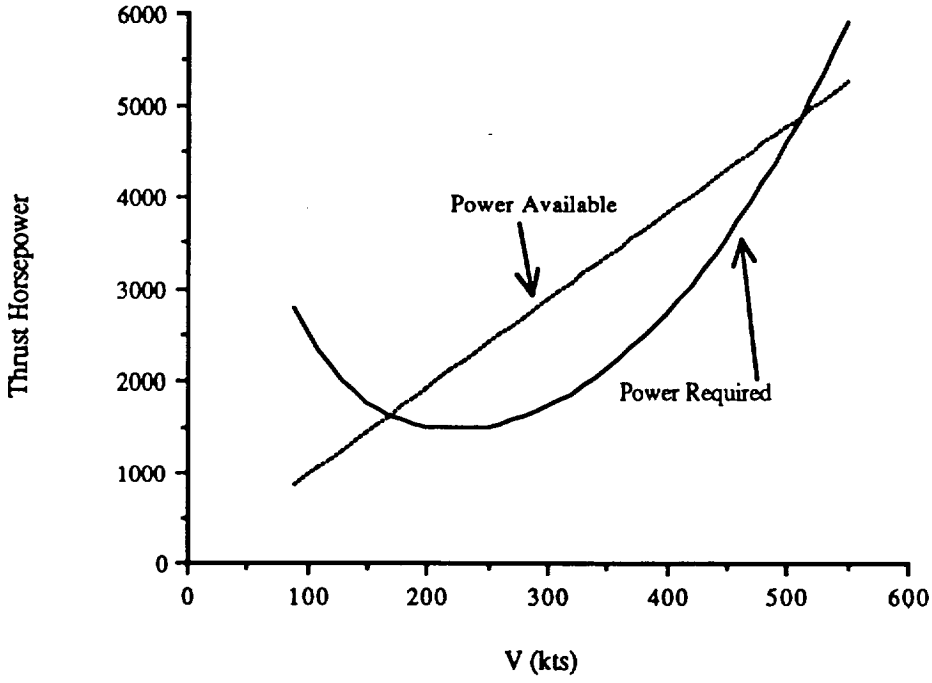

Figure 6 Power Available and Power Required vs. Velocity

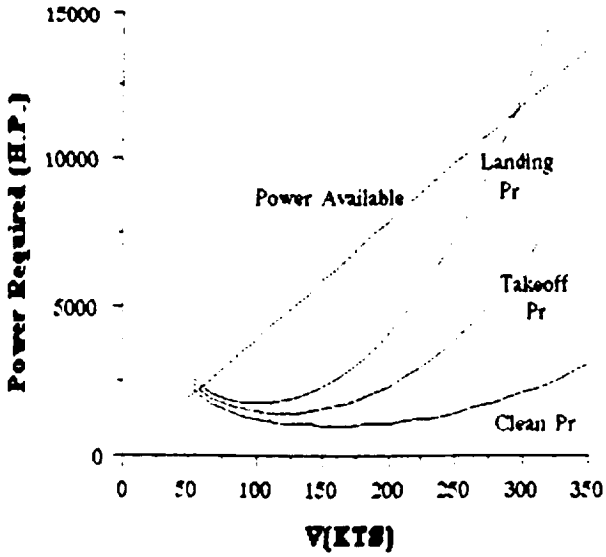

Figure 7a Power Available vs Power Required at 3000 ft

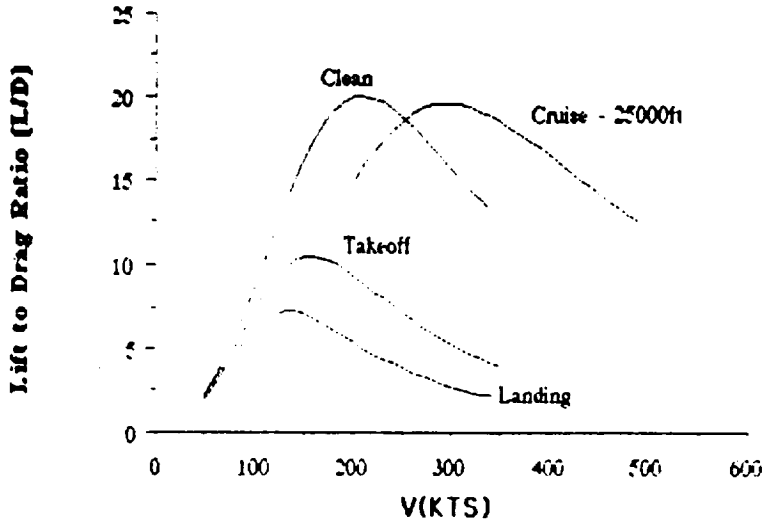

Figure 7b Lift to Drag Ratio vs Speed

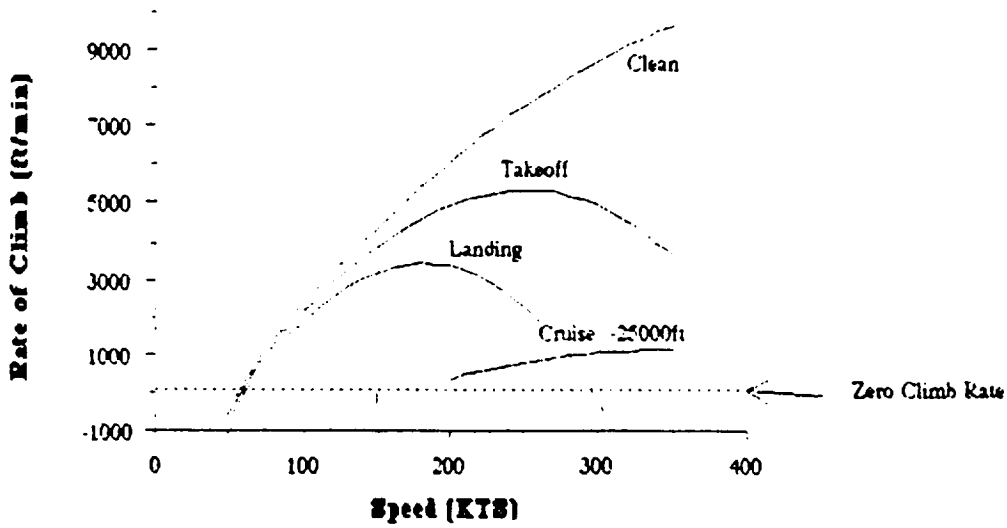

Figure 7c Climb Rate vs Speed

Geometry Summary

Table III presents the geometric charaacteristics or the California Sky-hopper.

Table III CASH Geometric Characteristics

	Wing	Horizontal Tail	Vertical Tail
Area	406 ft^2	113 ft^2	81 ft^2
Span	63.7 ft	23.8 ft	9.86 ft
MGC	6.89 ft	4.93 ft	8.52 ft
Aspect Ratio	10	5	1.2
Sweep Angle	15 deg.	15 deg.	38 deg.
Taper Ratio	.34	.5	.5
Thickness Ratio	.17	.12	.13
Airfoil:	LS(1)-0417	NACA 0012	NACA 0013
Dihedral Angle	-1.4 deg.	0 deg.	-------
Incidence Angle	-3.5 deg.	variable	-------
Aileron Span Ratio	.8 - 1	elevator chord ratio	rudder chord ratio
Aileron Chord Ratio	.23/.22	.4	root/tip
Flap Span Ratio	.14 - .8	———	.27/.35

Fuselage	Cabin Interior	Overall
Length	44.8 ft	81.8 ft
Maximum height	6.17 ft	11.8 ft
Maximum width	8.75 ft	9 ft

Structures Summary

The purpose of this section is to discuss how the structural layout was designed. This includes the integration of the wing, fuselage and the empennage structure. In the design of all structural members, it was necessary to obtain the shearing forces and the bending moments at various cross sections of the members. After determining the structure of the aircraft, a V-n diagram was constructed to determine the design limit and the design ultimate load factor as well as the corresponding speeds to which CASH structures are designed.

According to the aerodynamic loads on CASH's wing, the load per foot span is shown in **Fig. 8**. This is based on the assumption that the CASH's wing has an elliptical lift distribution. By using the load curve, the shear and bending moment diagram was constructed. (**Fig. 9 & Fig. 10**)

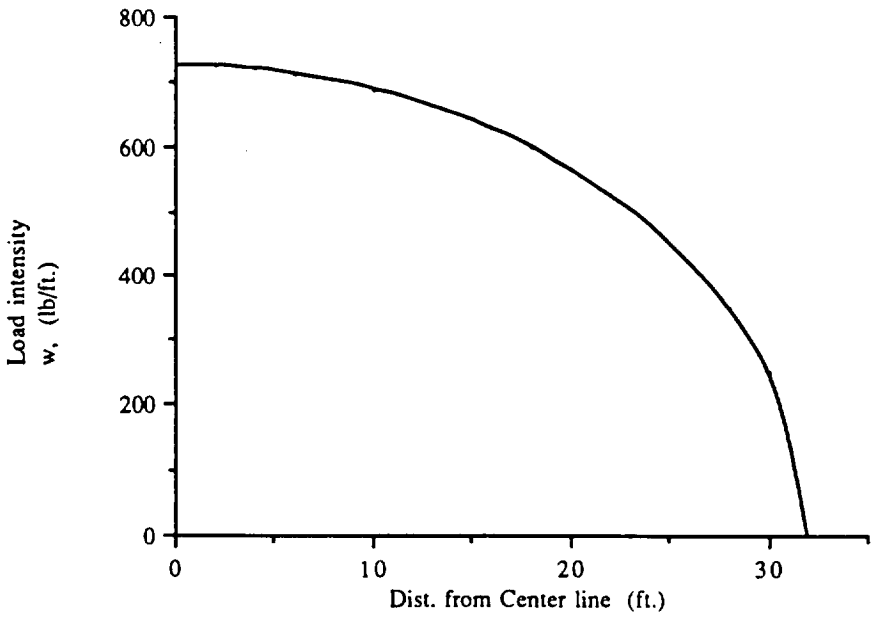

Figure 8 Lift Distribution Curve

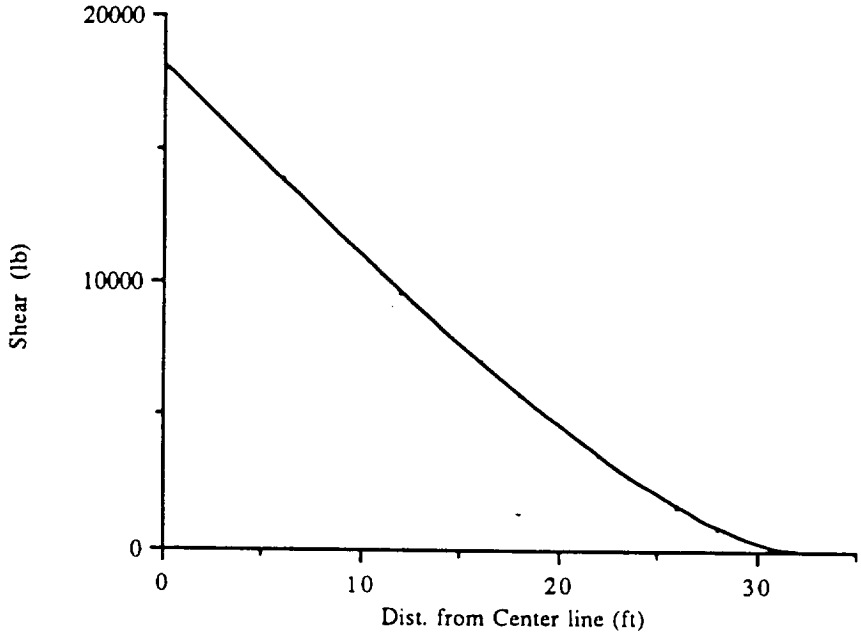

Figure 9 Shear Diagram

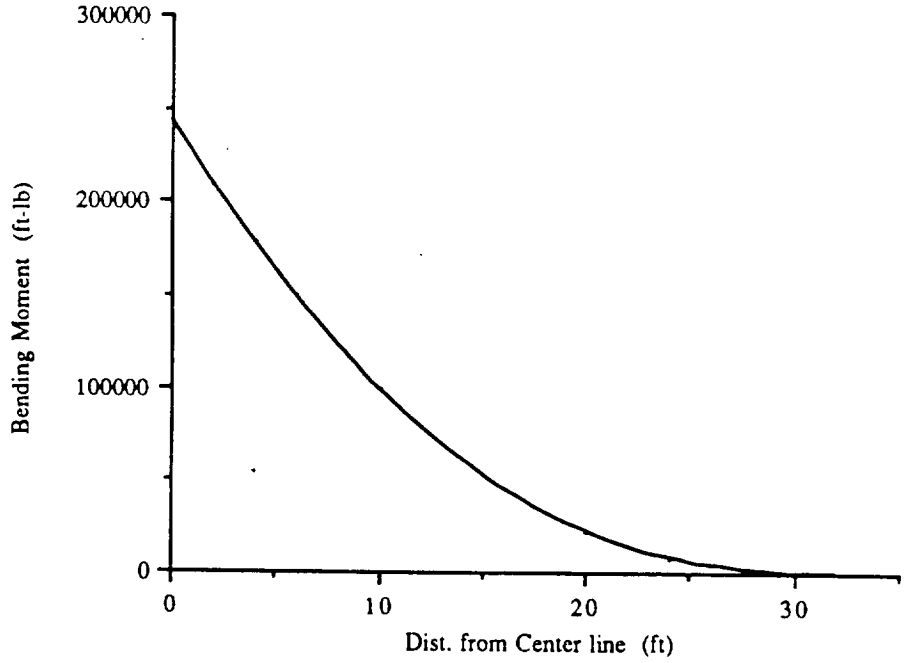

Figure 10 Bending Moment Diagram

The result of the shear and bending moment is shown in Table IV. Based on these data, the wing spar location was designed.

Table IV Shear and Bending Moment

Stations	Load Intensity	Distance Between Stations	Shear Increment	Shear	Moment Increment	Bending Moment
Dist. from Center line	From airload computation	From Col.(1)	Wav Δy	$\Sigma \Delta V$	Vav Δy	$\Sigma \Delta M$
y, ft.	w, lb/ft.	Δy, ft.	ΔV, lb	V,lb	ΔM, ft-lb	M, ft-lb
32.00	0	0.0	0	0	0	0
30.00	253	2.0	253	253	253	253
28.00	351	2.0	604	856	1109	1361
26.00	423	2.0	774	1631	2487	3848
24.00	480	2.0	903	2534	4164	8012
22.00	527	2.0	1007	3540	6074	14086
20.00	566	2.0	1093	4634	8174	22261
18.00	600	2.0	1166	5800	10434	32695
16.00	628	2.0	1228	7029	12829	45523
14.00	652	2.0	1281	8309	15338	60861
12.00	673	2.0	1325	9635	17944	78805
10.00	689	2.0	1362	10997	20631	99436
8.00	703	2.0	1392	12388	23385	122821
6.00	713	2.0	1415	13804	26192	149014
4.00	720	2.0	1433	15236	29040	178054
2.00	724	2.0	1444	16681	31917	209971
0.00	726	2.0	1450	18130	34811	244782

Wing Spar Locations

CASH's wing uses a so-called torque-box (wing-box) as the main load carrying component. The torque box is located in order to take the maximum advantage of the structural height available within the LS(1)-0417 supercritical airfoil contour. The torque box is closed off by a front spar (F.S), a rear spar(R.S), and an upper and lower skin. As a result, the front spar is located at 25% chord and the rear spar located at 70% chord.(Fig. 11)

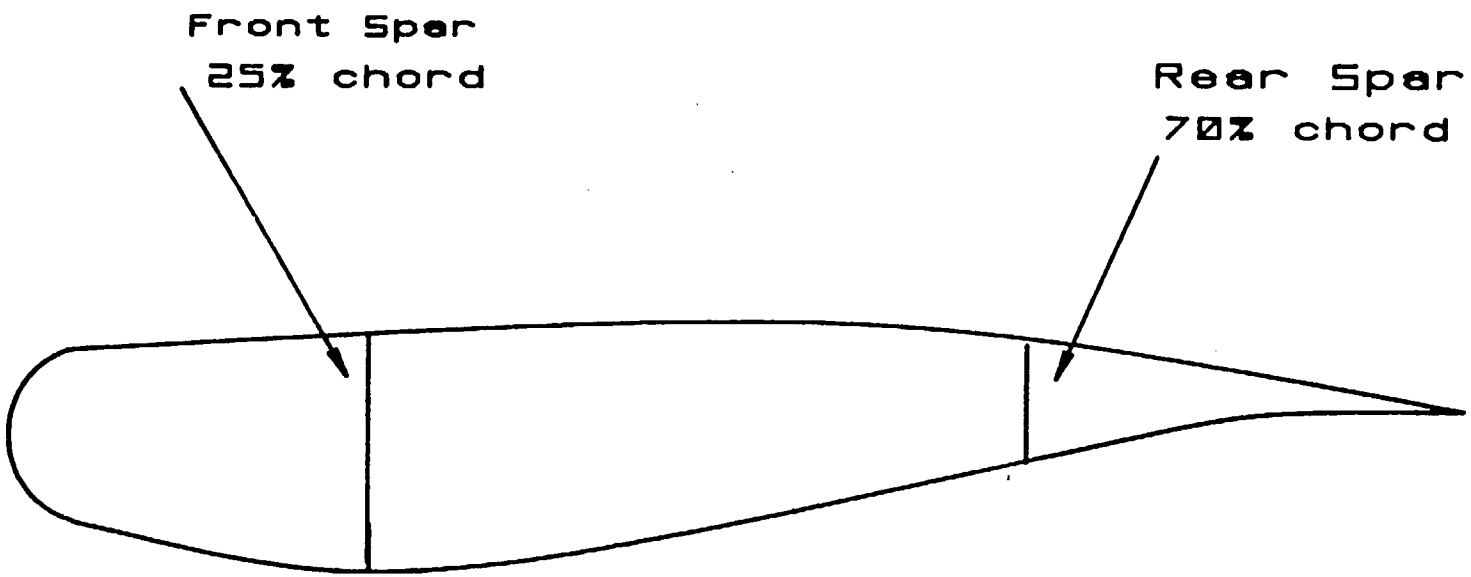

Figure 11 Wing Structure Cross-sectional Arragnement

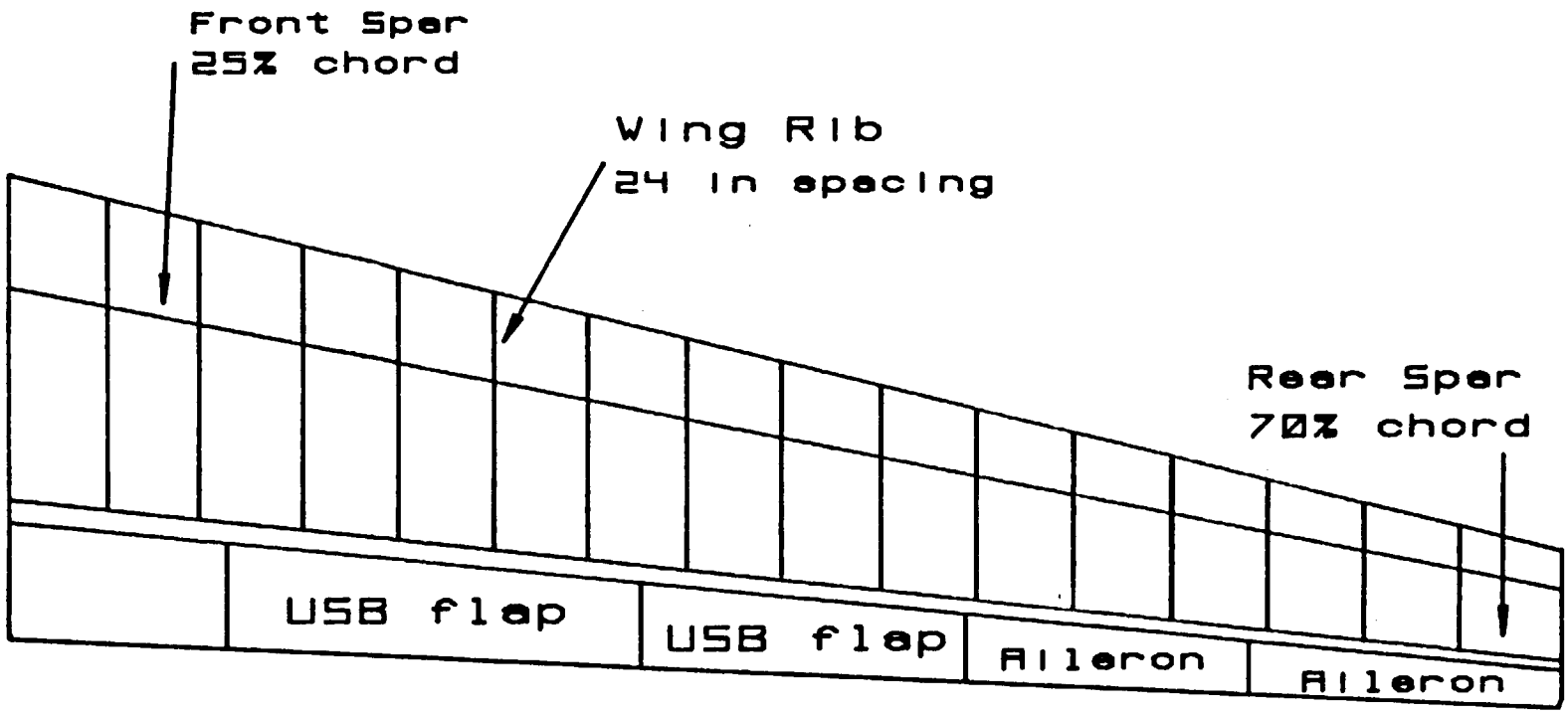

Figure 12 Wing Structural Arrangement

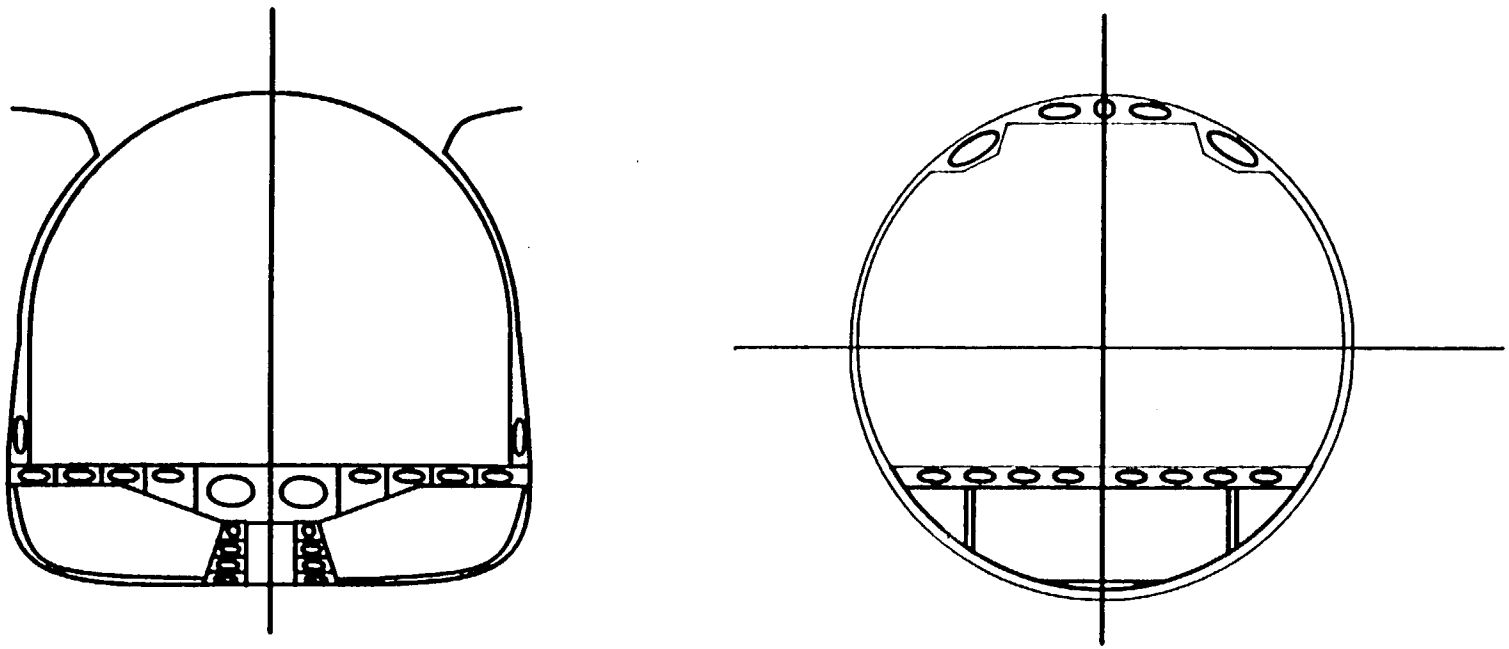

Figure 13 Fuselage Shell and Skin Layout

Wing Rib Locations

The outer skin helps stabilize the torque box, and also serves as attachment points for the leading edge skin, trailing edge skin, flaps, ailerons and spoilers, wing ribs are used. The rib spacing are 24 in. apart.(**Fig. 12**)

Fuselage Structure

For the structural arrangements for CASH's fuselage, the frame depth is 1.6 in. with a frame spacing of 20 in. and longeron spacings of 12 in.(**Fig. 13**) These numbers are based on the average load for which CASH is designed. **Figure 14-16** shows the design limit and design ultimate load factors as well as the corresponding speeds to which CASH structures are designed.

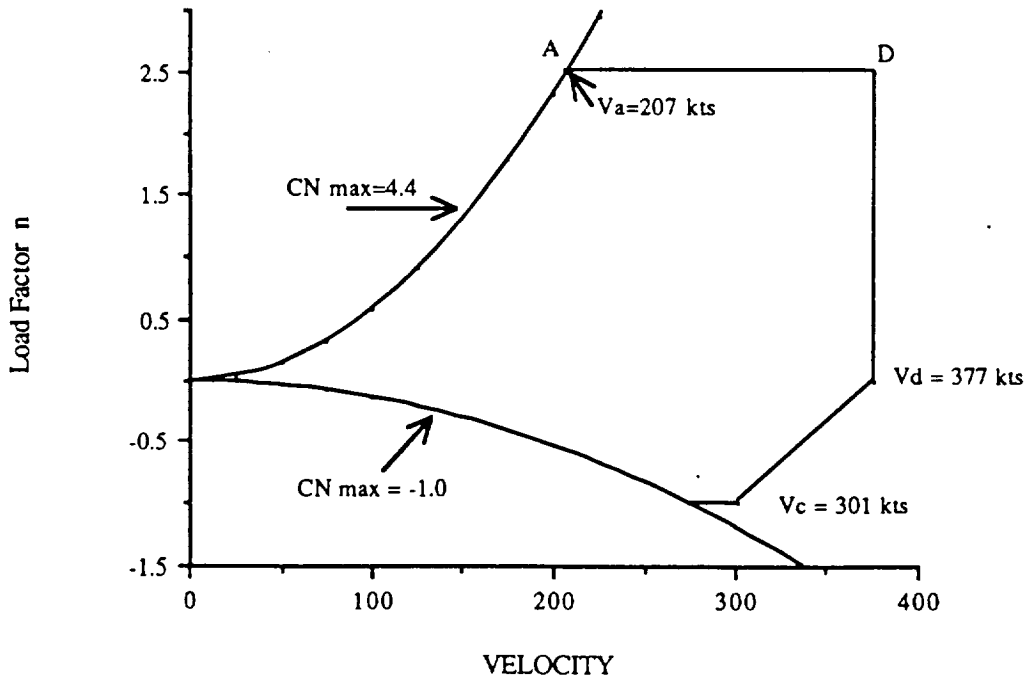

Figure 14 V-n Diagram (sea level)

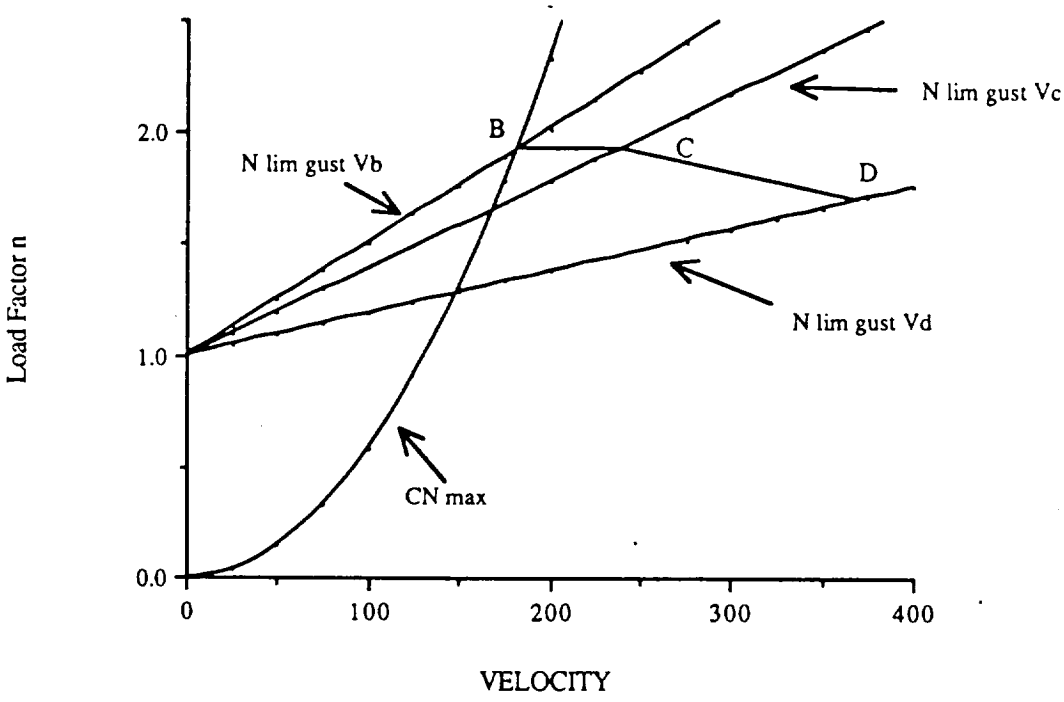

Figure 15 V-n Gust Diagram (Sea level)

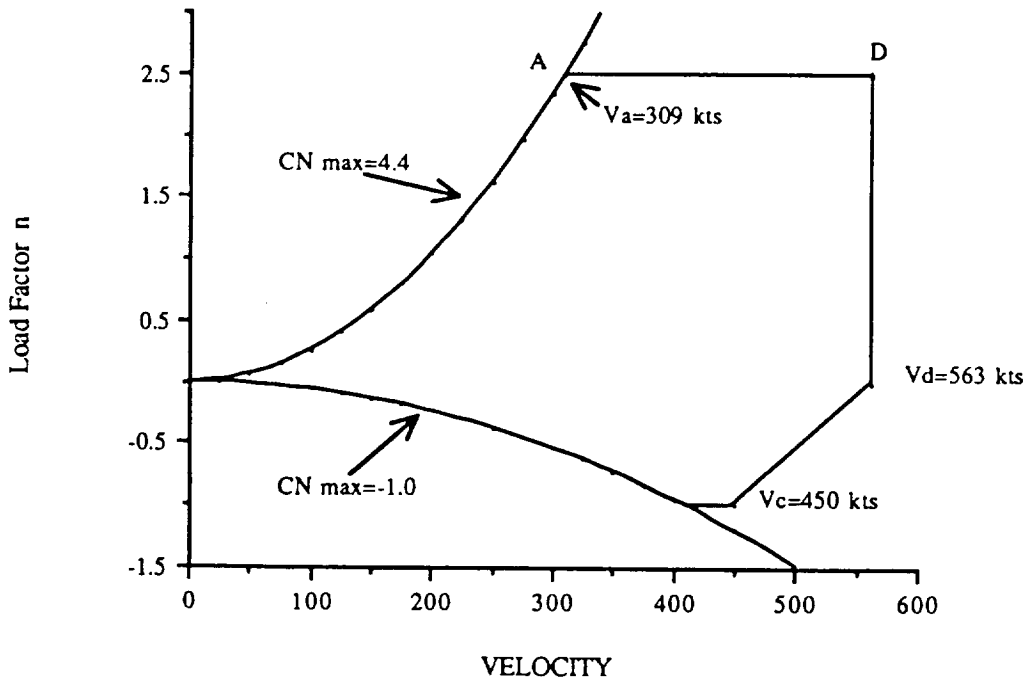

Figure 16 V-n Diagram(Cruise Altitude)

Aircraft Configuration

In order to achieve efficient high cruise speed and low speeds for short landings, it is necessary to incorporate a propulsion system that generates high lift. **Figure 17** shows the different types of propulsive lift.

The propeller slipstream system was not considered, since the propellers are not efficient for our selected cruise speed. Vectored thrust allows for very high lift generation, but at the cost of increased noise. Since our aircraft will operate in noise sensitive areas, we felt this system would prove inadequate.

The externally blown flap vectors the thrust down by placing the engine close to the lower section of the wing. This system has shown improvement in lift, but the turbulent flow of the exhaust on the flap, makes a lot of noise. This highly turbulent flow causes vibrations on the flap. This means strengthening of the flap is required.

The internally blown flap uses a small percentage of the engine power to blow over the top of a retracted flap, this energizes the boundary layer and delays separation. The disadvantage of this system is a lot of ducting is required to provide blowing. The long ducts will lose pressure, therefore, more power is needed to overcome the losses.

Upper Surface Blowing

The powered lift configuration selected is upper surface blowing. This system ducts the flow over the upper surface of the wing. This energizes the boundary layer, and allows for high flap angles with the flow remaining attached. This is known as the ***coanda effect***. Reference 4 contains data that shows lift coefficients as high as 10 can be achieved. USB powered lift has the highest lift generating capability than other systems studied. USB configuration is very quiet. Furthermore, since the engine exhaust is mounted above the wing, much of the noise is deflected up rather than down over the community. **Figure 18** shows the noise foot print of the QSRA.

In designing around the requirements for upper surface blowing configuration, five aspects of configuration design are carefully studied.

Fuselage

The conventional fuselage is adopted for this airplane. The well-proven data available for the conventional fuselage minimizes designing and building costs and maximizes safety. In order to minimize the drag due to the fuselage, a circular cross section is selected. An aluminum alloy structure has been selected as the primary material for the aircraft. There are two advantages to selecting aluminum alloy.

First of all, aluminum alloys have been well proven for safety. Secondly, since alloys have been around for a long time, certification costs will be minimized. However, in order to improve payload capacity, composite materials are expected to replace non critical components. Reference 5 states that it is possible to achieve up to 3% structural weight reduction by substituting secondary and medium primary components with composites.

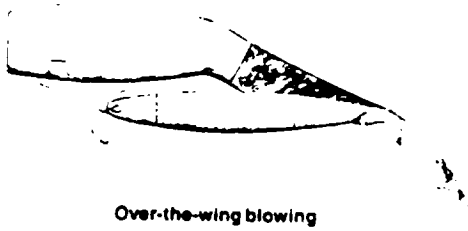

Over-the-wing blowing

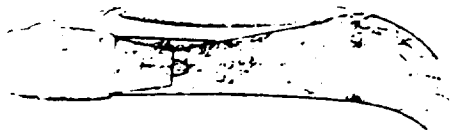

Externally blown flap

Upper surface blowing

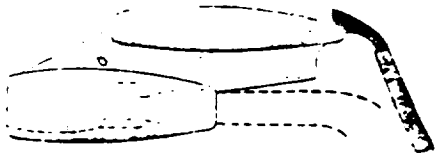

Augmentor wing

Figure 17 Powered Lift Systems

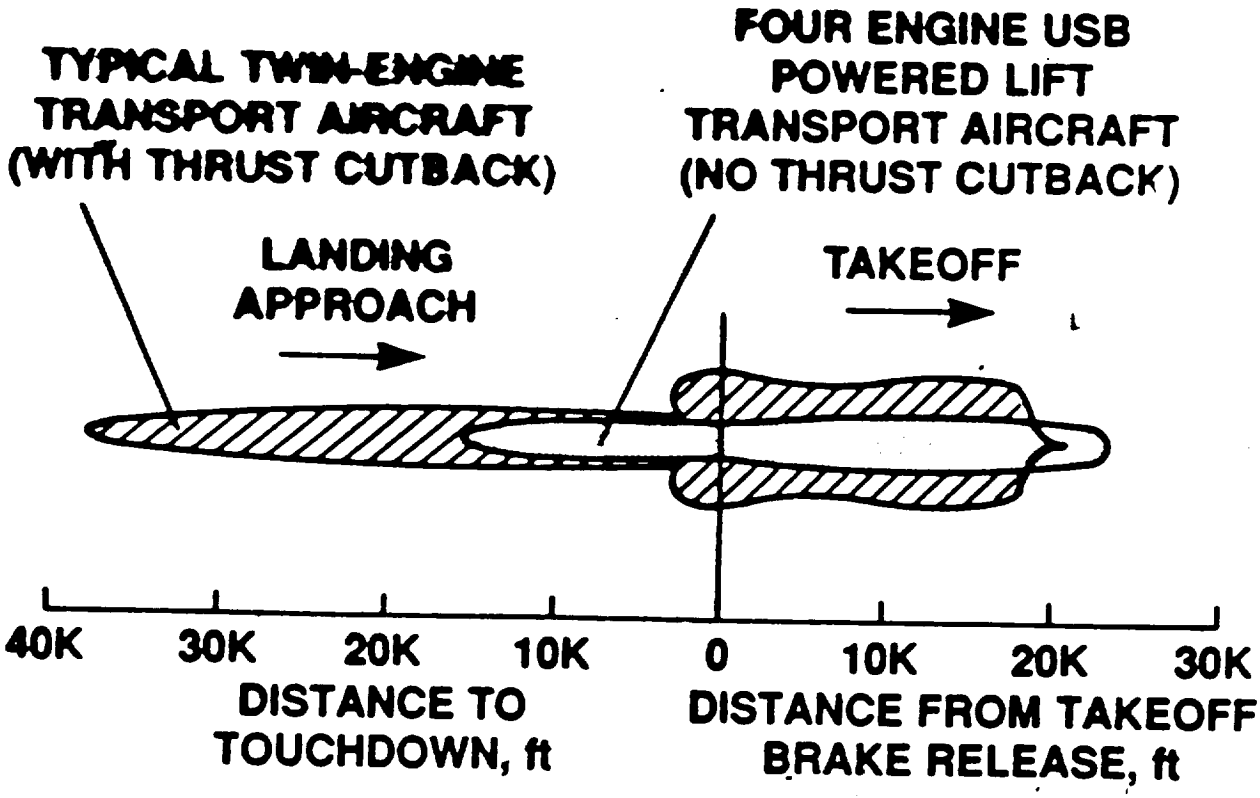

Figure 18 Comparison of Noise Footprints

Engine Locations

CASH has four turbofan engines in a tractor configuration. They are positioned above and forward of the wing. For USB, this tractor configuration is mandatory. It was desired to have two engines, but stringent FAR requirements for safety in an engine out condition prevented this. The boeing YC-14 is an example of a two engine USB aircraft. This aircraft was designed to replace the aging fleet of C-130's. The YC-14 had to incorporate a complicated control system in order to assure safety in the event of an engine failure. A boundary layer control system was used to blow over leading edge slats. The USB flap was capable of being converted into a slotted flap in case of engine failure.

In order to achieve simplicity in design, four engines are used on CASH. Four engines do provide more upper surface jet flow over the span and requires less oversize of the engines in order to meet FAR 25 one engine out takeoff and landing requirements.

Propulsion System

Turbofan engines were selected for three reasons. Firstly, the turbofan has a lower specific fuel consumption than turbojets. Secondly, turbofans produce less noise. Finally, since part of the flow by-passes the turbine, the mixed flow at the exit nozzle has a lower temperature than a turbojet. Since the flow is directed over the wing it is crucial not to overheat the upper surface.

Telescoping Nozzle Modification

The purpose of USB powered lift is to allow an aircraft designed for high cruise speed to land and takeoff from a short runway. But when the flaps are retracted, the engine exhaust is still attached to the top of the wing, creating high circulation. Two things would most likely occur with the attached flow. First, there is a loss of net thrust due to scrubbing losses. Second, shock waves would form over the top of the wing aft of the flow. In order to achieve efficient cruise, we are proposing a telescoping nozzle. During cruise, this circular nozzle telescopes out to 70% chord length. This circular nozzle improves net thrust by directing it off the wing. At slower speeds, the circular telescoping nozzle is retracted into the nacelle, and a D shape nozzle is used to attach and spread the flow over the wing.

Wing

A high wing is required in order to reduce excessive ground effect due to the high circulation flow. This configuration assures positive dihedral effect. The high wing also provides better views for the passengers.

Empennage

The selection of the conventional two surface configuration over the three surface was the result of the tradeoff study. Despite the fact that a properly designed canard generates higher lift, overall it could cause a problem at high angles of attack due to canard tip vortices impinging on the wing and, therefore, causing higher drag. (**Ref. 6**) Also, the canard, depending on its location, could restrict the pilot's vision. But, most of all, the canard increases cost, weight, and the complexity of the mechanisms. CASH designed without the complex mechanisms for the canard is simpler and less expensive to maintain. The study made on NASA's QSRA, Boeing' YC-14, and Japan's Asuka, USB concept airplanes designed with the conventional two surface (T-tail) configuration, shows no problems for stability.

Landing Gear

To minimize cost and maximize safety, a conventional tricycle gear layout was selected. The landing gear is retracted into the fuselage. This configuration reduces drag. It is noted that the main gear under the strongest point in the fuselage reduces weight.

Propulsion

To satisfy the takeoff weight of 36,475 lbs with the takeoff thrust-to-weight ratio of 0.306 at sea level, each of the four engines must be able to produce 3,500 lbs of thrust. Four engine configuration is selected over two engine configuration for stability reasons as explained before.

Garrett TFE 732-2 turbofan engines were seleted for the preliminary design (**Fig. 19**). This engine produces 3500 lbs net thrust for takeoff at sea level and 755 lbs for maximum cruise speed at 40,000 ft (Mach=0.8). Specific fuel consumptions (sfc) are 0.504 and 0.815 at sea level and 40,000 ft respectively. General speculation on the development of more efficient engines forecasts probable improvement of 20 to 30% on sfc in the near future. There already exist new-generation engines with sfc in the 0.4 range (**Ref. 7 & 8**). With average 20% of improvement on sfc accounted for, 0.403 for sea level and 0.625 at 40000 ft are newly found. New sfc values reduce the amount of the total fuel by approximately 15% from the original amount of fuel needed. TFE 732-2 has a bypass ratio of 2.67, which is relatively lower than what CASH needs to be more efficient and less noisy. Bypass ratios between 5 and 6 would provide better results for CASH. For the present time, a specific engine that provides 3,500 lbs net thrust with a by-pass ratio of 5 or 6 is not available.

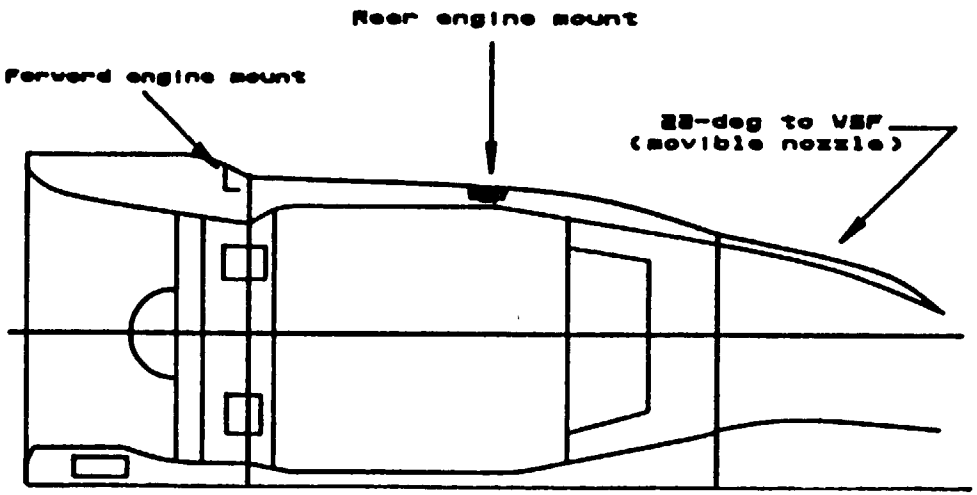

Figure 19a Propulsion System Installation
TFE731-2 Turbofan

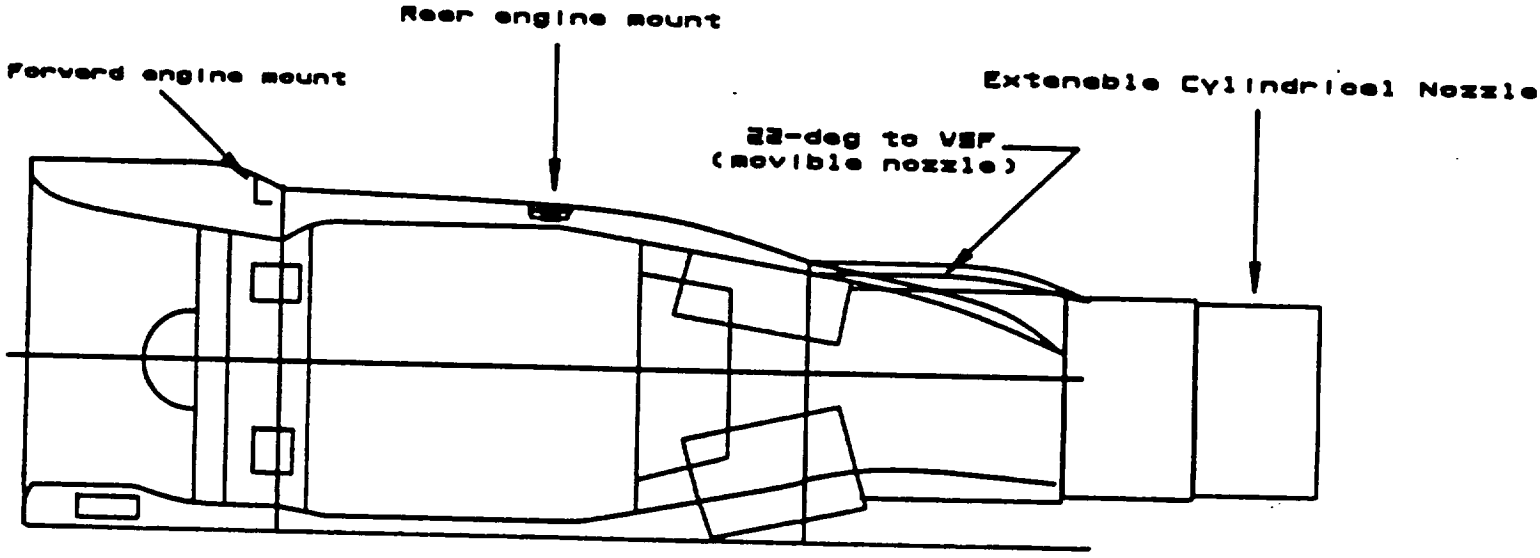

Figure 19b Engine Installation
TFE731-2 Turbofan

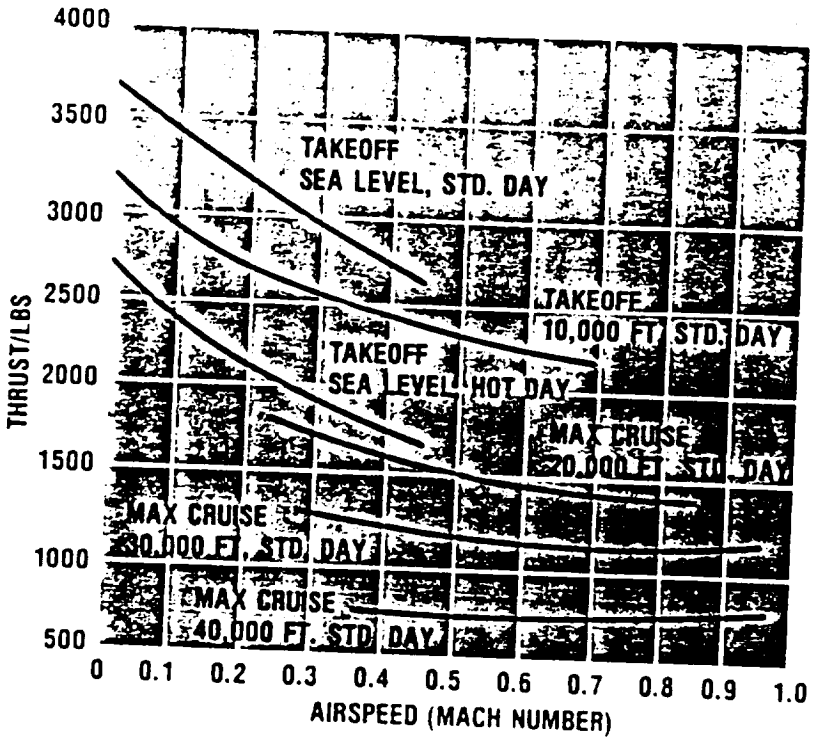

Figure 19c Garrett's TFE 732 Turbofan Engine Data

Wing Design

Table V shows the following platform design characteristics of the wing:

Table V CASH Wing Geometric Characteristics

Wing Area:	406 ft^2
Aspect Ratio:	10
Sweep Angle:	15 deg
Thickness Ratio:	.17
Airfoil:	**LS(1)-0417** (supercritical)
Taper Ratio:	.34
Incidence Angle:	-3.5 deg
Dihedral Angle:	-1.4 deg
Root Chord	9.51 ft
Tip Chord	3.23 ft
Mean Chord	6.89 ft

Based on one engine out takeoff requirements, a wing loading of 90 psf was selected. giving a wing area of 406 ft^2.(**Fig. 20**)

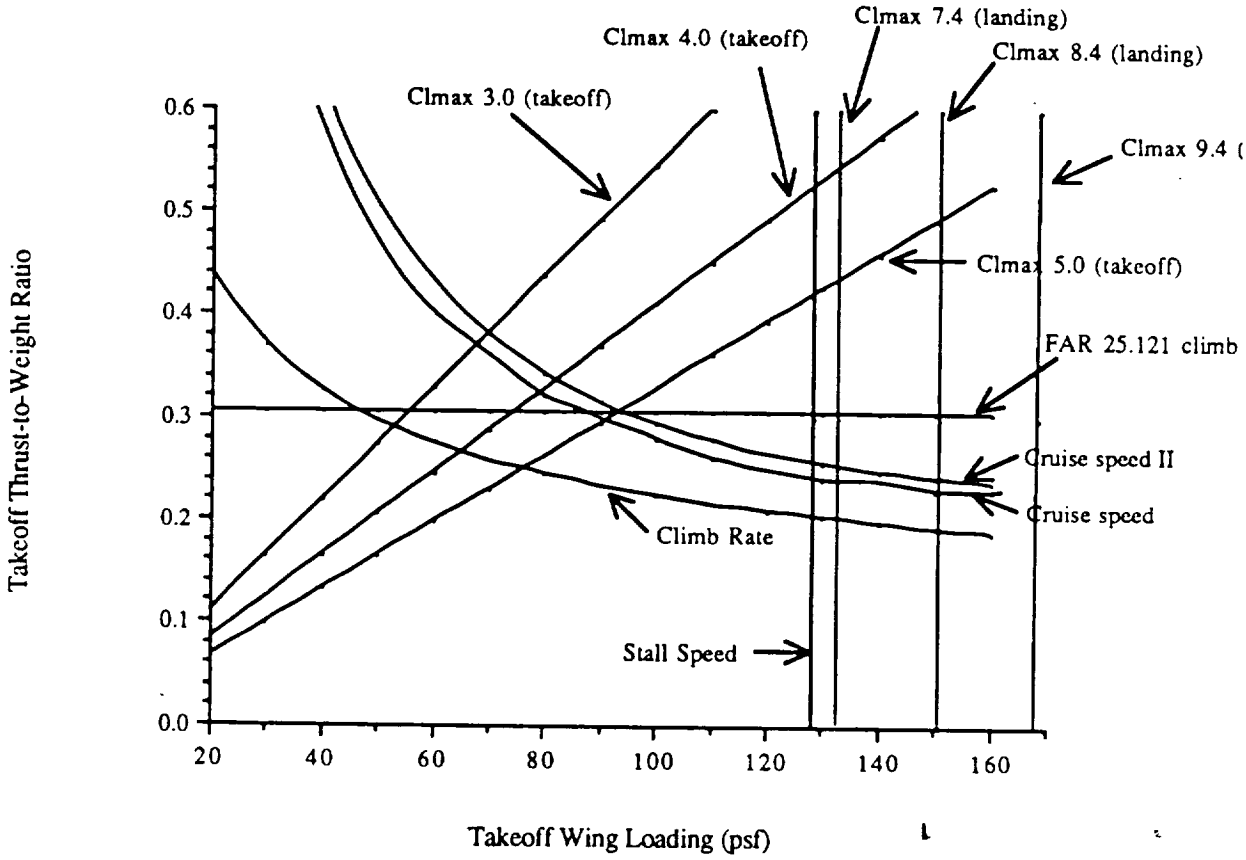

Figure 20 Sizing of California Sky-hopper

Since our aircraft generates high circulation, a high aspect ratio wing was selected. To minimize induced drag, it was decided to use a supercritical airfoil rather than a NACA 60 series. A supercritical airfoil allows CASH to adopt a higher thickness ratio without added compressibility drag as compared to NACA 60 series airfoils. Also, this airfoil helps to achieve a higher maximum lift coefficient, which is advantageous for low speed flight.

The sweep angle was determined by using a wing design method by corning,(**Ref 9**). **Figure 21** shows how the sweep angle selection changes with thickness ratio and critical Mach number. Since our cruise speed is .75 Mach, it is necessary to have a sweep angle of around 15 deg. in order to avoid wave drag.

A taper ratio of .34 was selected by using the taper ratio of a 737-200 (**Ref. 10**). Because the 737 flies at about the same cruise speed as CASH. **Figure 22** shows the complete airfoil section data for the selected airfoil. A cruise lift coefficient of .4 is expected, this was assumed for the condition after 40% of the fuel weight is consumed. It can be seen from **Figure 22** that our zero lift occurs at alpha of -4 deg. This will require an incidence angle of -3.5 deg in order for the floor line to be level during cruise. For roll

control, ailerons are placed along the outer portion of the wing. Based on typical aircraft configurations a preliminary aileron length of 80% of the half span of the wing was selected . Ailerons were selected over spoilers, because ailerons produce less drag.

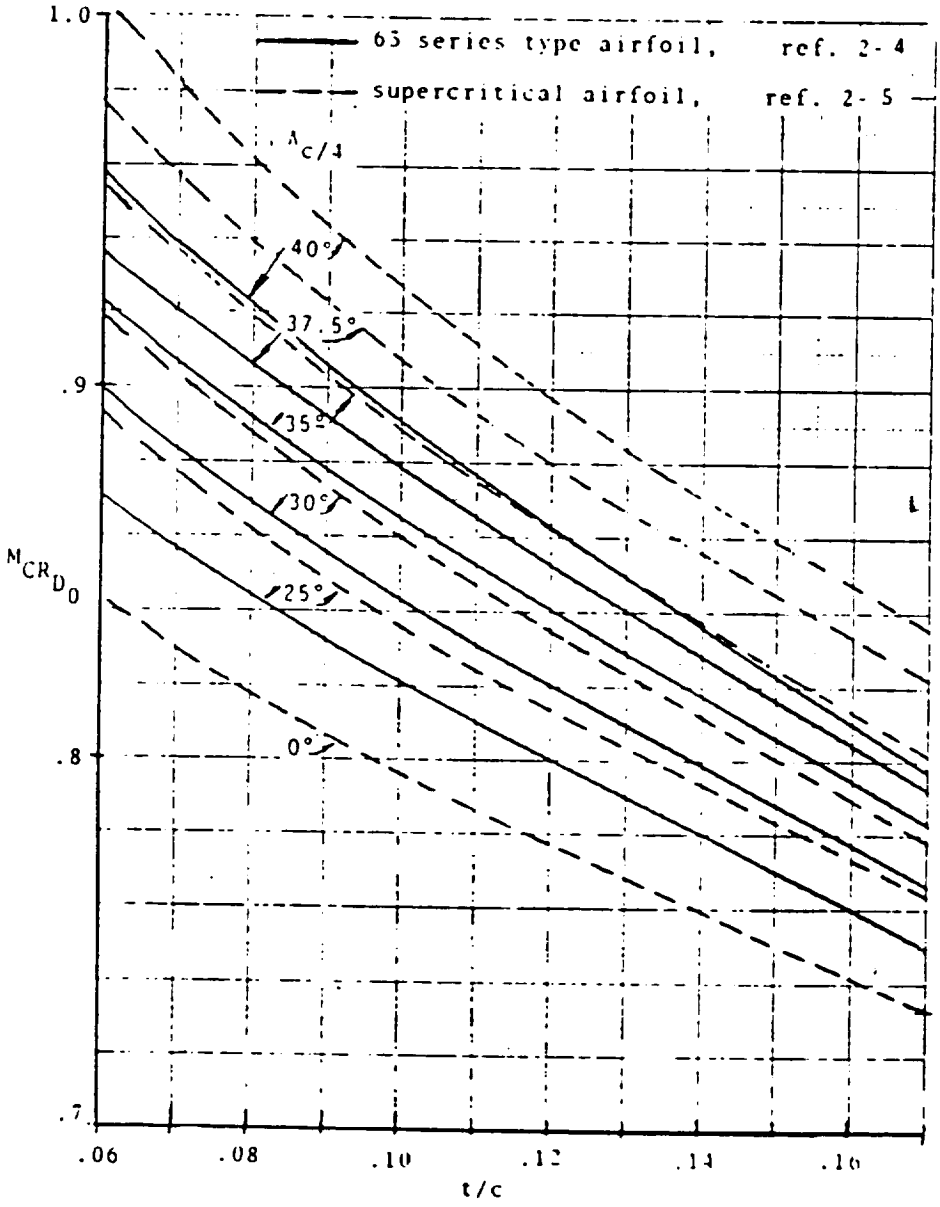

Figure 21 M_{CRD0} vs. Equivalent t/c

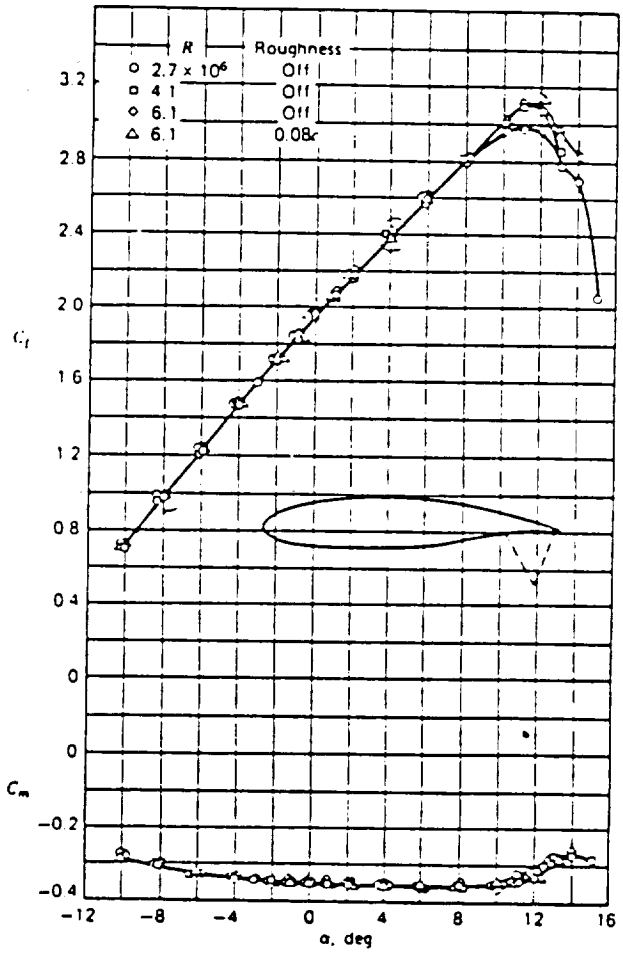

Figure 22 Effect of Reynolds Number on Section Characteristics of GA(W)-1 airfoil Model smooth, M=0.15

A preliminary calculation of wing fuel volume was performed by using Roskam's method in Book II (**Ref 10**). It was assumed, that no fuel is placed beyond 85% span in order to insure safety from lightening strikes. Results show that 192 ft^3 are available where CASH only needs 141 ft^3. This indicates that it will not be necessary to have additional tanks in the fuselage.

Figure 23 & 24 shows the wing geometry of the CASH.

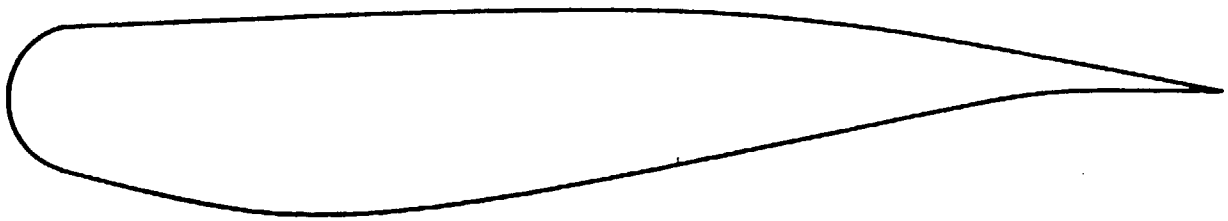

Figure 23 LS(1)-0417 Supercritical Airfoil

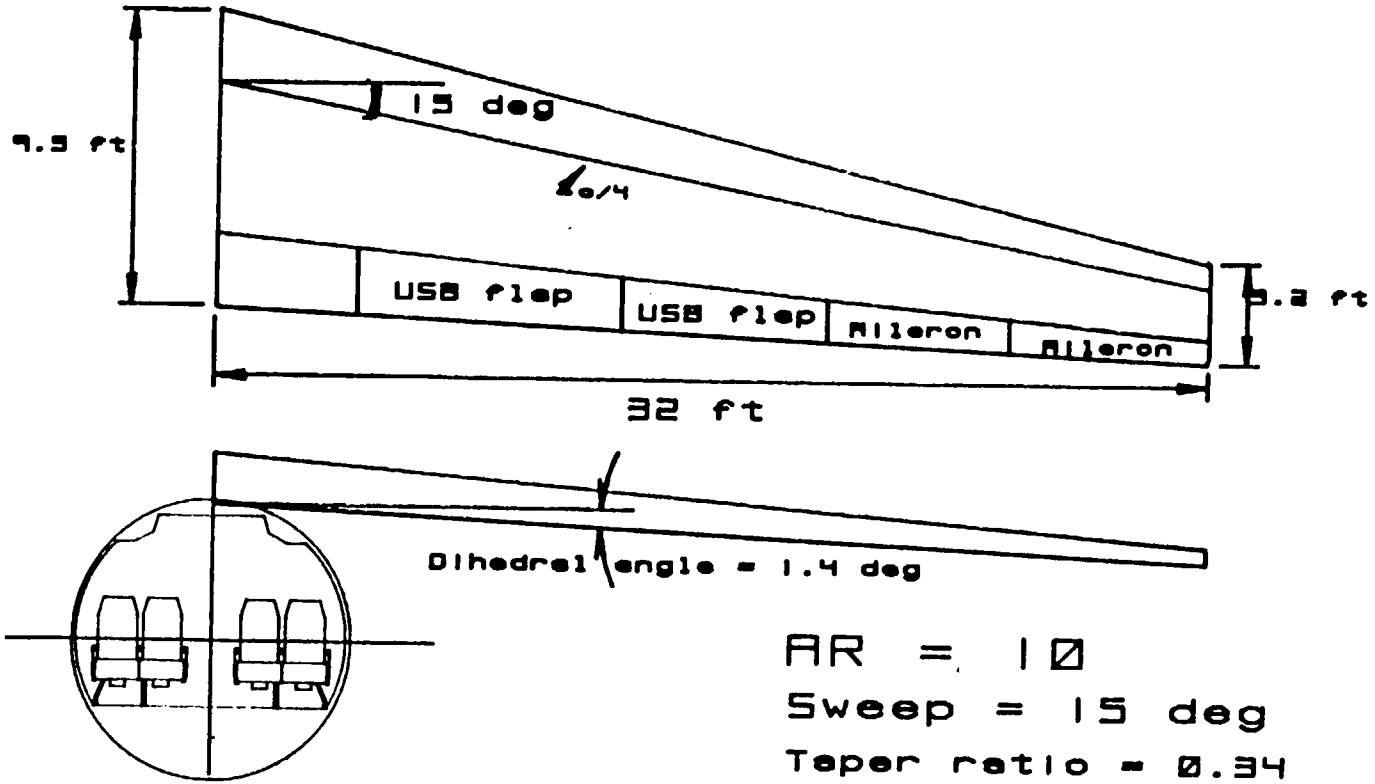

Figure 24 Wing Drawing Layout

Empennage Sizing

Roskam's class I method was used to determine size and disposition of the empennage as well as the longitudinal and directional control surfaces. A T-tail configuration was selected to reduce the incidence angle range due to the strong downwash angles induced by the USB configuration at high flap angle settings. Also by selecting a T-tail, higher pitching moments can be achieved. The empennage is placed as far aft of the wing as possible in order to keep the empennage area as small as possible. This method requires selection of volume coefficients. Tail volume coefficients are defined as follows:

$$V_h = X_h \, S_h / S \, c \qquad \text{(eqn 1)}$$

$$V_v = X_v \, S_v / S \, b \qquad \text{(eqn 2)}$$

Volume coefficients were selected from a Dehavilland DASH 8 STOL aircraft since this aircraft has basically the same landing and takeoff requirements as well as fuselage geometry. By estimating our furthest possible moment arms, vertical and horizontal tail areas are calculated from the above equations. The elevator and rudder sizes were obtained from the Dehavilland DASH 8 and 7 respectively.

The platform geometry was selected based on ballpark figures given in Roskam's book for Jet transports. Sweep angle and thickness ratio were selected such that the critical Mach number for the empennage is higher than that of the wing. **TABLE VI** and **Figure 25 & 26** summarize the preliminary size of the empennage.

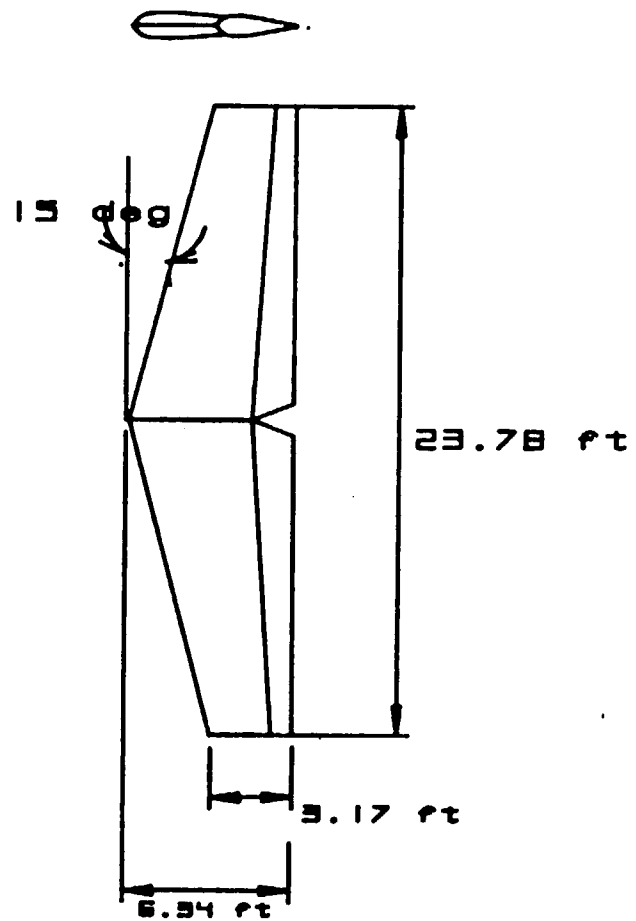

Figure 25 Empennage Configuration

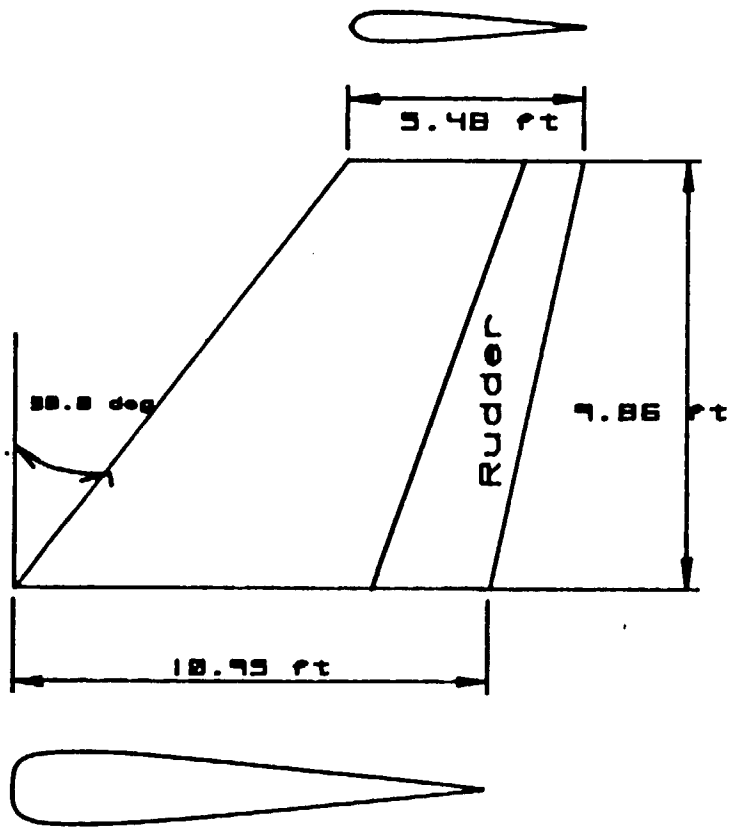

Figure 26 Vertical Tail Configuration

TABLE VI Empennage Geometric Characteristic

	Vertical Tail	Horizontal Tail
X_v / X_h	31.4 ft	36.3 ft
V	.0985	1.47
S	81 ft^2	113 ft^2
AR	1.2	5
	38 deg	15 deg
t / c	.13	.12
Airfoil	NACA 0013	NACA 0012
Incidence	------	variable
b	9.86 ft	23.78 ft
C_r	10.95 ft	6.34 ft
C_t	5.48 ft	3.17 ft
C	8.52 ft	4.93 ft
S_e / S_h	---	.42
S_r / S_v	.26	-----
Elevator Chord (% C_h)	.41	.43
Rudder Chord (% C_v)	.27	.35

Riblets

Recently, riblets have been tested and proven to be effective in reducing skin friction drag due to turbulent boundary layer buildup. Riblets are grooved surfaces placed in the flow direction. The depths and spacings of the grooves are in the order of the turbulent wall streak and burst dimensions. High and low speed streaks exist very near the surface. The low speed streaks burst, and cause high turbulent energy. Riblets space the high and low speed streaks farther apart, to reduce burst intensity per unit area. A highly viscous sublayer forms in the riblet valley, and pushes the skin-friction producing turbulence away from the surface.

Reference 11 describes extensive studies done on different geometries. The "v" shaped grooves produced the highest drag reduction which is in the order of 7-8%. This drag reduction depends on geometry, machining accuracy, spacing and alignment with the flow. The study indicated, however, that maximum drag reduction is unaffected by different upstream boundary layer histories. Thin vinyl sheets with adhesive backing have already been tested on a business Lear jet at Mach numbers ranging from 0.3-0.7. Drag reduction in the order of 6% were found. More information can be found in **reference 12.**

CASH will have riblets installed over the entire fuselage, empennage, and outer wings. Vinyl sheets will be used. The advantage of using the vinyl sheet is light weight and easy application. A conservative drag reduction of 5% on zero lift parasite drag coefficient was applied for the Class I preliminary calculations. This resulted in a 25% reduction of required thrust to weight ratio for cruise.

Fuselage Design

CASH is capable of hauling 40 passengers and their baggages for each short haul flight. The total length of the fuselage with a diameter of 108 in. is 982 in. The 10 rows of 4 seat abreast should provide a very roomy seating environment. The closets, toilets and galley are located at the rear of the fuselage in order to save space. **Figures 27-32** show the overall layout. To achieve a short turnaround time, the passenger access door is located on the port side and the servicing access door is located on the starboard side. This allows loading and unloading passengers and baggage at the same time. The fuselage cross section is the result of compromises among weight, drag, systems and creature comfort considerations. For pressurized airplanes, the most efficient cross section viewpoint is the circle. To compromise with all these aspects, CASH adapted a circular shape fuselage. **Figure 28** shows our cross section. The designed cabin allows 4 seats abreast with significant space enough for an average height person to walk down the aisle without any discomfort.

Most of the carry on luggage can be stored underneath the seat. This increases the safety of the passengers compared to overhead storage of baggage. The seat covers on CASH are fire resistant. The material used is a flame resistant foam - Metzoprotect FR - from Germany's Metzeler. Reference 13 gives a complete description of this material. **(Fig. 27)**

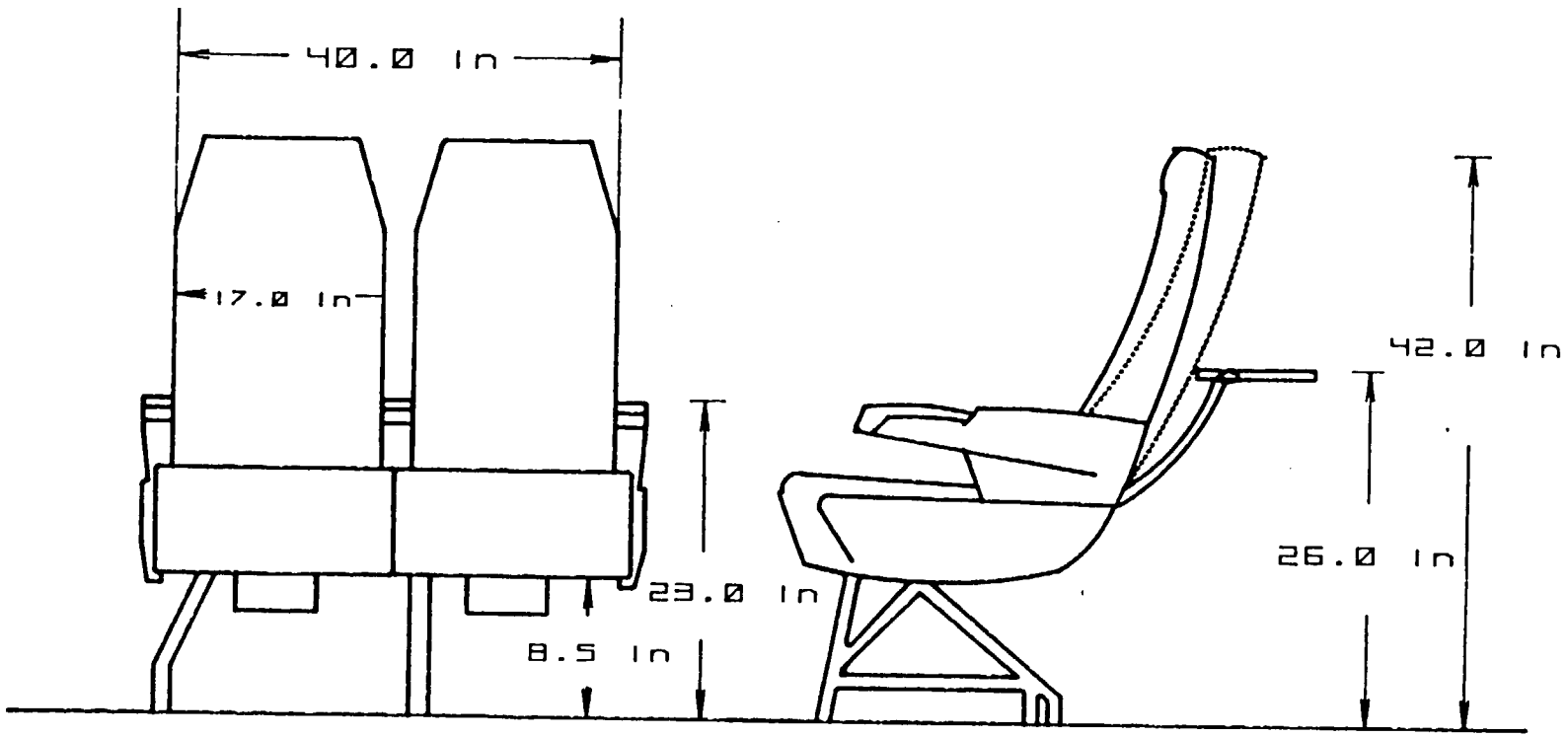

Figure 27 Airline Seat

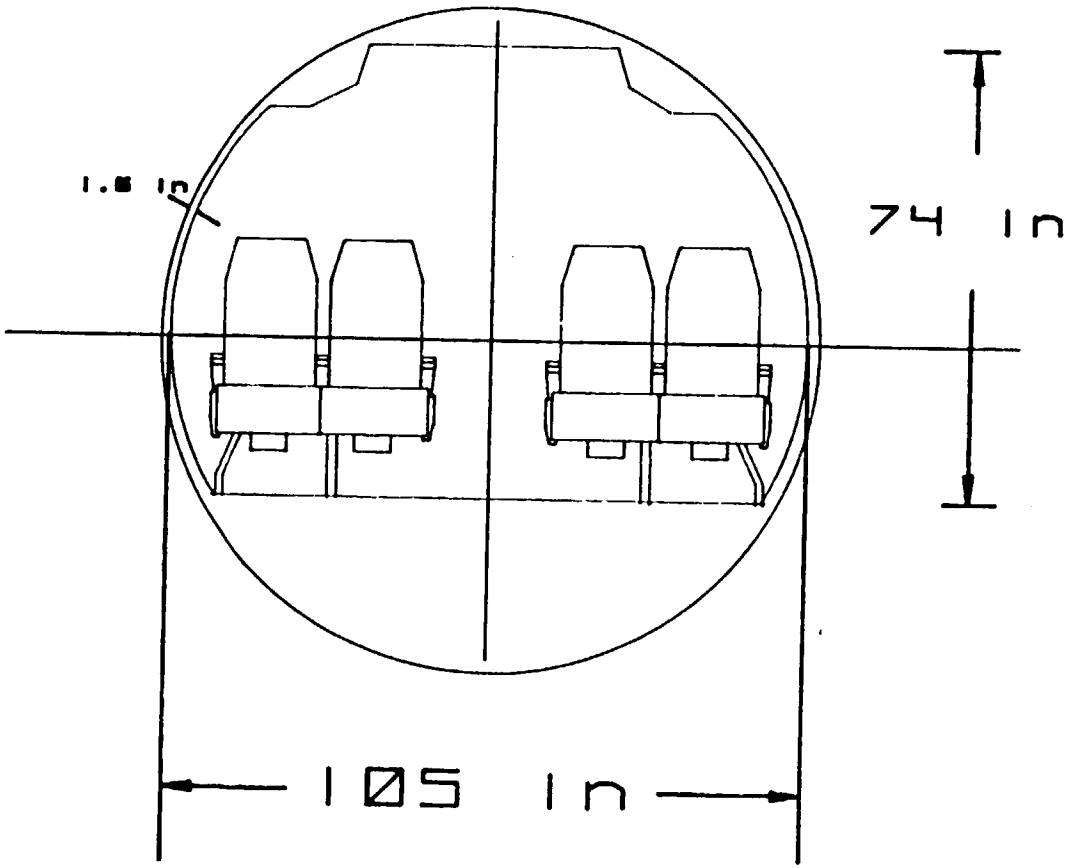

Figure 28 Fuselage Cross Section

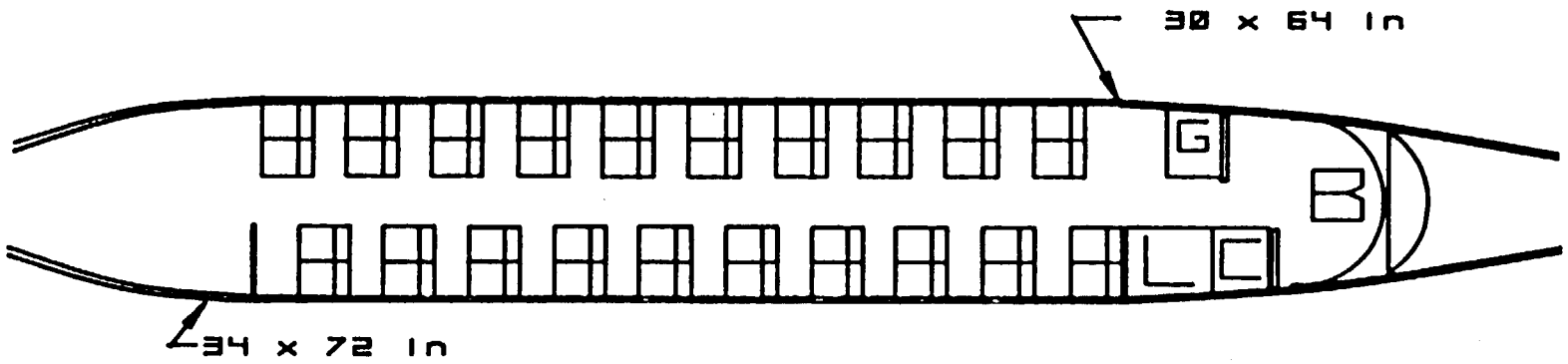

Seating capacity-40 passengers

Figure 29 Fuselage Layout

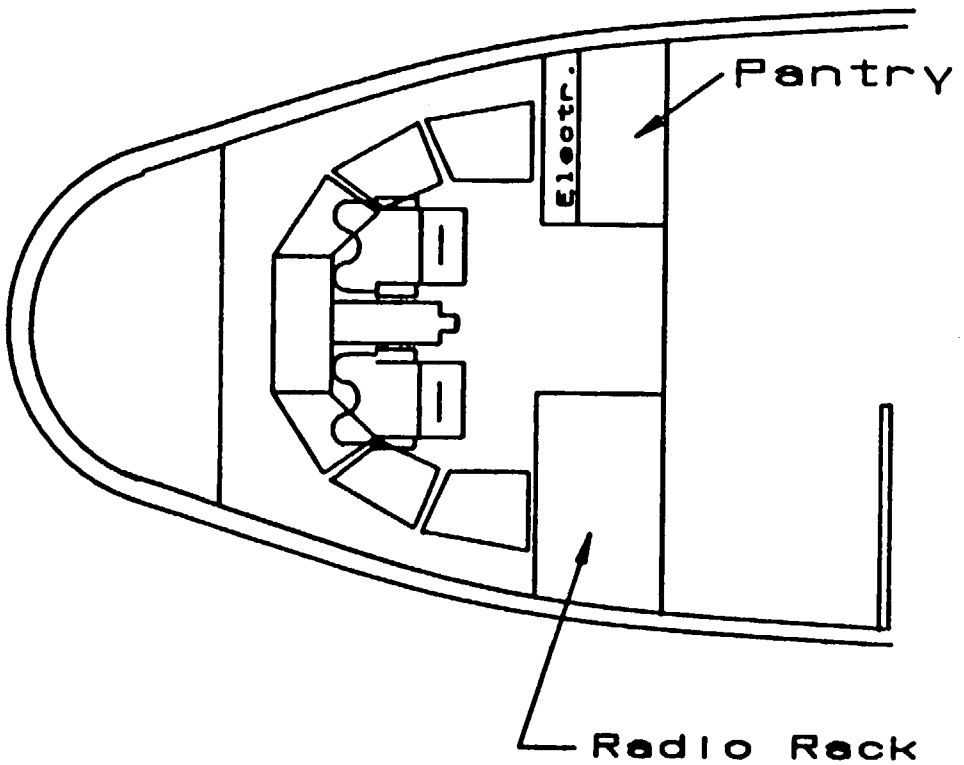

Figure 30 Cockpit Layout

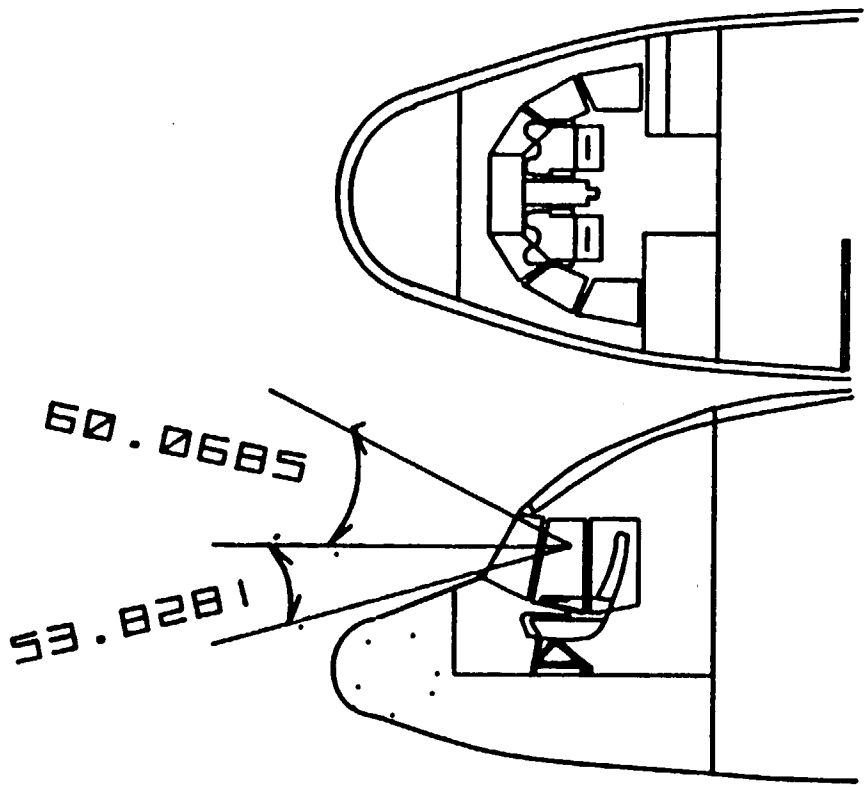

Figure 31 Flight Deck Arrangement

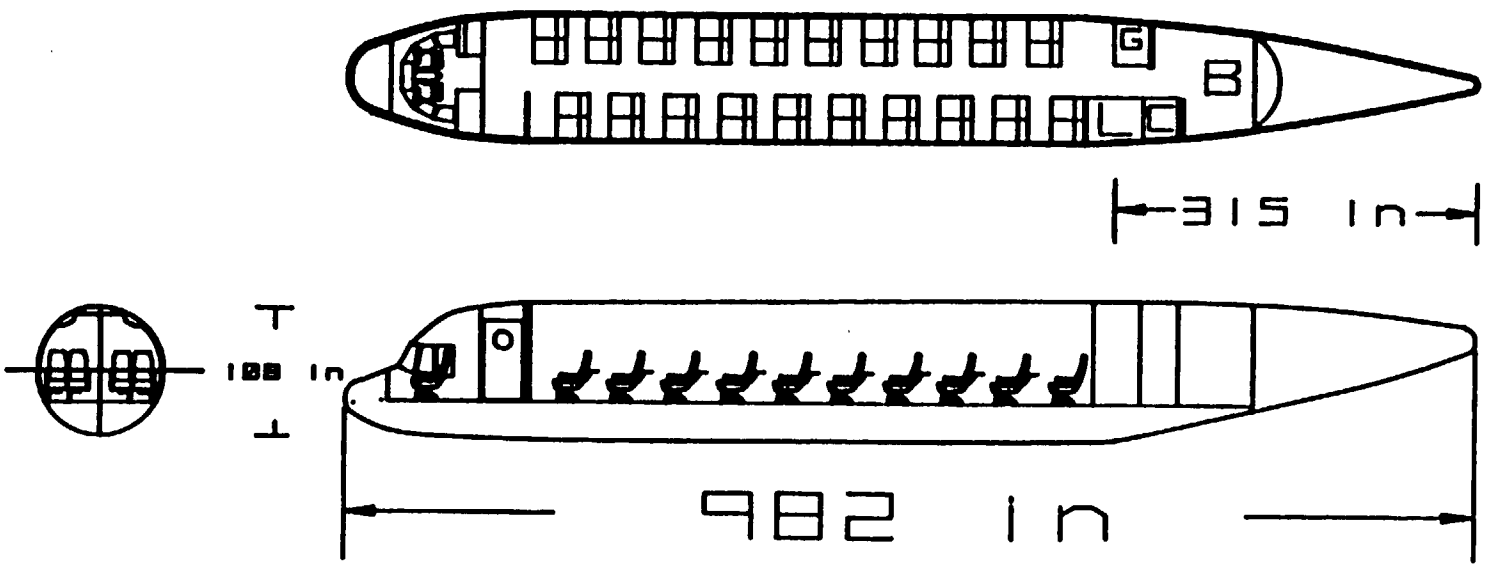

Figure 32 Fuselage Layout: 3-view

Class I Weight and Balance Analysis

The purpose of this analysis is to determine roughly whether or not the center of gravity of the proposed airplane design is in the right place for different loading scenarios. This method uses Roskam's class I method of weight and Balance analysis **Reference 10.**

A preliminary weight breakdown analysis is achieved by observing the breakdown in terms of percentage of empty weight of comparative aircraft. The following aircraft were compared:

Fokker F-27-100
DHC7-102
Fokker 614

Ratios of component weight to gross weight were averaged and used to calculate the CASH weight break-down. Table VII gives the breakdown.

Table VII CASH weight breakdown

component	weight (lbs)	
wing	4,170	
empennage	949	
fuselage		3,900
nacelles	1,119	
landing gear	1,288	
power plant	3,730	
fixed equipment	5,426	
empty weight	20,582	
payload	8,200	
crew	410	
fuel	7,101	
trapped fuel	182	
takeoff weight		36,475

The C.G. locations of each component were calculated and logged with respect to a datum 200 in. forward of the nose and 100 in. below the bottom part of the fuselage. Main C.G. components were tabulated. The wing was placed such that the overall C.G. for a full load is slightly forward of the wing aerodynamic center. This was done on a computer spreadsheet (see appendix). Different overall C.G. locations were calculated for empty, operational empty, operational empty + fuel, takeoff, and takeoff - fuel configurations. From this, the most forward and rearward C.G. locations were obtained. **Table VIII** gives the C.G. travel with respect to the mean aerodynamic chord and **Figure 33** shows how the C.G. and weight changes with different loadings.

Table VIII Maximum C.G. Travel

position	x/c
most forward	.06
most rearward	.22

The baggage weight balances over the C.G. such that the total travel distance is only 6 in. It is assumed, however, that the passengers are evenly dispersed in the cabin for loads less than capacity. For uneven loads, the C.G. travel is expected to change significantly. In order to minimize trim drag, it is recommended that a seat reservation system assign passengers to seats in an even fashion.

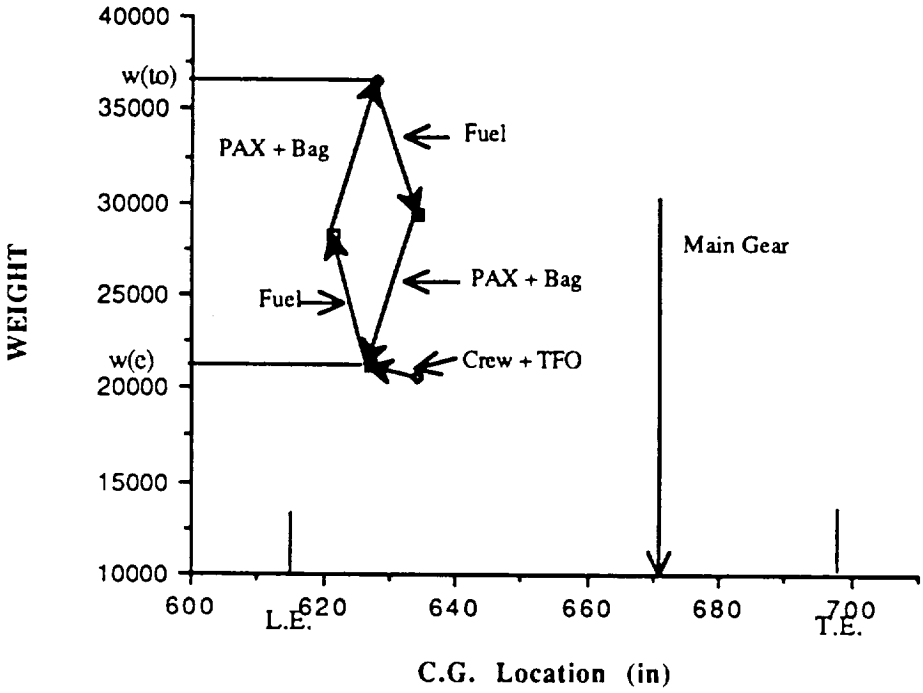

Figure 33 Weight-C.G. Excursion Diagram

Avionics

In order to achieve more complex transition and approach patterns in the terminal area under instrument conditions, it will be necessary to incorporate a digital fly-by-wire flight control system. Studies done on the QSRA using a fully computer controlled system proved feasibility in achieving complex precision approaches. This system will have heads-up and multi-function display screens.

The HUD will give the pilot more clear instrument readings on flight path, airspeed and other important flight parameters. The multi-function display will provide the pilot various mode screens in which he/she can easily switch. All flights coming into the terminal areas will be preprogrammed by the pilot before reaching the destination airport. The multi-function display will provide a map of the selected approach grid upon the arrival to the terminal area. The computer will fly the approach all the way to touchdown. The pilot will monitor all the systems and provide new information to the computer for any deviations in the flight plan. **Figure 34** is an example of a complex transition and approach to a terminal airport. Flight path, airspeed and stabilization command modes are accomplished by the computer by using a nonlinear, inverse model following methods. **Figure 35** shows the operation of this system. The computer system will have a high-tech Traffic and Collision Avoidance System (TCAS). This system will be required equipment in all airliners. If two aircraft are on a collision course, the computer from both planes will calculate a course of evasive action and steer out of danger automatically.

A complete fly-by-wire system allows CASH to have precise control of the aircraft in already overcrowded airspace in the terminal area. If the FAA requires preprogrammed flight plans for all aircraft inbound to the STOL port, lower aircraft spacings under instrument conditions can be achieved without compromising safety.

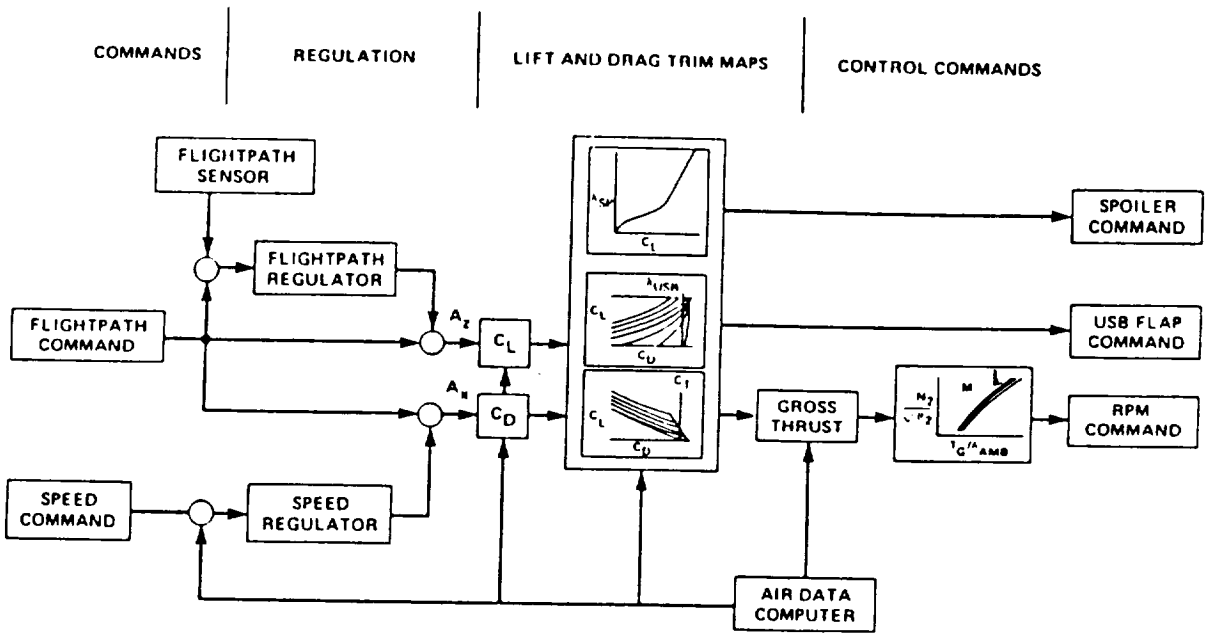

Figure 34. Nonlinear Inverse Concept for Flightpath and Airspeed Command and Augmentation System

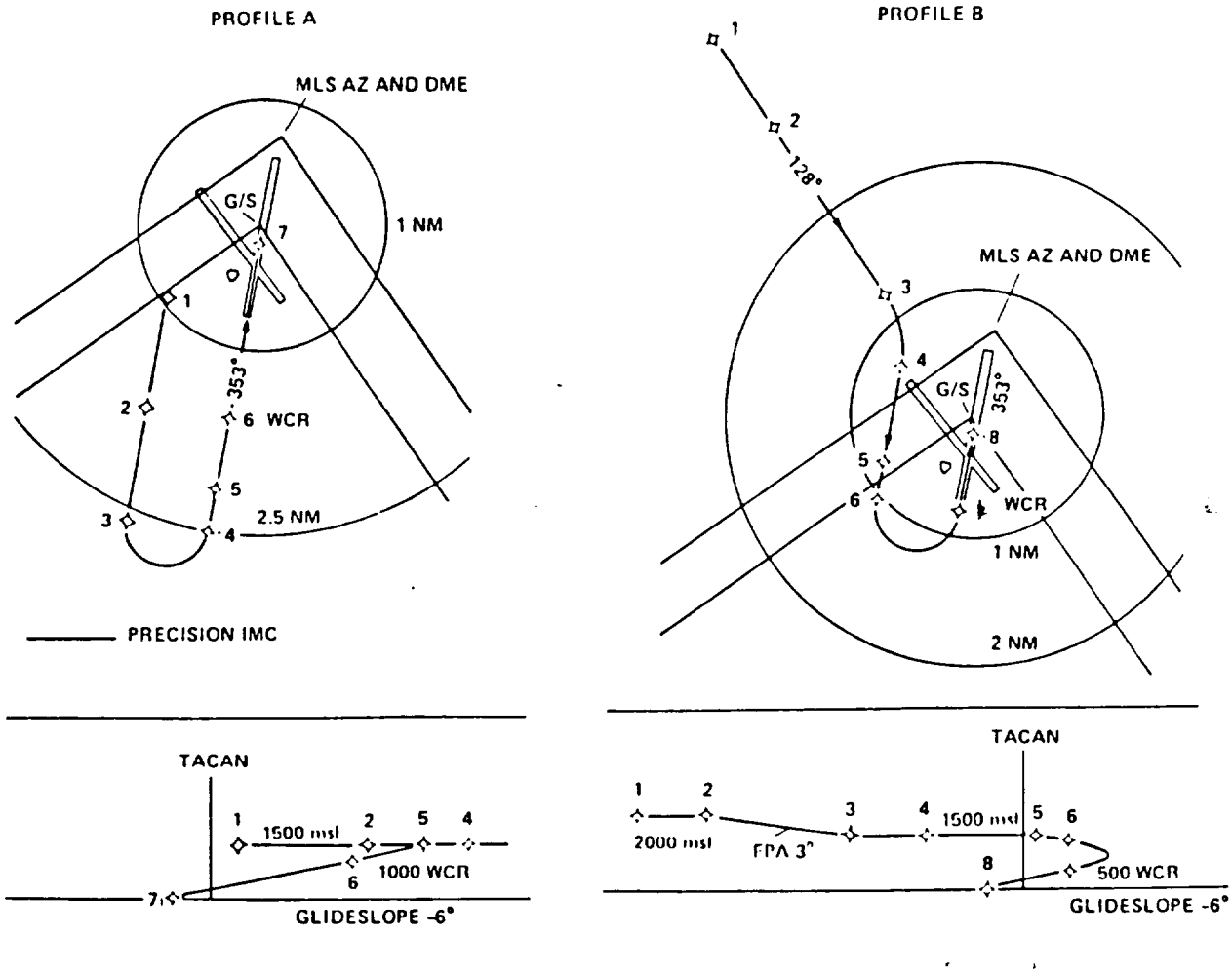

Figure 35 Reference Flight Trajectories for Transition and Approach

Landing Gear

Roskam's Class I method for landing gear sizing was used for CASH. It was necessary to calculate a rough estimate of C.G. location of the aircraft. A preliminary landing gear start disposition was selected at a point just forward of the cone angle. Two geometric criteria needed to be considered in deciding the disposition of the landing gear struts:

1) Tip-over criteria and θ , Ψ
2) Ground clearance criteria Ø

The longitudinal tip-over criteria must be greater than 15 deg. The main wheel is located so far aft that equals 20 deg. Since the main gear is designed to retract into the fuselage, the distance between the main gears is critical for lateral tip over criteria. This angle must be less than or equal to 55 deg. By setting Ψ equal 55 deg., the minimum main gear gap is 67.5 inches.

Based on typical landing gear data for a 44,000 lb regional turbo-propeller driven airplanes, wheel geometries were obtained. It was decided that two wheels per strut were sufficient to handle static loads. And two wheels per strut also minimize the size of the wheels, since the volume in the bottom part of the fuselage is limited. **Table IX** illustrates the dimensional parameters as well as static loads on gear.

Since the gear retraction volume is not sufficient to handle tandem wheel configuration, it is necessary to place the main gear wheels end to end. **Figure 36** is the selected main landing gear retraction system. It will be similar to the BAE 146.

Table IX Landing Gear Geometric Characteristic

Static Load per Strut

P_n:	4228 lbs
P_m:	16124 lbs
P_n / W_{to}:	.116
P_{mns} / W_{to}:	.884

Wheel Geometry:

	Diameter (in)	Width (in)
Main Gear	30	9
Nose Gear	23.4	6.5

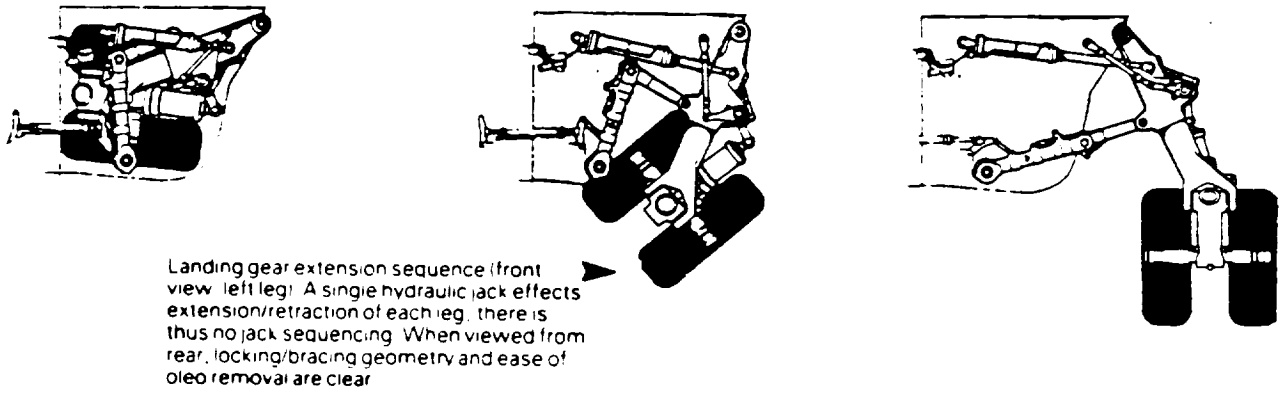

Landing gear extension sequence (front view, left leg). A single hydraulic jack effects extension/retraction of each leg, there is thus no jack sequencing. When viewed from rear, locking/bracing geometry and ease of oleo removal are clear

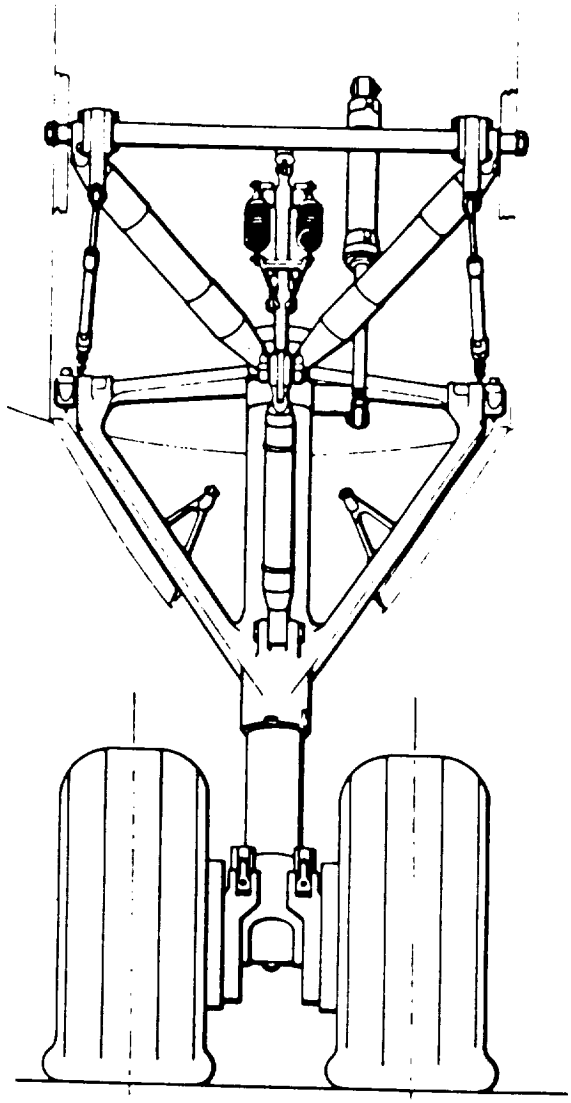

Figure 36 Landing Gear Arrangement

Stability Analysis

The stability analysis contained in this report is limited to static stability analysis for the preliminary design purpose (**Ref 10**). To achieve appropriate longitudinal and directional stability without losing in maneuverability and to minimize the initial cost, CASH adopted the conventional two surface control system. For the horizontal tail, a relatively larger area was suggested to compensate for the high thrust line and USB flap pitching moment. Also, the result from the C.G study shows that the C.G would not travel in wide range; therefore, the two surface control system with the relatively larger horizontal tail was expected to satisfy the stability criteria for CASH. CASH also uses an active fly-by-wire control system for its lighter weight and greater data handling capability. In the beginning of the analysis, the three surface control system was considered carefully. An addition of a flapped canard would increase the Cl_{max} during landing and take-off and decrease the size of the horizontal tail, however, it would also create unnecessary drag during cruise and increase the weight and initial cost of the aircraft. The final report of the QSRA from NASA shows that the QSRA designed with the two surface control system achieved satisfactory stability control. The final result from the calculations shows that CASH satisfies the stability requirement. To improve the aircraft handling quality for the low speed STOL regime, lateral, longitudinal, and directional stability augmentation systems are available.

Static Longitudinal Stability

With the estimated area of 113 ft^2 for the horizontal tail, the static margin of 0.058 was found for the most AFT C.G.(**Fig. 37**)

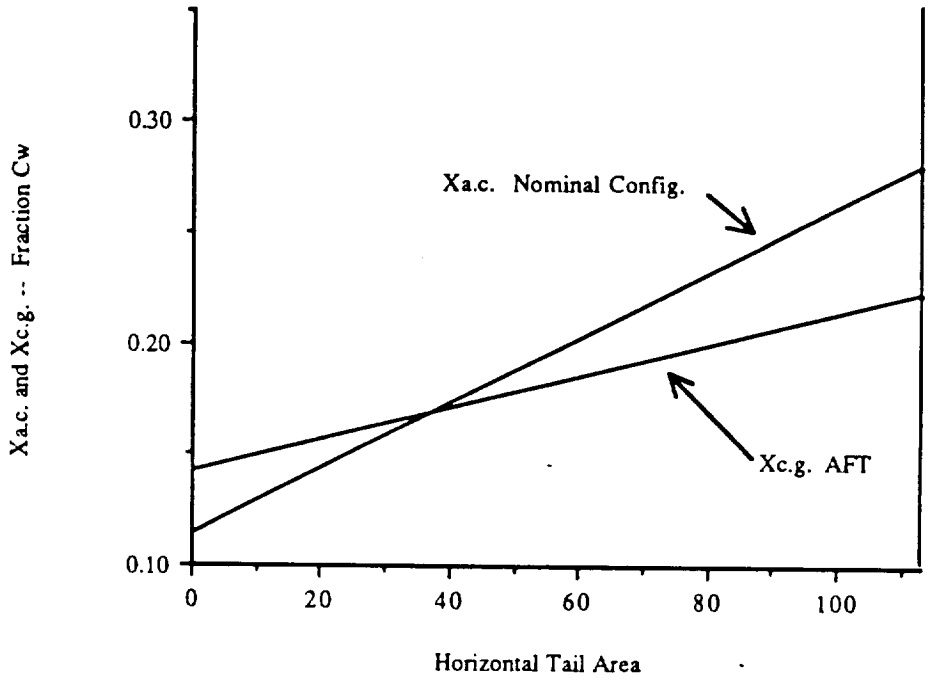

Figure 37 Longitudinal X-Plot

This static margin satisfies the minimum requirement requested by Roskam's Design Book II. The equation applied to compute the static margin is as follow:

$$dC_m / dC_l = (X_{cg}-X_{ac}) / c \qquad \text{(eqn 3)}$$

where

$$X_{ac}/c=[X_{acwb}/c+\{C_{lah}(1-de/da)(S_h/S)X_{ach}/c-C_{lac}(1+dec/da)X_{acc}/c(S_c/C)/C_{lawb}\}/F \qquad \text{(eqn 4)}$$

where

$$F=[1+\{C_{lah}(1-de/da)(S_h/S)+C_{lac}(1+dec/da)(S_c/S)\}/C_{lawb}] \qquad \text{(eqn 5)}$$

(note: since the CASH was opted for the conventional two surface control system, the terms for the canard are ignored)

The minimum static margin required by Roskam's Design Book II is 0.05c.

A sample calculation is provided for the most AFT C.G in the Appendix, since the most AFT C.G generates the smallest static margin. All data used in the calculations were generated from the appropriate equations and diagrams contained in **Ref. 10 and 14.**

Static Directional Stability

The major preliminary static directional stability concern was the determination of the size of the vertical tail that can overcome the most critical condition of one outer engine inoperatiove. To decide the

size, The procedures from Roskam's design text was followed. From the calculation, the maximum critical speed was found to be 72 kts by manipulating the landing stall speed of 60 kts (V_{mc}=1.2Vs). Approximately, 10 deg. rudder deflection, of the 25 deg. maximum allowed by **Ref. 10**, was estimated for the most critical condition. Therefore, the directional stability control is not a problem with the suggested size of the vertical area. For directional stability equation:

$$C_{nB}=C_{nBwb}+C_{lav}(S_v/S)(X_v/b) \qquad \textbf{(eqn 6)}$$

where

$$C_{nBwb}=C_{nBw}+C_{nBb} \qquad \textbf{(eqn 7)}$$

(note: Roskam recommends C_{nBw}=0 for the preliminary design purpose since the wing contribution is important only at high angle of attack)

Roskam's text suggests to assume the overall level of directional stability to be C_{nB}=0.0010/deg. Without counting the wing contribution C_{nB} was found to be -0.0048/deg. This value reduced the size of the vertical tail to 62 ft^2.(**Fig. 38**) But, after reviewing the **Ref. 15**, originally suggested size of 81 ft^2 was found to be more beneficiary for the CASH, since the CASH has relatively high angles of attack for landing and take-off.

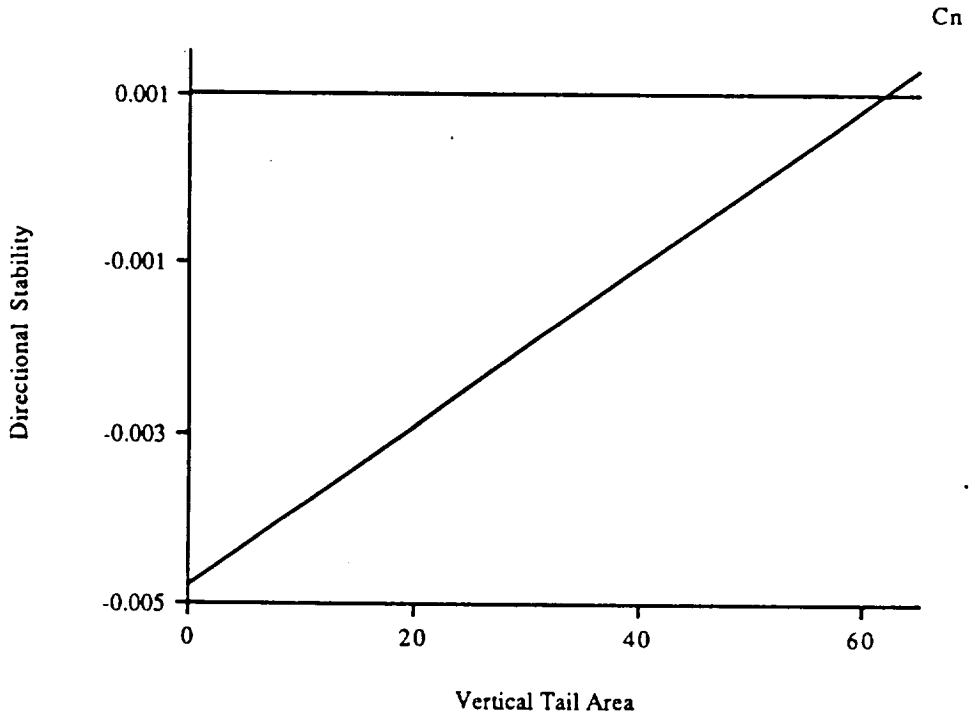

Figure 38 Directional X-Plot

Baggage and Passenger Handling

CASH is designed to have a short turn-around time at major city airports. For this reason, baggage and passenger handling must be accomplished at minimum time. For CASH, baggage and cargo is carried in "standard" containers. From a competitive viewpoint, it is important to be able to carry as many different types of containers as possible. CASH is designed for conversion from a 40 passenger airplane to a cargo plane within a short period of time.(**Fig. 39**) When CASH is converted to a cargo plane, it becomes capable of carrying four 118 x 75 x 90 in. containers. For cargo, a workable average density is: 10 lbs/ft^3.

Inspection, Maintenance and Servicing

In transport operations it is essential that the "turn-around" time be minimized as much as possible. This means that a large number of vehicles need to have simultaneous access to the airplane when parked at the gate. CASH is designed for a maintenance "turn-around" time of less than 30 minutes.(**Fig. 40**) It allows loading and unloading passengers, refuel and reoil, replenish potable water, clean airplane cabin, and service lavatories at the same time.

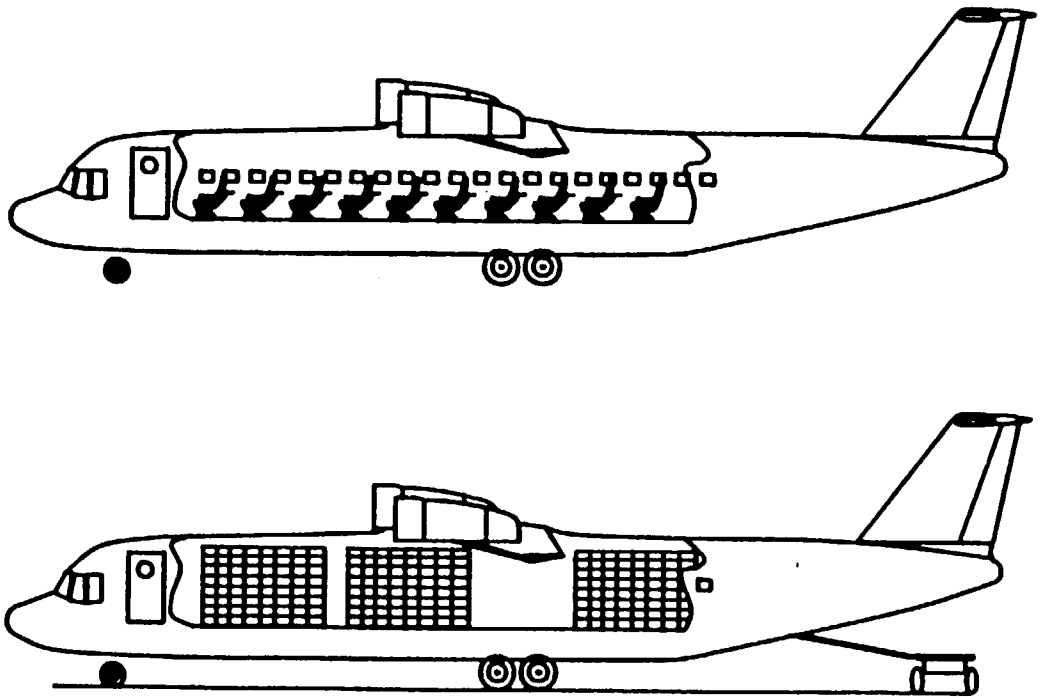

Figure 39 Passenger / Cargo Arrangement

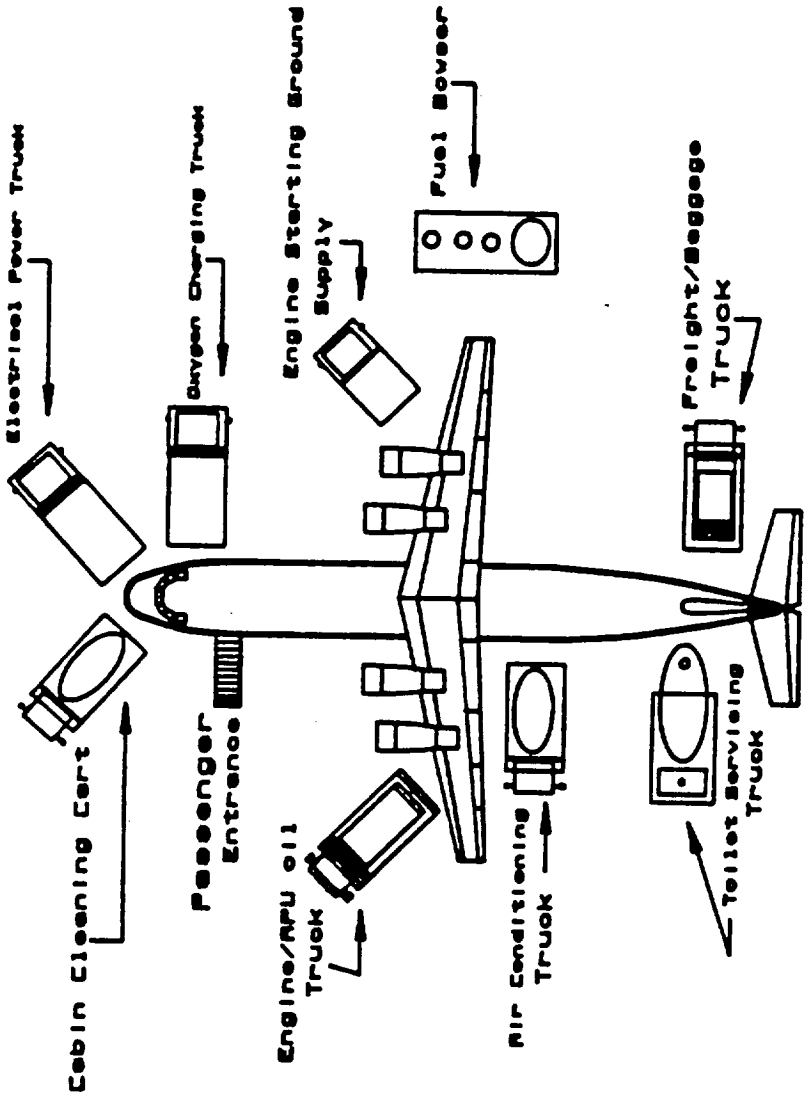

Figure 40 Inspection, Maintenance and Servicing

Cost Analysis

The estimation of the unit cost or the cost estimating relationship (CER) for the development, testing evaluation and production will be based upon the methods presented in **Ref. 16**. The procedures and sample calculations are well illustrated in **Ref 15**. Procedures and assumptions made for the calculations of the cost analysis are shown in appendix A. The results show a unit cost of 5,969,409.29 dollars, which is very competitive to any aircraft in the same class with CASH. For example, Canada's De Haviland DHC-8, Czechoslovakia LT610, and Swedish SAAB SF 340 would be categorized as the same class as CASH and their unit costs fall between 5,000,000 and 6,000,000 U.S. dollar.(**Ref. 17**) However, CASH with the higher cruise speed and shorter field length required for takeoff and landing easily outperforms any of the three aircraft.

The total operating cost consists of direct and indirect operating cost. Direct operating cost is directly associated with a specific flight. The cost of fuel, payroll of crew, overhaul time of engine, insurance, depreciation rate and maintenance of aircraft are direct functions of each flight. The indirect operating cost includes office payroll, advertising, hangar costs and other miscellaneous items. The total operating cost was very difficult to determine with any degree of accuracy since they often vary drastically from one airline to another. For a very rough estimate, the indirect operating cost is often assumed to be equal to the direct operating cost. The estimation of direct operating cost (dollars per ton mile) was based on **Ref. 18**. The methodology contained in this reference is still the basis of the D.O.C. calculations, but the coefficients of the formulas have been revised to accommodate the differences in cost of labor, materials, fuel and also different practices in maintenance. These revisions are based on the work done by Boeing. It is well explained in **Ref. 9**. The direct operating cost in this report is evaluated for a one way trip of 500 nm. The D.O.C for CASH is 1.41485 dollars per ton-mile. This means 0.14502 dollar per passenger-mile and 42.06 dollars to carry a passenger from San Luis Obispo to LAX airport, assuming the distance is 200.00 statute miles and 55% of the 40 seats are occupied. American Eagle, a major commuter airline operating between LAX and San Luis Obispo, is currently charging a passenger 90 dollars for the one way trip as of May, 1989. If CASH is in operation today for the same route, it would bring in 114% of the total cost as the net profit.

Conclusion

To meet the needs of the California Corridor in the year 2010, two mission profiles were defined in the very beginning of the design: intermetro flights and commuter flights. For designing CASH, the decision was made to focus on the travelers flying any routes that are within the radius of 250 nautical miles from Los Angeles or San Francisco as well as the direct route between the two cities. A considerable increase of air traffic volume in these routes are expected by the year 2010. In order to accommodate this increase without creating massive air traffic congestion in already overcrowded LAX and San Francisco International airports, innovative CASH that minimizes layover time and noise was designed. Upon the completion of the preliminary design of CASH, a speculation was made that quiet CASH with STOL capability can outperform the aircraft in current service.

Roskam's Aircraft Design was used as a guideline. After the preliminary design was completed, few newly developed technologies were recognized and are strongly recommended for further research in the future to achieve better results for CASH. The following list shows the subjects recommended for future study.

* Manufacturing Processes of composite materials

* Small efficient high by pass ratio engines

* Optimization of engine disposition for efficient high speed cruise

* Fully automated flight control system

Further detailed studies of these subjects will considerably increase the credibility of CASH. Equipped with these new innovative technologies, CASH will be able to produce valuable service for the California Corridor in the year 2010.

REFERENCES

1. F.A.A. Aviation Forecasts Fiscal Year 1988-1999, Department of Transportation, Federal Aviation Administration, FAA APO 88-1, February 1988.

2. Sponseller, Michael, "Magnetic Train", Popular Science, December 1988.

3. Lemonick, Michael D., "2001 Transportation, On Track But Off The Rails", Discover, November 1988.

4. The Development of a Quiet Short-Haul Research Aircraft - Final Report, NASA #152298

5. Aircraft Composites Energy Efficiency Technology, ACEE Composites Structures Technology Conference, August 1984, NASA-cr-172358

6. DeMeis, Richard, "Another Chance For Canards", Aerospace America, October 1988.

7. Larson, George C., "Let's Stop Fueling Around With Inefficient Engine Designs", Aviation Week and Space Technology, August 10, 1987.

8. Brown, Alan, "Taming Ceramic Fiber", Aerospace America, May 1989

9. Corning, Gerald, Supersonic and Subsonic, CTOL and VTOL, Airplane Design, 1960

10. Roskam, J. , Airplane Design: Part II, Preliminary Configuration Design and Integration of the Propulsion System.

11. Walsh, MJ, Turbulent Boundary Layer Drag Reduction Using Riblets, AIAA 20th Aerospace Sciences Meeting, Orlando, FL, January 11-14, 1982. AIAA paper no. 82-0169

12. Walsh, MJ : Sellers, W.L.; McGinley, C.B. : Riblet Drag Reduction At Flight Conditions. AIAA 6th Applied Aerodynamics Conference, Williamsberg, Virginia, June 6-8, 1988. AIAA paper No 88-2554.

13. Marsh, George, "Breathing Space", Commuter World, April-May 1988.

14. Perkins, Hage, Airplane Performance Stability and Control, John Wiley & Sons, 1949.

15. Nicoli, Fundamentals of Aircraft Design, 1975

16. Levenson, G.S., Boren H.E., Tihansky, D.P., and Timson, F., "Cost-Estimating Relationships for Aircraft Airframes", Rand Report R-761-PR, Rand Coorp. Santa Monica, CA DEC. 71.

17. Pilling, Mark; Smrcek Ladislav, "Let's Lift Off", Commuter World, April-May 1989.

18. Air Transport Association of America, "Standard Method of Estimating Comparative Direct Operating Costs of Turbine Powered Transport Airplanes", 1967.

HCSRT

High Capacity Short Range Transport

A Design For the Year 2010

Designed by:

Brent Bauer

Lincoln Keill

Michael Kelly

David Mounkes

Donald Wilmot

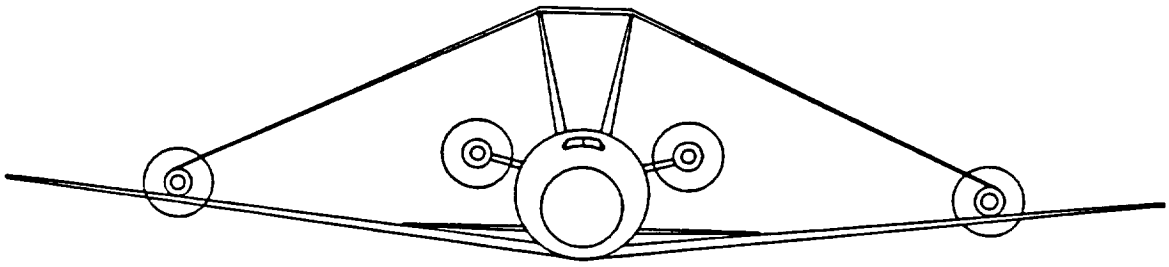

California Polytechnic State University

Aeronautical Engineering Department

Aero Design Class 1989

ABSTRACT

An effort was made to design an aircraft which would fulfill the high demands of the California corridor in the year 2010. It was determined that a 600 passenger vehicle would provide a possible solution by reducing airspace congestion and still meet the transportation needs of the populous. By utilizing current and projected technology, the most efficient aircraft was sought. The results were a joined wing vehicle, powered by unducted fan engines which burn hydrogen fuel. Herein lies the results of that research.

Table of Contents

List of Figures

List of Figures Cont.

List of Tables

List of Symbols

AC	Aerodynamic center
a	Lift curve slope
AR	Aspect ratio
b	Wing span
c	Chord/Specific fuel consumption
cg	Center of Gravity
D	Distance/Drag
d_f	fuselage diameter
E	Endurance
e	Oswald efficiency factor
f	Parasite area
k	Correction factor
L	Lift
l_f	Fuselage length
l_m	Length from gain main gear to cg
l_n	Length from cg to nose gear
M	Mach number/Mission fuel factor
n	Number of main struts
P_m	Static force on main struts
P_n	Static force on nose struts
R	Range

RC	Rate of Climb
Re	Reynolds number
S	Wing area
T	Thrust
t	thickness
U	Velocity in x-direction
V	Velocity
W	Weight

GREEK SYMBOLS

α	Angle of attack
α_i	Incidence angle
δ	Deflection angle
Λ	Sweep angle
γ	Climb angle
λ	Taper ratio
ν	Kinematic viscosity
ρ	Density

SUBSCRIPTS

a	Aileron
c	Canard
CL	Climb

1.1 Introduction

The California Corridor is one of the most heavily traveled airways in the world. Air traffic is increasing at an alarming rate, with California's population growth rate being one of the highest in the nation. The Corridor is a system that is already operating at its capacity and is unable to meet the transportation needs for the year 2010.

To solve this problem a transportation system was conceived that comprised of two elements. The first element proposed was a network of STOL and VTOL community airports to relieve a large portion of the traffic at the major hubs. However, this network was not considered able to accommodate all of California's growth. The construction of the community airports would have major problems in funding, noise, and safety concerns for the surrounding communities. These concerns were expressed in the interview in reference 6. These problems will most likely limit the number of STOL and VTOL airports possible thus compromising the ability of this system to handle all of the corridors needs. Therefore, a second element was incorporated in to the transportation system. This second element was designed to improve of the transportation system at the major hubs. The major hubs concentrated on were LAX, SFO, San Diego, San Jose and Sacramento.

It was considered that the most effective way to reduce the traffic at the hubs was to reduce the number of aircraft

in service by increasing the passenger capacity per aircraft. A large high capacity aircraft would result in fewer aircraft needed to accommodate a given number of passengers. These large aircraft were found to improve all aspects of airport and airspace overcrowding. The air traffic control system is already over stressed and any reduction in the volume of air traffic would be beneficial. Although there has been much consideration and investigation in the computerization of the ATC system it was considered not to be sufficiently developed for the year 2010. It would almost certainly not be accepted by the public in this time frame. Typically corridor traffic is enroute for only one hour but must loiter for another half hour waiting for an open runway. A large aircraft for the Corridor would decrease the number of aircraft requiring a runway time slot. This would improve the efficiency of the runways by increasing the number of passengers per runway slot. Reference 6 indicated the possibility of airlines being charged for runway slots to try and push for more efficient runway use. The large commuter transport would maximize the number of passengers handled for a given runway fee. The reduction in the number of aircraft would also reduce the problems of accommodating these aircraft in the airport terminals and taxiways.

The High Capacity Short Range Transport was designed to fulfill the need to improve the traffic at the major hubs. The mission specifications developed, are listed in table 1.1.

Table 1.1 Mission Specifications

Payload:	600 passengers at 175 lbs each and 30 lbs of baggage each.
Crew:	Two pilots and twelve cabin attendants at 175 lbs each and 30 lbs baggage each.
Range:	870 nautical miles (1000 statute miles), which includes a 45 minute loiter, followed by a 100 statute mile flight to alternate (This range enables the aircraft to operate in other similar corridors, or to make a round trip without refueling).
Altitude:	Cruise at 30,000 feet (for the design range).
Cruise Speed:	M = 0.80 at 30,000 feet (for 1 hour cruise time).
T.O. and Landing:	FAR 25 fieldlength, 8600 feet (use of existing conventional hubs).
Mission Profile:	Typical passenger transport operation in the California Corridor.

Destination Distances

Los Angeles to/from San Francisco	292 nm	(336 sm)
Los Angeles to/from Sacramento	312 nm	(360 sm)
San Diego to/from San Francisco	387 nm	(446 sm)
San Diego to/from Sacramento	407 nm	(469 sm)

2.0 Results

The following tables and figures of sections 2.1 (specifications) and 2.2 (geometry) are the results of the HCSRT design.

Table 2.1 includes a tabular form of the HCSRT's specifications. Figures 2.1-1 through 2.1-4 contain the power and thrust curves for sea level and cruise altitude conditions. Figures 2.1-5 through 2.1-7 contain the drag polar curves for take-off, landing and clean configurations. All results may be verified in the sample calculations (appendix 1). Finally, figure 2.1-8 is a rate of climb against altitude plot.

Table 2.2 is a review of the HCSRT geometries. Because of the unique joined wing geometry, figure 2.2-1, a diagram of the wing, has been included. Table 2.2-1 is a comparison of some parameters of the HCSRT to the Boeing 747 short range model and the McDonnell Douglas DC-10 series 10.

Section 2.3 contains the results of the wing structure sizing. Most of this data was obtained from the NASA code JWAOPT, obtained from reference 18. The results of this program were recently verified in the NASA wind tunnel test results of their own experimental joined wing aircraft (reference 17).

2.1 HCSRT Performance

Table 2.1 Performance Specifications

Velocities:

Stall at sea level:	145 knots
Stall at 30,000 ft:	237 knots
V_{ne} at Sea Level:	422 knots
V_{ne} at 30,000 ft:	572 knots
Take-off:	231 knots
Rotation:	206 knots
Best Angle of Climb:	273 knots
Best Rate of Climb:	359 knots
Cruise:	458 knots

Weights:

W_{to} = 438,682

W_E = 295,982

W_{OE} = 300,800

W_F = 14,880

W_{PL} = 123,000

Cruise:

CL_{alpha} = .0968 deg^{-1}

CN_{beta} = .0065 deg^{-1}

Static Margin = 7.4 feet

DOC = .0309 $/ton-mi.

SFC = 40 pass-mi/lb-fuel

$CL_{cruise} = .471$

$W/S_{cruise} = 125\ lb/ft^2$

$L/D_{cruise} = 17.9$

Range = 1000 sm

Endurance = 1.06 hours

$T_{max} = 121{,}000$ lbs

T/W = 0.274

Service Ceiling = 40,000 ft

Take Off Length = 8600 ft

Drag Polars:

Clean:

$.0195 + .031CL^2$	$L/D_{max} = 20.3$	$CL = .793$

Take-Off:

$.0545 + .034CL^2$	$L/D_{max} = 11.6$	$CL = 1.27$

Landing:

$.1045 + .037CL^2$	$L/D_{max} = 8.0$	$CL = 1.68$

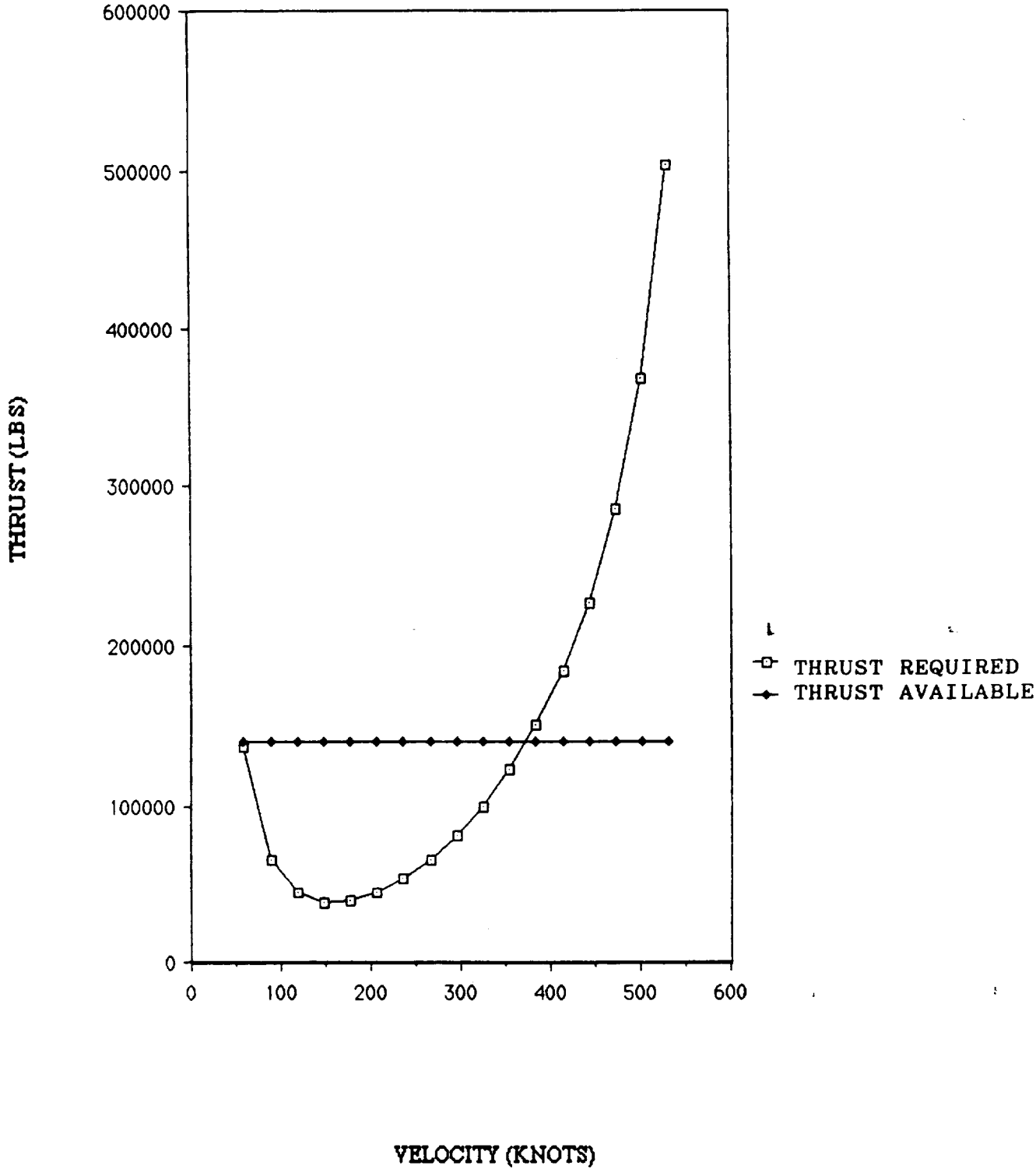

Figure 2.1-1

THRUST REQUIRED, T.O. & SL CONDITIONS

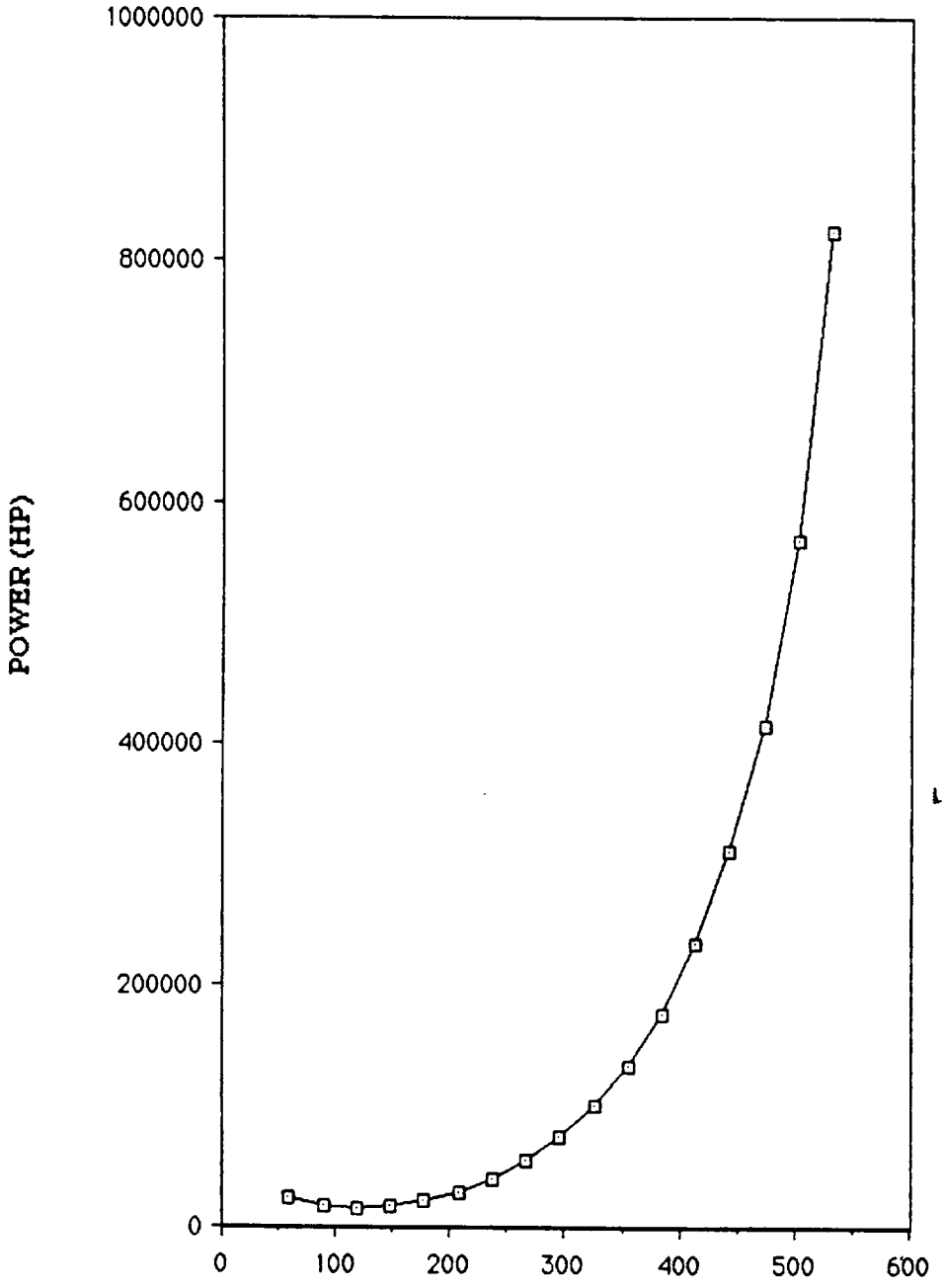

Figure 2.1-2

POWER REQUIRED, T.O. & SL CONDITIONS

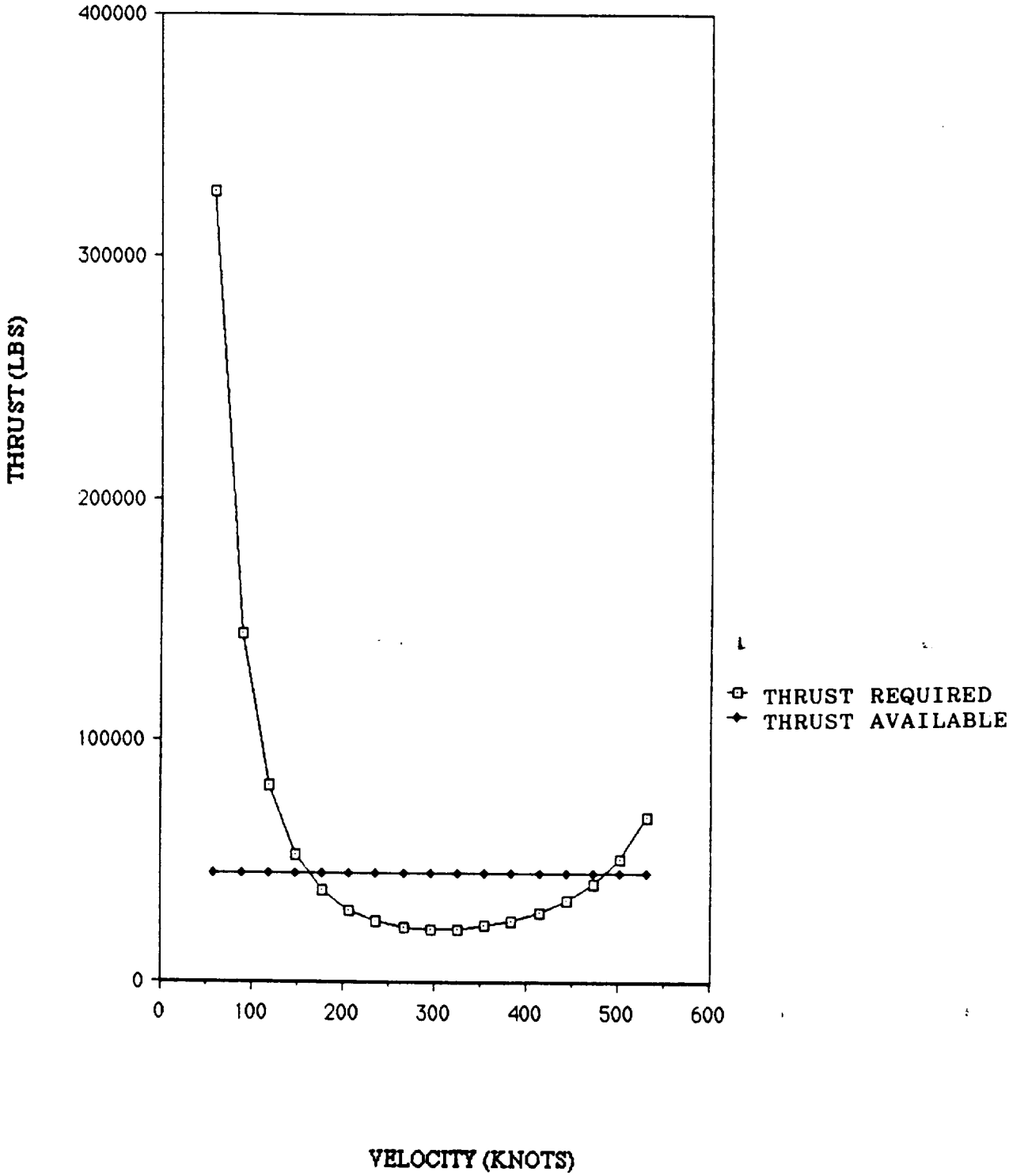

Figure 2.1-3

THRUST REQUIRED, CLEAN @ 30,000 FEET

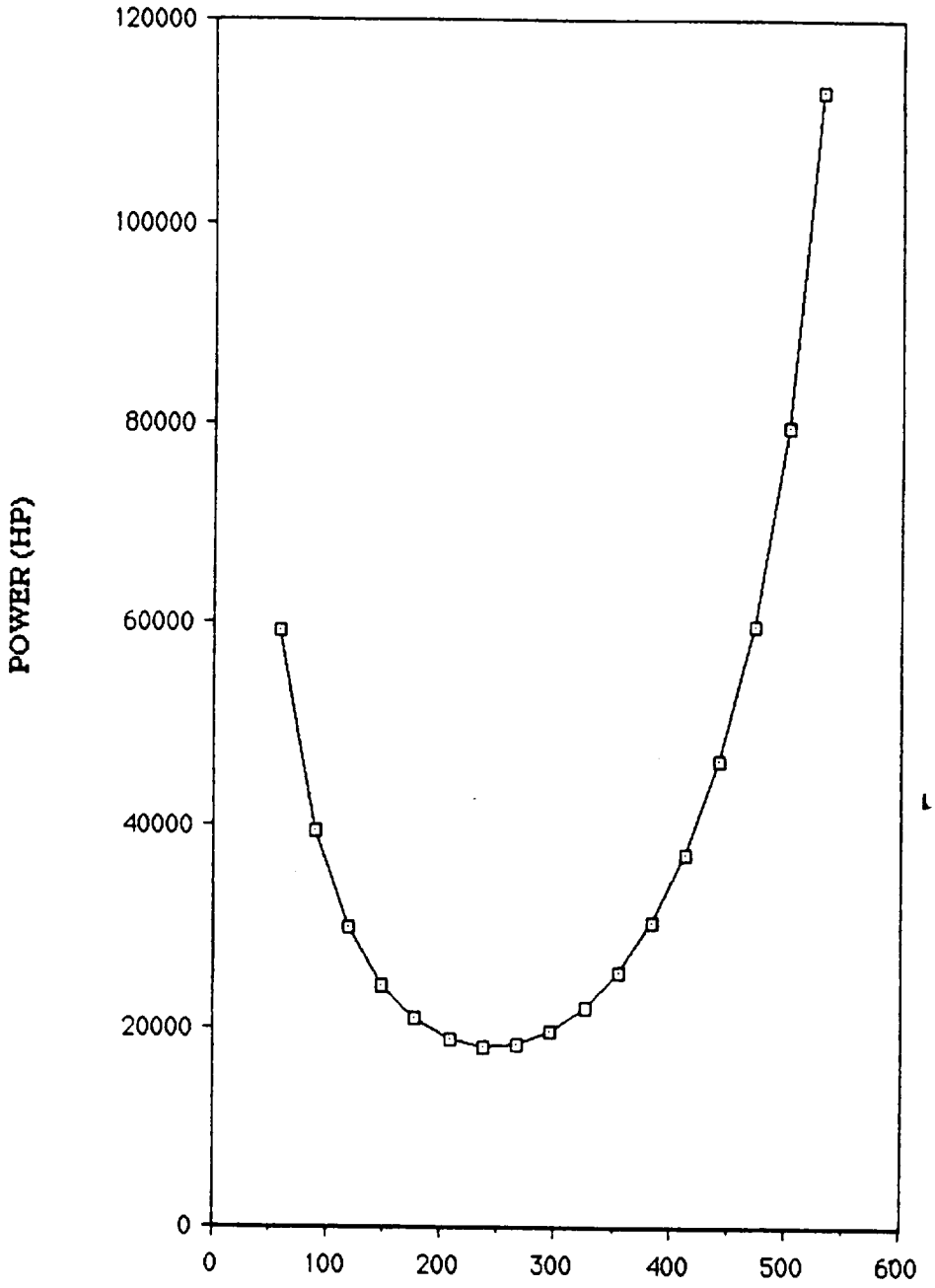

Figure 2.1-4

POWER REQUIRED, CLEAN @ 30,000 FEET

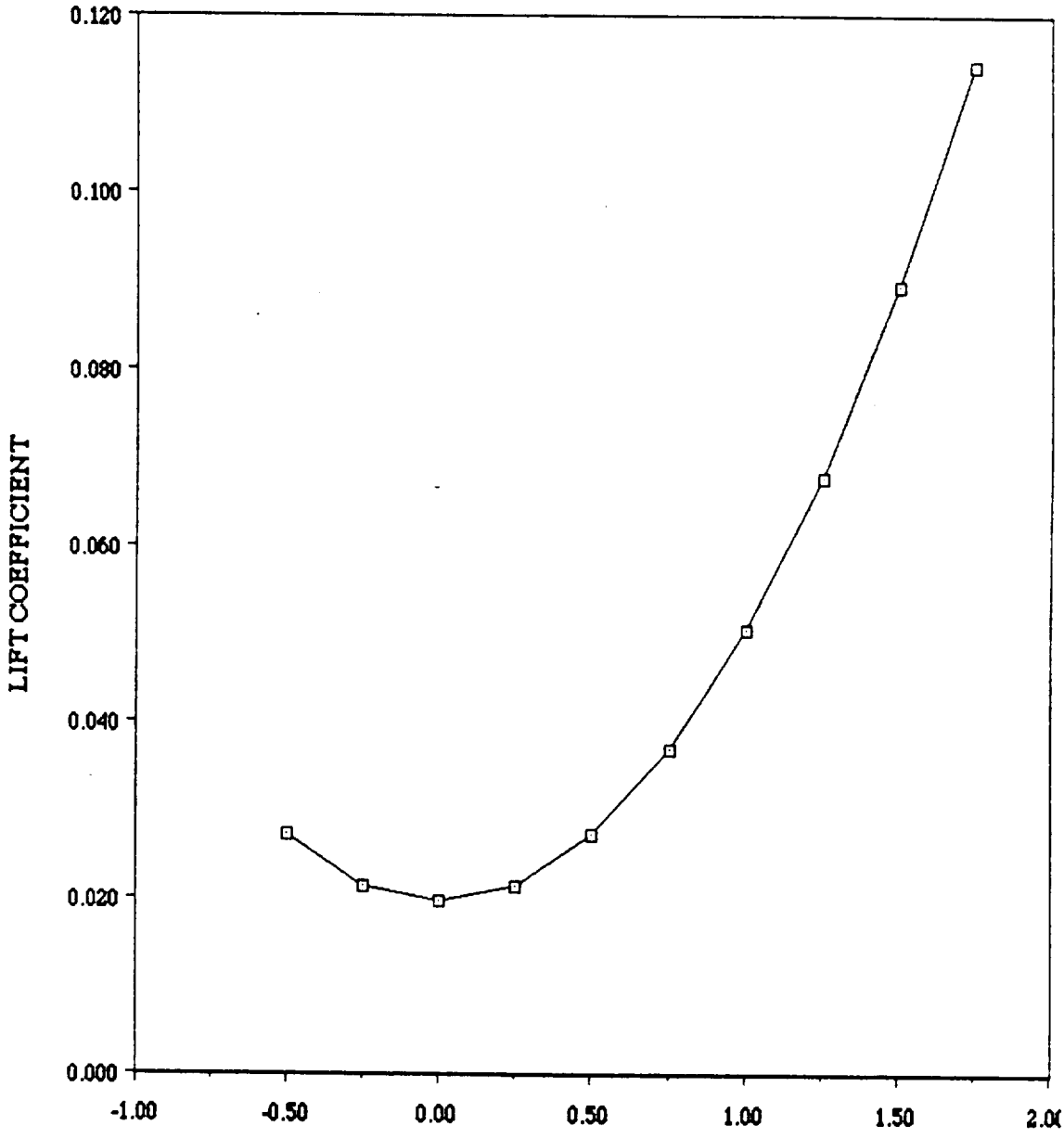

F:

Drag Polar (Clean)

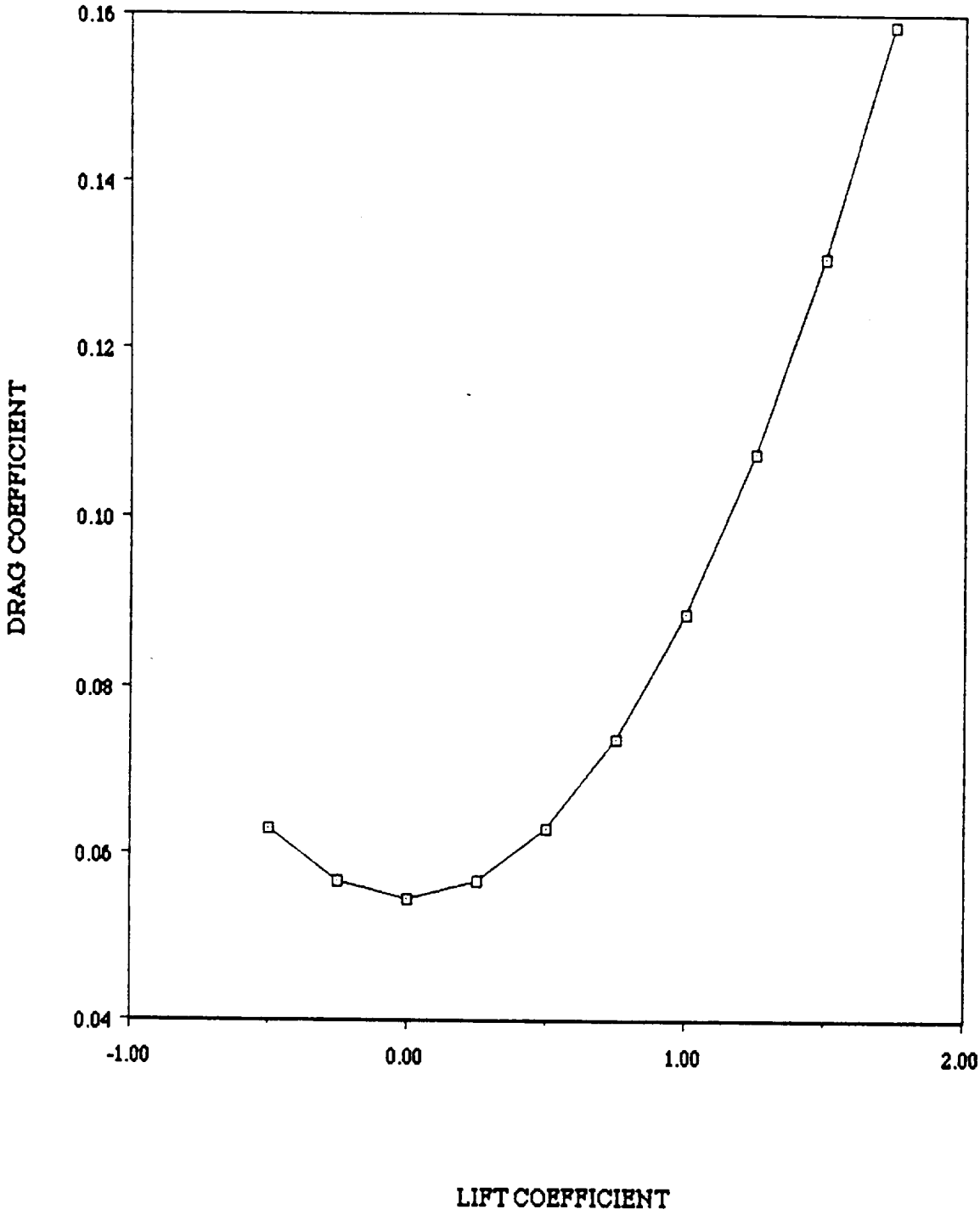

Figure 2.1-6

Drag Polar (Take off)

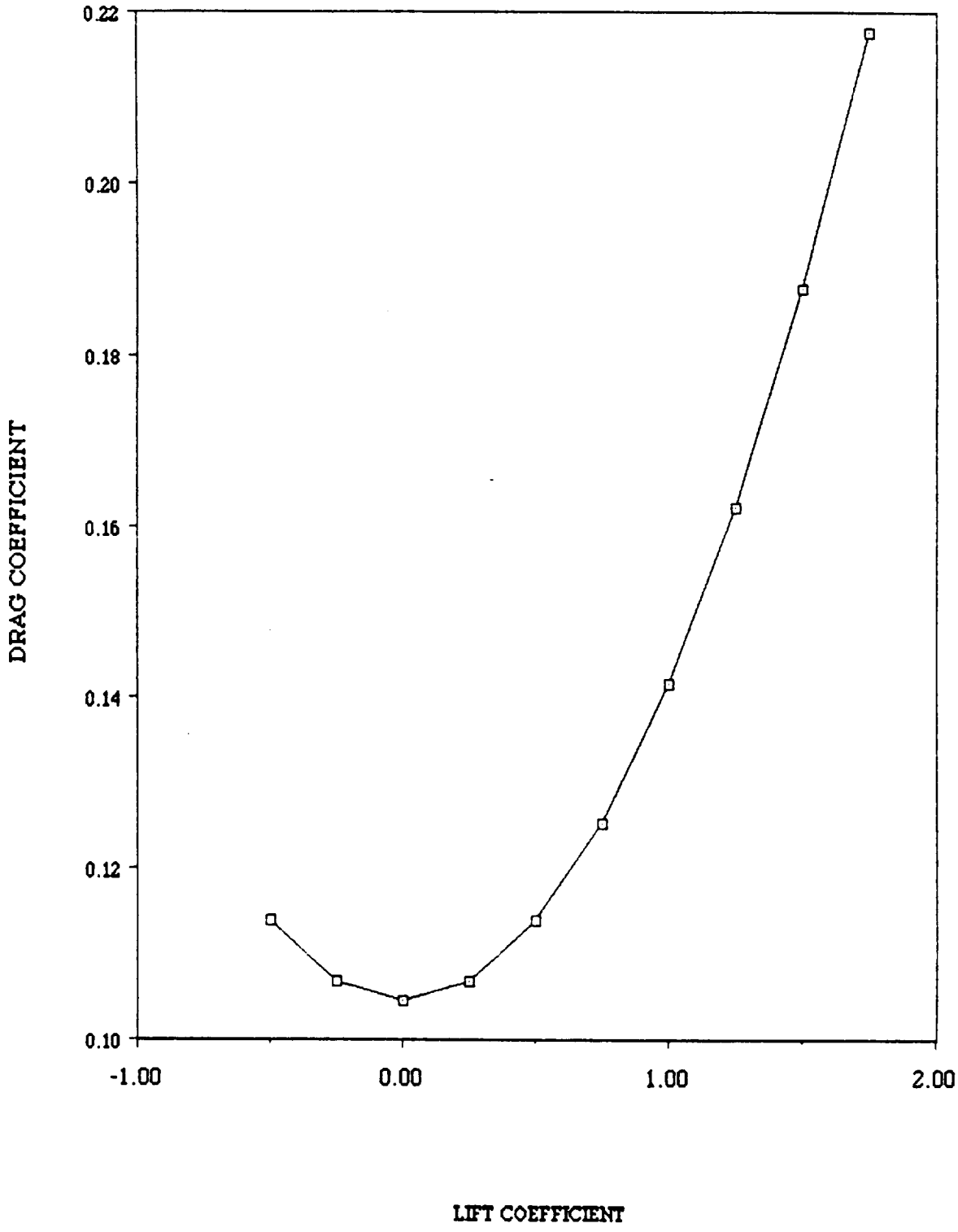

Figure 2.1-7

Drag Polar (Landing)

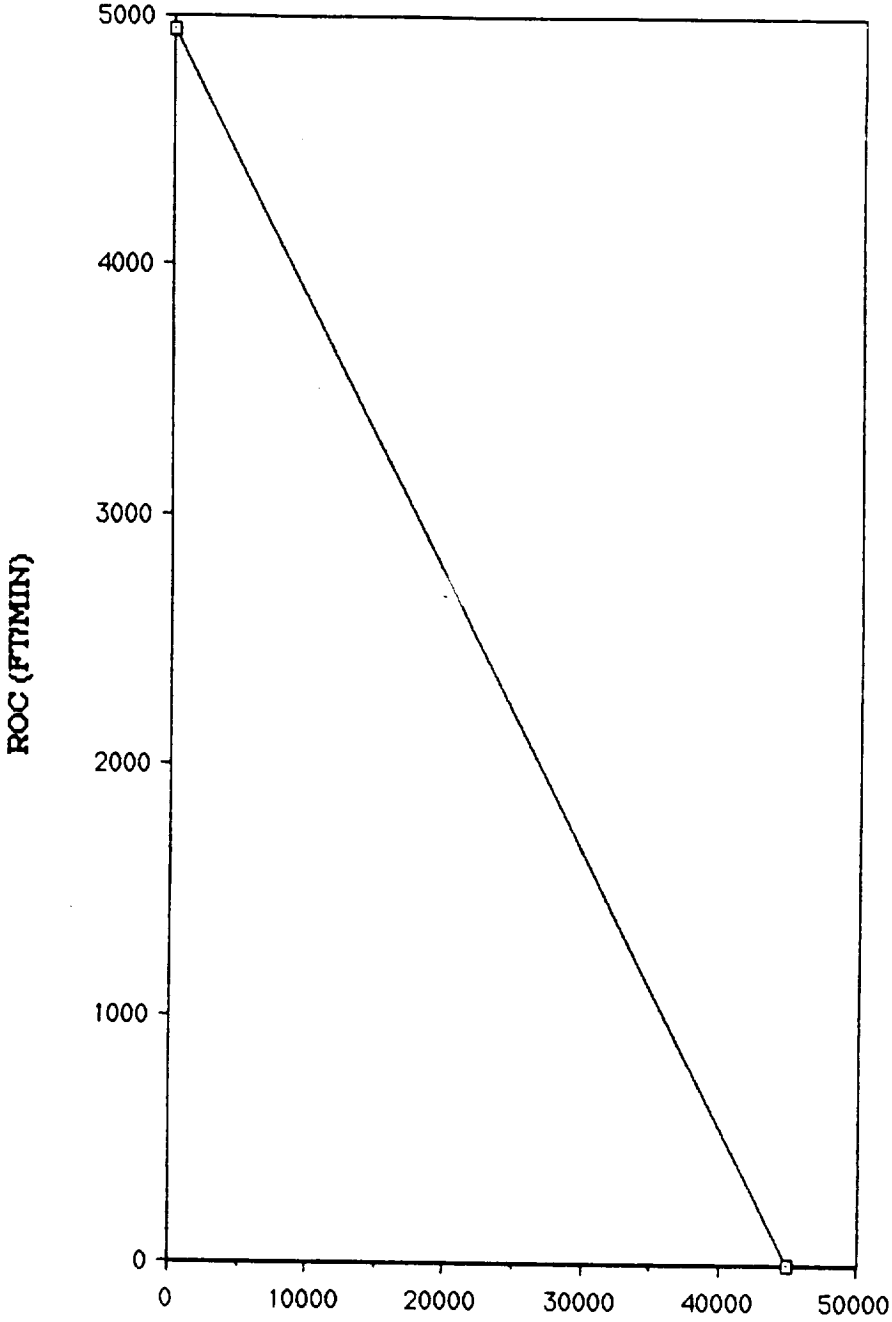

Figure 2.1-8

RATE OF CLIMB VS. ALTITUDE

2.2 HCSRT Geometry

Table 2.2: HCSRT Geometry

Fuselage:	Diameter	22.5 feet
	Length	225 feet
Front Wing:	Aspect Ratio	15.5
	Span	195 feet
	Surface Area	2450 square feet
	Sweep Angle	30 degrees
	Taper Ratio	0.35
	Wing Dihedral	6 degrees
	MAC	12.6 feet
	Root Chord	18.6 feet
	Tip Chord	6.5 feet
Rear Wing:	Aspect Ratio	17.7
	Span	136.5 feet
	Surface Area	1050 square feet
	Sweep Angle	-40 degrees
	Taper Ratio	0.35
	Wing Dihedral	-20 degrees
	MAC	7.69 feet
	Root Chord	11.4 feet
	Tip Chord	4.0 feet

Table 2.2 HCSRT Geometry continued

Canard:	Aspect Ratio	6.2
	Span	60 feet
	Surface Area	580 square feet
	Sweep Angle	30 degrees
	Taper Ratio	0.35
	MAC	9.67 feet
	Root Chord	13.0 feet
	Tip Chord	5.5 feet
Vertical Tail (Each):		
	Surface Area	400 square feet
	Height	20 feet
	Sweep Angle	30 degrees forward
	Root Chord	20 feet
	Tip Chord	9 feet
Miscellaneous:	Total Wing Surface Area	
	With Canard	4080 square feet
	Without Canard	3500 square feet

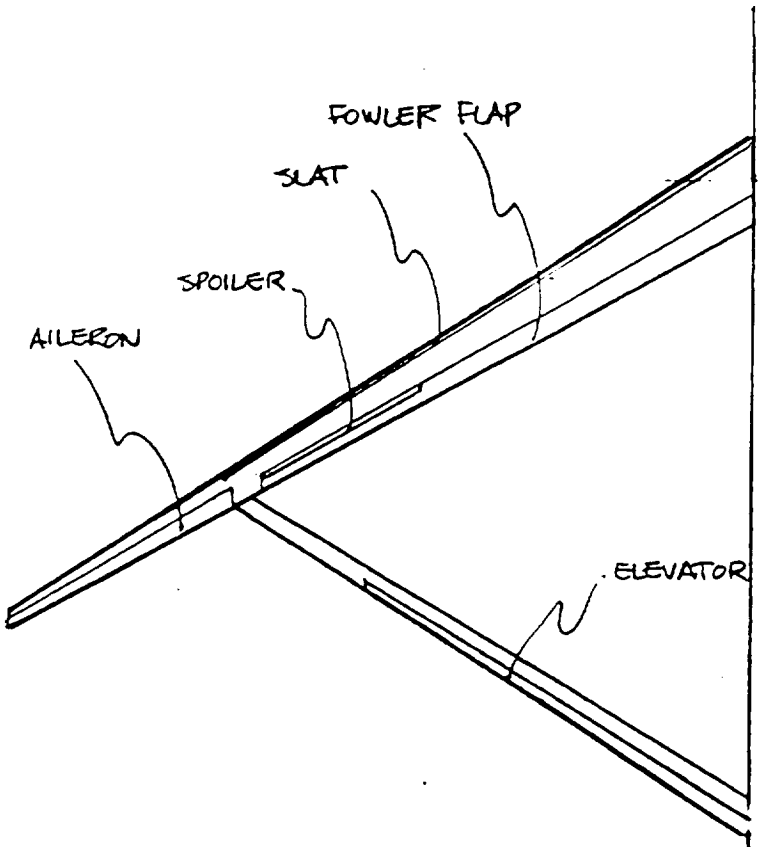

Aileron Span	.70-.97 b_f (30.4 ft)
Avg. Aileron Width	.50-1.00 c_f (34 ft)
Spoiler Span	.50-.70 b_f (22.5 ft)
Avg. Spoiler Width	(1.89 ft)
Elevator Span	0-.70 b_r (42.2 ft)
Avg. Elevator Wth.	.70-1.00 c_r (2.31 ft)
LE Slat Span	0-.70 b_f (65.3 ft)
Fowler Flaps	0-.70 b_f (65.8 ft)
Avg. Flap Chord	C_{flap}/C_f = 0.30

Fig. 2.2-1
HCSRT Wing Geometry

Table 2.2-1 Comparative Studies

PARAMETER	MD DC-10 series 10	BOEING 747-SR	HCSRT
W_{TO}	455,000 LBS	520,00 LBS	438,682 LBS
W_E	244,000 LBS	347,000 LBS	295,982 LBS
RANGE	2,706 s.m.	3,000 s.m.	1000 s.m.
LENGTH	181' 5"	231' 10"	225'
WING AREA	3861 sq. ft.	5500 sq. ft.	4080 sq. ft.
PASS. CAP.	250-300	400-500	600
CONFIG.	standard	standard	joined wing
ENGINES	3 41 k# turbofans	4 turbofans (47-52 k#)	4 unducted fans (35 k#)

2.3 Wing Structure

The NASA program JWOPT (Joined Wing Optimization) was run in order to size the spar caps and shear webs. A full description of the program as well as its verification is in section 3.6. An aluminum structure was input with the following parameters:

Youngs Modulus	1.0E+07 psi
Shear Modulus	3.7E+06 psi
Yield Stress	3.7E+04 psi
Safety Factor	1.5
Load Factor	2.5 G's
Gross Weight	452,000 lbs

The program output in tabular form is contained in appendix 2. The program divided the wing and tail into twenty sections and output the local loads and sizes for each element. The maximum shear stress and bending moments occured at the wing root. With the joined wing there were significant loads in all three directions. The resultant shear and moments were computed to be 6.4035E+05 lbs and 5.208E+08 in-lbs respectively.

The maximum loading configuration for each wing and tail element was then calculated by the program. Then the caps and webs were sized so they would yield at this loading

(which includes the safety factor). This insured the lightest possible wing and tail which could carry all of the design loads.

The wing box is asymmetrical so that it could resist the out of plane twisting moments imposed by the joined wing configuration. At the root the following cap and web thicknesses were computed.

Web	.5 in
Skin	.18 in
Cap 1	5.7 in
Cap 2	1.4 in

These dimensions will become clearer by observing fig 2.3-1. For the complete size listing, see appendix 2. Once the structure was optimized, a second run was completed which used a conventional design with the same weight and wing dimensions. It was found that the joined wing had a weight savings of 20,000 lbs or 6% of the empty weight.

A very detailed analysis would be needed to arrive at the proper rib placement. Since this is beyond the scope of this design phase, the typical value for transports was used. Using Ref. 12, a value of 24 inches was used.

The spar carry through box also could not be designed in detail, so again, a typical transport design was used. Fig. 2.3-2 shows the arrangement taken from Ref. 12. It is the same one used on the DC-10.

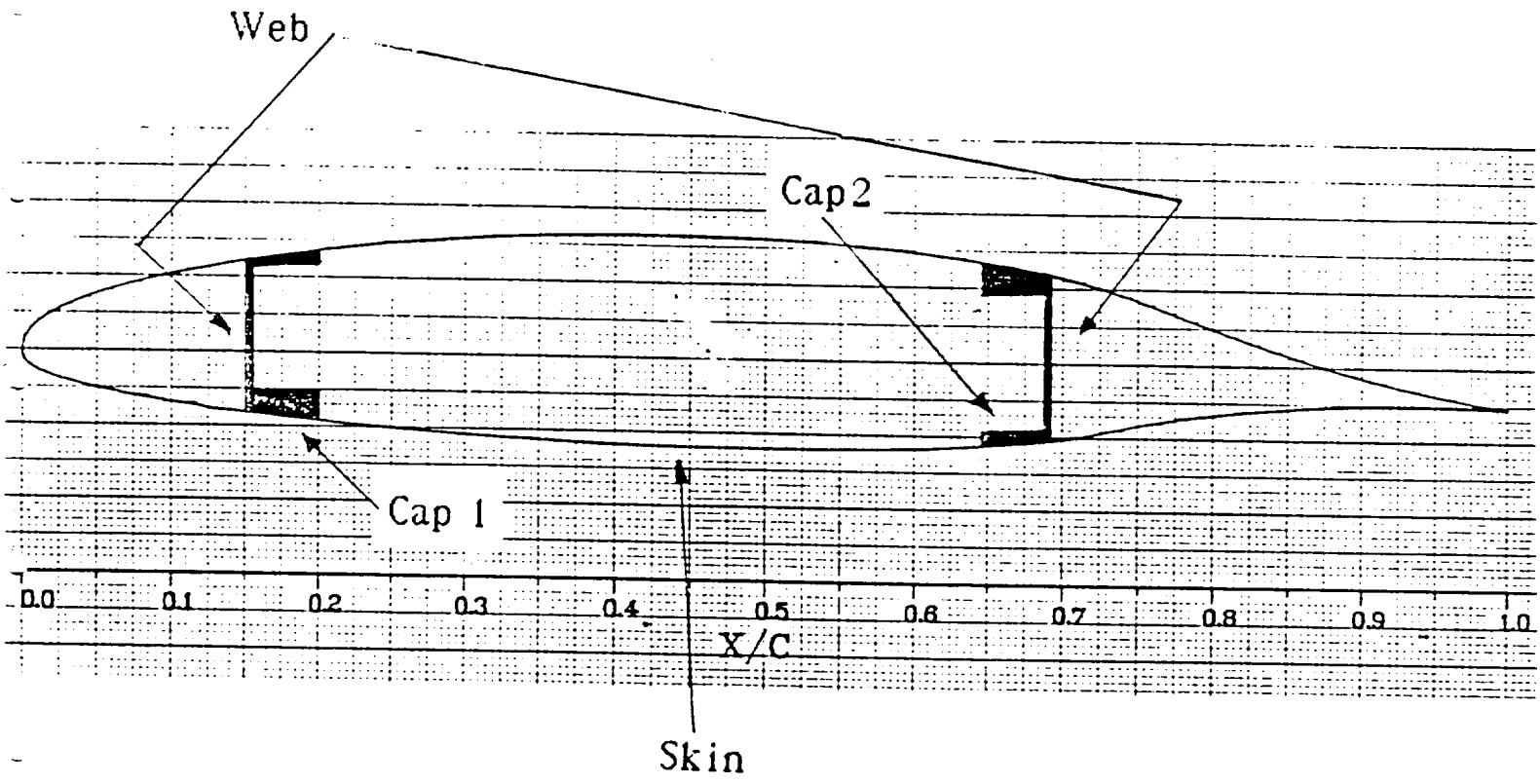

Fig. 2.3-1 Wing Profile

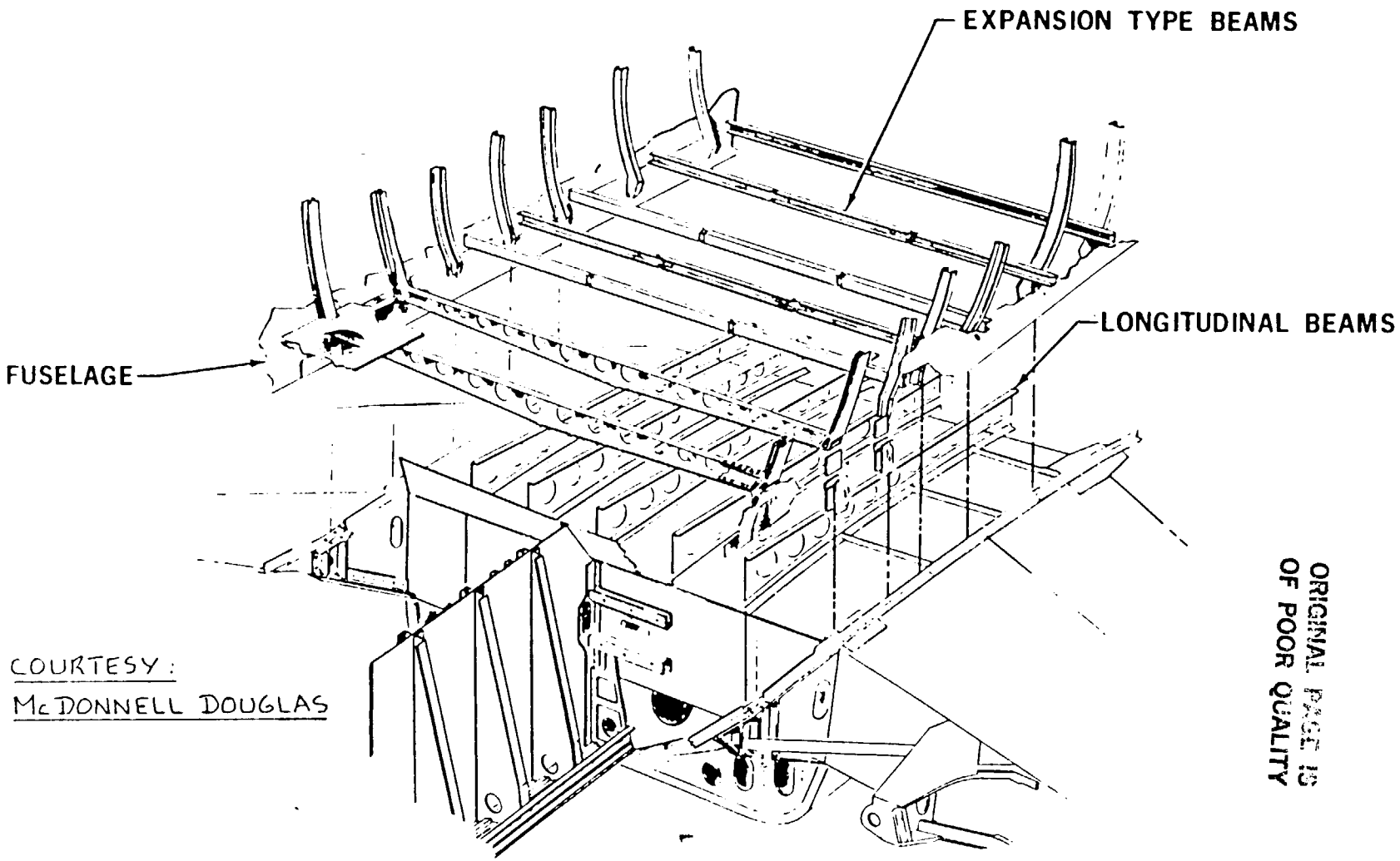

Fig. 3.2-2 Wing/Fuselage Attachment

3.1 Configuration

The initial concept for the HCSRT was a traditional, large transportation aircraft redesigned with modern and upcoming technologies to make passenger flying safer and more efficient, as well as to address the specific problems of the California Corridor. As various technologies were researched (such as upper surface blowing, composite materials, propeller and jet technologies, tandem wings), the field of possibilities for utilization of these technologies was narrowed.

The joined wing configuration was the first major decision for the HCSRT group, due to the large weight savings with induced drag savings. The advantage of less weight allows for a more economical flight. Though some of the joined wing technologies were rather theoretical, its proof of concept has recently been verified in wind tunnel tests at NASA Ames (reference 17).

The sizing of the wing planform was done as suggested by Dr. Jan Roskam (reference 11). However, the location of the joined wing on the fuselage was a variable which turned out to be very convenient for both weight and balance design and landing gear placement. The wing was adjusted, keeping all planform parameters fixed, so that the main gear of the aircraft could be mounted under the wings, such as traditional landinng gear, satisfying all landing criteria as well as all weight and stability requirements for safe and comfortable passenger flight.

3.2 Wing Configuration

Upon surveying the various possible configurations, the HCSRT group decided to look into the joined wing configuration. After talking with Mr. Julian Wolkovitch from ACA industries, and reading his papers (references 19 - 20), a number of surprising and enlightening facts were discovered concerning the joined wing, and it was decide to integrate the configuration into the design. The joined wing claims a number of advantages:

- -reduced aircraft weight
- -increased wing stiffness
- -reduced induced drag
- -increased trim lift coefficients
- -direct lift and side force capability
- -improved crash resistance (the original motivation for the joined wing)

The joined wing employs tandem wings arranged to form diamond shapes in both the plan and front views (see figure 3.2-1 for three view drawing). It derives its structural advantages and weight savings from tilting the wing's bending axis, which allows the plane's lift vector to be broken into two reduced components. One of these vectors is in plane, and is easily resisted by the wing truss structure, while the other is out of plane, and is what a normal cantilever wing has to resist (see figure 3.2-2). Since the out of plane vector is reduced (approximately by the cosine of the tilt axis), the wings can be built lighter and thinner, which saves

weight. A consequence of this is an increase in aspect ratio, which in turn reduces induced drag. The interaction of the front and rear wing flow increases the Oswald efficiency factor (it's not totally known why, but wind tunnel tests have shown this), which again decreases induced drag (see figure 3.2-3). Since the joined wing is self bracing, flexure of one wing is resisted by torsion from the other. This results in high stiffness which can be realized in the real world as higher aileron effectiveness and higher flutter speeds (figure 3.2-4). In addition, since the fuselage is being lifted in two places instead of one (as in a conventional configuration), fuselage bending moments are also reduced (figure 3.2-5). Theoretically, trimmed lift coefficients can also be increased for the same reason that is true for a canard. Instead of a download on the tail, the vehicle's lift is divided between two wings, with aerodynamic centers at different longitudinal locations, which allows the vehicle to be longitudinally stable with only uploads. With proper aileron/elevator coordination, direct side force and lift capability can be realized with the joined wing (figure 3.2-6). Lastly, the front, lower wing offers a good crash barrier, although it is hoped that such a benefit will not be needed.

Initially, the HCSRT group decided to optimize the joined wing's aerodynamic advantages, in order to reduce drag, and hence reducing fuel consumption as much as possible. To do this, a planform was chosen that employed tip-jointed wings, thirty degrees sweep on both front and rear wings, a taper ratio of 0.30. and an aspect ratio of 21.7 (each wing). It was hoped that it would be possible to mount two of our four

engines in the wing joints, which would neutralize the wing vortices and decrease the induced drag yet further. After further evaluation, and talking with Mr. Steve Smith of NASA Ames (reference 18), it was decided that emphasizing aerodynamic advantages was not the proper decision given the mission specifications the HCSRT (with its short range). The high Oswald efficiency factors that were expected (around 1.30) did not seem to find justification, and since our cruise time was relatively short (one hour), drag savings, no matter how great, could not be exploited to any great extent. At this time it was decided to redesign the wing, this time emphasizing the weight savings gained by using the joined wing, which in turn would lower manufacturing, maintenance and fuel costs.

To optimize weight savings, sweep needs to be minimized, aspect ratio maximized, wing dihedral maximized, taper ratio maximized and the joint location needs to be as close to the 0.70 wing span position as possible. Due to the cruising velocity restriction (M=0.80), it was necessary to employ sweep angles of at least thirty degrees (with the vertical tail possessing a thirty degree sweep forward for the same reasons) with a thickness-to-chord ratio of 0.10 to avoid drag divergence, and hence unacceptably high levels of wave drag. At this time, it was decided to split the total surface area required so that the front wing was seventy percent and the rear wing was thirty percent. With this wing area distribution, the rear wing functions more as a tail than a wing. Having made this decision, the option of direct side/lift force control was lost because the coupling between the ailerons and elevators was thought to be too complex and

maybe not possible. It was determined that take off rotation would not be sufficient given the position of the landing gear (see section 3.5), therefore a canard was added to compensate for this as well as to increase longitudinal stability. The HCSRT group surveyed various airfoils, keeping in mind a thin (t/c=0.10) airfoil with a maximum lift coefficient of at least 1.5 (determined from initial sizing in reference 10). Supercritical airfoils were not considered because it was discovered to be quite difficult to keep the airfoil thin while maintaining good lift coefficients. The NACA 64A410 (figure 3.2-7) was decided upon because it gave the required lift coefficients with the required thickness ratio and provided a drag bucket between lift coefficients of 0.3 to 0.6, which is where the HCSRT will cruise. Arbitrarily, the span ratio was set equal to 0.70 and the taper ratio was set equal to 0.30 (to come as close to elliptical lift distribution as possible). Knowing these values, plus the sweep angles and the surface area requirements, all the planform parameters were determined (table 2.2). At the same time, two other design aids were used in conjunction with the research conducted on the joined wing.

The HCSRT group obtained a copy of JWAOPT, a joined wing structural analysis code from Gallman and Kroo (reference 7). This code was used to help design the NASA experimental joined wing, which was recently wind tunnel tested with very good results. After entering the data for the HCSRT into this code, a list of optimized results was obtained. The optimized results were fairly consistent with the theoretical calculations that had previously been performed. The only major difference was the sweep angle for the rear wing. It

had been determined that thirty degrees (forward) sweep would be sufficient to avoid drag divergence, which was the only restriction considered. JWAOPT, however, recommended a forward sweep angle of approximately forty one degrees, in order to move the aerodynamic center forward. A rear sweep angle of forty degrees was subsequently adopted into our design.

After preliminary sizing (reference 10), the HCSRT group also went through reference 11 to further refine our wing design. As outlined in chapter two of reference 11, a survey was made of existing aircraft with similar mission profiles to the HCSRT, including the McDonnell Douglas DC-10 series 10 and the Boeing 747. It was decided that the important characteristics of the HCSRT that would impact design the most significantly were:

- -relatively long field length (the shortest being Sacramento Metro Airport which has 8600 feet of runway)
- -the large number of passengers carried (600)
- -short range (1000 statute miles)
- -required travel time of no more than one hour between LAX and SFO
- -improved fuel economy over existing aircraft of similar type

After reviewing all the possible configurations, it was decided to go with the joined wing configuration (considered braced both high and low when using conventional design procedures) because of the reasons listed previously. Knowing

the desired cruising Mach number (0.80) and knowing it was possible to use a thin airfoil and still retain structural integrity (advantage of the joined wing), it was decided on a ten percent thick airfoil, which required a sweep angle of thirty degrees to avoid drag divergence. Lateral control devices were sized using data on existing aircraft and adapted to optimize the advantages of the joined wing . Having sized the vertical tail in parallel with our wing design, the vertical distance from tail to bottom of fuselage was known which made it simple to calculate the dihedral angles of the front and rear wings (also taking into account the numbers generated by JWAOPT). Since the joined wing is a highly integrated concept, incidence and twist angles need to be tailored individually depending on the aircraft's mission; no set rules exist when making these decisions. Unfortunately, CFD work is necessary to optimize incidence and twist, which the HCSRT group did not have access to, nor did time permit. Instead, the basic requirement was used that the front wing should stall before the tail for longitudinal stability, which means that the front wing incidence angle is higher than the rear wing incidence, so that the front wing stalls first (and the canard must stall before the front wing, so it is at the highest incidence). All the planform parameters are summarized in table 2.2.

Once these decisions were made, a class I drag polar analysis was done, in accordance with reference 11. A detailed analysis of total surface area was completed to find profile drag. Knowing the aspect ratio, and with an educated guess made of the Oswald efficiency factor, induced drag could be calculated.

Sizing for the high lift devices was calculated according to reference 11, and indicated that the maximum lift coefficients initially assumed were difficult to obtain. Since the HCSRT takes off and lands at existing airports, there was noted to be no real necessity for very high maximum lift coefficients. The high lift device sizing calculations were reiterated with only slightly lower maximum lift coefficients and resulted in easily obtainable high lift device sizing, with Fowler flaps and leading edge slats. The maximum lift coefficients are still at the higher end of the spectrum when compared with today's most recent similar aircraft.

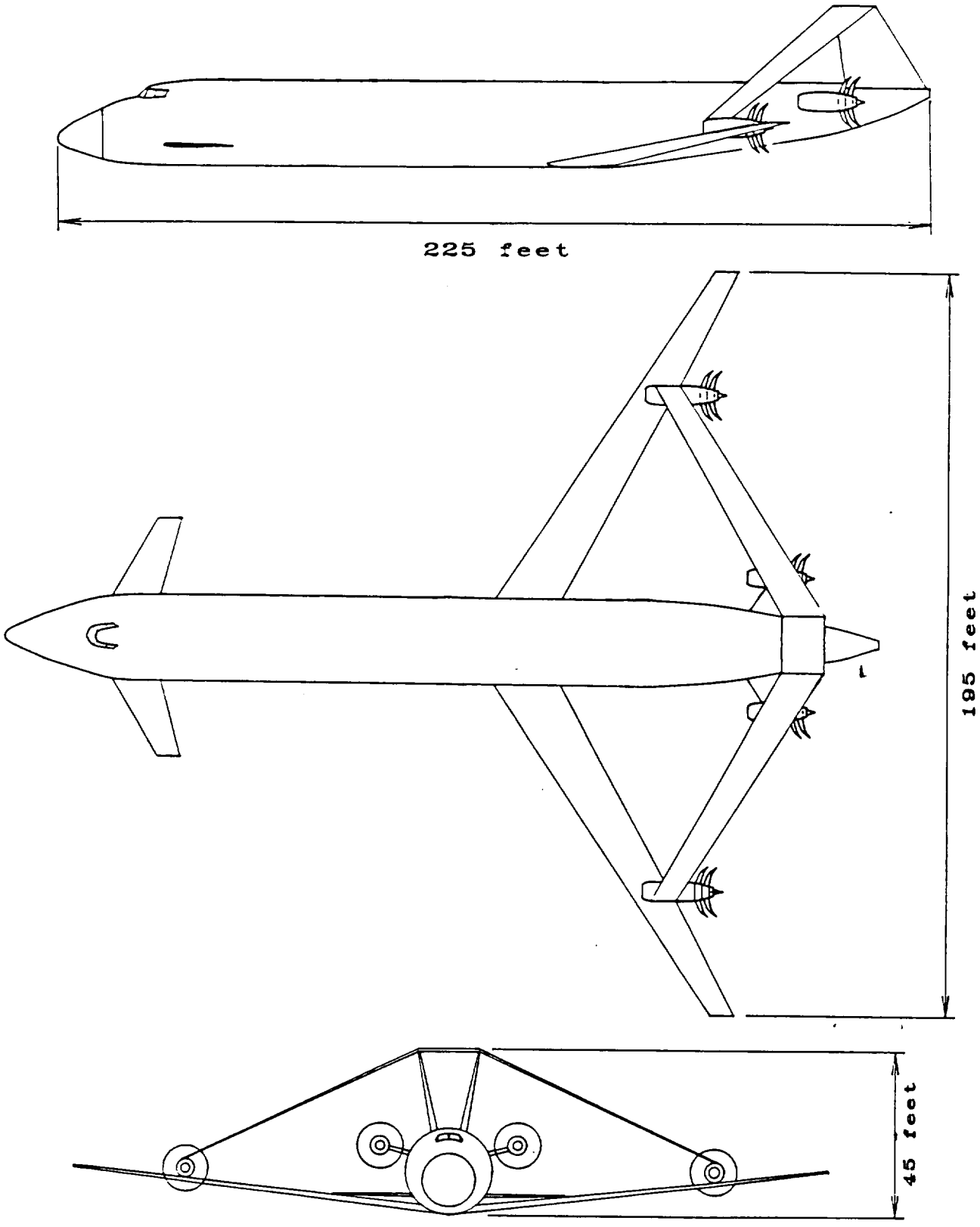

Figure 3.2-1
HCSRT Three view

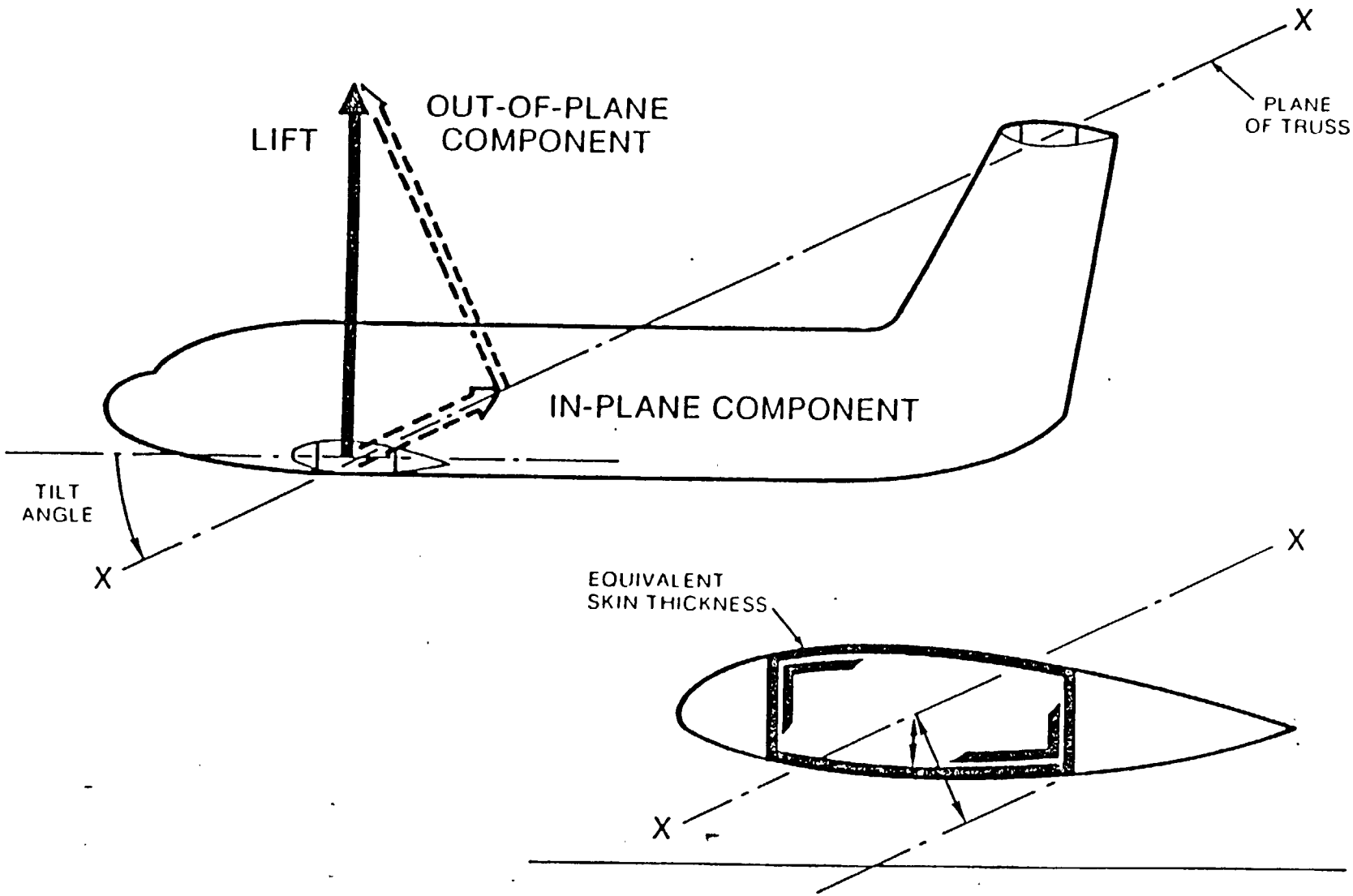

Figure 3.2-2 IN-PLANE AND OUT-OF-PLANE LIFT COMPONENTS

Source: Wolkovitch, J. "The Joined Wing: An Overview", AIAA-85-0274

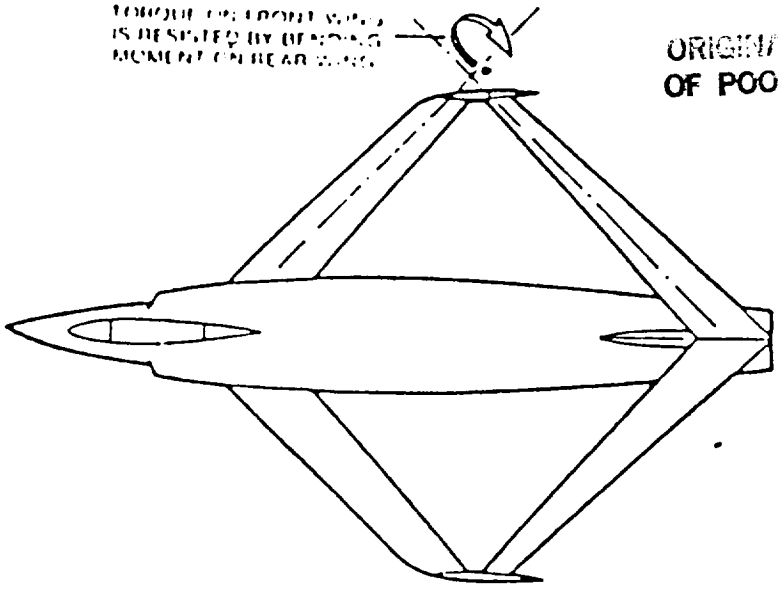

Figure 3.2-4 Resistance of Torsion of One Wing by Flexure of the Other

Source: Wolkovitch, J. "The Joined Wing: An Overview", AIAA-85-0274

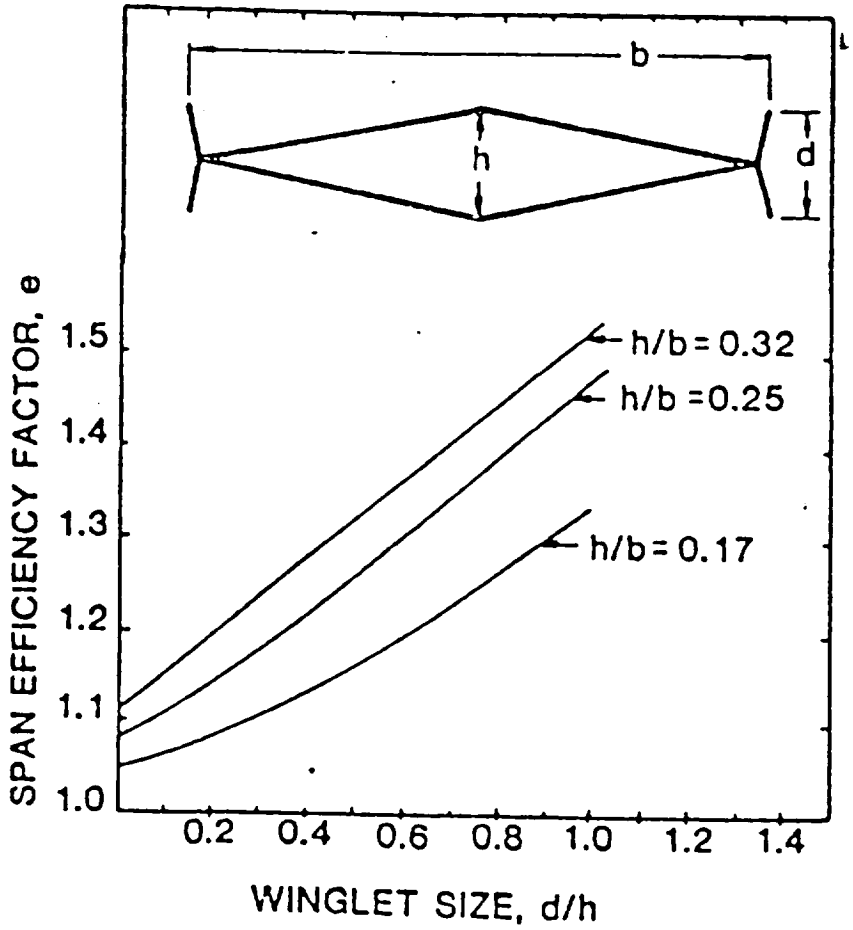

Figure 3.2-3 Theoretical Span-Efficiency Factor for Joined Wing with or without Symmetric Inclined Winglets (3)

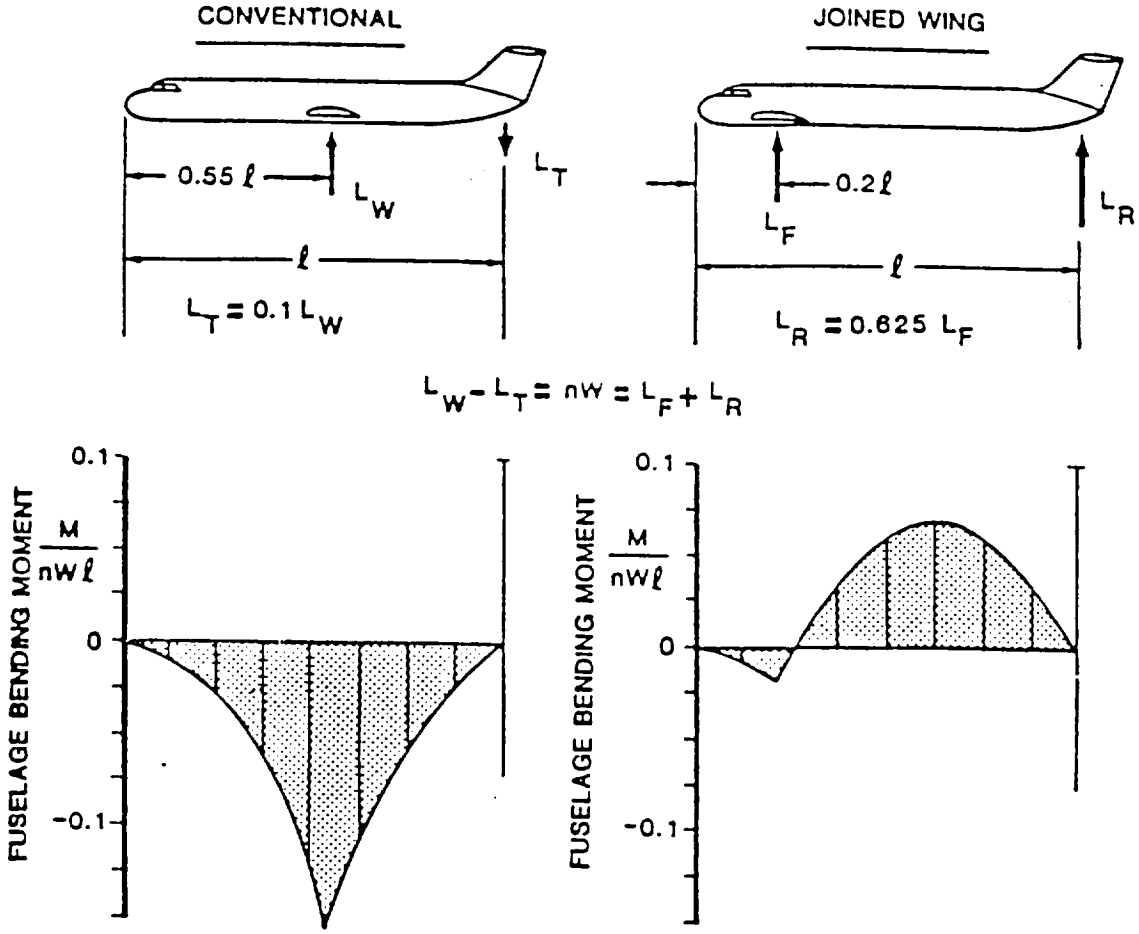

Figure 3.2-5 FUSELAGE BENDING MOMENTS FOR JOINED WING AND WING-PLUS-TAIL SYSTEMS

Source: Wolkovitch, J. "The Joined Wing: An Overview", AIAA 85-0274

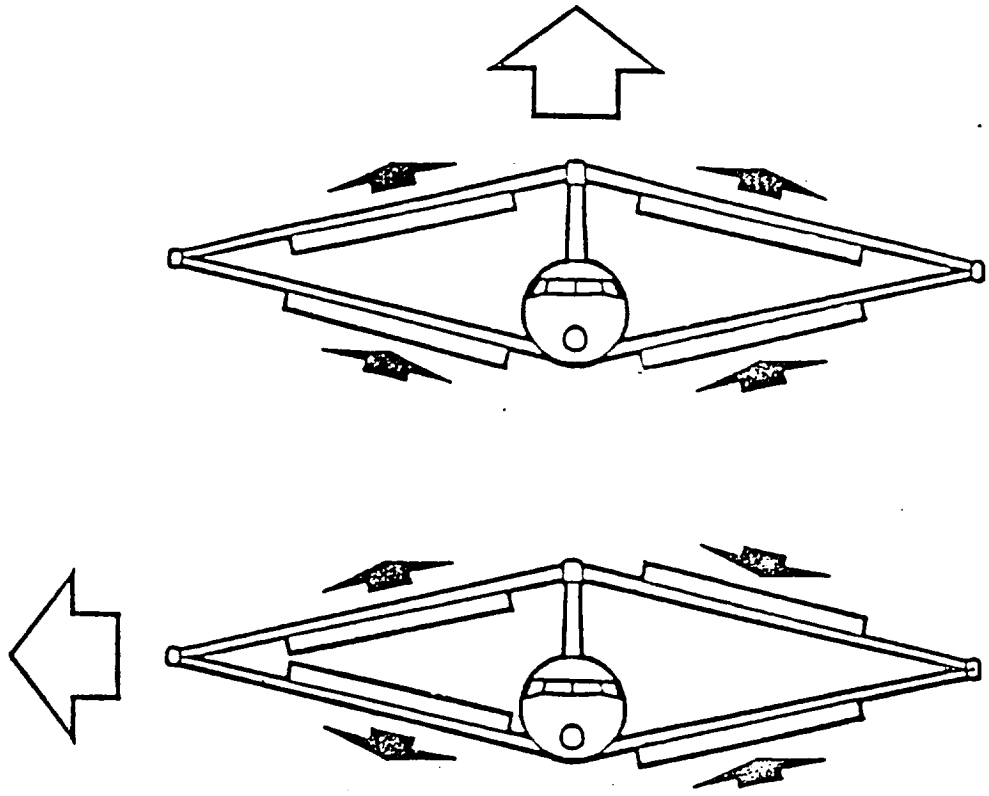

Figure 3.2-6 DIRECT LIFT AND SIDEFORCE CAPABILITIES OF JOINED WINGS

Source: Wolkovitch, J. "The Joined Wing: An Overview", AIAA 85-0074

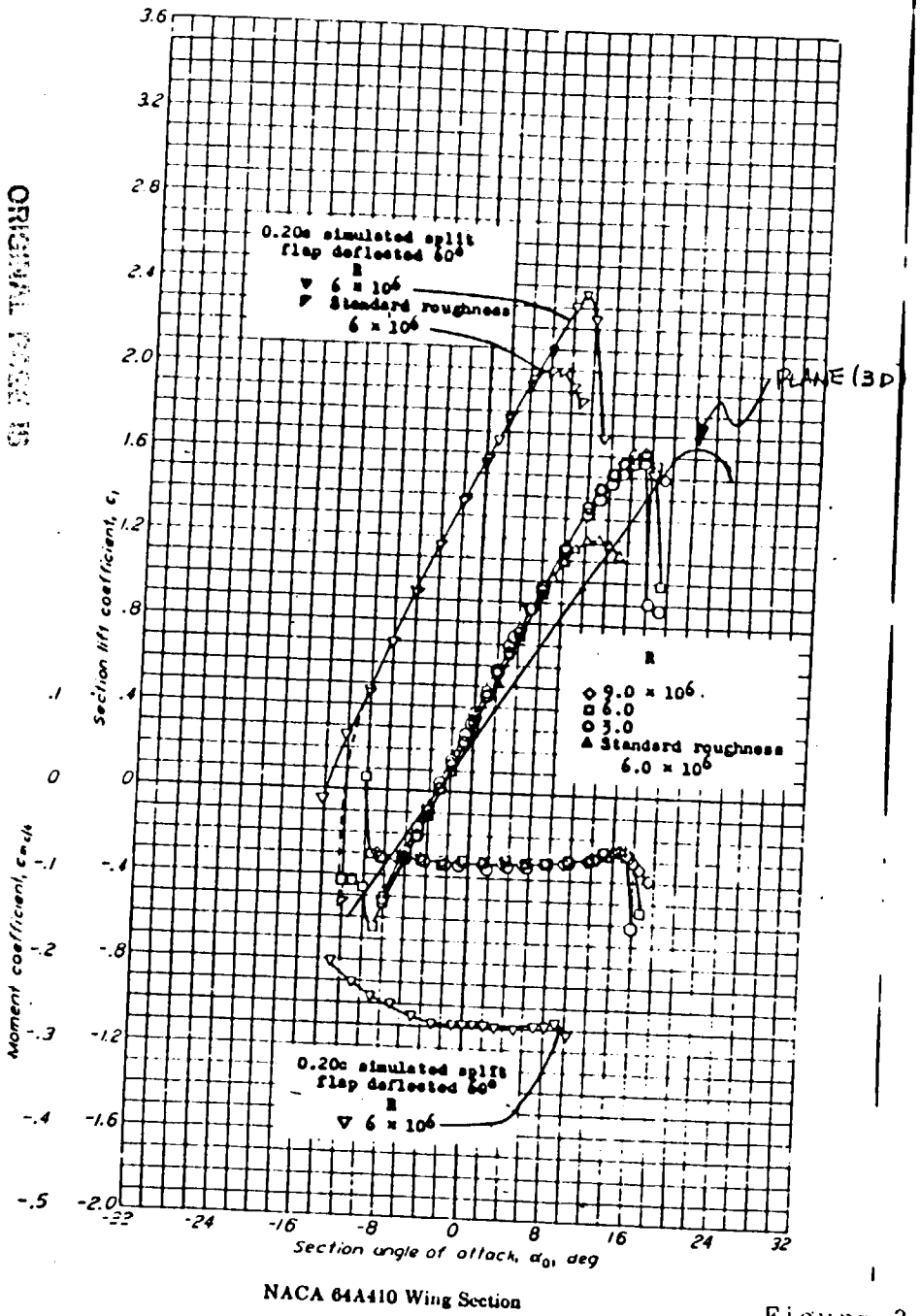

NACA 64A410 Wing Section

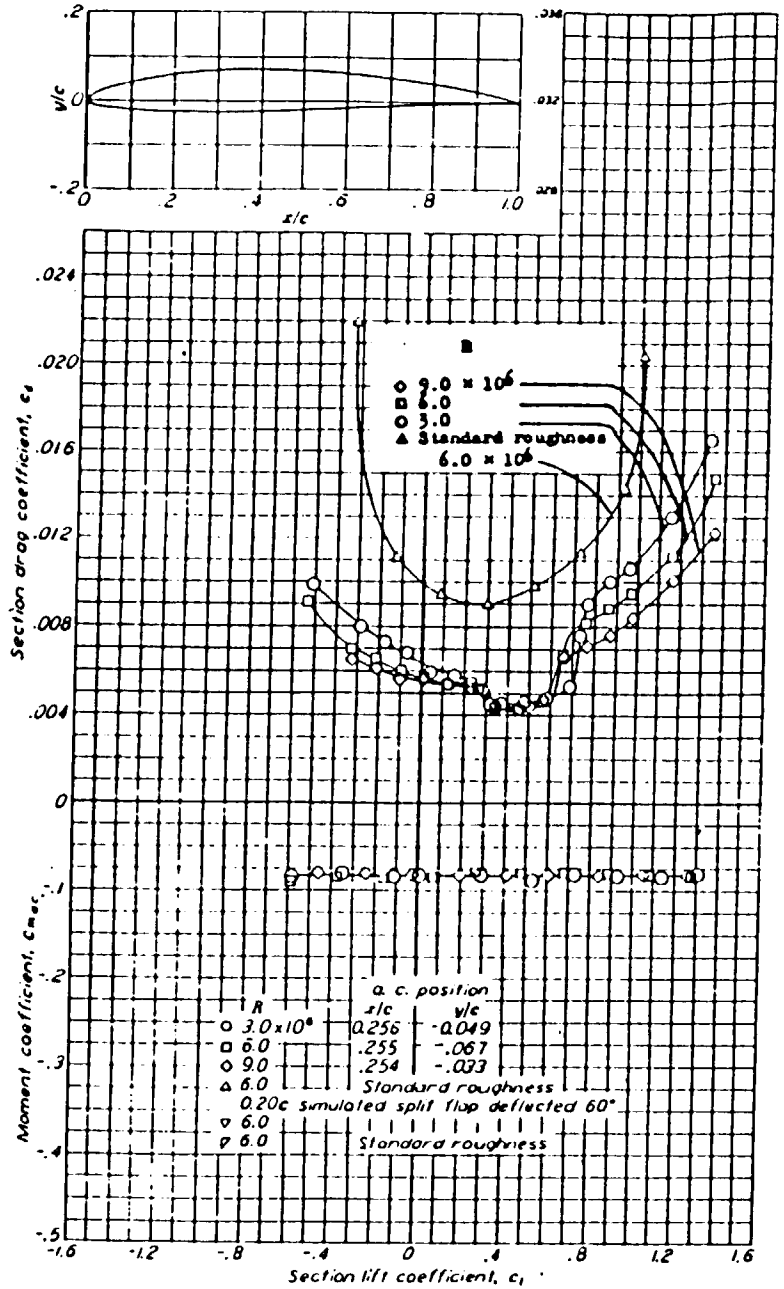

NACA 64A410 Wing Section (Continued)

Figure 3.2-7

Source: Abbot, Ira, "Theory of wing sections", Dover Publishing, 1959

3.3 Fuselage Design

The accommodation of 600 passengers presented considerable problems for the fuselage layout. Since there was insufficient time to investigate the feasibility of a considerably larger fuselage, it was desired that the fuselage dimensions be comparable to that of an already proven aircraft. Therefore, the fuselage layout of the Boeing 747, the largest airliner, was looked at closely. Although the HCSRT would carry more passengers, it would have a smaller luggage volume requirement because of its application as a commuter rather than a tourist coach. For this reason it was logical to assume that the HCSRT fuselage could be designed to a size similar to the 747's.

The 747 has passengers ten abreast for a fuselage length of 225 feet and a diameter of twenty one feet. For the HCSRT, it was found that ten abreast seating would result in a fuselage over 300 feet long. The fineness for such a fuselage was fifteen, far higher than suggested in reference 12. The major concern in this was the large wetted area. If twelve abreast seating was used, the fuselage length would be 250 feet with a diameter of 23 feet. This fineness ratio was in the range recommended in reference 12. For large transports, circular cross-sections result in most of the fuselage volume being above and below the passenger deck (see fig. 3.3-1). For typical transport jets this volume is used for check-in luggage and aircraft systems.

However in the case of the HCSRT the commuter passengers would not require a large check-in luggage volume. A circular cross-section would result in wasted volume above and below the passenger deck. To reduce this extra volume, an elliptical cross-section was investigated. This option was rejected however, the fuselage being a pressure vessel would need to be much heavier structurally to accommodate the stress concentrations of an elliptical fuselage. This would be particularly true of the HCSRT. The fatigue life of an aircraft is not dependent on flight hours as much as it is on the number of cycles (flights) an aircraft has logged. Therefore a quick flight fatigues the aircraft almost as much as much as a long flight. Since the HCSRT was designed for the short commute, the stress concentration of the elliptical fuselage coupled with the need for structural strengthening for fatigue life would be too much of a weight compromise.

The next configuration investigated, and eventually chosen, was a bi-level fuselage (see fig. 3-3.2). It was found that for a lower deck seating of eight abreast and an upper deck of six abreast with a six foot, eight inch aisle height, the resulting fuselage diameter was 22.5 feet and the frame depth 6.5 inches. This cross-section resulted in a fuselage length of 225 feet. The lower deck had two aisles while the upper deck only required one. Reference 12 recommended an aisle width of twenty inches which was incorporated into the HCSRT. This still allowed sufficient

room for aircraft systems and baggage stowage. The cargo compartments below the lower deck could accommodate the LD-2 standard pallet container.

The aircraft seating was decided to be entirely coach although the configuration was adjustable if a first class section was desired. The seat chosen was a standard coach model found in reference 12. The cabin layout (see fig 3.3-3, and 3.3-4) is void of any galleys. For the short haul, no meals would be served. A total of eight lavitories were incorporated into the front and rear of both decks.

Emergency exit requirements indicated the need for eight exits per deck, four on each side. The emergency exits were placed so that the lower deck exit was separated somewhat from the closest upper deck exit. It was considered that if both exit doors were placed close together, the local fuselage cross-section would be cluttered, and room for the aircraft's systems travailing through the fuselage would be compromised. In addition, if the two emergency exits were placed too close together, the passengers unboarding from these exits could interfere with one another during an emergency situation.

Passenger boarding and unboarding was considered an important design concern for the HCSRT. For other large aircraft that are designed for long flights, the boarding time is not as big of a concern. For a short haul commuter aircraft, ground turnaround time must be as short as possible. On todays aircraft passengers are boarded through a single side door and must enter in single file. For the

HCSRT's capacity and trip length the boarding time for this technique would not be acceptable. For this reason a different boarding technique was developed. In observation of a number of cargo aircraft it was noticed that many, such as the C-5, had swiveling nose cones for cargo loading. If this was incorporated into the HCSRT, passengers could load three abreast. This would allow the HCSRT to be loaded in roughly the same time as a 200 passenger aircraft. This is similar to the size of aircraft being used today for the same mission. In addition, the required modifications to the airport terminal gates would be minimal. The HCSRT was designed to taxi directly into the terminal gate alleviating the need for loading gates. This technique seemed feasible and was adopted for the HCSRT. The forward pressure bulkhead was blunt faced and nearly semi-spherical, for minimum structural weight of the pressure vessel. It was placed immediately in front of the cockpit (see fig. 3.3-3). The large boarding door was placed at the foremost end of the bulkhead (see fig. 3.3-5). The portion of the nose that actually swivelled was only for aerodynamic purposes and was not pressurized. It was considered feasible to manufacture it from lightweight, non-metalic materials. This lower weight would reduce the required size of the swivel hinge. The nose was swivelled to the side rather than up as in most cargo aircraft. This was to maintain pilot visibility while the nose was open.

The conventional system for baggage stowage and handling was used for the HCSRT. However , it was found that all of the passenger luggage could be accommodated by the

stowage areas in the passenger cabin alleviating the need for check in luggage. This would be very beneficial to the passengers since they would not be required to retreive their luggage in the terminal which saves time. This leaves the volume below the lower passenger deck completely free for aircraft systems and possibly airfreight. The systems placed under the deck were the hydrogen fuel heat exchanger/ air conditioning unit, hydraulic and electrical systems. The auxilary power unit was placed in the tailcone volume behind the main fuel tank.

A typical configuration was decided for the cockpit layout. There were no real reasons to alter this convention. The HCSRT was designed to be as simple of an aircraft as possible. Also the navigation requirements would be relatively simple so it was decided that only two pilots would be required. The general cockpit layout is shown in fig. 3.3-6.

Three of the liquid hydrogen fuel tanks were located in the fuselage. The main tank was placed immediately behind the rear pressure bulkhead (see fig. 3.3-4). Two of the tanks were located in the nose below the lower deck immediately behind the forward pressure bulkhead (see fig. 3.3-3). These positions placed the tanks as far away from the passengers as possible. However, it was proposed that a system be incorporated to vent the forward tanks to the exterior of the aircraft and that this be a part of the pilot's emergency checklist.

The structural layout of the fuselage was approximated by comparison to other large transport aircraft found in

reference 12. However, the frame and longeron spacing was chosen to be smaller than the average of the other aircraft. This was due to the fatigue life concerns for short haul aircraft discussed earlier. The frame spacing was chosen to be twenty-one inches and the longeron spacing ten inches (see fig. 3.3-7). To help support the upper deck it was considered that perhaps a number of columns would need to be placed between the two decks (see fig. 3.3-2). It was considered that these columns would not seriously compromise passenger accommodation. A weight comparison would have to be made between this solution and strengthening the upper deck to withstand the loading by itself.

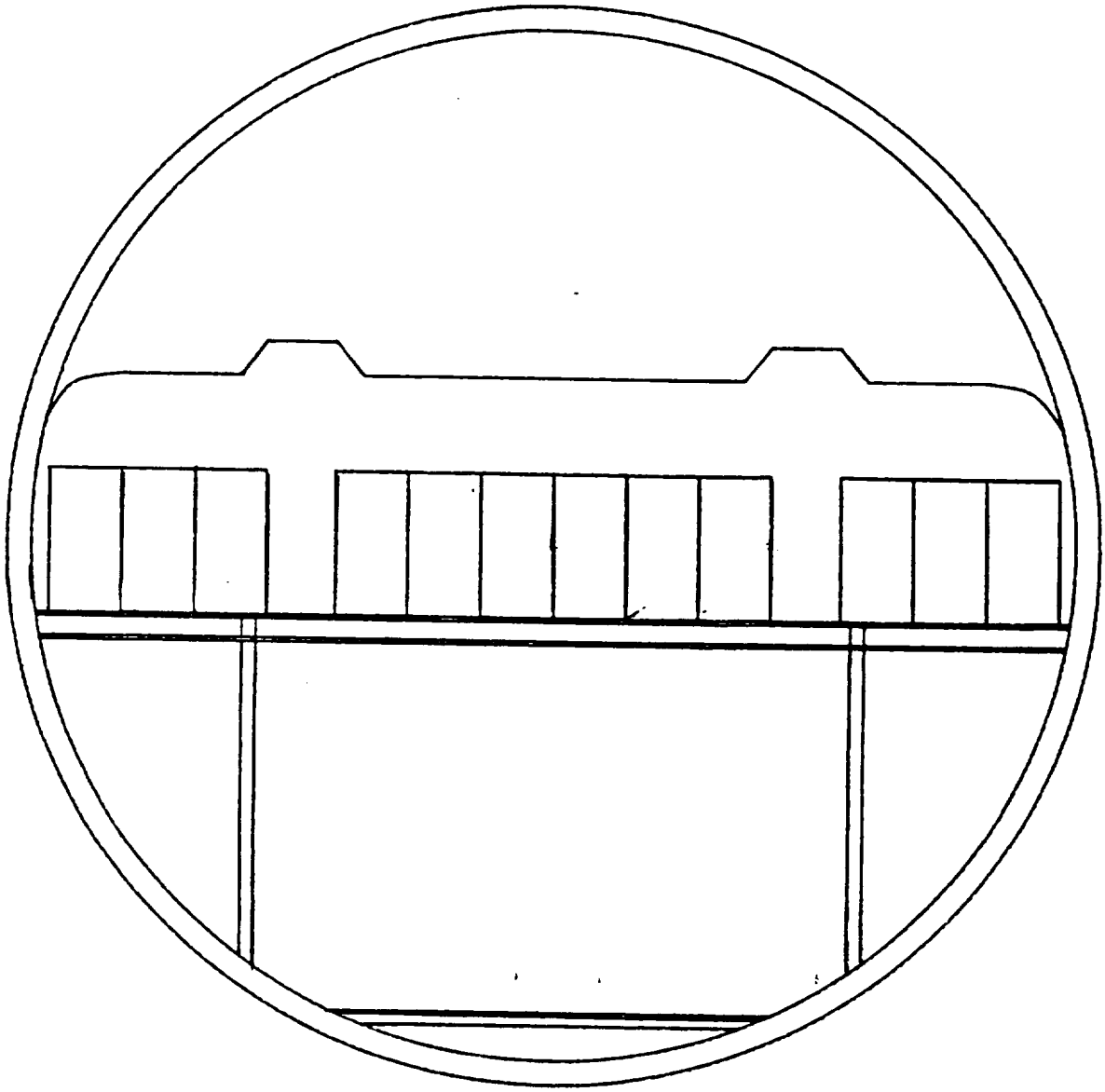

Figure 3.3-1

Cross Section for Twelve Abreast Seating

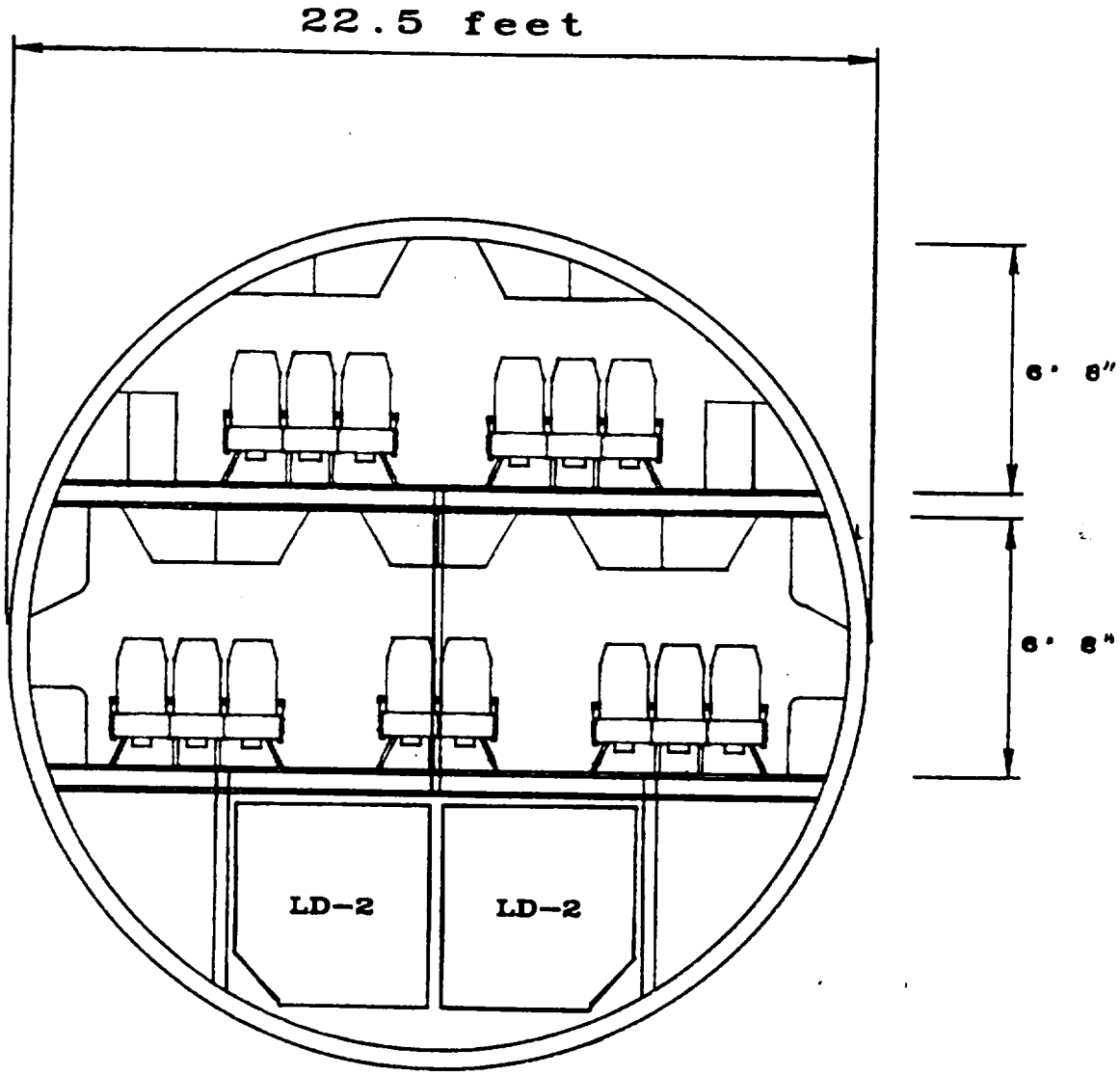

Figure 3.3-2
FUSELAGE CROSS SECTION

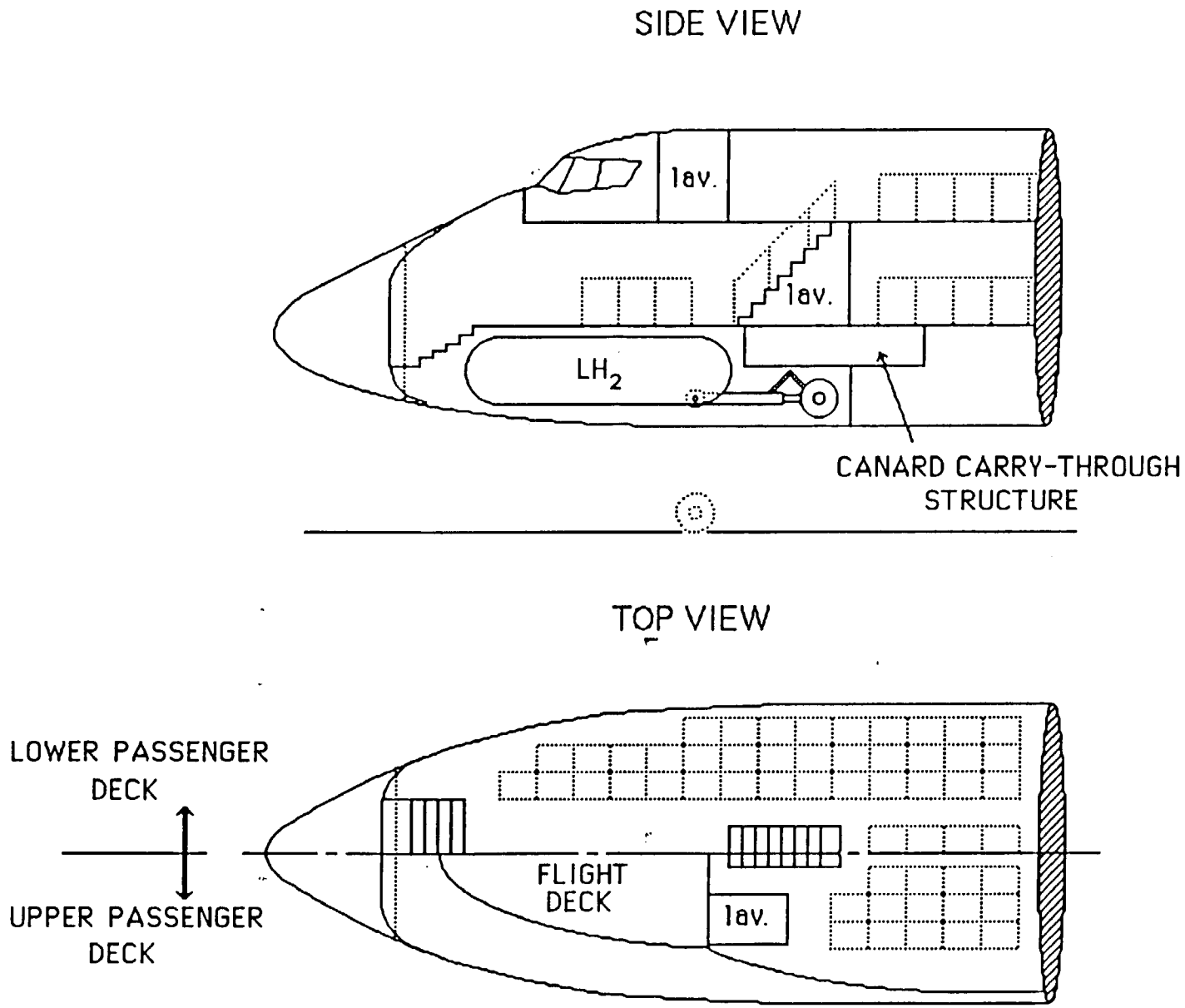

Figure 3.3-3
Forward Cabin Layout

TOP VIEW

LOWER PASSENGER DECK

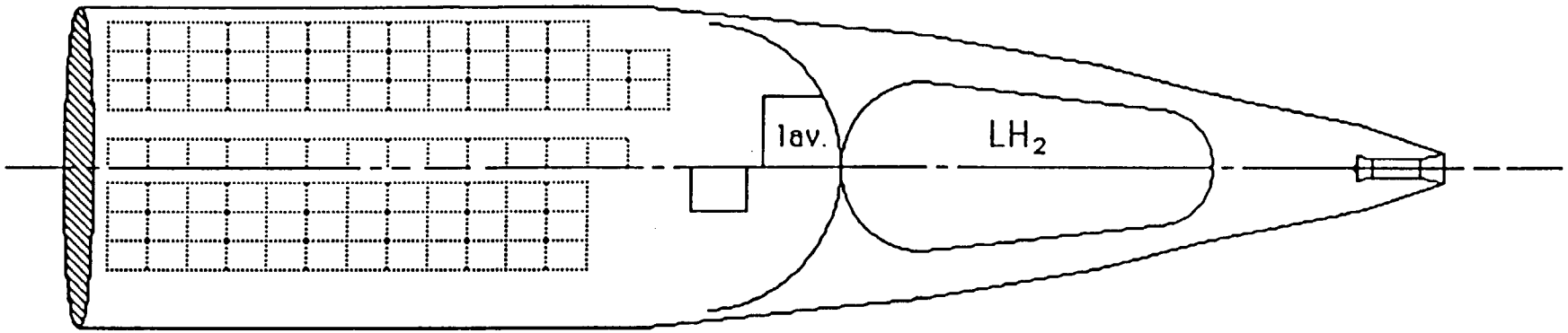

UPPER PASSENGER DECK

SIDE VIEW

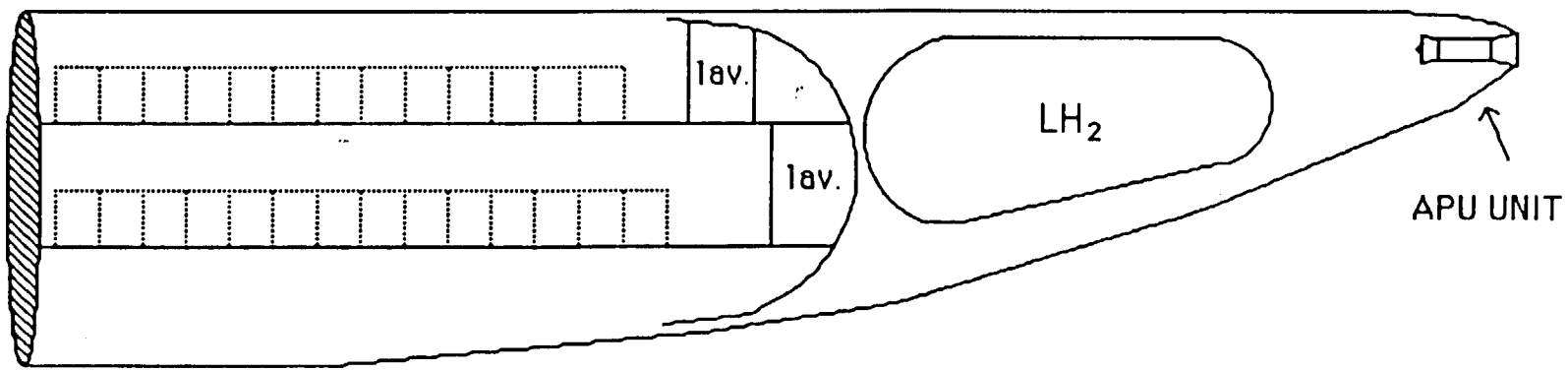

Figure 3.3-4

Aft Cabin Layout

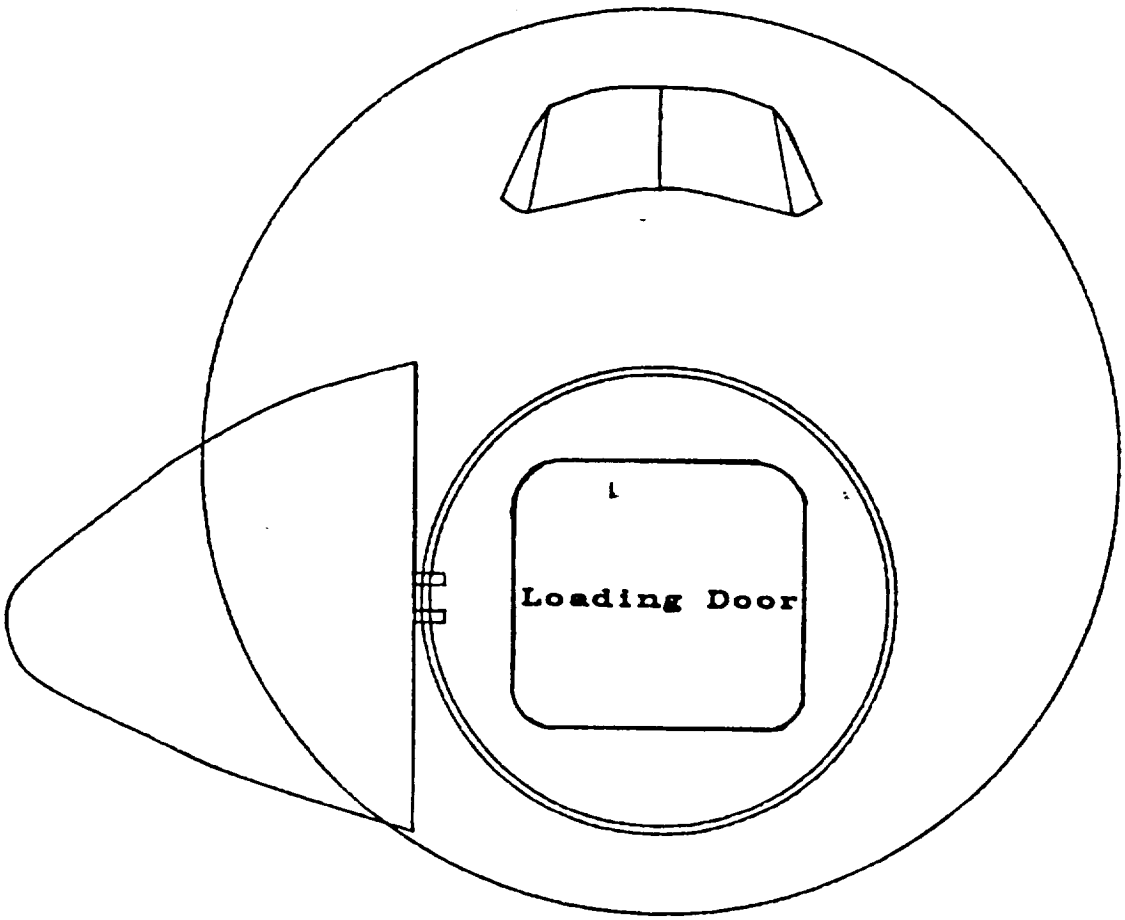

Figure 3.3-5

Front View of Swivel Nose

and Loading Door

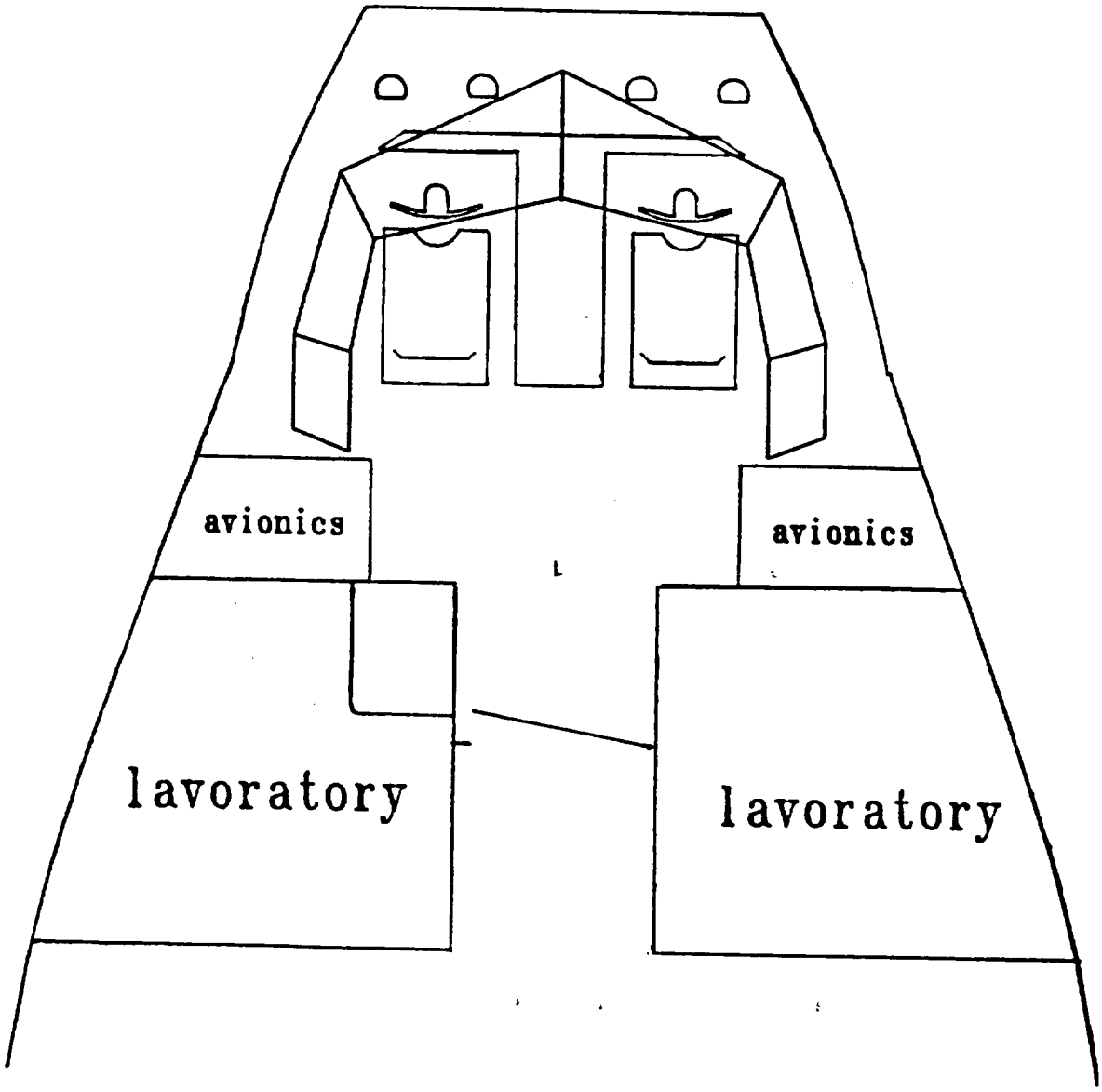

Figure 3.3-6

Cockpit Layout

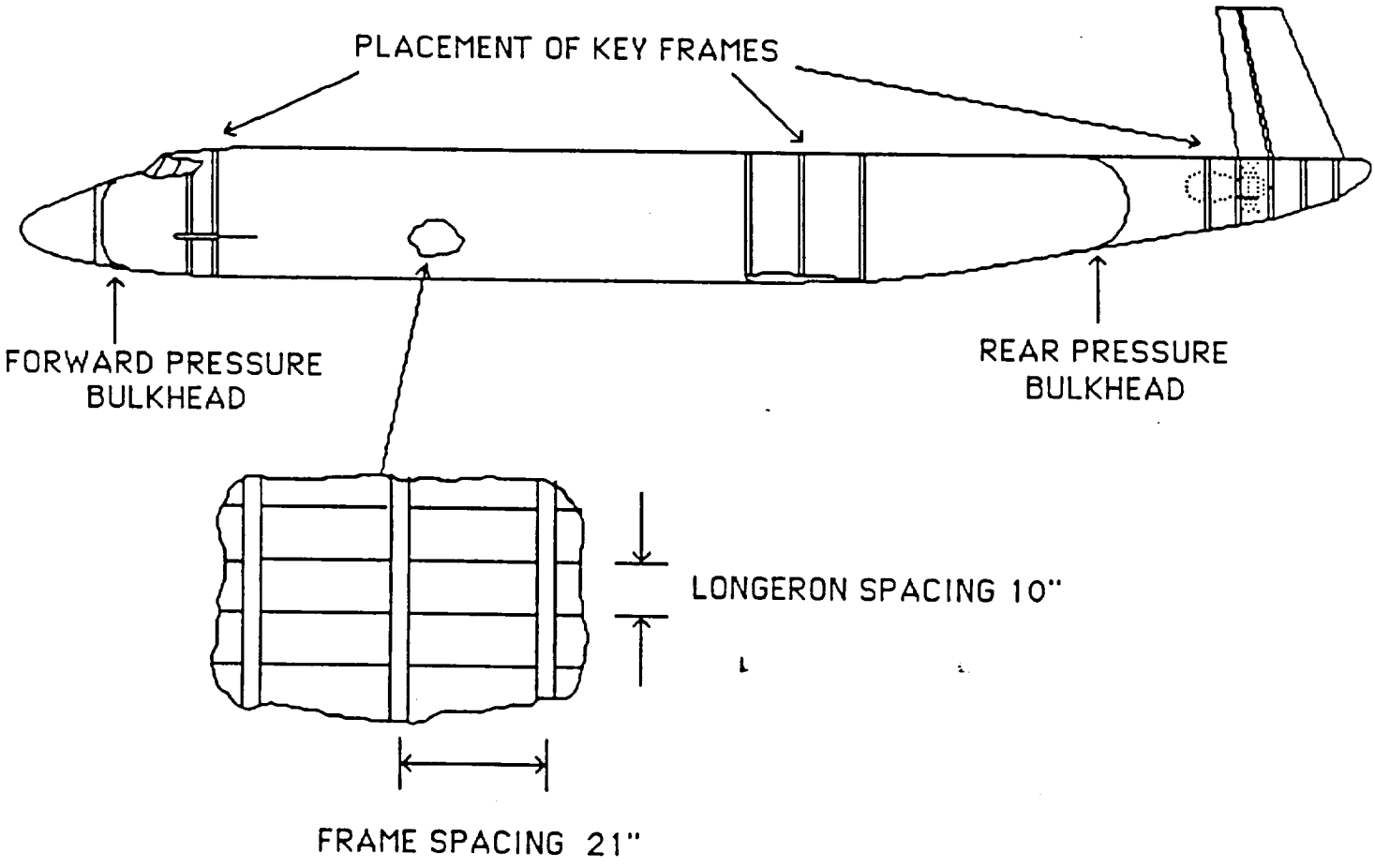

Figure 3.3-7

Fuselage Structural Layout

3.4 Propulsion System Design

The selection of the type of propulsion system to be installed on the HCSRT focused on two major concerns, fuel efficiency and noise. The manufacturing and airport storage of hydrogen are the greatest drawbacks in incorporating this fuel into an aircraft. Minimizing the quantity of fuel required for the mission was considered crucial. The noise emitted by an aircraft as it climbs away from the airport is also crucial for environmental and public acceptance reasons. Presently, there is extensive research into a propulsion system that reduces both fuel consumption and noise and yet still operates in the mach number and altitude regime of today's airliners. This system is the unducted fan. Most of the flight testing of this system was conducted at mach .8 at 30,000 feet. This is the exact speed and altitude the HCSRT was designed to cruise at. For these reasons the unducted fan was the selected propulsion unit.

To determine the number of engines, it was decided to investigate other large airliners. Both the McDonnell Douglas DC-10 and the Lockheed L10-11 are three engined aircraft. The Boeing 747 has four engines. Since the HCSRT is closest in size to a 747, a four engine configuration was selected. The preliminary sizing of the HCSRT indicated a thrust requirement of 121,000 lbs. For a four engine configuration, the thrust requirement for each engine was

30,250 lbs. The flight testing of the unducted fan used an engine of 25,000 lbs. thrust. However it was determined from Reference 2 that the technology could easily be expanded to the thrust requirement of the HCSRT. The testbed model had a fan diameter of ten feet. Assuming the diameter to be proportional to the square root of the thrust as is the case with propellers, this indicated a fan diameter of eleven feet for the HCSRT. Engine weight was considered to be similar to a turbofan of the same thrust class. Other engines such as the Pratt & Whitney 2037 and the Rolls-Royce 535 indicated a dry weight of 10,000 lbs. would be reasonable. No information could be found on the center of gravity location for an unducted fan so it was estimated to be at the middle of the fan unit. If it differed from this by a few feet, it was considered to be insignificant for the preliminary design phase due to the size and weight of the HCSRT.

Two of the engines were placed on the fuselage sides near the tail. This placement was used of several airliners such as the Boeing 727, McDonnell Douglas DC-9, BAC 111 and the Fokker F.28. Reference 9 indicated that with a pusher configuration this position was best in terms of acoustics, installation drag, and propeller inflow (see fig. 3.4-2). The engines were placed back far enough so that if a fan or turbine blade were to be lost, it would not rupture the hydrogen fuel tank. Initially the wings were to be joined at the tips. The possibility of integrating the two remaining

engines at the wing joint was considered. Provided the engine out yawing moment was controllable, this type of engine placement would have offered an advantage. If the fans were designed to rotate counter to the wingtip vortices they would partially diffuse these vortices, thereby reducing the induced drag. However, the wings were altered to join inboard of the main wingtip. Another position considered was placing the other two engines where the rear wing joined the vertical tails (see fig. 3.4-3). This was rejected however because of the distance between the thrust centerline and the aircraft center of gravity. This would induce a large trim inbalance during changes in power setting. In addition, the engines being fifty feet off the ground would severly complicate maintenance. Reference 9 indicated the next best engine placement was on the wing. A tractor unit was preferred because it received a better propeller inflow than a pusher. It was decided to place the two engines at the wing joint location to reduce the cabin noise as much as possible. Stability considerations indicated this to be the farthest outboard installation possible with a feasible tail size. However, it was decided to install pushers rather than tractors. The high speed flow behind the fan would increase the interference drag at the wing joint. This was considered more important than the air inflow to the fan. In addition, the two different engine types would complicate maintenance and increase repair costs. Geometric clearance requirements for both takeoff rotation and five degree bank angle during approach were satisfied with these engine placements (see fig.3.4-4).

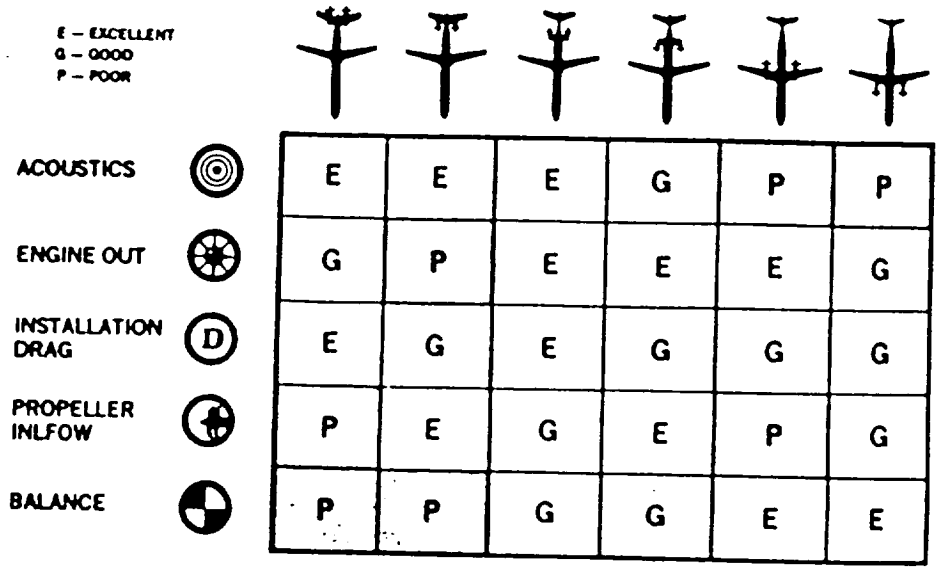

Figure 3.4–2 UHB CONFIGURATION COMPARISON

Source: Page and Ivey, "Ultra High Bypass Engine Applications to Commercial and Military Aircraft", SAE Paper 861720

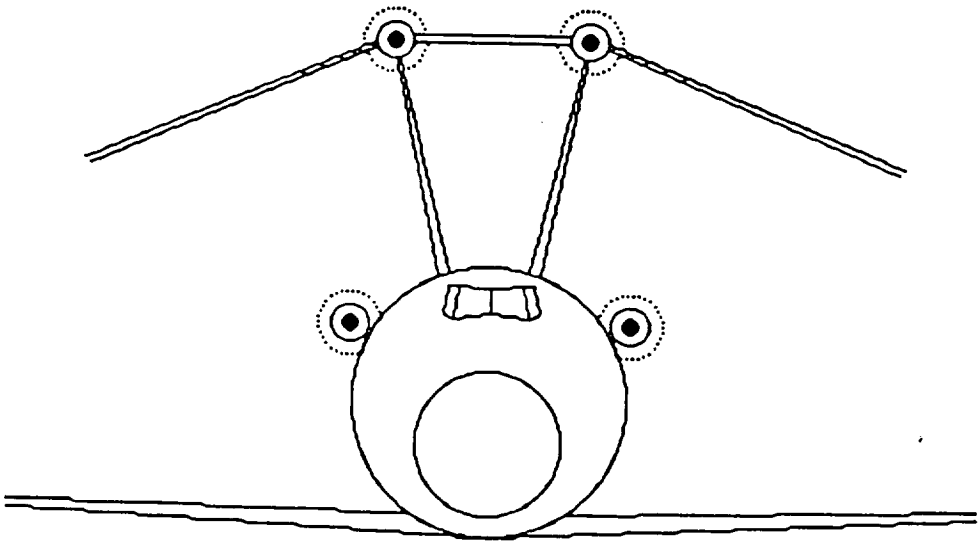

Figure 3.4–3

Engine Placement In Tail and Rear Wing Joint

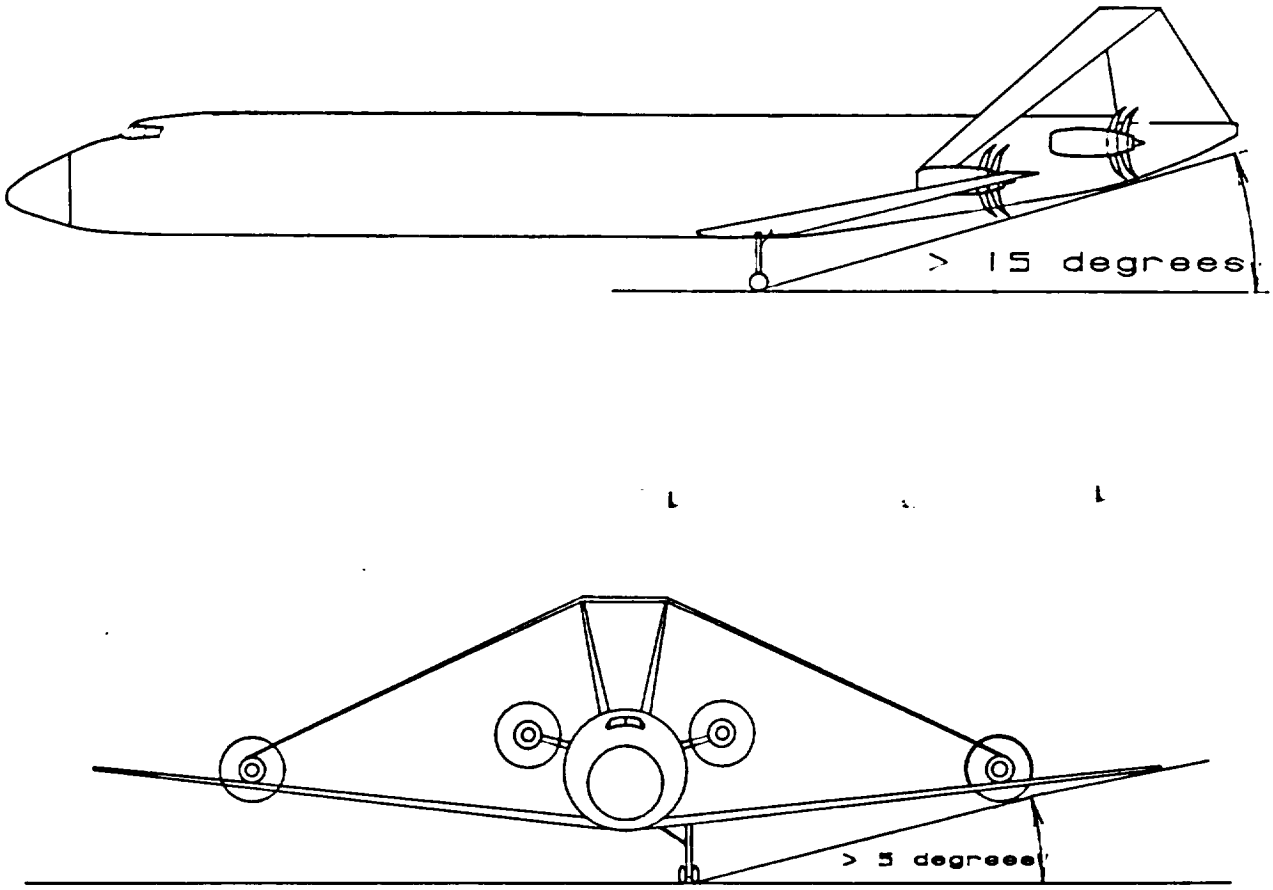

Figure 3.4-4

Geometrical Ground Clearances

3.4.1 Fuel: Liquid Hydrogen

In the interest of exploiting as much new technology as possible, liquid hydrogen was looked into as a possible source of fuel, instead of the conventional jet-A petroleum based product currently used. Upon further research, (see reference 4), the following advantages were discovered for LH2:

- -manufactured from products that cannot be cartelized
- -higher engine efficiencies resulting from even-burning and pre-cooling of air
- -lower fuel consumption by a factor of three
- -nominal pollution (see table 3.4-1)
- -safer to use than jet-A (see table 3.4-1)
- -possibility to cool wing surface to extend laminar boundary layer

In addition, the following disadvantages were also found:

- -extra weight of insulation and auxiliary equipment
- -higher fuel required fuel volume by a factor of four
- -losses due to evaporation
- -higher cost

Liquid hydrogen is stored at 21 psia and -421.3 degrees fahrenheit. It is three times lighter than jet-A, and although it burns three times more efficiently, it needs four times the volume to store the equivalent amount of fuel energy. Since LH2 can be manufactured from coal or water, both of which the United States has an abundant supply of, we

need not worry about fuel shortages once the industry is set up. LH2 produces higher specific fuel consumption (.58 lbs/hr/lb for jet-A, .23 lbs/hr/lb for LH2) and it can be used to pre-cool inlet air, so higher compression ratios and inlet turbine temperatures can be used (40:1, 3800 degrees fahrenheit).

It was finally decided to implement LH2 as our fuel for the following reasons. Since our mission specifies a short range, the mission fuel requirement is low. That, coupled with the fact that the HCSRT is a large plane, means that there will be no problem storing the needed amount of LH2, despite the fact that it is four times more voluminous than jet-A. It is also assumed that fuel availability will not be a problem since the HCSRT is designed to mainly function at major hubs. Again, since the trip length is short, evaporation losses which make the LH2 prohibitive on long flights, can be neglected for the HCSRT. Lastly, since the additional weight needed to use LH2 (pumps and tanks) is fairly constant and not a strong function of range, it becomes a small percentage of the take off weight. So in summary, LH2 was utilized because it has advantages that the HCSRT is able to take advantage of, and the disadvantages were able to be minimized. In accordance with the Lockheed study (see reference 4), it is estimated (there is as of yet no existing concrete data for exact numbers) that our fuel weight will be decreased by a factor of 2.9 over that of conventional jet-A fuel, and take off gross weight will be nominally increased. The effect of fuel cost on direct operating cost is hoped to be a smaller percentage in the year 2010 with LH2 than it would if jet-A was used. This is because the cost of jet-A is expected to increase (at

least) from $2 per million BTU (1973) to $3.5 per million BTU in 2010, while LH2 is expected to increase from $3 per million BTU (1973) to $3.7 per million BTU in 2010 (reference 4). Since direct operating cost is a strong function of fuel cost, it is hoped that using LH2 will be a financially beneficial decision.

Initially, it was decided to fit all the fuel in two cylindrical tanks, one aft and low, the other below and forward of the passenger deck. Cylinders were used for structural integrity in containing constant internal pressure loads. However, it was found that the tanks' radii would be to big to hold the required 3231 cubic feet. It was then decided to complement these two tanks (volumes of 1672 and 778 cubic feet) with tapering cylindrical tanks that would fit inside the front wing and run from the fuselage out to the wing joint (0.70c). Six of these of these tanks could be fit into the front wing and hold a total of 781 cubic feet of fuel, giving a total aircraft fuel volume of 3231 cubic feet. In the interest of minimizing evaporation, operating procedures will dictate that fuel is pulled from the wing tanks first. In addition, for flights of less than 700 statute miles (i.e. SDO to Sacramento, all California Corridor one way flights), the wing tanks would not be needed.

Table 3.4-1: Emissions and Safety Comparison Between LH_2 and Jet A

EMISSIONS COMPARISON
(PARTS PER 10^6)

	Jet A	LH_2
CO	30	0
unburned HC	4	0
smoke	15	0
NOx	12	3

SAFETY COMPARISON

	Jet A	LH_2
vapor space flammable?	YES	NO
burning rate	slow	fast
emissivity	high	low
by products	noxious	safe
leakage danger	low	high
health hazzard	skin irritant	tissue freezing
evaporation	slow	fast
hot surface ignition	420°F	1100°F
spark ignition	safe	unsafe

Source: Brewer, Morris, Lange, Moore, "Study of the application of hydrogen fuel to long-range subsonic transport aircraft", Jan. 1975, Lockheed Aircraft Corp., Contract NAS 1-12972

Table 3.4-2 COMPARISON OF FINAL DESIGNS: LH_2 VS JET A PASSENGER AIRCRAFT (SHORT RANGE)

[M = 0.85; 400 PAX; 5560 km (3000 n mi)]

	SI	CUSTOMARY	LH_2		JET A		FACTOR (JET A/LH_2)
			SI	CUSTOMARY	SI	CUSTOMARY	
Takeoff Gross Weight	kg	lb	152,000	335,200	183,200	404,300	1.21
Operating Empty Weight	kg	lb	96,500	212,900	95,500	210,600	0.99
Block Fuel Weight	kg	lb	12,700	28,000	37,400	82,400	2.95
Total Fuel Weight	kg	lb	15,600	34,300	47,800	105,700	3.08
Wing Area	m^2	ft^2	283	3,047	301	3,235	1.06
Wing Loading, Takeoff	kg/m^2	lb/ft^2	537	110	610	125	1.1.
Landing	kg/m^2	lb/ft^2	488	100	488	100	1.0
Span	m	ft	50.5	165.6	52	170.6	1.03
Fuselage Length	m	ft	64	210	60	197	0.94
Lift/Drag (Cruise)			14.86	14.86	16.66	16.66	1.12
Specific Fuel Consumption (Cruise)	$\frac{kg}{hr}/kN$	$\left(\frac{lb}{hr}\right)/lb$	0.203	0.200	0.592	0.582	2.91
Thrust per Engine (SLS)	N	lb	110,000	24,720	114,500	25,770	1.04
Thrust/Weight (SLS)	N/kg	-	2.90	0.295	2.51	0.255	0.87
FAR T.O. Distance	m	ft	1,790	5,860	2,437	7,980	1.36
FAR Landing Distance	m	ft	1,770	5,804	1,760	5,760	0.99
Approach Speed (EAS)	m/s	knots	69.5	135	69	134	0.99
Weight Fractions	percent	percent					
Fuel			10.2	10.2	26.2	26.2	2.57
Payload			26.3	26.3	21.8	21.8	0.83
Structure			31.7	31.4	27.8	27.8	0.89
Propulsion			10.7	10.7	6.7	6.4	0.60
Equipment and Operating Items			21.7	21.4	17.8	17.8	0.83
Energy Utilization	$\frac{kJ}{seat\ km}$	$\frac{Btu}{seat\ n.m.}$	1,510	1,204	1,580	1,260	1.05

Source: Brewer, Morris, Lange, Moore, "Study of the application of hydrogen fuel to long-range subsonic transport aircraft", January 1975, Lockheed Aircraft Corp., contract NAS 1-12972

3.5 Landing Gear Configuration

For the preliminary landing gear design of the HCSRT, retractable landing gear was preferred to fixed, due to the large drag component that would be imposed at high cruise speeds from fixed gear. The first landing gear configuration that was considered was tail dragger gear because the lateral tip over criterion required the ground span to be ten feet wider than the fuselage is. The front wing being low allows the font gear to be placed out on the wing.

This tail dragger design was dropped and replaced by tricycle gear after a weight and balance was done and it was seen that with some minor weight corrections, the tricycle gear would work most effectively. The placement of the rearward, main gear, under the front wing, is designed to utilize one strut five feet out on each side of the fuselage, with one strut at the same longitudinal position in the center of the fuselage. The nose wheel is centered on the fuselage thirty-six feet behind the nose. This positioning keeps less than 100 feet between the main gear and the nose gear, which allows for optimal ground maneuvering while still maintaining the lateral tip over criterion.

The change from tail dragger to tricycle gear did require a small change in the tail cone shape to allow for a proper ground clearance for take off rotation. The wing design inherently took care of the lateral ground clearance since the dihedral is greater than the clearance angle required.

Three main struts with four tires on each were chosen for

the main landing gear. This configuration yields stress values which are comparable to aircraft working today such as the Boeing 737 and 747.

3.6 Structural Design

As has been described earlier, the main advantage of the joined wing configuration is its structural weight savings. There was major concern during the early stages of joined wing technology which delt with the large out of plane bending moments induced by the rear wing on the forward wing. This has been eleviated however by the use of an asymetric spar.

This spar is constructed by making the caps in the wing box different thicknesses. Since the forward lower and rearward upper sparcaps must take the majority of the torsion loads, they will be thicker while the other two caps can be reduced. Also the caps can be tapered in thickness along the span since the loads decrease toward the tips. All these factors will decrease wing weight in addition to the savings already incorporated by the aerodynamic advantages of the configuration.

In order to optimize the wing weight, an iterative process must be used between the wing weight and the material thickness. This process was performed by a program called JWOPT (Joined Wing Optimization), written by Ilan Kroo and John Gallmann of NASA. A flow chart which shows the sequence of calculations is shown in fig. 3.6-1. First, the input file is read and initialized. The subroutine PLANF is then called to determine the wing position which provides the required static margin and calculates other geometric

properties. TLOAD is then used to calculate calculate the load distributions which trim the aircraft at CL=CLref and produce minimum drag. The subroutine LASUB is used by TLOAD to calculate aerodynamic loadings using extended lifting line theory. The structural optimization loop starts by computing the cross sectional area and moments of inertia. The data from TLOAD is used to calculate the minimum beam dimentions needed to support the structural loads. The structural weight is now calculated by integrating the cross-sectional area distribution along the span to get structural volume and multiplying by the material density.

A test is now made to see if the weight equals the initial guess (or the last iterative value). If not, the new weight value is used to calculate shear and moment distributions and the minimum cap and web thickness needed. This process continues until the minimum weight is achieved. JOAPT then exits the loop and the results are printed out. Detailed discriptions will now be given for each of the primary analysis sections.

Subroutine LASUB

LASUB is a subroutine version of the program LinAir published by Desktop Aeronautics. This subroutine calculates the forces, moments, and lift distributions on multi-element, nonplanar lifting surfaces using a discrete vortex Weissenger method. Forces and moments are computed using Trefftz plane induced velocities. LinAir solves the Prandtl-

Glauert equation, a linear partial differential equation describing inviscid, irrotational, subsonic flow. The equation gives a relation between the flow in the x,y, and z directions and the freestream Mach number. This is solved by representing the wing surfaces with discrete vortex lines forming skewed horseshoe vorticies. The vortex strengths are adjusted so that the flow is tangent to the surfaces at a series of control points. These points are located on the 3/4 chord line of each element. The "bound vortex" is located at the 1/4 chord line. The equation for each element is put into a matrix and the system is solved. The force and moment contribution is then calculated from the Kutta-Joukowski relation.

Subroutine PLANF

The planform geometry which is consistant with wing sweep, wing dihedral, wing span, joint location, the ratio of wing and tail aspect ratios, and the desired static margin is determined by the subroutine PLANF. The assumptions are, (1) that the parameters defining the wing geometry are fixed, and (2) that the distance between the aircraft center of gravity and the tail root quarter chord is a fixed input value. The basic idea is to move the wing forward or aft until the desired static margin is achieved. Since the wings are joined, this requires changing the tail sweep and dihedral.

Subroutine TLOAD

The aerodynamic load distributions need to be determined before the structure can be optimized. Subroutine TLOAD is an aerodynamic optimization routine which minimizes the drag, and trims the aircraft at CL=CLref. The aerodynamic solution is determined for an aircraft cruising at zero angle of attack. The drag is minimized with respect to root incidence and tip twist angles for the wing and tail, where the twist distributions are linear. Consequently subroutine TLOAD calculates the lift distributions, root incidence and tip twist angles, and the minimum drag of the lifting system.

Subroutine BEAM

The subroutine BEAM is responsible for the structural analysis. Its primary function is to compute and return the structural moment distributions, and deflections due to aerodynamic loads, structural weight, and wing joint reaction forces. The structural analysis assumes that the wing and tail can be represented by inextensible beams. These beams are represented by a finite number of sections with known inertial properties. Asymmetric box beams are used for both the wing and tail and are optimized for minimum total structural weight. The web and cap thicknesses are sized such that a maximum allowable stress is not exceeded and minimum cross sectional area is obtained at each spanwise station.

Once the analysis is complete, JOAPT prints out several output files which can be chosen in the input file. The seven files include aerodynamic forces, 3-D load distributions, shear and moment distributions, deflections, Thickness of the caps and webs, the convergence history of the weights, and the three dimentional coordinates of the wing and tail. The output for the HCSRT is included in the results and calculations section.

Verification of JOAPT could not be done by hand as it would take many weeks. But the program has been tested extensivly by NASA and is documented in a number of articles. Joined Wing Optimization Program Mannual written by John Gallman and Ilan Kroo is the users guide and describes the program fully. Reference 17 is an unpublished document which gives wind tunnel results of a joined wing model designed using JWOPT. The results show very good accuracy of the program.

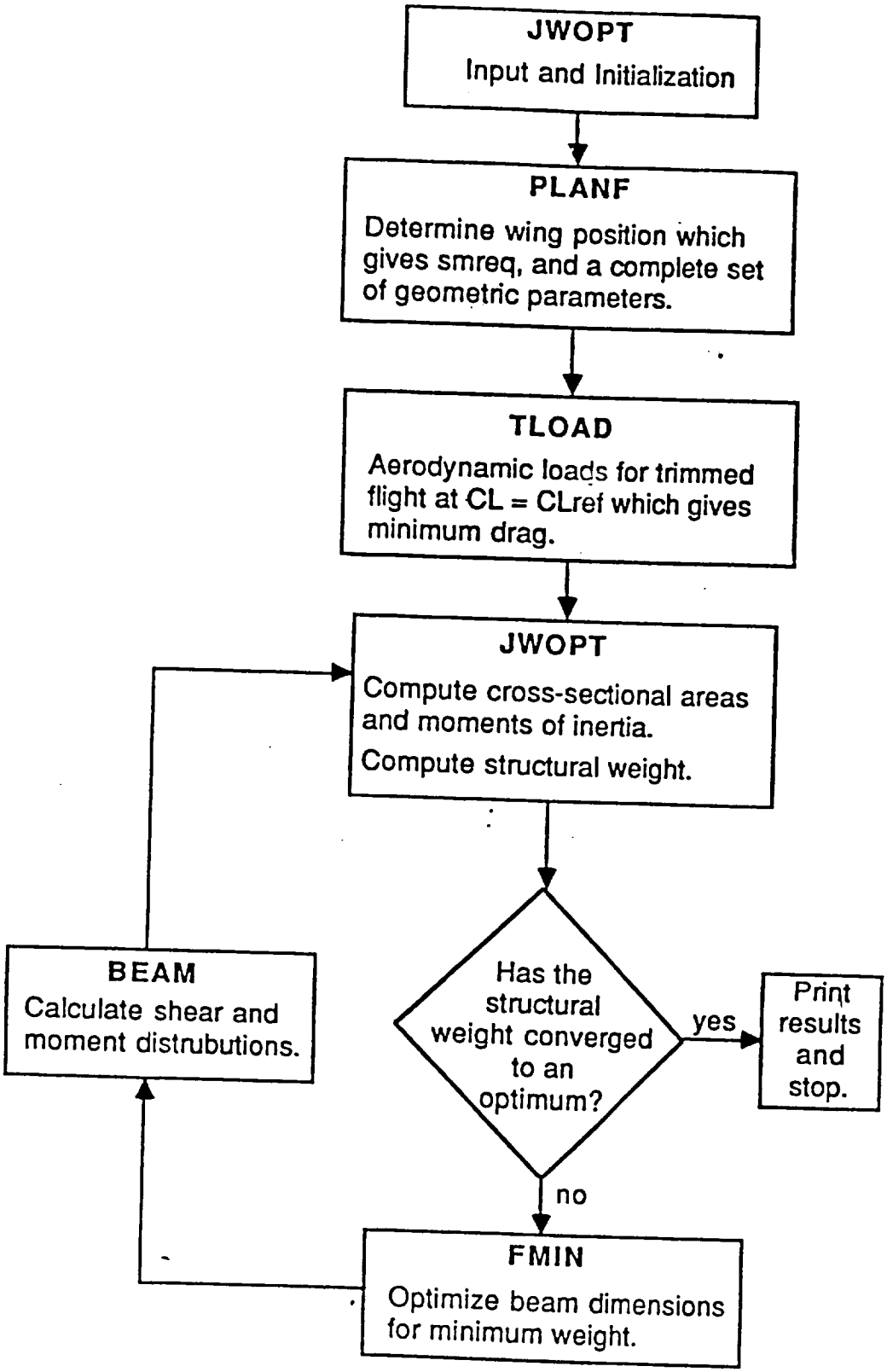

Source: REFERENCE 17

Fig. 3.6-1 JWOPT Flow Chart

3.7 Weight and Balance

The HCSRT was broken up into components and each component was given a weight fraction of the total plane (as per indicated in reference 11). These fractions were obtained from comparable aircraft such as the McDonnell Douglas DC-10 and the Boeing 747. Each component weight fraction was adjusted up or down to account for expected differences in structure supports and required equipment. Once the weights were all decided, the center of gravity of each component was calculated to obtain a moment arm. The moment of each component was calculated about the longitudinal balance (table 3.7-1), as well as about the vertical balance (table 3.7-2), at ten feet below the fuselage. These center of gravity locations (119.4 feet from the nose longitudinally and 10.9 feet up from the bottom of the fuselage) allowed the landing gear to be changed from a tail dragger landing gear configuration to a more conventional tricycle configuration, due to the forward location of the longitudinal center of gravity.

Prior to the current locations of the fuel tanks in the HCSRT, a weight excursion diagram was done once all the component's variations were calculated, and it was found that the no passenger, no cargo and no full tanks scenario did not keep the center of gravity in front of the main gear. This required that some of the fuel from the rear tanks be moved forward. The solution was easy since there was open space near the nose, just in front of the nose wheel. A tank as

large as could be fit was placed in the free space (hence the current fuel tank locations) and another excursion diagram was done (figure 3.7-1). The current configuration meets the required limit of fifteen degrees forward of the landing gear as required for the longitudinal stability during ground maneuvers and take off.

Table 3.7-2 Vertical CG

Component	Weight	Z_{cg}	Moment
Fuselage	79,786	22.1	1,763,271
Wings Forward	42,789	16	684,624
Rear	18,738	35	641,830
Vertical Tail	6,600	36	237,600
Horizontal Tail	904	48	43,392
Canard	4,400	18	79,200
Engines	44,076	23.75	523,402
Landing Gear:		up dn	
Main	25,480	12 / 7	305,760
Nose	6,370	12 / 7	76,440
Equipment	62,413	21.25	1,326,276
Nacelles	4,826	23.75	114,618
Fuel - Main	7,700	23.75	182,875
Nose	3,583	14.6	53,312
Wing	3,597	15	53,955
Pax	105,000	22.5	2,362,500
Baggage	18,000	14.6	262,800
Crew	3,075	22.5	69,188
W_{tfo}	1,744	20.1	35,054
W_{to}	438,682		9,176,520

Zcg = 20.9 ft (gear up)

Zcg = 20.6 ft (gear down)

Table 3.7-1 Longitudinal CG

Component	Weight	X_{cg}	M_{nose}
Fuselage	79,786	110	8,776,460
Wings Forward	42,789	150	6,418,350
Rear	18,738	185	3,392,530
Vertical Tail	6,600	209	1,379,400
Horizontal Tail	904	206	186,224
Canard	4,400	26	114,400
Engines	44,076	168	7,404,768
Landing Gear:			
Main	25,480	130	3,312,400
Nose	6,370	20	127,400
Equipment	62,413	95	5,929,235
Nacelles	4,826	180	868,680
Fuel - Main	7,700	189	1,455,300
Nose	3,583	27	96,741
Wing	3,597	120	431,640
Pax	105,000	93	431,640
Baggage	18,000	c.g.	-
Crew	3,075	93	285,975
W_{tfo}	1,744	168	292,992
W_{to}	438,682		50,237,495

X_{cg} = 119.4 feet

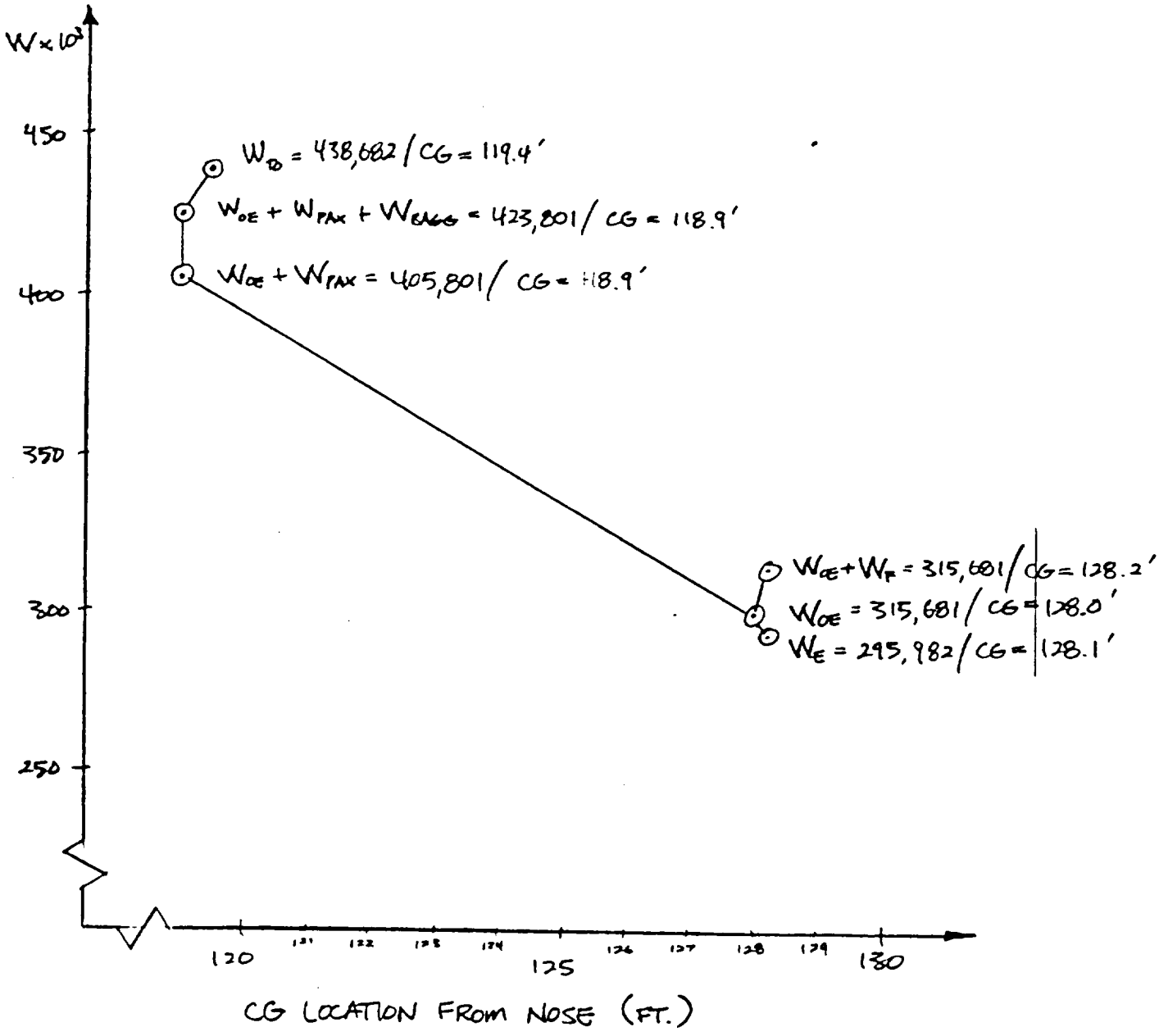

Figure 3.7-1
Weight Excursion Diagram

3.8 Static Stability

Since the HCSRT is a passenger plane and cost is a major concern, the aircraft was designed to be inherently stable. The canard was sized at 580 square feet, which gave a static margin of 7.4 feet, or forty percent of our root chord of the front wing (figure 3.8-1). At first this seemed large, according to reference 11. However, the joined wing has a much larger aspect ratio, which creates a smaller root chord than the conventional cantilever wing, besides the fact that the total wing area is divided between the front and rear wings. This canard size also allows enough lift on the front of the aircraft to counter the large moment keeping it from rotating at take off.

When resizing the vertical tail (the vertical tail had previously been sized from comparisons to similar existing aircraft), inherent stability was desired to avoid large computer costs. The vertical tail size required for a cantilever aircraft of comparable size to the HCSRT would be 400 square feet (figure 3.8-2). The joint wing, however, has slight directional instability in side slip conditions due to the large anhedral of the rear wing. Therefore, the vertical tail size was doubled, which resulted in a twin vertical tail of 400 square feet each. This tail size allows for a sufficient stability factor and requires only 9.4 degrees deflection of the rudders for the most critical engine out condition. It may be possible to reduce the size of the vertical tail with further study.

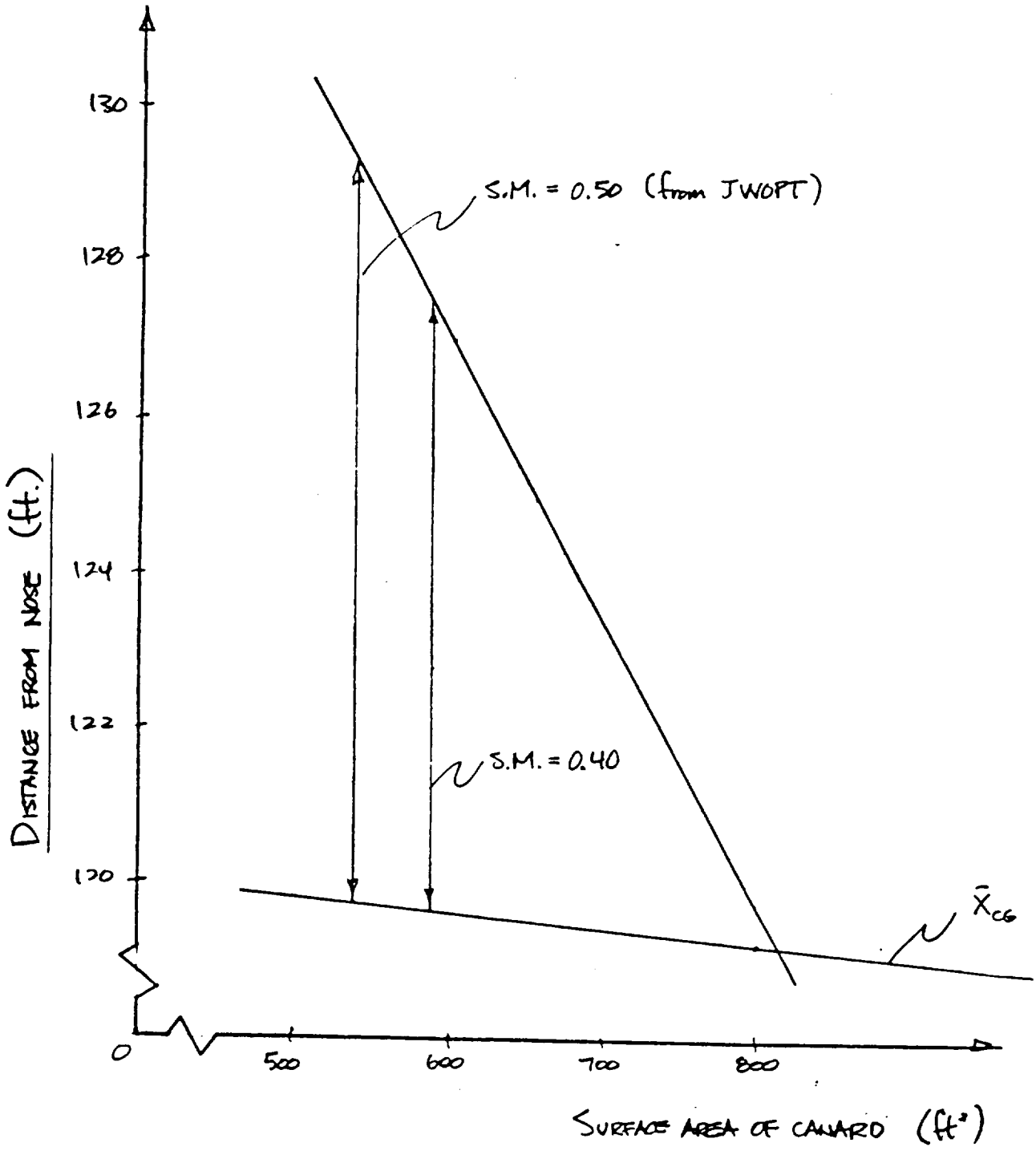

Figure 3.8-1
Stability X - Plot

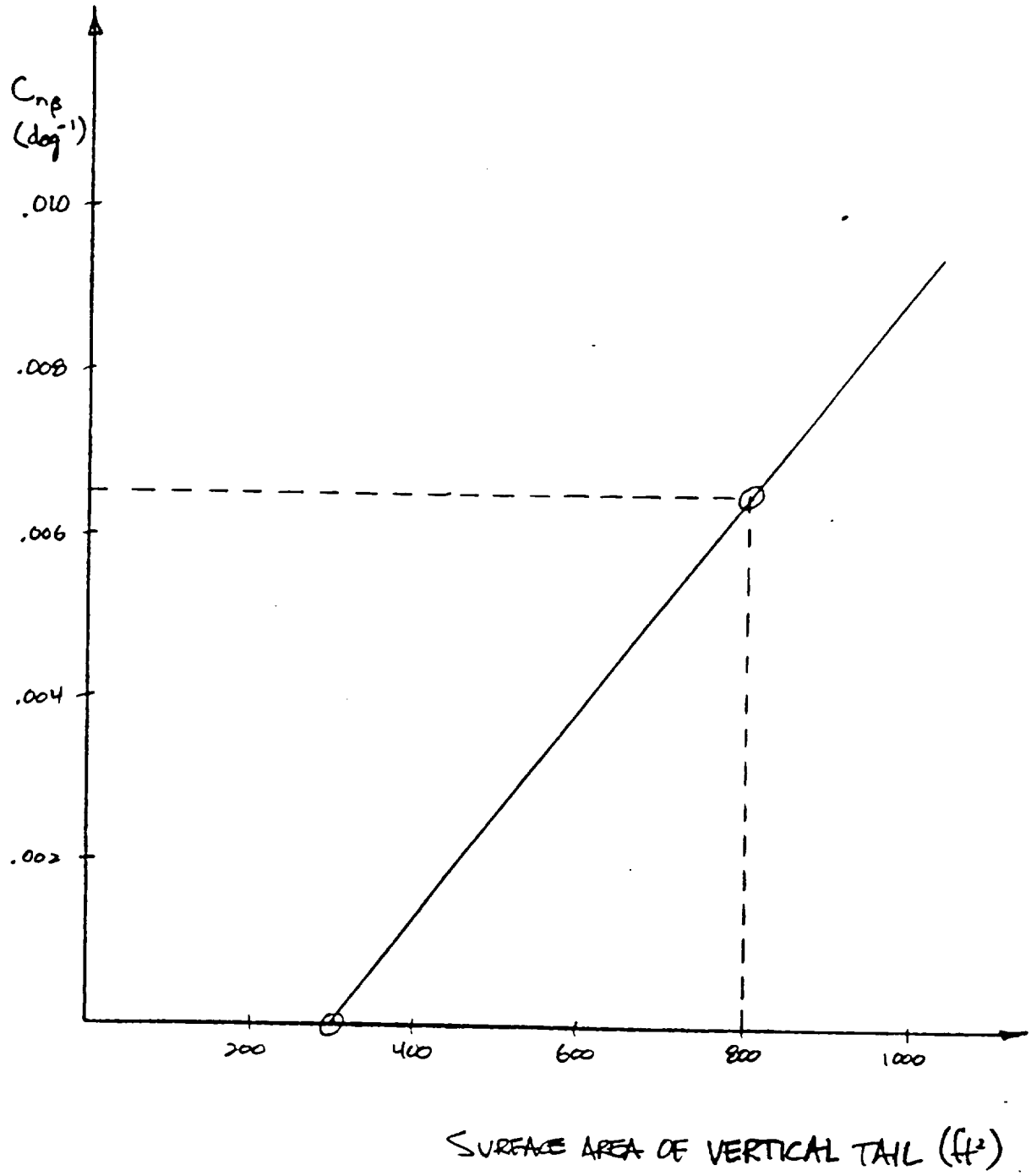

Figure 3.8-2
Vertical Tail Sizing

3.9 Conclusion

The design of the HCSRT was a complete preliminary aircraft design with some aspects being researched beyond the preliminary stage. However, there are some other areas that could still use some more research.

The joined wing has the potential for direct side force control if the proper sizing is used for front and rear "elevons." The use of these elevons would require a computer augmentation system, and it would allow for good cross wind landings with the bank angle requirements.

With all its advantages, the joined wing may have some disadvantages with interference drag and flow patterns off the wing joints. This would be an area of extreme concern for the HCSRT. A brief study showed no major problem with the choice of location. However, the effects are not totally understood.

The liquid Hydrogen system has not been completely researched. Insulation, pumping and storage still need to be looked into. The Hydrogen integration into the engines is known to be possible but since engine technology is always changing, an actual design needs to be developed. Since this is still a developing technology, not all of the information is available yet.

A complete landing gear system still needs to be developed. The preliminary report only covers it's height

and location. Still needed are the specifications of the tires, struts, structure, and retraction system.

There are many areas that need more research before this design is ready for construction. However, this report is a thorough preliminary design, and shows the definite ability of the HCSRT to fulfill the mission requirements in a very economic way.

References

1. Abbott, Ira, VonDoenhoff, Theory of Wing Sections, Dover, 1959

2. Bell, Bob, General Electric Company, 5933 W. Century Blvd., Suite 800, Los Angeles, CA, 90045

3. Brewer, "A Proposed LH2 development Program For Aircraft", Lockheed Aircraft, Burbank CA

4. Brewer, Moris, Lange, Moore, "Study of the Application of Hydrogen Fuel to Long Range Subsonic Transport Aircraft", Jan. 1975, Lockheed Aircraft Corp., Contract NAS 1-12972

5. Darrow, "Joined-Wing Aircraft: Wave of the Future?", Design News, April 7, 1986

6. Hockaday, Steve, Chairman, Civil Engineering Dept., California Polytechnic State University

7. Kroo, Gallman, "Aerodynamic and Structural Studies of Joined Wing Aircraft", AIAA-87-2931

8. Kroo, I. Desktop Aeronautics, P.O. Box 9937, Stanford CA, 94305, Aug. 1987

9. Page & Ivey, "Ultra High Bypass Engine Applications to Commercial and Military Aircraft", SAE Technical Paper Series 861720

10. Roskam, Jan, "Airplane Design", Part I, Roskam Aviation and Engineering Corporation, 1985

11. Roskam, Jan, "Airplane Design", Part II, Roskam Aviation and Engineering Corporation, 1985

12. Roskam, Jan, "Airplane Design", Part III, Roskam Aviation and Engineering Corporation, 1985

13. Roskam, Jan, "Airplane Design", Part IV, Roskam Aviation and Engineering Corporation, 1985

14. Roskam, Jan, "Airplane Design", Part V, Roskam Aviation and Engineering Corporation, 1985

15. Roskam, Jan, "Airplane Design", Part VI, Roskam Aviation and Engineering Corporation, 1985

16. Smitch, Cliff, "The Design of a Joined Wing Flight Demonstrator Aircraft", AIAA-87-2930

17. Smith, Stephen, "Experimental Aerodynamic Characteristics of a Joined-Wing Rearch Aircraft Configuration", NASA Ames Research Center, Moffett Field, CA

18. Smith, Stephen, correspondance

19. Wolkovitch, J, "Joined Wing Research Airplane Feasibility Study", AIAA-84-2471

20. Wolkovitch,. J, "The Joined Wing: An Overview", AIAA-85-0274

T R A N S I T

PRELIMINARY AIRCRAFT DESIGN

PREPARED FOR:

Aero 445
Dr. Doral R. Sandlin
Aeronautical Engineering Department
California Polytechnic State University
San Luis Obispo

PRESENTED BY:

Kipp Howard
Byron Proshold
Jim Rogers
Teana Suggs-Chandler

Spring, 1989

Abstract

Projections show that the population of California will continue to increase, which will cause a severe strain on an already impacted transportation system. This problem has been recognized and solutions are being investigated. This report contains the justification, design and analysis of one possible solution which will improve the transportation system of the California Corridor in the year 2010. The resulting design is a forty passenger transport aircraft which has the ability to takeoff and land like a helicopter but cruise as a conventional aircraft.

Table of Contents

List of Tables

List of Figures

List of Symbols

a	Lift curve slope
A or AR	Aspect ratio
a.c.	Aerodynamic center
b	Wing span
c	Chord length
C_D	Total drag coefficient
$C_{d,o}$	Profile drag coefficient
$C_{D,o}$	Parasite drag coefficient
c_f	Coefficient of friction
CG	Center of gravity
CGR	Climb gradient
CGRP	Climb gradient parameter
C_l	Section lift coefficient
C_L	Total lift coefficient
C_m	Moment coefficient
C_{mac}	Moment coefficient (aero. center)
C_T	Thrust coefficient
D	Drag
DL	Disk loading
e	Oswald efficiency factor
gc	Gravitational constant (32.2 ft/sec^2)
i_t	Tail incidence angle
i_w	Wing incidence angle
L	Lift
L/D	Lift to drag ratio
mac	Mean aerodynamic chord
M	Mach number
M_{ff}	Mission fuel fraction
M_{res}	Reserve fuel fraction
n	Load factor
nm	Nautical mile
P	Power (horse-power)
P_a	Power available
P_r	Power required

P_s	Specific excess power
q	Dynamic pressure
R	Range
R/C or ROC	Rate of climb
RCP	Rate of climb parameter
S	Wing area
S_e	Elevator area
S_h	Horizontal tail area
S_r	Rudder area
S_v	Vertical tail area
S_{wet}	Wetted area
t	Time
T	Thrust
T_a	Thrust available
T_r	Thrust required
V	Velocity
W_e	Empty weight
W_f	Mission fuel weight
W_{pl}	Payload weight
W_{to}	Takeoff gross weight

Greek Symbols

α	Angle of attack
β	Side slip angle
δ_e	Elevator deflection
ε	Downwash
η_t	Dynamic pressure ratio at horizontal tail to freesteam dynamic pressure
η	Propeller efficiency
λ	Thickness ratio
π	Pi = 3.14159
ρ	Air density
σ	Density ratio, or solidity
Λ	Sweep angle

Acronyms

AEI	All engines inoperative
AEO	All engines operating
APU	Auxiliary power unit
DOD	Department of Defense
FAA	Federal Aviation Administration
FAR	Federal Aviation Requirements
IGE	In ground effect
NASA	National Aeronautics and Space Administration
OEI	One engine inoperative
OGE	Out of ground effect
SL	Sea level
STOL	Short takeoff and landing
TRANSIT	Tilt rotor aircraft needed to simplify intercity transportation
VTOL	Vertical takeoff and landing

Introduction

The population in California is projected to reach 36 million by the year 2010. This increase will cause a major impact on the present transportation system. Therefore, new transportation systems must be incorporated to accommodate the needs of the expanding population. Specifically, this report focuses on the design of a Tilt Rotor Aircraft Needed to Simplify Intercity Transportation, TRANSIT, in the California Corridor for the year 2010.

Preliminary investigations showed that a system which incorporates both VTOL and STOL aircraft is needed for the California corridor. The need for a VTOL aircraft becomes more apparent as the population increases outside of major city centers. This expansion will result in further congestion of already impacted freeways. VTOL aircraft can provide intercity service for travelers who would like to minimize time spent in traveling to and from airports as well as service the commuter who does not want to spend time on a congested freeway. Other markets which could utilize VTOL aircraft include package express, resource development (offshore oil), law enforcement, disaster relief, and corporate travel.

To achieve the portal-to-portal service that will make VTOL aircraft cost competitive with other means of transportation, vertiports must be incorporated into the present transportation system to allow VTOL access close to a traveler's destination. Examples of potential vertiport locations are above freeways, on top of buildings, on waterfront property, or at existing airports.

TRANSIT was designed to fulfill the VTOL requirements for the California corridor. The tilt rotor aircraft has many advantages which made it the best VTOL configuration for the given mission. The advantages include VTOL and STOL capabilities, less noise, lower weight, flexibility in operation (vertiports and short runway accessibility), and marketability for other missions. In addition, TRANSIT uses the Telescoping Rotor Aircraft (TRAC) variable diameter rotor system developed by Sikorsky Aircraft (Ref. 1). Although the TRAC rotor increases the weight of the aircraft, the advantages pay off overall. Lower disk loading, better cruise efficiency, and greater speeds are all advantages of the TRAC rotor system. This report contains a discussion of the methodology and results of the design of TRANSIT.

Mission Requirements

TRANSIT was designed primarily to fulfill the needs of the high-density, intercity, civil market for the California corridor in the year 2010. However, the demand for TRANSIT in other markets, such as government public service, resource development (offshore oil), intracity/metropolitan, and package express, was taken into consideration for increased marketability. The TRANSIT design specifications were chosen according to various reports on the tilt rotor aircraft and California corridor. The specifications are summarized in Table I and the mission profile is illustrated in Figure 1.

Table I. Mission Specifications

Number of Passengers	40
Crew	1 Pilot, 1 Attendant
Cargo Weight	8610 lbs
Range	375 nm
Cruise Speed	325 knots
Cruise Altitude	16,000 ft
Pressurized Cabin	@ 8,000 ft
Critical Hover Condition	OEI, 200 fpm, 95° F, 3000 ft
Noise Level	85 PNdB

The payload was chosen based on the potential market demands for the year 2010. Figure 2 shows that the greatest demand (1200 units) for the high density market is 36-45 passengers (Ref. 2). With a seating capacity of 40, TRANSIT will fit this optimum range as well as fulfill the capacity needs in other markets. The weight per passenger was chosen to be 175 lb/person plus 30 lb baggage for short to medium flights (Ref. 3). Thus, the total cargo weight is 8610 lbs.

A flight crew of 1 pilot and 1 attendant was selected. The current Federal Aviation Requirements, FAR's, (Ref. 4) require two pilots; however, with increasing technology, it is reasonable to say that automated piloting systems will alleviate the need for two pilots by the year 2010.

The range and speed specifications were determined in order to be competitive with other means of transportation. First, the range was chosen to be 375 nm to accommodate transportation from within a 45 nm radius of Los Angeles to within a 45 nm radius of San Francisco. The Los Angeles-San Francisco route was

found to be the most traveled in the California Corridor. The speed was chosen to have a portal-to-portal trip time better than other transportation means. With a speed of 325 knots, TRANSIT can accomplish this and stay within the limitations of the tilt rotor aircraft design.

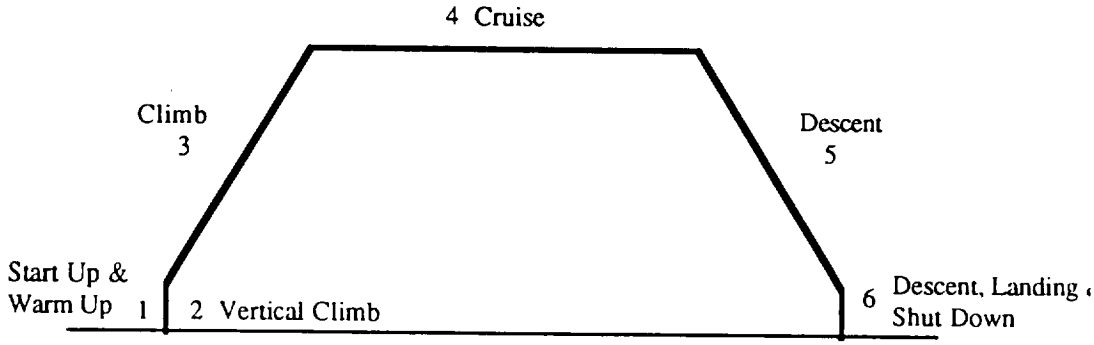

Figure 1. Mission Profile

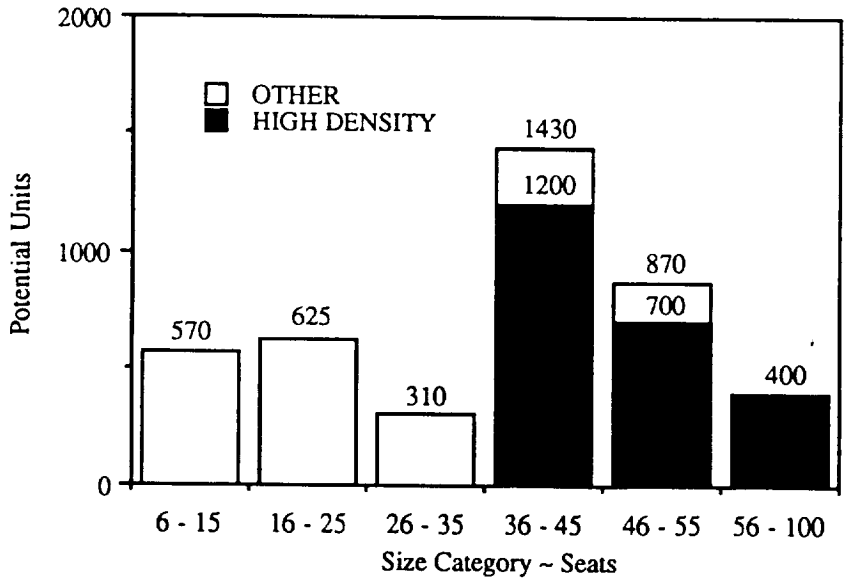

Figure 2. Potential Market Demand

A prime consideration in the design of future aircraft is the noise they produce. Current noise requirements limit the effective perceived noise levels as follows: 89 EPNdB for takeoff, 94 EPNdB for sideline, and 98 EPNdB for approach (Ref. 5). The noise requirement for TRANSIT was chosen to fit community acceptance and the limits of tilt rotor aircraft. A maximum perceived noise level of 85 PNdB was chosen.

Design Approach

After researching the needs of the California corridor and choosing the mission specifications, several steps were taken in designing the optimum VTOL aircraft. First, several VTOL configurations were considered and the best one chosen based on a trade-off study which included the following parameters: speed, noise, weight, efficiency, safety, complexity, and cost. The configurations considered were fan in wing, lift fan, compound helicopter, stowed rotor, tilt rotor, tilt wing, and lift jet. The tilt rotor aircraft was determined to be the best configuration.

Tilt rotor cruise speeds are only greater than the compound helicopter but the trade-off between the speed, weight and noise of an aircraft made the tilt rotor a better VTOL design. The lift fan, fan in wing, and lift jet especially had very high perceived noise levels, which is undesirable for the specified mission. A variable diameter tilt rotor aircraft could provide much higher hover and cruise efficiencies than a conventional tilt rotor aircraft. Although the variable diameter configuration rates high in complexity, the performance and other benefits that accrue will enable it to survive in a competitive economic market.

Once the configuration was selected, preliminary design analysis was conducted to determine the characteristics for performance, stability and control, and structures. The direct operating cost was also calculated. Since a tilt rotor aircraft consists of both vertical and forward flight capabilities, the methodology used combined the design approaches of helicopters and conventional turboprop aircraft.

Results

Performance

Table II contains the performance results for both vertical and forward flight. The power curves are given in Figures 3 and 4 for conditions at sea level and 16,000 ft. Because the power required for the critical climb condition is large, the power available exceeds the power required in cruise by over 4,100 hp. The maximum rate of climb at sea level is over 8,400 fpm, as shown in Figure 5. Climb speeds of this amount will never be used because passenger comfort would be sacrificed. The service ceiling is 28,172 ft. Again, this limit will never be reached because the efficiency of the aircraft would significantly decrease and larger weights due to pressurization would occur. Figure 6 shows the results that altitude and ground effect have on the vertical rate of climb. TRANSIT has the ability to land vertically at any altitude below 19,000 ft. and hover continuously out of ground effect up to altitudes of 4,500 ft. Figure 7 shows the power required to climb

vertically. TRANSIT can climb at rates up to 5000 fpm at sea level with the installed power. These overall performance characteristics for hover and cruise are indicative of the excess power necessary to hover in the critical climb conditions. The drag polar, C_D vs. C_L, curve is shown in Figure 8.

The results of the noise are based on an overall sound pressure level at 300 ft. and are shown in Figure 9. The results show that the maximum perceived noise level reached would be 84 PNdB which is within the 85 PNdB limit specified for TRANSIT.

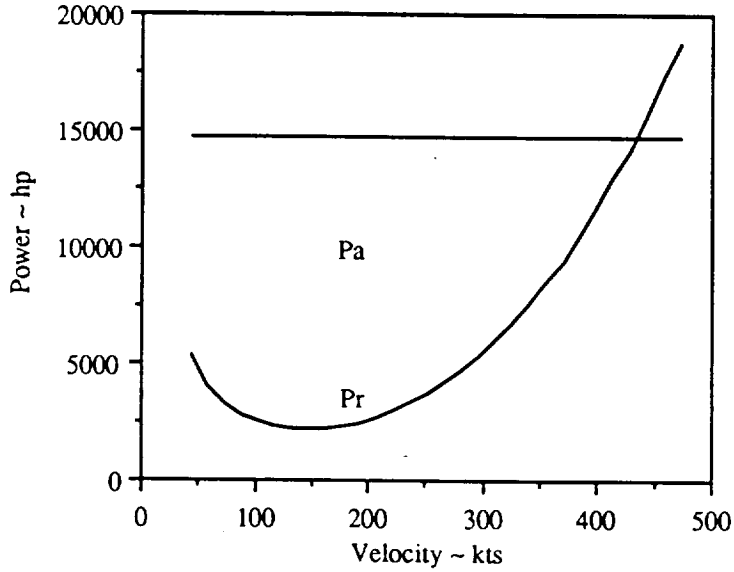

Figure 3. Power Available and Power Required Curves, @ SL

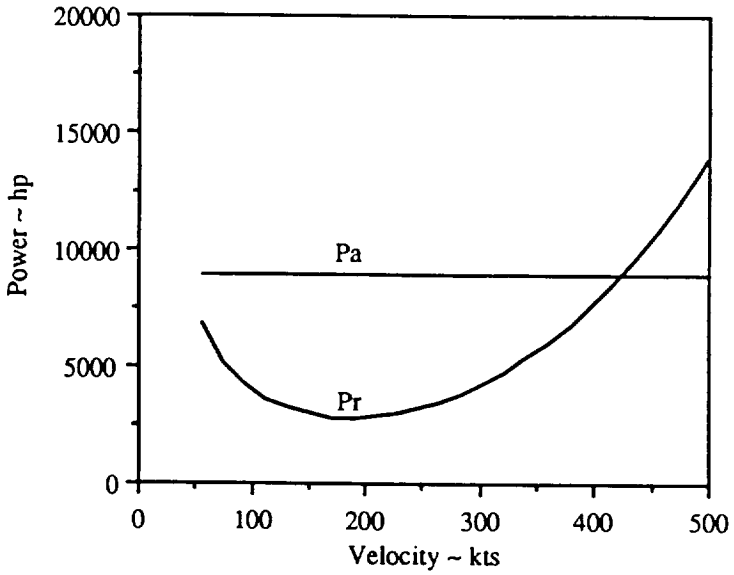

Figure 4. Power Available and Power Required Curves, @ 16,000 ft.

Table II. Performance Results

Weights	
$W_{payload}$	8,610 lbs
W_{to}	48,789 lbs
W_{empty}	31,724 lbs
W_{fuel}	6,813 lbs
Rotor	
Number of Blades	4
Radius (Cruise)	14.61 ft
Radius (Hover)	24.36 ft
Blade Chord	2 ft
Torque Tube Chord	0.8 ft
Twist	-30 deg
ß @.75 r/R	47.5 deg
Collective Pitch	33 deg
Solidity (Cruise)	0.174
Solidity (Hover)	0.101
Figure of Merit	0.779
Autorotative Rate of Descent	105 fps
Disk Loading	13.1 psf
Advance Ratio	2.48
Blade Taper Ratio	1.0
Rotor Airfoil	Bell XN-12
Cruise Efficiency	0.748
Tip Speed (Cruise)	690 fps
Tip Speed (Hover)	645 fps
Performance Parameters	
Cruise Speed (@ 16,000 ft.)	372 mph
L/D	10.7
P_r (Cruise)	3,458 hp
P_r (Hover)	2,991 hp
P_r (OEI)	6,129 hp
T_r (Cruise)	24,394 lbs
T_r (Hover)	2,619 lbs
Stability Derivatives	
$C_{m_{\delta e}}$	-1.57/rad
$C_{m_{\alpha}}$	-0.54/rad
$C_{n_{\beta}}$	0.057/rad
$C_{n_{\delta r}}$	0.14/rad
Powerplant	
No. of Engines	2
Type of Engines	Allison 501-M62
Horsepower, per engine (max)	7,305 hp
Specific Fuel Consumption (cruise)	0.520 lb/h/ehp

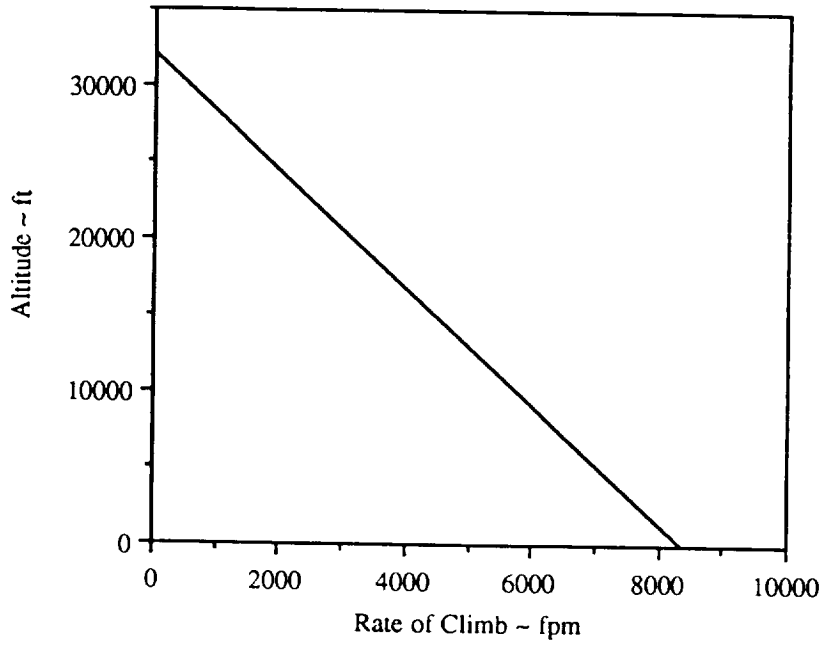

Figure 5. Altitude Vs. Rate of Climb, Cruise

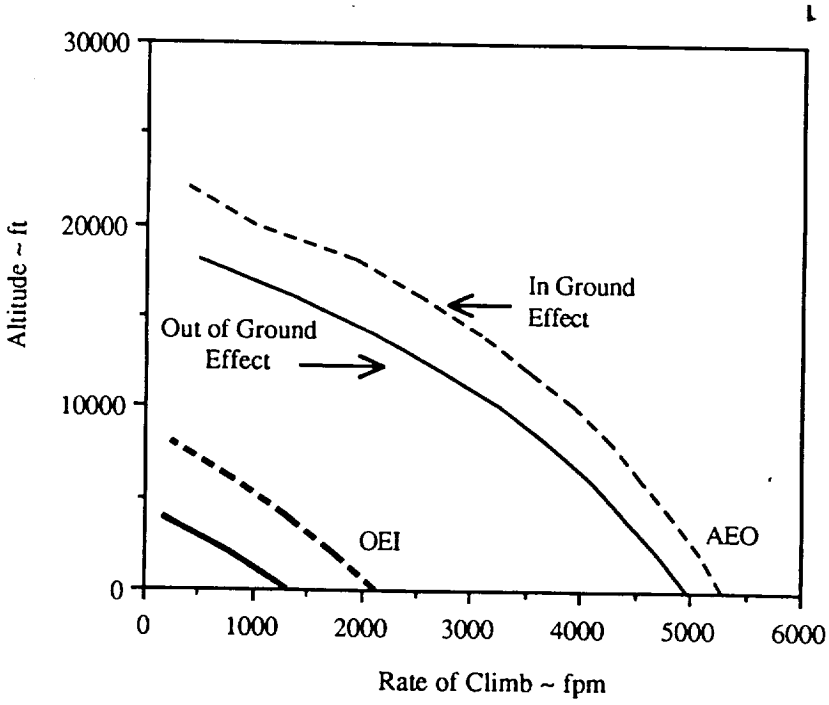

Figure 6. Altitude Vs. Rate of Climb, Hover

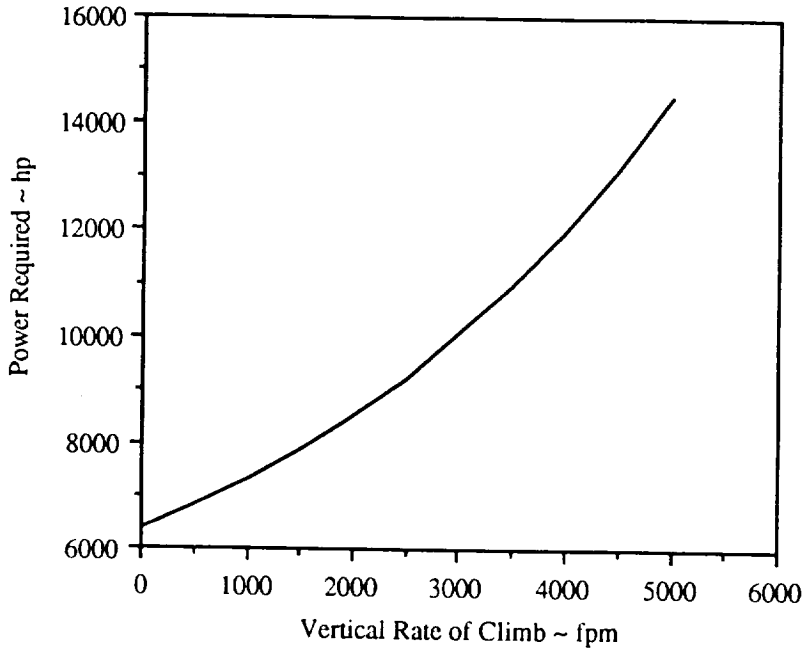

Figure 7. Power Required Vs. Vertical Rate of Climb

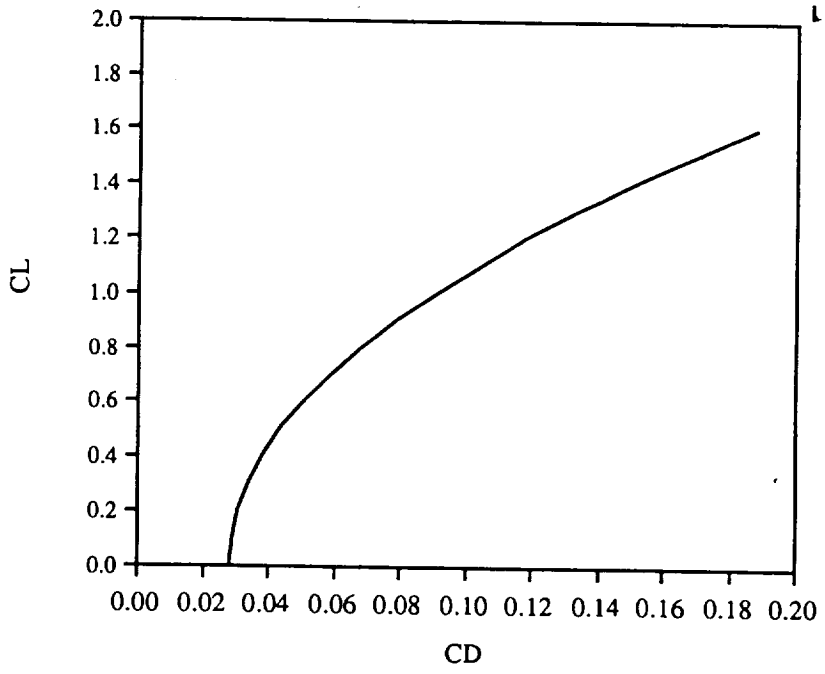

Figure 8. Drag Polar, Cruise

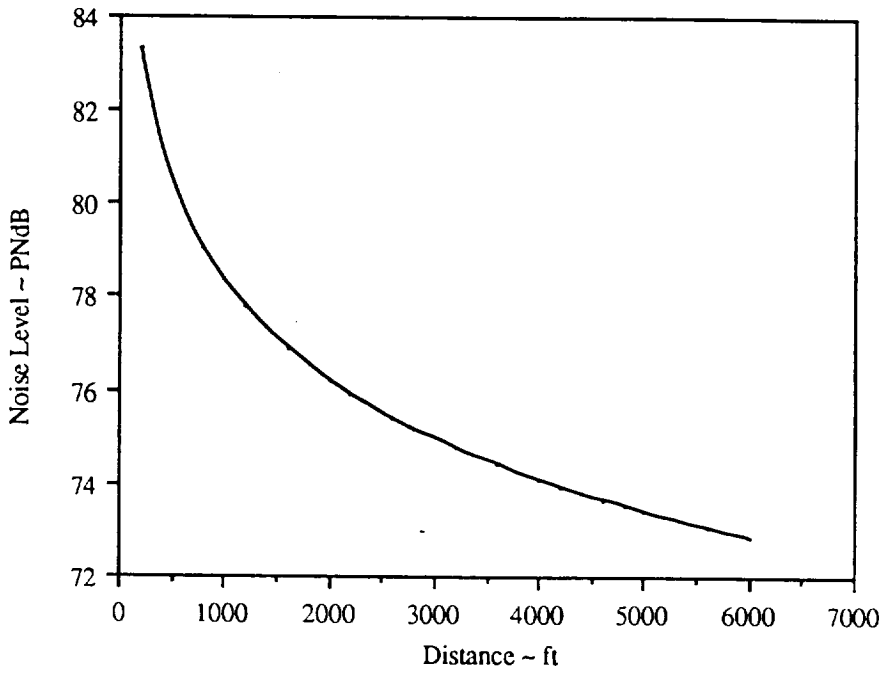

Figure 9. Perceived Noise Levels

Geometry

Table III contains the list of the design geometry for TRANSIT. Three-view drawings for TRANSIT in cruise mode and in hover mode are shown in Figures 10 and 11, respectively.

Table III. Design Geometry

Wing:	W/S	85
	Area	574 ft^2
	Span	58.7 ft
	Aspect Ratio	6
	Taper Ratio	0.9
	Sweep Angle	- 6.0 deg.
	mac	9.27 ft
	t/c	0.18
	Airfoil	64-218
	C_{l_α}	6.7/rad
	$(C_{l_\alpha})_{M=0}$	4.7/rad
	$(C_{l_\alpha})_{M=0.5}$	5.68/rad
Ailerons:	S_a/S_w	0.15
	Span	0.5b
	Chord	0.3b
H. Tail:	Area	190 ft^2
	Span	27.6 ft
	Aspect Ratio	4
	Taper Ratio	0.7
	Sweep Angle	15 deg.
	mac	5.92 ft
	Airfoil	64-215
	C_{l_α}	5.7/rad
	$(C_{l_\alpha})_{M=0}$	3.7/rad
	$(C_{l_\alpha})_{M=0.5}$	4.3/rad
Elevators:	S_e/S_h	0.3
	δ_e	-15 to +15 deg.
V. Tail:	Area	90 ft^2
	Span	14.4 ft
	Aspect Ratio	1.5
	Effective Aspect Ratio	2.1
	Taper Ratio	0.35
	Sweep Angle	15.9 deg.
	mac	7.51 ft
	Airfoil	0012
Rudder:	S_r/S_v	0.09
	c_f/c	0.3
	b_r/b_v	0.3
Fuselage:	Length	61.1 ft
	Outside Diameter	9 ft

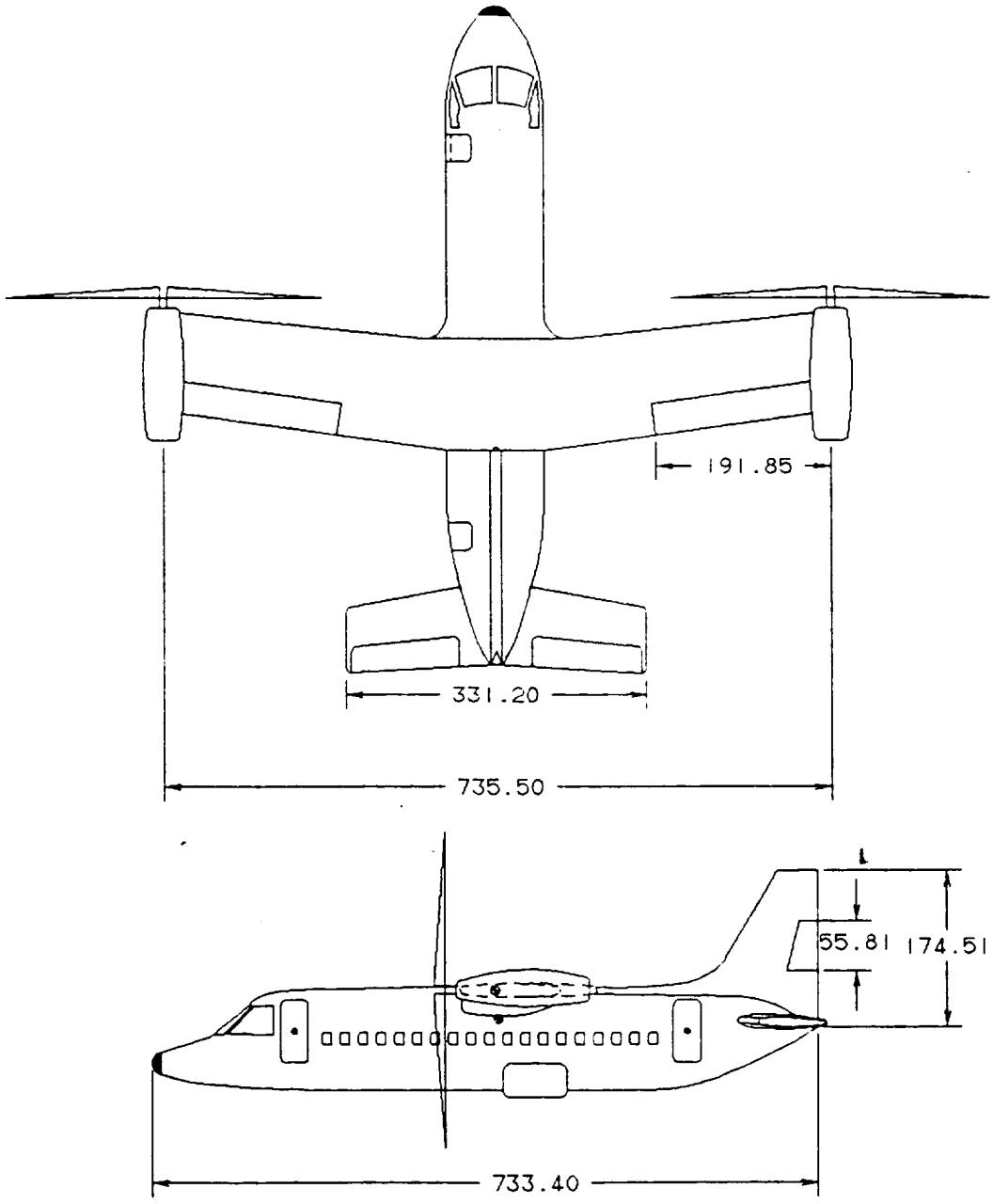

Note: All dimensions in inches

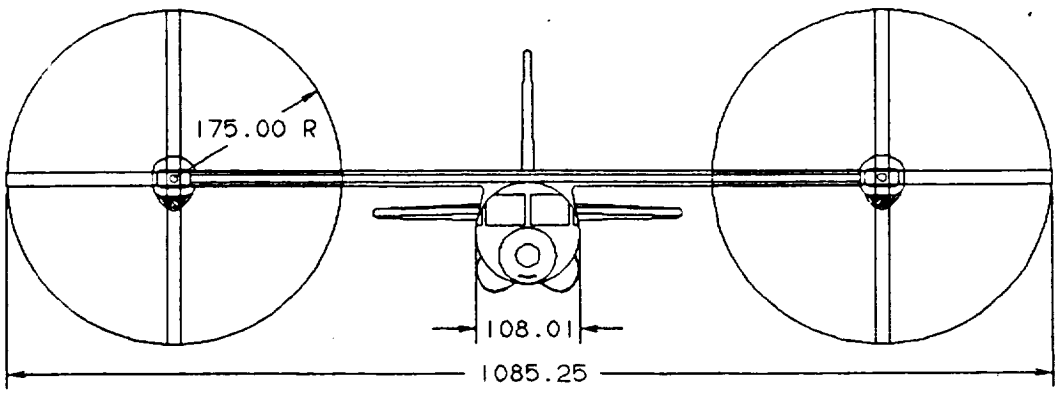

Figure 10. Preliminary Three-View in Cruise Mode

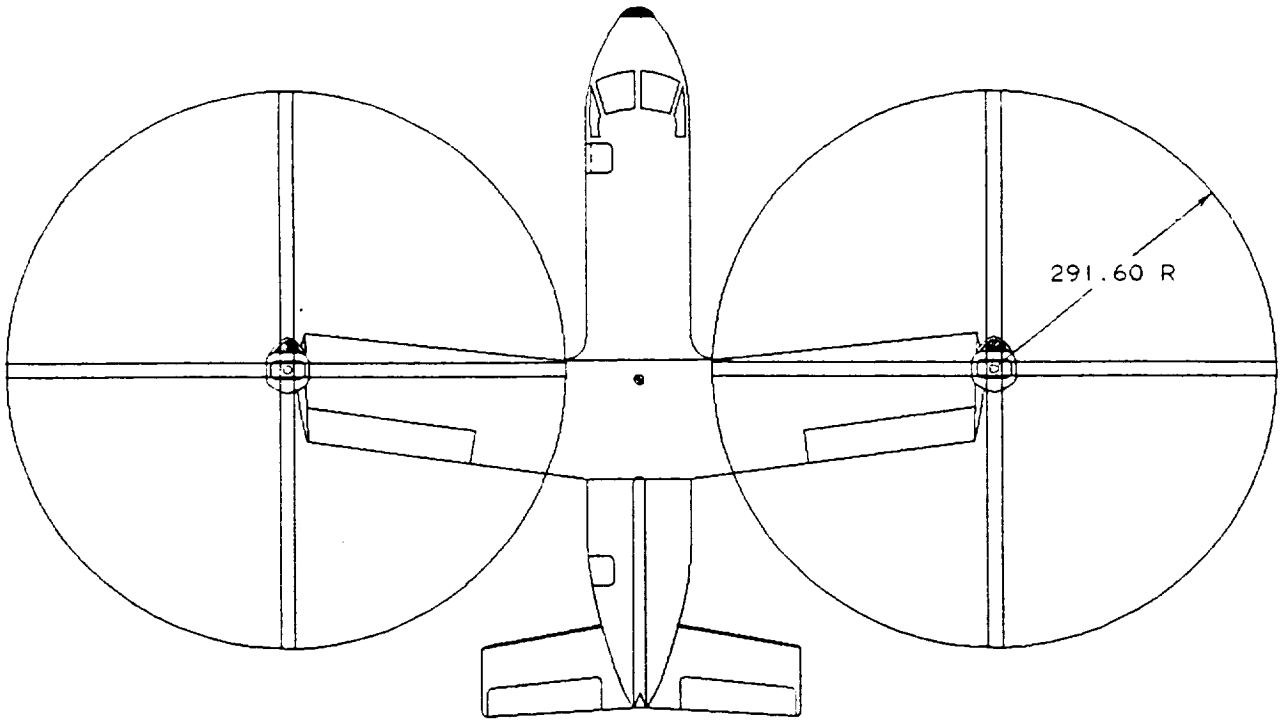

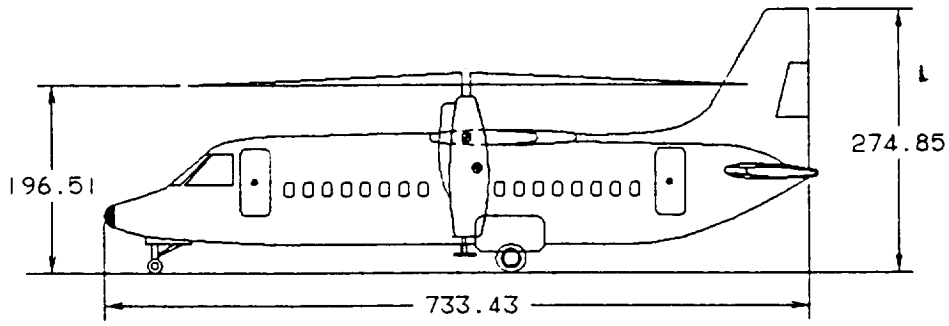

Note: All dimensions in inches

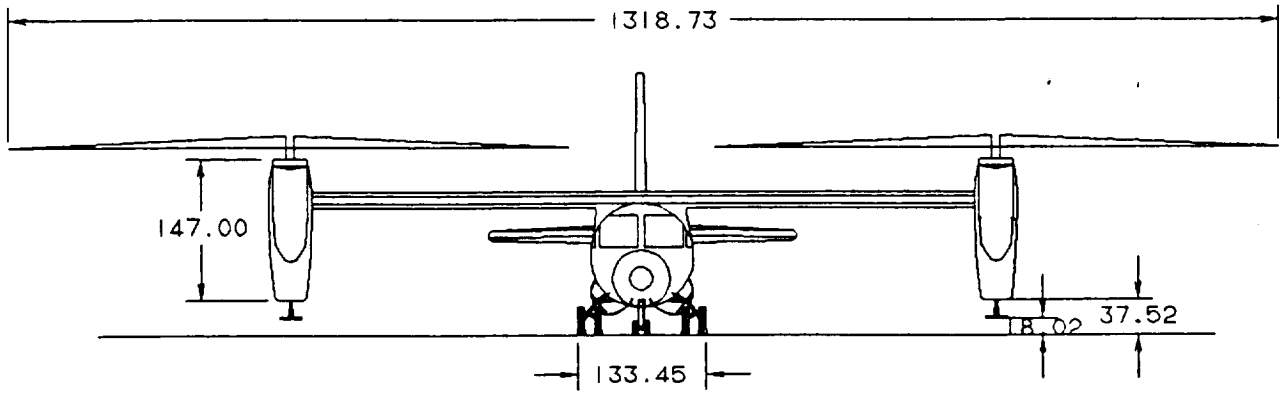

Figure 11. Preliminary Three-View in Hover Mode

Structures

The V-n and V-n_{gust} diagrams are shown in Figures 12, 13, and 14. The positive load limit is 3.34 g's at a velocity of 545 fps. The analysis showed that the conditions for cruise produced the most critical loading condition. The results indicate that the wing moment of inertia needs to be at least 3489 in^4 and the wing attachment area must be no less than 4.73 in^2. The airfoils chosen for this aircraft have high thickness ratios and, therefore should have no problem accommodating the supporting structures needed to obtain these values. This structure would have to withstand a maximum shearing force of 151,362 lbs and a root bending moment of 1,415,127 ft-lbs. A rib spacing of twenty-four inches was used, which correlates with industry standards. The front and rear spars were located in order to take greatest advantage of the wing thickness and so that the cross-shafting and front spar transverse the wing in a straight manner. These locations are shown along with other wing parameters in the wing structural diagram (Fig. 15).

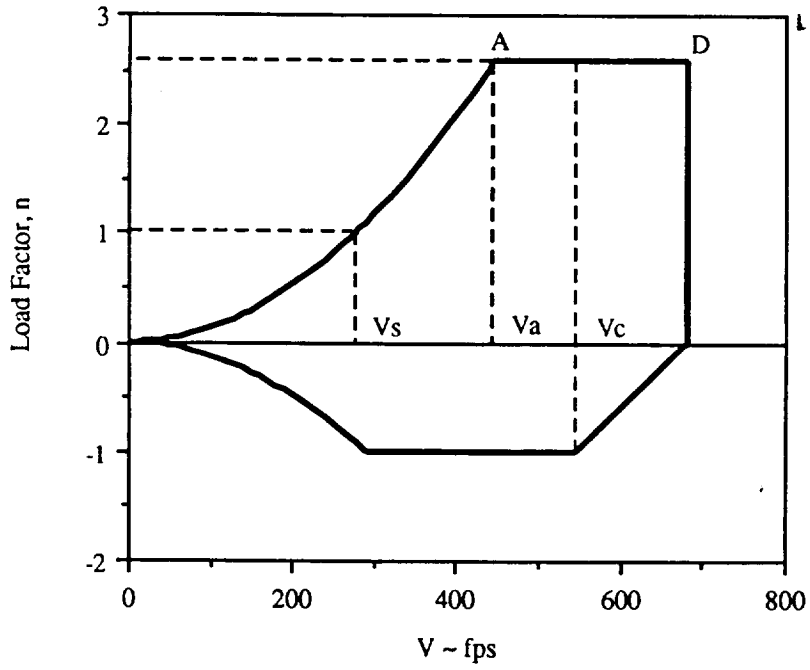

Figure 12. V-n Maneuver Diagram at 16,000 ft.

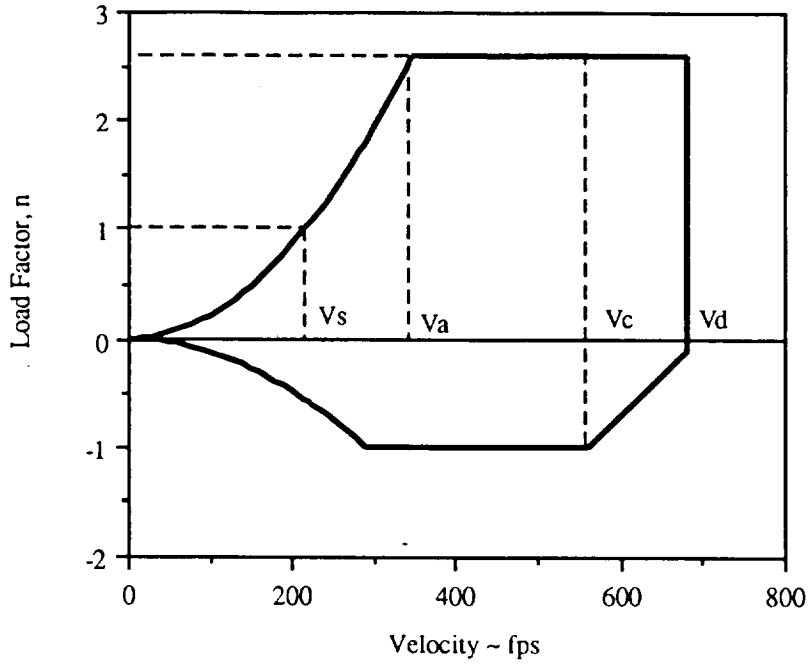

Figure 13. V-n Maneuver Diagram @ SL

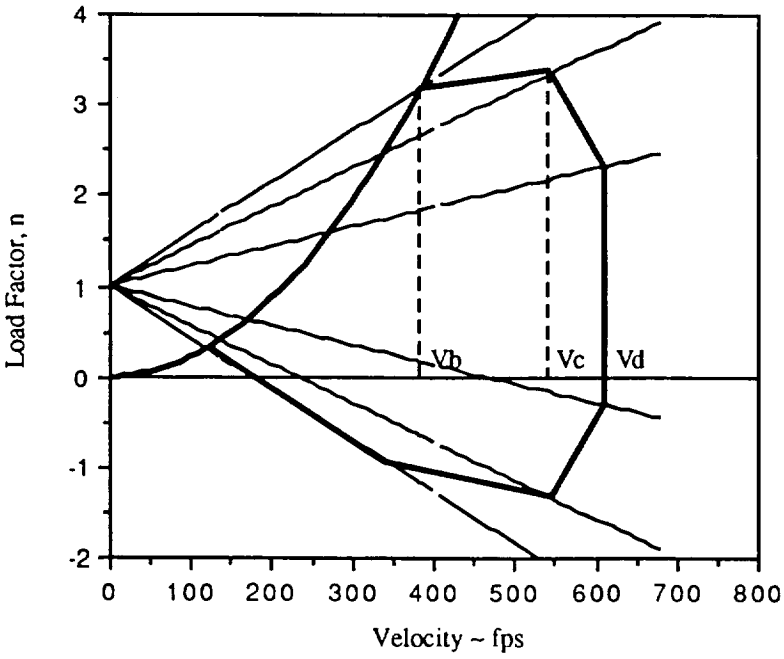

Figure 14. V-n Gust Diagram, @ SL

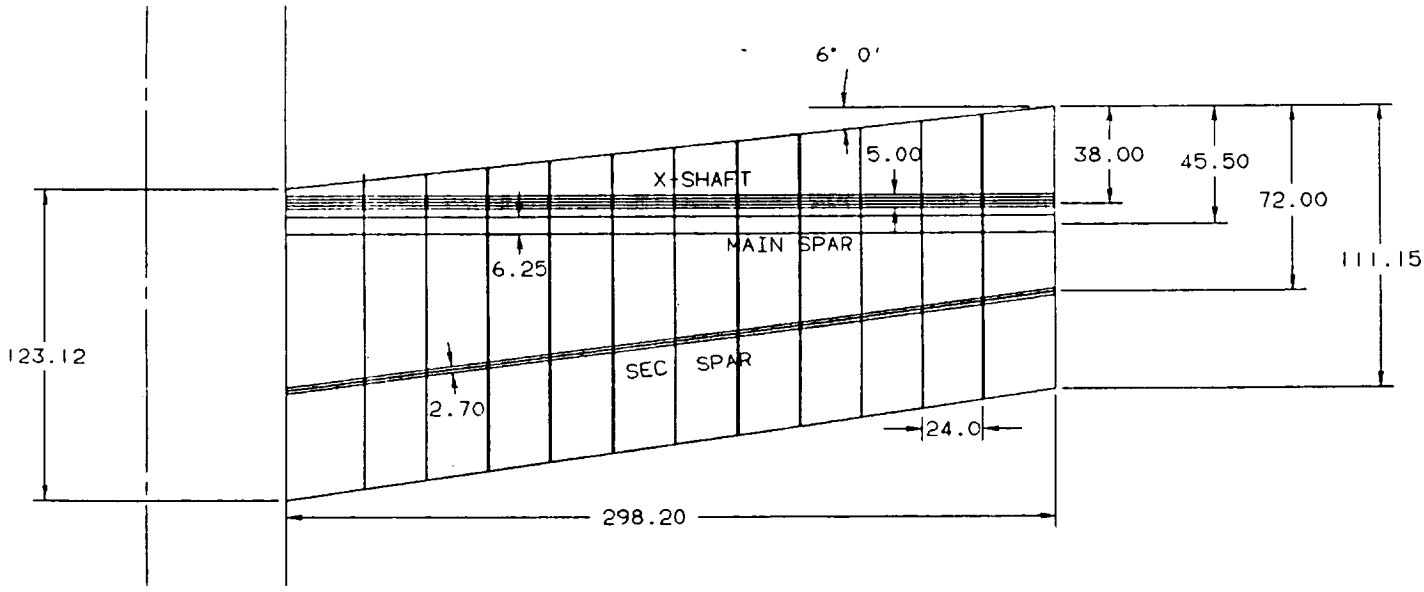

Note: All dimensions in inches

Figure 15. Wing Structural Diagram

Preliminary Sizing

The preliminary sizing of TRANSIT was accomplished using the methods outlined in Reference 3. However, since tilt rotor aircraft data was not available in Reference 3, comparisons were made to regional turboprop aircraft data when applicable. For tilt rotor comparisons, data on the XV-15, V-22 and derivatives were used (Refs. 2 and 6).

Preliminary weights were estimated first. An initial takeoff weight was determined using the linear correlation which exists between the logarithmic scales of takeoff weight and empty weight. Figure 16 shows this correlation for tilt rotor aircraft based on the data from the above sources. Using an iterative method, the preliminary design weights were determined. The weight due to a variable diameter rotor (Ref. 1) was then added to the takeoff weight to achieve the design weights listed in Table II.

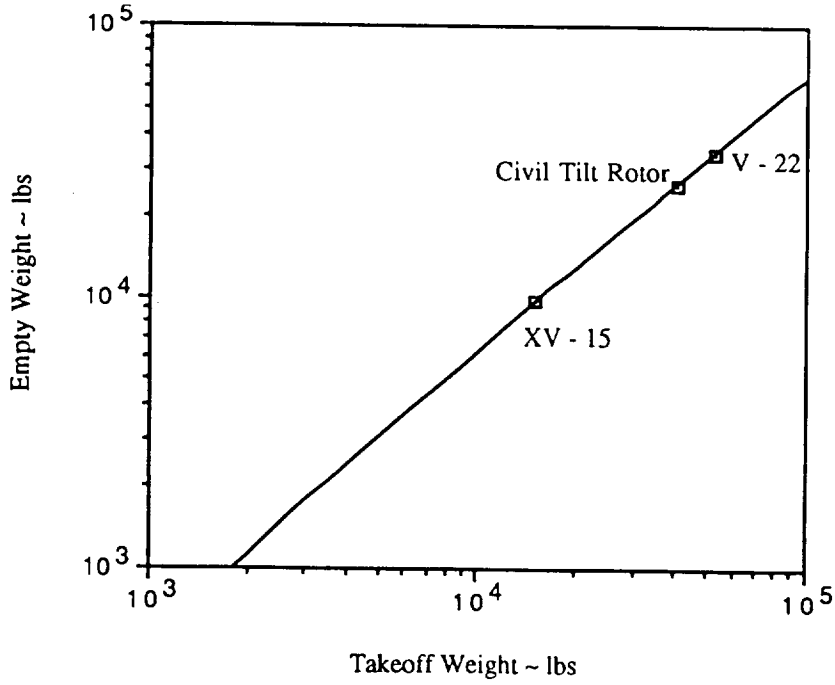

Figure 16. Weight Trends for Tilt Rotor Aircraft

The next step in sizing the aircraft was to estimate certain performance parameters. This was accomplished by sizing to meet specific performance requirements as listed in the FAR's (Ref. 7). Due to the VTOL capabilities of TRANSIT, the conventional takeoff and landing distance requirements were neglected.

Also, the parameters associated with conventional takeoff and landing, such as $(C_{Lmax})_L$ and $(C_{Lmax})_{TO}$ were neglected. The methods used provided a way to determine the desired combination of a high wing loading (W/S) and a low power loading (W/P) which would meet all performance requirements. Figure 17 shows the results of power loading vs. wing loading for cruise and climb as a conventional aircraft. Since a high wing loading increases the lift-to-drag ratio, increases the ride quality, and decreases the weight, a high wing loading is preferred. However, the need for a large rotor radius limited the wing loading and a W/S of 85 psf was chosen to be reasonable for this design. For comparison, the wing loading of the XV-15 is 77 psf. Point P on Figure 17 indicates the operating point for the chosen wing loading.

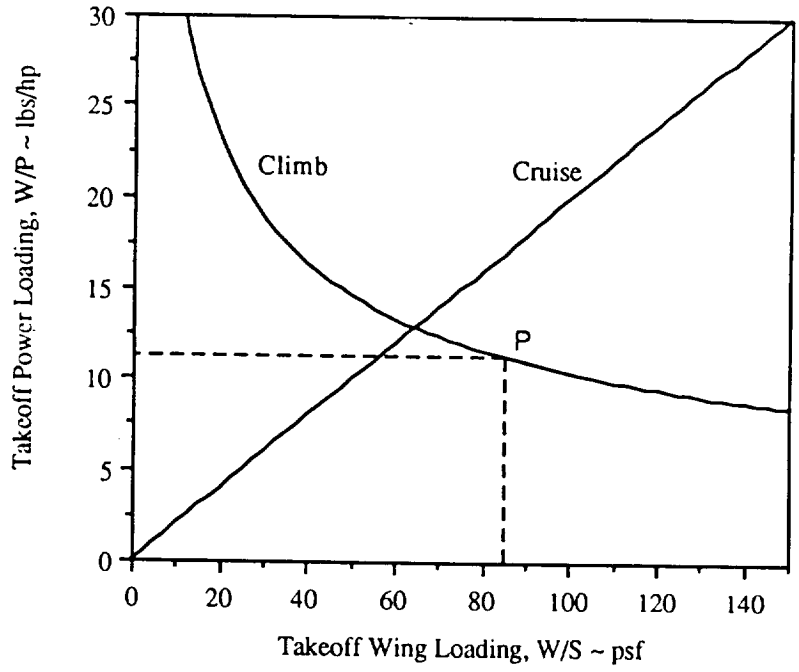

Figure 17. Matching Results for Sizing of TRANSIT

Rotor Design

The rotor design proved to be a complex problem. Since the rotor configuration (blade twist, chord, radius, etc.) had to be designed for both cruise and hover efficiency, trade-offs had to be made. The variable diameter mechanism also added an extra dimension of complexity. Due to these problems, two computer

programs were written by members of the design team to find the optimum rotor configuration for variable diameter and fixed diameter designs. The outlines for each program are shown in Figures 18 and 19.

First, the momentum-blade element theory outlined in Reference 8 was used to determine the cruise performance. For each rotor configuration, the cruise program calculated the horsepower required to produce the thrust necessary to cruise at 16,000 feet. The following parameters were used:

Number of Blades, B
Radius of Rotor, R
Cruise Velocity, V_{cr}
Cruise Tip Speed, V_{tip}
Blade Chord, c
Blade Twist
Pitch (at 0.75R), ß

These parameters were varied individually over various ranges determined through trial and error as well as sample calculations. The final result for a particular rotor configuration was calculated by finding the specific radius necessary to produce the cruise thrust.

Next, the results for cruise were integrated into the hover program which used the combined momentum and blade element theory given in Reference 9. For each rotor configuration used in the cruise program, the horsepower required to produce the thrust needed to hover was calculated. Additional variables used in the hover program were:

Hover Tip Speed, V_{tip}
Pitch (at 0.4R), ß

The final result for a particular rotor configuration was calculated by finding the hover tip speed which produced the necessary thrust for hover.

Final results were examined to find the best rotor configuration. A number of factors were important in determining the best rotor configuration. The most significant factor was the power required for cruise. Since the most amount of time would be spent in cruise, a high cruise efficiency was necessary for an economically feasible design. Horsepower to hover was also important. Since TRANSIT has the capability to hover with one engine inoperative, the OEI condition dictated the engine size and weight. Better hover efficiency produced less engine weight.

Secondary importance was placed on a number of other factors, including disk loading and tip speeds in hover and cruise. Disk loading, the ratio of the airplane's weight to disk area of the rotors, is inversely dependent upon the radius of the rotor blade. Thus, a higher disk loading correlates to a smaller rotor radius, and

less weight. Unfortunately, a high disk loading also has adverse effects. For instance, high disk loadings produce lower efficiencies in hover due to comparatively larger amounts of tip losses. In addition, disk loadings greater than 14 psf create hurricane force winds in the landing zone, a condition that should be avoided (Ref. 1). For this design, lower disk loadings (below 14 psf) were regarded as beneficial. Tip speed in hover was another important consideration. Higher tip speeds in hover correlate to greater noise problems. The limiting tip speed for noise considerations is 750 fps (Ref. 9). Thus, it was necessary to reduce the tip speed as much as possible without sacrificing too much cruise efficiency. Tip speeds in cruise must also be kept low to avoid reaching the critical Mach number; therefore, tip Mach numbers were kept below 0.85.

A variable diameter rotor was measurably the best design. Although the variable diameter increased the weight of the aircraft, it provided the thrust required for cruise with less power than the fixed diameter did. The analysis showed that the optimum variable diameter configuration needed 3460 hp for cruise conditions. Conversely, the optimum configuration without variable diameter needed 3860 hp for cruise. This difference in cruise power was an important factor in choosing a variable diameter system.

Especially important to the rotor design was the twist and the collective pitch of the blade. For twist, a trade-off was necessary because the most efficient cruise twists are generally found above -30 degrees while ideal twist for hover correlates to around -10 degrees. Even so, a blade twist of -30 degrees most effectively satisfied both hover and cruise requirements. The blade must also have a variable pitch mechanism to produce the optimum performance levels as well as autorotative capabilities. The airfoil selected is the Bell XN-12 designed for optimum performance of the V-22. The C_l vs. α curve for the XN-12 airfoil is shown in Figure 20.

TRAC Rotor System

The TRAC mechanism developed by Sikorsky Aircraft was pioneered in the late 60's and 70's. TRAC was one of the few variable diameter rotor systems that had an actual working model. The TRAC program was very successful in meeting all of its program goals and was therefore chosen for the TRANSIT design.

A schematic arrangement of the blades is shown in Figure 21. The basic mechanism consists of a torque tube and a jackscrew which, upon rotation, imparts a linear retraction or extension of the retention nuts. The retention nuts connect to the outboard blade by tension-torsion straps. The torque tube, which contains the jack screw, provides increased stiffness in the blade while its airfoil shape produces a small percentage of the total lift of the blade. The maximum change in diameter is 40%.

Figure 22 illustrates the system used to actuate the jack screw. Basically, the system consists of bevel gears which are connected by coaxial shafts to a brake at the bottom of the transmission. When one of the brake shoes is applied, the pinions of the differential rotate around the bevel gear causing the jack screw to rotate. Depending upon which brake is applied, the blade will retract or extend.

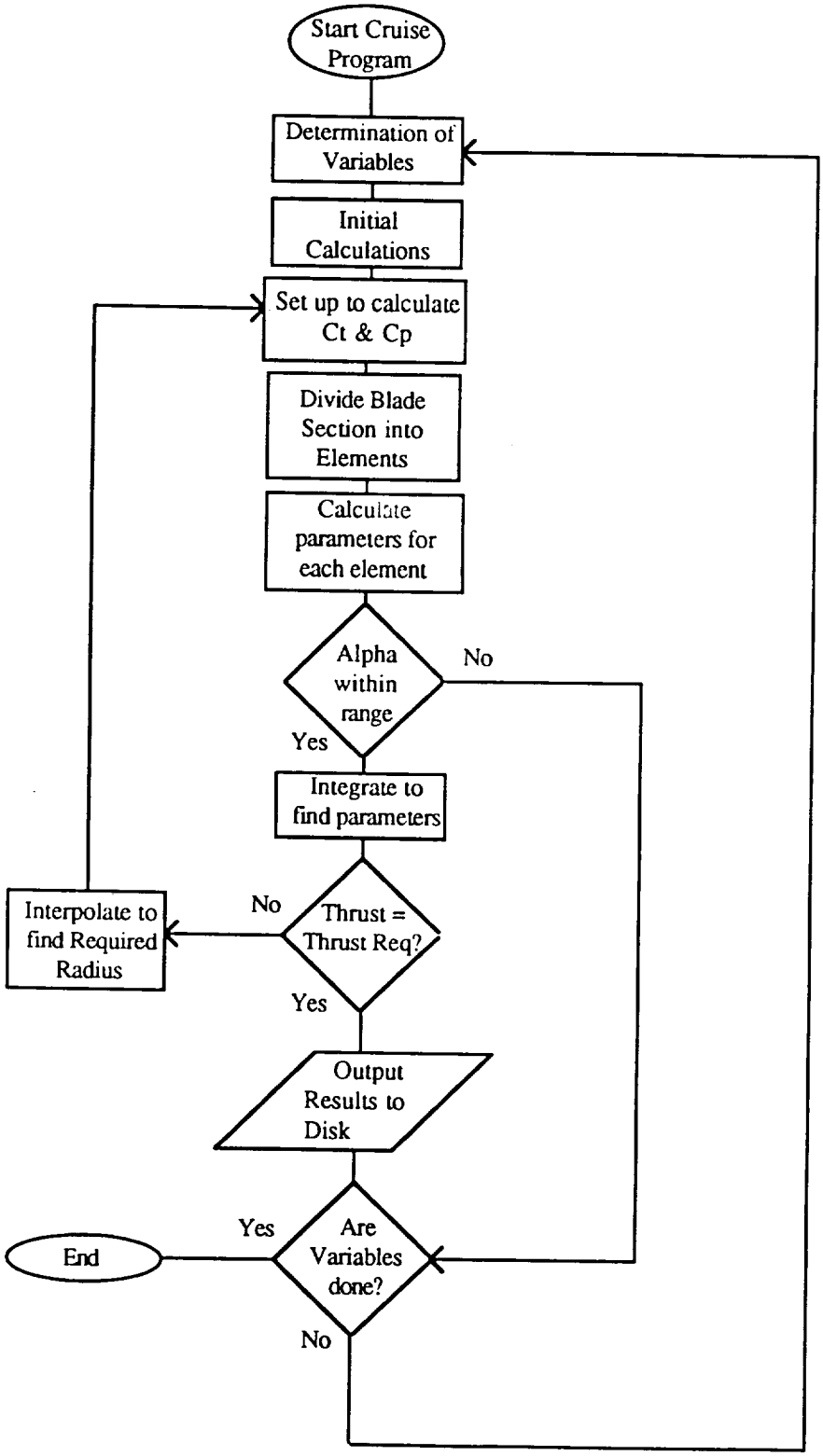

Figure 18. Flow Diagram for Cruise Program

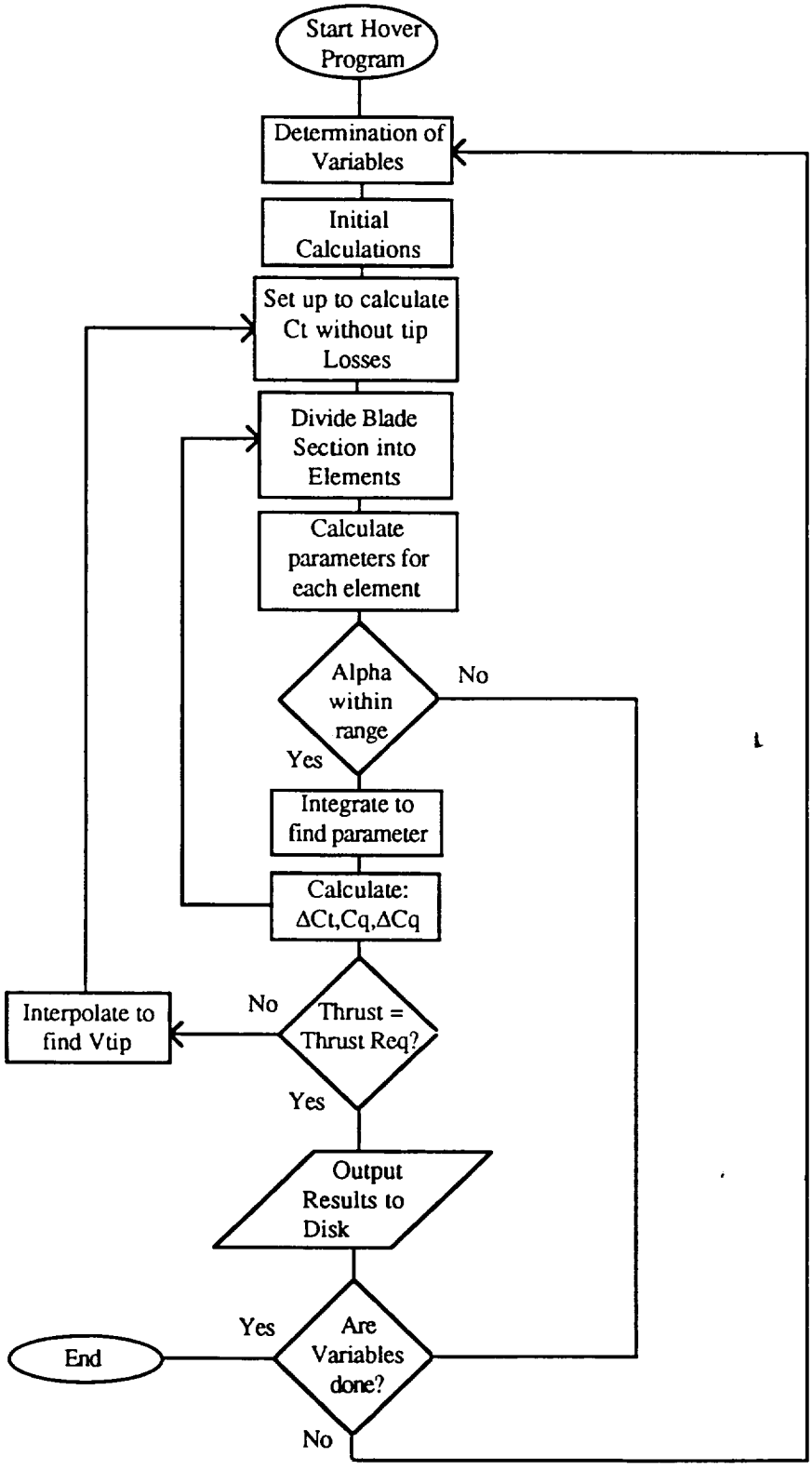

Figure 19. Flow Diagram for Hover Program

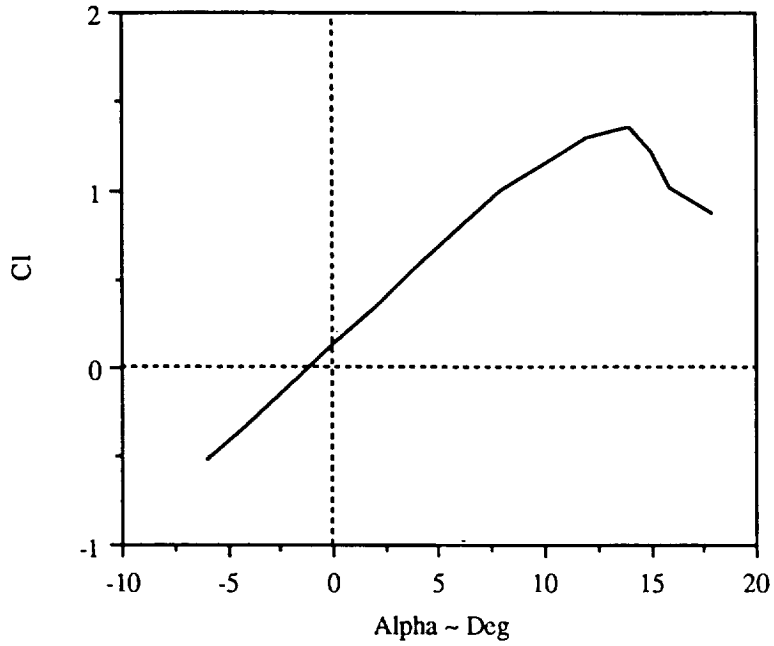

Figure 20. Cl Vs. Alpha, Bell XN-12

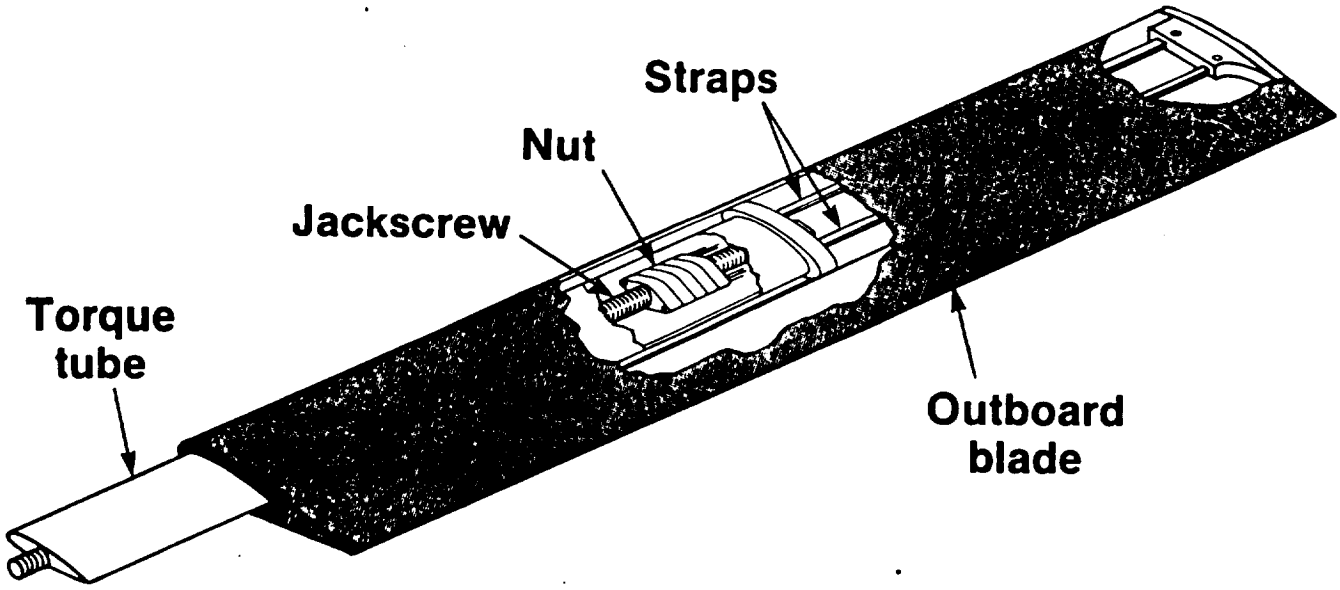

Figure 21. Telescoping Rotor Blade Schematic Arrangement (Sikorsky)

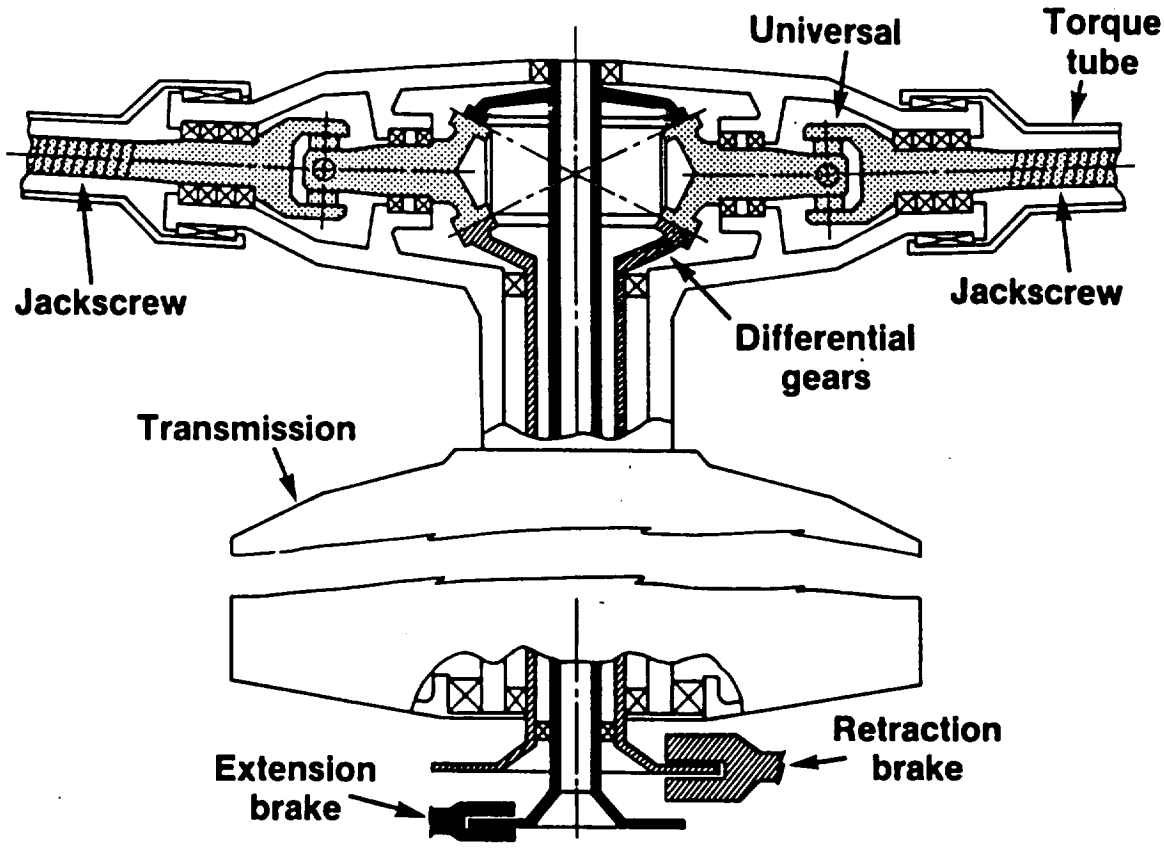

Figure 22. Retraction Mechanism Schematic Arrangement (Sikorsky)

The variable diameter is as reliable as an automobile differential. It does not require an extra power supply because the mechanism is driven by the rotor shaft. The system is also fast; capable of full retraction or full extension in about four seconds.

Powerplant Selection and Integration

The horsepower required to meet the critical climb condition in hover, with one engine inoperative, was used to determine the engine size. The selected engine must have over 7000 hp. During the design process, both two and four engines were considered. A simple analysis determined that two engines will supply the necessary power, while weighing less than four engines. The type of engine chosen was the ALLISON 501-M62 (Ref. 10), which is a derivative of the engine used for the V-22 Osprey.

The integration of the powerplant included mounting, transmissions, gear boxes and cross-shafting. The engines are mounted at the wing tips to accommodate the size of the rotors when the engines are in the vertical configuration. The transmission and gear box configuration was chosen similar to the one used for the

XV-15 (Ref. 6). It has been proven in both the XV-15 and V-22 that one engine can provide the power to both rotors using this configuration. Figure 23 illustrates the transmission and gear box arrangement in the XV-15.

The cross-shafting was sized to the meet the critical OEI climb conditions. During OEI conditions, the shaft must carry the torque necessary to drive the propeller connected to the inoperative engine. Torsional theory (Ref. 11) for circular shafts was used to determine the size of the cross-shaft. Three different materials were considered for the sizing: steel, aluminum and titanium. Aluminum was chosen to be the best material based on strength, weight and cost. A cross-shaft diameter of 5 in. was chosen based on the thickness ratio of the wing. The thickness of the shaft necessary to withstand torsional loads only was found to be 0.074 in, but a greater thickness was needed to withstand possible bending moments on the shaft. A wall thickness of 0.25 in. was chosen. Using the density of aluminum and the length of the shaft, the weight was calculated to be 451 lbs. The cross-shafting is located at the CG of the engines and directly in front of the main spar, as shown in Figure 15.

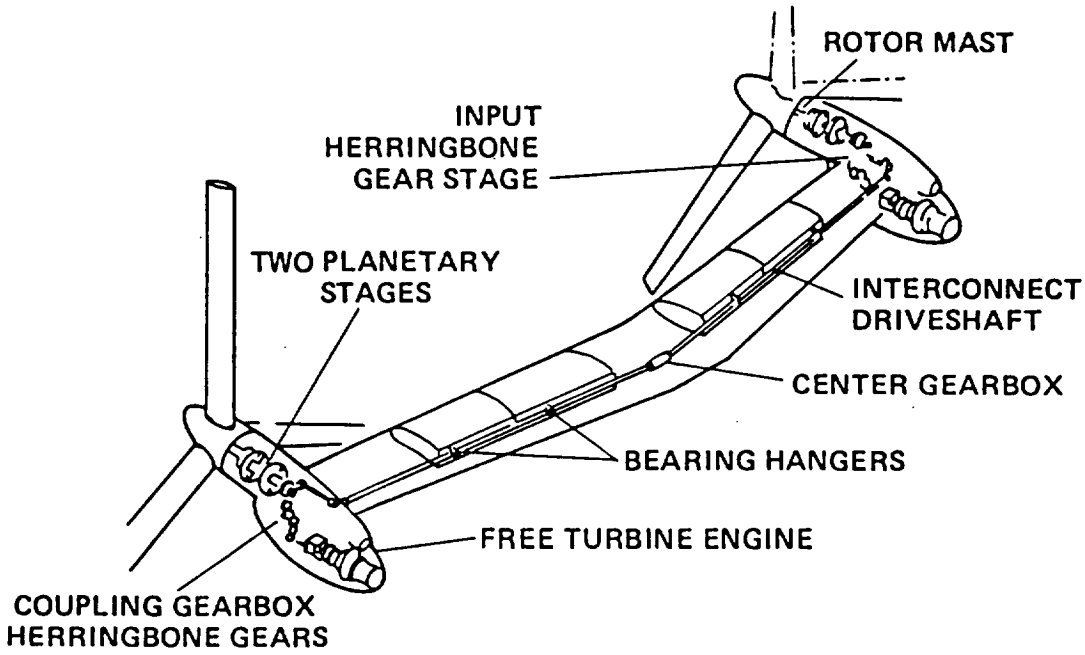

Figure 23. Propulsion System (NASA)

Fuselage Design

The fuselage was designed according to the payload, crew and operational items which needed to be located in the fuselage. Based on these parameters, a preliminary interior cabin layout was produced. For a 40

passenger payload, ten rows with four seats abreast were chosen. Although passenger comfort is important, the cost effectiveness of TRANSIT was predominate in choosing the seat classes. For economic feasibility, only the economy class size was considered. However, first class and business class seating could easily be incorporated into future TRANSIT designs. Dimensions for seat width, aisle width and seat pitch were obtained from industry standards (Ref. 13). Distances, such as those required for depth of fuselage frame and bulkheads were added to the layout. The lavatory, galley, and two closets were also added, again using industry standards for the dimensions. A three view drawing of the resulting fuselage design is shown in Figure 24 and Figure 25 is a detailed cross-sectional drawing.

Wing Design

The design of the wing was the next step in the design procedure. First the configuration was chosen based on the mission of the aircraft. A high wing configuration with forward sweep was chosen. A high wing design was chosen to meet the ground clearance requirements for the engines. The parameters to be determined were the area, taper ratio, leading edge sweep, thickness ratio, incidence angle and dihedral. First the wing surface area (S) was determined from the wing loading (W/S) that was found during the preliminary sizing. Using the gross weight of 48,789 lbs. and a wing loading of 85 psf, the surface area was calculated to be 574 ft^2. From this area, the span and mean chord were determined for an aspect ratio of 6, which was determined through comparisons with the XV-15 and V-22.

A high taper ratio is usually desired to improve the tipstall characteristics of the wing. For a tilt rotor, this is not an important consideration since the rotors are located at the wing tips. However, a high taper ratio will also yield greater fuel volumes and increased the wing weight. Taking these into consideration, a taper ratio of 0.9 was chosen.

Forward sweep was necessary for clearance between the rotor tip and the wing in airplane mode since the rotors are fully articulated. That is, clearance was required to allow for rotor flapping. The assumptions were that the rotor extended 1 ft. from the wing tip and a 2.5 ft. clearance from the rotor tip to the wing was desired. The necessary leading edge sweep was calculated to be 6 degrees.

A low thickness ratio is generally desired to increase the critical Mach number. However, the cruise speed for TRANSIT is well below the critical Mach number so this was not a factor in determining the thickness ratio. A higher thickness ratio will decrease the structural weight of the wing, increase fuel volume, increase the maximum lift coefficient, and provide sufficient area for the cross-shafting. Thus, a thickness ratio of 0.18 was chosen. Once the thickness ratio was chosen, the airfoil with the maximum lift coefficient was

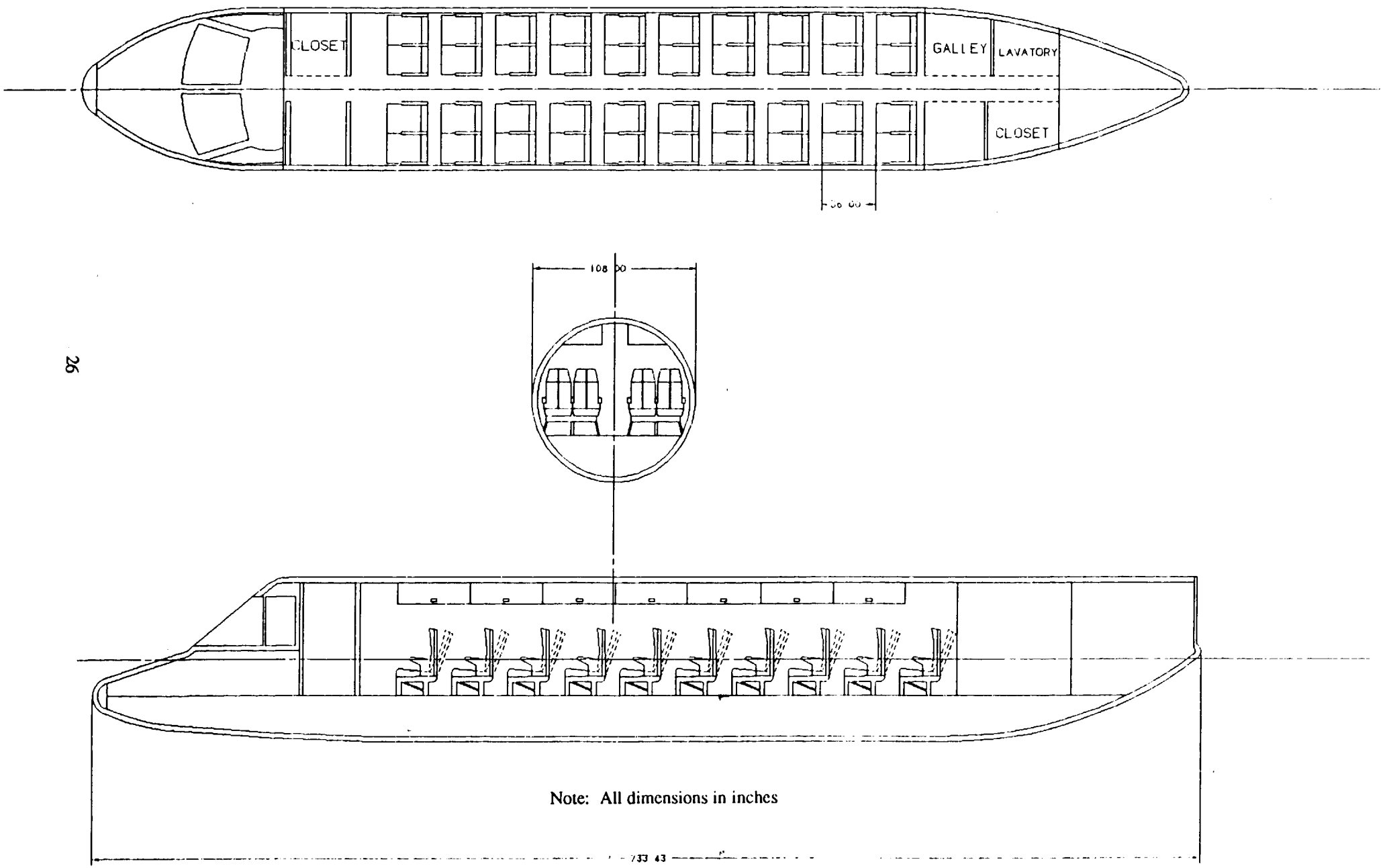

Note: All dimensions in inches

Figure 24. Preliminary Fuselage Layout

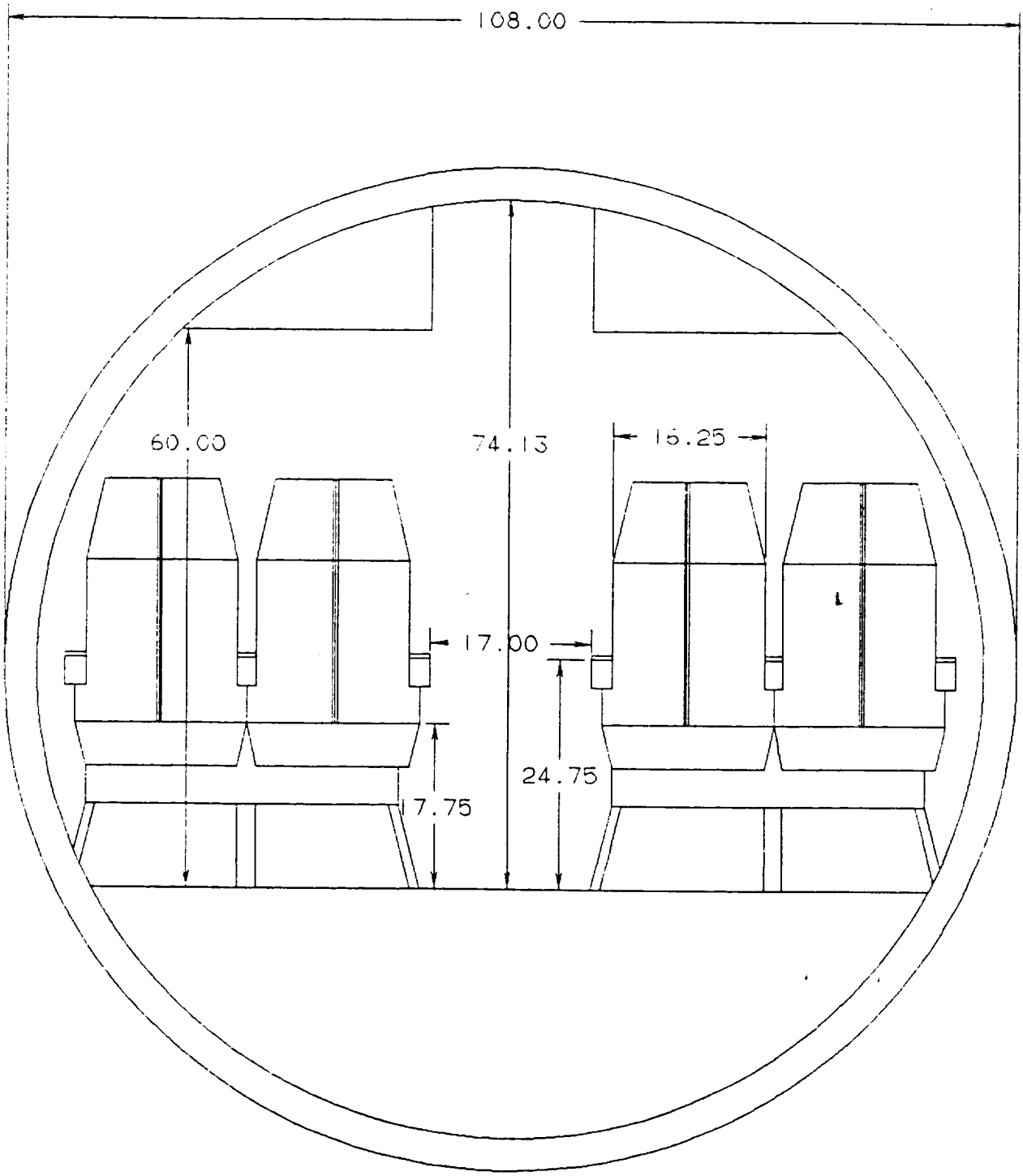

Note: All dimensions in inches

Figure 25. Cross-Section of Fuselage

chosen. Figure 26 is a plot of the C_l vs. α curve for the NACA 64-218 airfoil (Ref. 14) which was chosen for this design.

A wing incidence angle of 2 degrees was selected to give the fuselage a zero angle of attack. No dihedral was necessary for this design since a high wing configuration has inherent dihedral effects (Ref. 15). Also, as noted in Reference 15, the dihedral angle is usually not determined from analytical methods because of the large errors involved. A preliminary drawing of the wing planform is given in Appendix C.

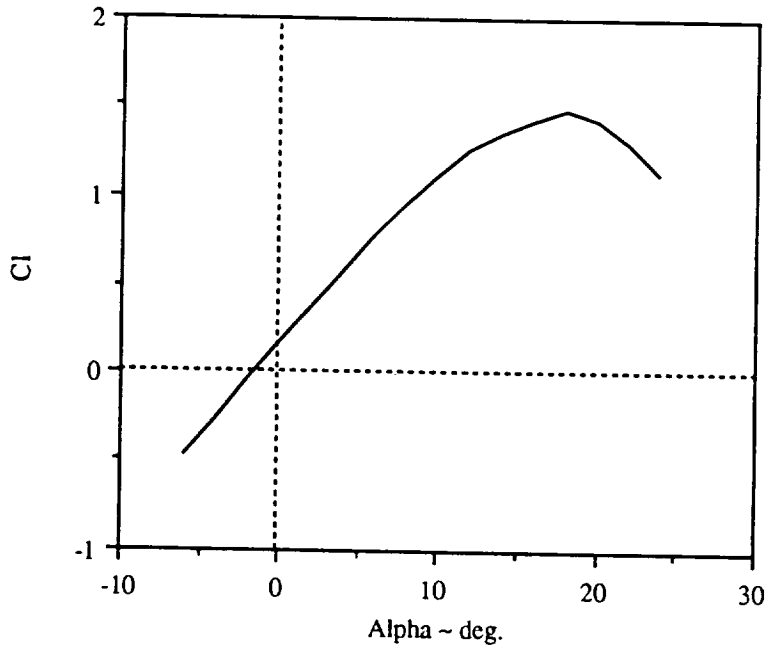

Figure 26. Cl Vs. Alpha, NACA 64-218

Empennage Design

The empennage configuration was chosen according to the methods outlined in Reference 12. A conventional configuration was chosen following an investigation of the XV-15 and V-22 empennage configurations. It was found that the H-tail configuration used on these two aircraft was chosen because of the military missions for which these aircraft are designed (hangar and carrier clearance). Airfoils were selected for both the horizontal and vertical tails, insuring that the wing would stall before the tail. This was accomplished by choosing sufficient sweep angles and thickness ratios. The final empennage sizing was governed by the results of the stability and control analysis.

Landing Gear

The initial design of the landing gear involved determining the static loads placed on both the front and rear gear. A safety factor was incorporated and the adjusted loads were used to determine the sizing of each gear. A CAD (Computer Aided Drawing) program was used to determine the correct orientation of the landing gear. A detailed drawing was made of both the stowed and extended configuration (Appendix C). Landing gear pods were necessary due to the fact that the wheel diameter of thirty inches could not fit into the bottom of the fuselage. Also, additional structures were added to the engine nacelles to prevent tip over. These structures are designed to retract into the engine nacelles during forward flight and to ensure that engine damage would not occur if a large gust caused the aircraft to tip while on the ground.

Weight and Balance

The weight and balance, landing gear placement, and stability and control are dependent upon each other; therefore, an iterative process was necessary to obtain the final results. The empennage, which was sized for stability and control, lead to changes in the CG position which made it necessary to re-locate the landing gear until there were matching results in CG location.

The weight and balance was determined using the design methodology in Reference 7. This method calculates component weights through comparisons to similar aircraft and gives a rough estimation of the center of gravity locations for each component. The weight ratios (component weight to W_{to}) of the wing, fuselage, empennage, and nacelles were estimated using turboprop airplane data (Ref. 16) and weight data from the XV-15 (Ref. 6). Using these ratios, the individual component weights were then determined. The weights for the powerplant (including engine, transmission, cross-shafting, and rotor), landing gear, and fixed equipment were found in the following manners. The weights for fuel, passengers, and baggage were determined previously during preliminary sizing. The resulting component weights are listed in Table IV and the components are shown in Figure 27.

The total powerplant weight was found by taking the engine data for the Allison 501-M62 and adding the estimated weight of the rotor blades. The weight of the rotor was determined using the rotor weight of the V-22 plus the weight due the variable diameter mechanism (Ref. 1) and the transmission weight was calculated by scaling the transmission weight of the XV-15. The weight of the cross-shafting was previously determined and explained in the powerplant integration analysis.

Using the assumption that the weight supported by the gear directly effects the weight of the landing gear, the landing gear weight was calculated by scaling up the weight of the XV-15 landing gear. The weight of the fixed equipment was likewise determined using XV-15 data. The ratio of fixed equipment to takeoff weight equals 0.131 which correlates with turboprop data (Ref. 6).

Center of gravity (CG) locations for each component were found using the methods in Reference 12. Estimations of CG positions were also made from the detailed drawings of TRANSIT.

Table IV. Component Weights and CG Locations

#	Component	Weight (lbs)	CG Location X_i (in)	CG Location Z_i (in)
1	Instrumentation	148	50	100
2	Landing Gear, Front	146	53	10
3	Electrical Equipment	741	70	20
4	Heating/Air Conditioning	593	200	110
5	Hydraulics & Flt Controls	1927	300	100
6	Fuselage	5655	348	60
7	Engine & Rotor	6088	378	120
8	Trapped Fuel & Oil	350	378	120
9	Cross Shaft & Trans.	2500	380	120
10	Misc (Seating, etc.)	3000	380	50
11	Nacelles	128	390	120
12	Wing	520	402	120
13	Full PAX & Baggage	8200	408	51
14	Fuel	6813	420	120
15	Main Landing Gear	1760	424	14
16	Wing Gear	300	459	108
17	Crew Attendant	200	554	54
18	Vertical Tail	226	684	149
19	Horizontal Tail	515	691	78

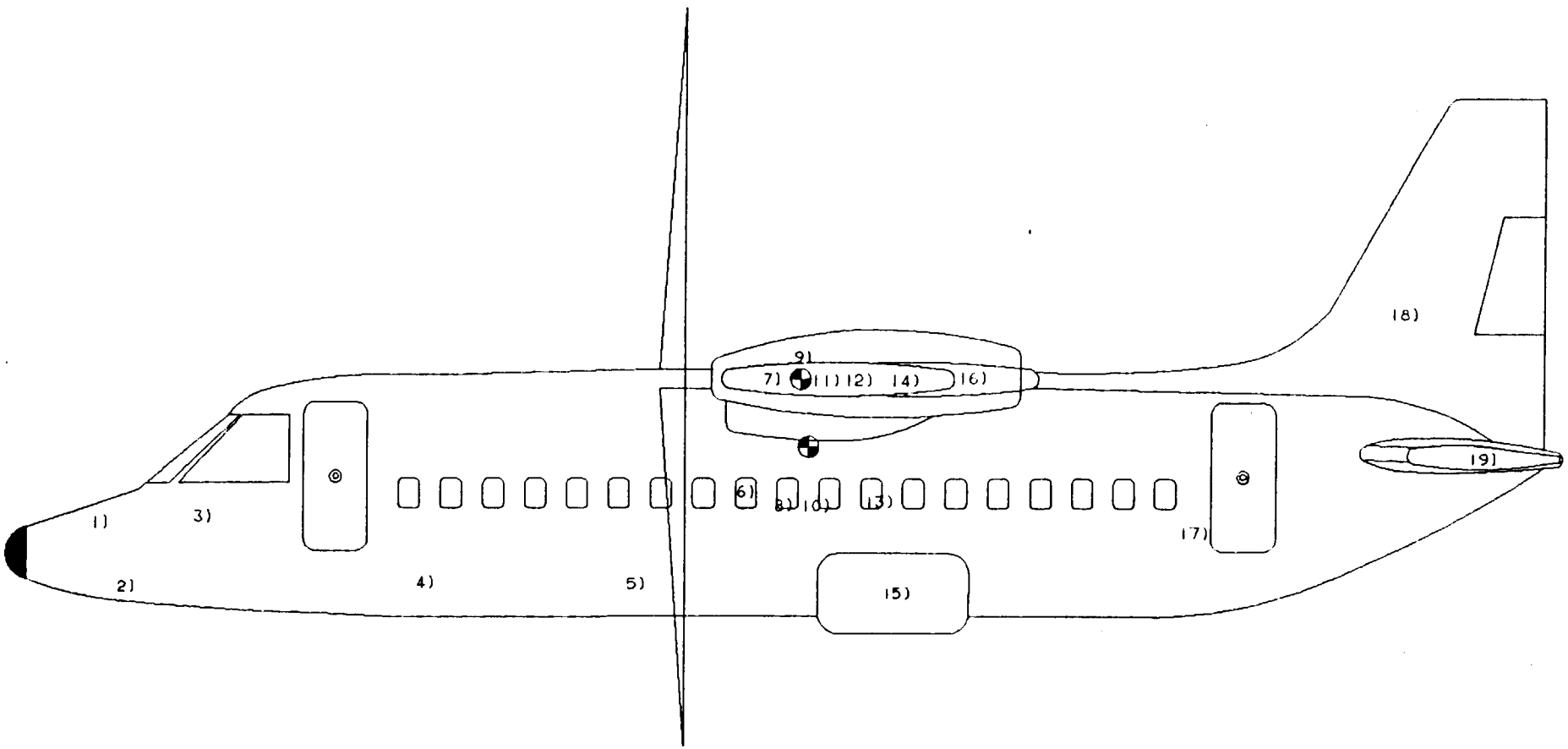

Figure 27. Component CG Location

An important consideration in tilt rotor design is the CG position. Besides stability and control considerations in forward flight, the CG position also effects hover stability. The CG position should be directly in line with the thrust of the engine while in hover. If it is not, the fuselage will incline. The magnitude of the inclined angle will depend upon the distance between the CG and the location of thrust. For the fully loaded condition (40 PAX), the engine is located six inches forward of the CG. This position produces a positive 10 degree angle of attack of the fuselage in hover. Large CG travel for different loading scenarios could cause problems.

Because of the importance of the CG position in hover, as well as for stability and control analysis, different passenger scenarios were studied to determine the limits of the CG position. These included 40 PAX, 30 PAX forward and aft, 20 PAX forward and aft, and 10 PAX forward and aft, as well as the fuel tanks empty and fully loaded. The most forward CG position is at 0.065 mac and occurs with 20 PAX forward and no fuel as shown in Figure 28. The most aft position occurs at 0.29 mac with 30 PAX aft and full fuel tank. For most aft CG location, the fuselage angle of attack is 13.7 degrees. For the most forward CG position, the angle of attack - 22 degrees. This condition might pose a problem and should be avoided.

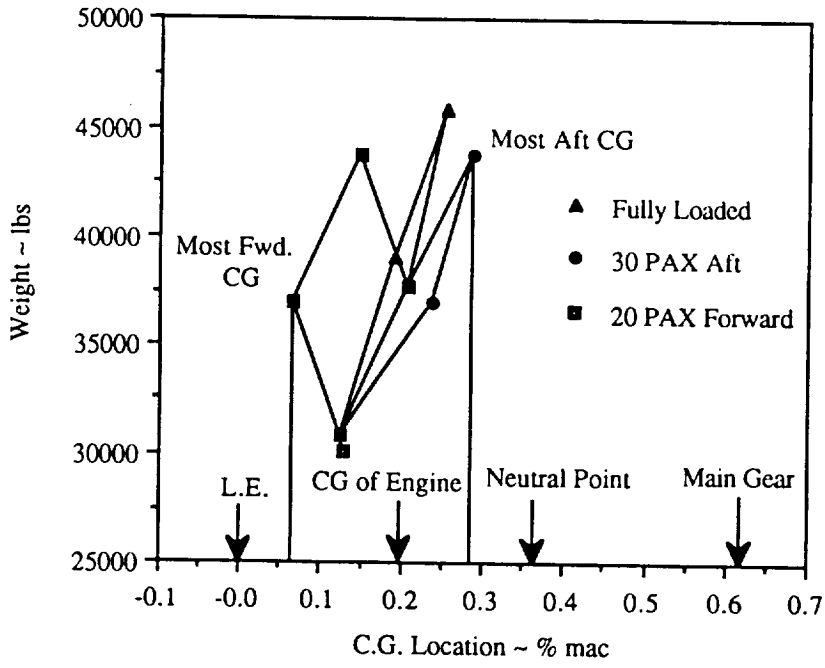

Figure 28. Excursion Diagram

Stability and Control

Stability and control was analyzed using a combination of methods (Refs. 12, 17, 18 and 19). The methodology of Reference 17 was used to develop the sizes of the vertical and horizontal tails, as well as the necessary control surfaces. Both the longitudinal and directional stability and control derivatives were developed.

Important considerations for the longitudinal stability were moment coefficients for each component of the aircraft. These included the effects of the fuselage, wing placement (in comparison to the CG), propeller (normal and thrust contributions), and horizontal tail. To decrease the destabilizing normal force of the propeller, the engines were designed to rotate parallel to the freestream air at high wing angles of attack. The moments referred to above were applied to the range of CG locations to ensure that the plane would not become statically unstable in any situation. Also taken into account was the elevator size and deflection necessary to keep the aircraft in trim for the most critical CG location shown in Figure 29.

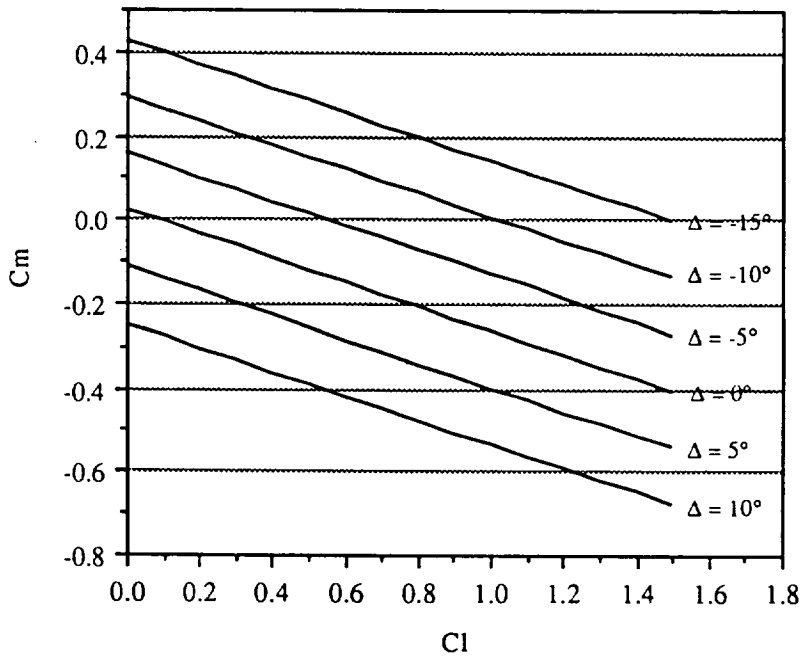

Figure 29. Cm Vs. Cl, Most Fwd. C.G. @ SL

Using the method in References 12 and 18, the neutral point was calculated to be at 0.35 mac. For an aft CG limit of 0.288 mac (Fig. 28), a C_m of at least -0.05 had to be produced for stability considerations.

Thus, the aft CG position was the limiting condition for sizing the horizontal tail. For three loading scenarios: fully loaded, most aft CG position, and most forward CG position the static margins were found to be -0.094, -0.057, and -0.2, respectively (Figs. 30, 31 and 32). Calculations for AEI conditions showed that a windmilling propeller would have minimum effect on the stability.

The directional stability was developed using the methods in Reference 12. The effects of the fuselage and the vertical tail on directional stability were taken into account and the vertical tail size was determined (Fig. 33). The rudder was sized using the methodology in Reference 17. Since cross-shafting eliminated the possibility of yaw due to one engine out, the rudder was only needed to correct for the yaw due to aileron deflection. The ailerons, which were sized according to the method in Reference 12, decrease the downwash drag of the wing in hover and provide for lateral control in cruise. The results found were comparable to turboprop planes.

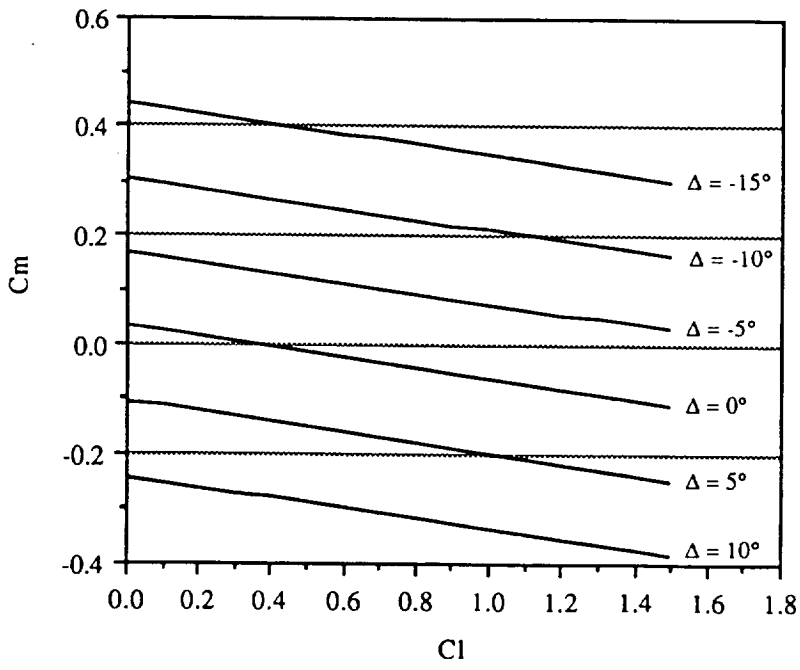

Figure 30. Cm Vs. Cl, Fully Loaded @16,000 ft

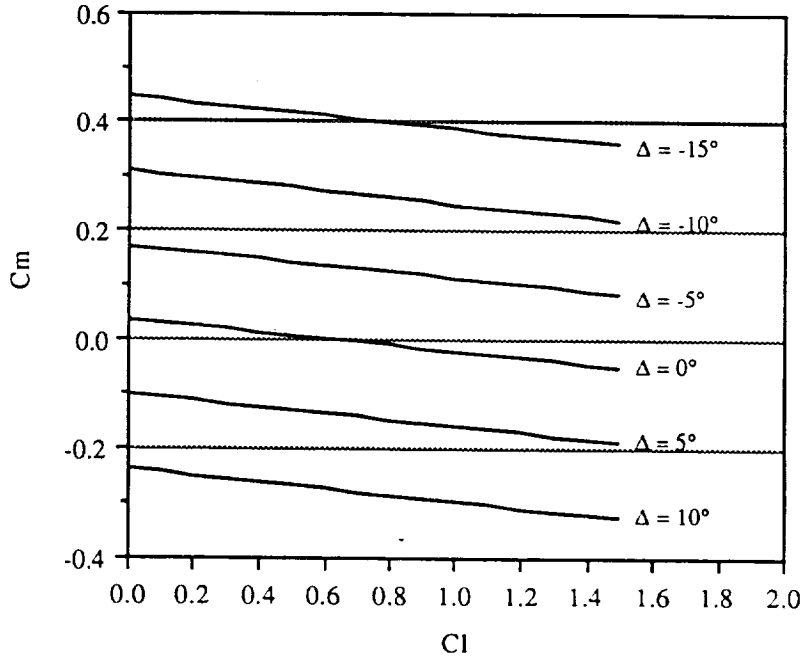

Figure 31. Cm Vs. Cl, Most Aft C.G. @ 16,000 ft

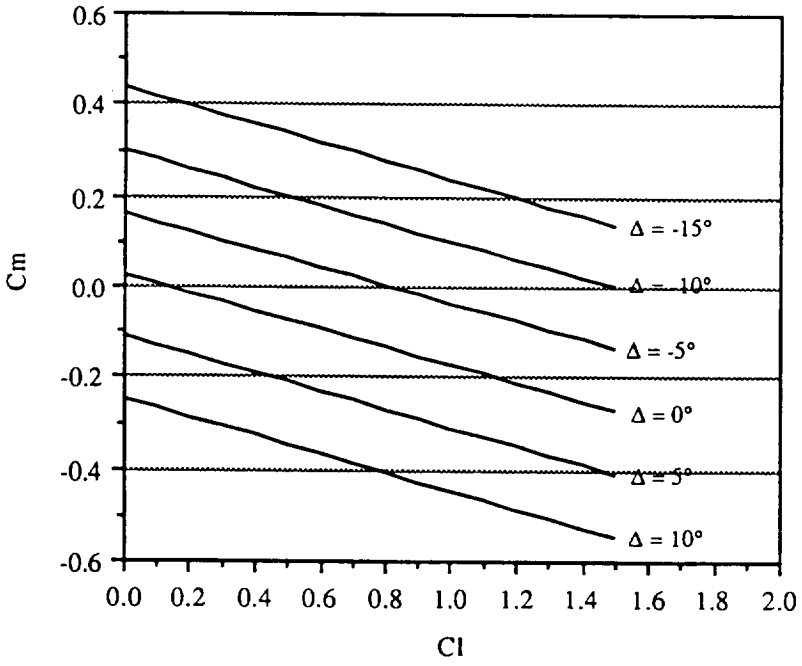

Figure 32. Cm Vs. Cl, Most Fwd. C.G. @ 16,000 ft

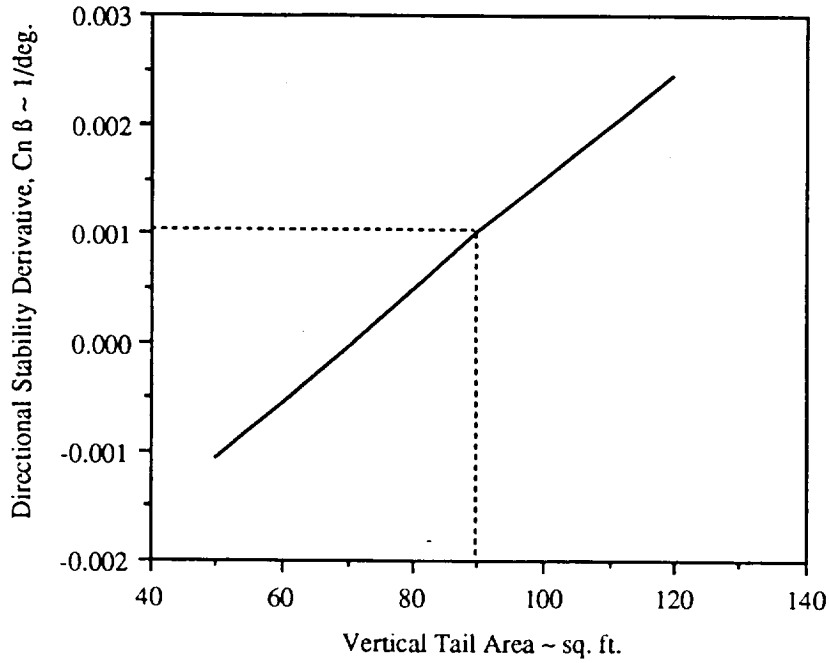

Figure 33. Directional X-Plot

Direct Operating Cost

Reference 20 provided a method for determining the direct operating cost (DOC). Reference 21 was also used to account for additional parameters for tilt rotor aircraft. To determine the DOC, certain assumptions were made. The time and fuel for descent were assumed to be zero and the rate of climb in airplane mode was assumed to be 2500 rpm. Also, the cost per ton-mile for direct maintenance labor was doubled to accommodate for the increased maintenance that tilt rotor aircraft require.

The cost per available seat mile was calculated to be 1.114 $/passenger mile in 1988 dollars. This would mean, for example, that a 350 nm trip at a load factor of 80% and a 20% profit margin would cost a passenger $68.95.

Conclusions

Upon completion of the preliminary analysis, an aircraft has been designed which meets or exceeds the mission requirements. The feasibility of TRANSIT is apparent and the potential for civil applications is promising. One drawback to this revolutionary aircraft may be the public's acceptance of such a concept. However, the inevitable gridlock on the California freeways will motivate travelers to utilize new and innovative aircraft. This will open the door for TRANSIT to fly right in.

For TRANSIT to reach its fullest potential, extensive design procedures must be completed. Since the scope of this report was confined to preliminary design over a nine month period, many details that could effect performance were not thoroughly investigated. Below is a list of recommendations for further study.

- Investigate propeller effects on wing tip vortices.
- Analyze compressibility effects on the rotor blades in cruise.
- Research rotor tip shapes to increase critical Mach number.
- Complete an analysis on vibrations.
- Research, in depth, various empennage configurations and the possibility of a canard or three surface configuration.
- Study the effects of wing blockage on rotor performance.

The redundancy of the variable diameter mechanism is also yet to be proven, especially on a aircraft as complex as a tilt rotor.

References

1. Fradenburgh, Evan, H,.Improving *Tilt Rotor Aircraft Performance With Variable-Diameter Rotors*, Sikorsky Aircraft Division United Technologies Corporation Presented Fourteenth European Rotorcraft Forum, Milano Italy,1988.

2. Boeing Commercial Airplane Co., *Civil Tiltrotor Missions and Applications: A Research Study*, Prepared for NASA/FAA/DOD, (NASA CR 177452).

3. Roskam, Jan, *Airplane Design: Part I, Preliminary Sizing of Airplanes*, Roskam Aviation and Engineering Corp., Ottawa, Kansas, 1985.

4. Federal Aviation Administration, Department of Transportation, Federal Aviation Requirement Designation, 25.XX.

5. Federal Aviation Administration, Department of Transportation, Federal Aviation Requirement Designation, 36.XX.

6. Tilt Rotor Research Aircraft Project Office Staff, *Army/NASA XV-15 Tilt Rotor Research Aircraft Familiarization Document*.

7. Federal Aviation Administration, Department of Transportation, *Interim Airworthiness Criteria: Powered-Lift Transport Category Aircraft*, 1988.

8. McCormick, Barnes W., *Aerodynamics, Aeronautics, and Flight Mechanics*, John Wiley and Sons, NewYork, 1979.

9. Prouty, Raymond W., *Helicopter Performance, Stability and Control*, PWS Publishers, Boston, Massachusetts, 1976.

10. Taylor, J.W.R., *Jane's All the World's Aircraft*, Jane's Publishing Co., London, England, 1987.

11. Bauld, Nelson R. Jr., *Mechanics of Materials*, PWS Publishers, Boston Massachusetts, 1986.

12. Roskam, Jan, *Airplane Design: Part II, Preliminary Configuration Design and Integration of the Propulsion Systems*, Roskam Aviation and Engineering Corp., Ottawa, Kansas, 1985.

13. Roskam, Jan, *Airplane Design: Part III, Layout Design of Cockpit, Fuselage, Wing and Empennage:Cutaways and Inboard Profiles*, Roskam Aviation and Engineering Corp., Ottawa, Kansas, 1985.

14. Abbott, I. & A. VonDoenhoff, *Theory of Wing Sections*, Dover Publications, New York, New York, 1959.

15. Nicolai, Leland M., *Fundamentals of Aircraft Design*, METS, Inc., San Jose, California, 1975

16. Roskam, Jan, *Airplane Design: Part V, Component Weight Estimation*, Roskam Aviation and Engineering Corp., Ottawa, Kansas, 1985.

17. Perkins, C. and R. Hage, *Airplane Performance Stability and Control*, J. Wiley and Sons, New York, New York, 1949.

18. Roskam, Jan, *Airplane Design: Part VI, Preliminary Calculation of Aerodynamic Thrust and Power Characteristics*, Roskam Aviation and Engineering Corp., Ottawa, Kansas, 1985.

19. Roskam, Jan, *Airplane Flight Dynamics and Automatic Flight Controls*, Roskam Aviation and Engineering Corp., Ottawa, Kansas, 1979

20 Corning, Geoff, *Supersonic and Subsonic CTOL and VTOL Aircraft Design*, University of Maryland, 1960.

21. *Standard Method of Estimating Comparitive D.O.C. of Turbine Powered VTOL Transport Aircraft*, Aerospace Industries Assoc. of America, Inc., Vertical Lift Council, Nov. 1968.

22 Anderson, John D. Jr., *Introduction to Flight*, McGraw-Hill Book Company, New York, New York, 1985.

23. Faulkner, Henry B., *The Cost of Noise Reduction in Commercial Tilt Rotor Aircraft*, Prepared for Aames Research Center, NASA, 1974.